Programa de Desarrollo de Ciencias Básicas (PEDECIBA)

Área: Biología

Sub-área: Biología Celular y Molecular

Tesis de Doctorado

"Estudio de la interacción *Physcomitrium patens* y *Botrytis cinerea*; un abordaje transcriptómico y funcional"

Guillermo Reboledo

Directora: Dra. Inés Ponce de León

Co-directora: Dra. Astrid Agorio

Departamento de Biología Molecular

Instituto de Investigaciones Biológicas Clemente Estable

Tribunal de Tesis:

Dr. Federico Battistoni, Dra. Mariana Sotelo y Dra. Ana López.

Julio 2022

Índice

Agradecimientos

A Inés y Astrid por ser excelentes tutoras, por su buena y pronta disposición, orientación, ayuda y motivación siempre que lo necesité. Por esas charlas y discusiones enriquecedoras esenciales para el crecimiento de uno en esta profesión, brindando la base para evaluar y resolver futuros desafíos. Pero, sobre todo por ser excelentes personas y preocuparse por uno día a día.

A Lucía V., con quién logramos, junto a Inés y Astrid, formar un gran equipo de trabajo generando una fuerte sinergia reflejada en la producción bibliográfica de estos últimos años, resolviendo muchos nuevos desafíos. Agradecerle principalmente por ese aire fresco, buena vibra y amistad que brinda y hace que el laboratorio sea un lugar aún más amigable donde estar y trabajar.

A Ricky y demás compañeros con quienes nos encontrábamos en el laboratorio diariamente compartiendo consejos, almuerzos, charlas personales, momentos lindos (y otros no tan lindos) así como festejos. A ellos un agradecimiento también por hacer que el trabajo, muchas veces, rutinario, extenso en horas y pesado, sea más fácil y mucho más llevadero.

A Alfo, Anto, Dani, Edu, Fer y Ger amigos que trajo la vida y/o la profesión, por estar siempre presentes en los momentos en que necesité algún tipo de apoyo, consejo o simplemente distracción y esparcimiento para tomar impulso y seguir con más fuerza.

A familiares importantes para uno, que por algún u otro motivo no están hoy en día para ver la culminación de esta etapa en mi vida, y de la cual seguro estarían muy orgullosos.

Principalmente y por sobre todas las cosas, me gustaría agradecer a mis padres, Julio y Carmen, y a mí hermano Gonza, por apoyar, escuchar, aconsejar y especialmente por **estar**. Han sido los pilares más importantes en mi vida y gracias ellos he logrado cumplir las metas que me he planteado y llegar a donde hoy estoy.

Agradezco el apoyo financiero brindado por: PEDECIBA, Beca de maestría ANII (Agencia Nacional de Investigación e Innovación), Beca de Movilidad Tipo Capacitación ANII, Beca para Pasantías de Corta Duración PEDECIBA, “Fondo Conjunto” Uruguay-México (AUCI-AMEXCID) y Programa para Grupo de I+D Comisión Sectorial de Investigación Científica, Universidad de la República (UdelaR).

Resumen

Las plantas vasculares activan diferentes mecanismos de defensa una vez que detectan la presencia de microorganismos patógenos, desencadenando un cambio masivo en la expresión de genes que codifican para proteínas con diferentes funciones en la defensa vegetal. A su vez, los patógenos han co-evolucionado con las plantas desarrollando diferentes mecanismos para interferir con estas defensas. En plantas no vasculares como las briofitas (musgos, hepáticas y antoceros), existe muy poca información sobre los mecanismos de defensas vegetal y virulencia de patógenos que actúan durante una interacción. El musgo *Physcomitrium patens* (*P. patens*), anteriormente conocido como *Physcomitrella patens,* representa una excelente planta modelo que junto con estudios comparativos con plantas vasculares, permite analizar la evolución de los diferentes mecanismos de defensa en el linaje de las plantas.

El objetivo de este trabajo es estudiar la interacción de *P. patens* con el hongo necrótrofo *Botrytis cinerea* (*B. cinerea*), el cual es un importante patógeno de cultivos. Mediante una aproximación transcriptómica, evaluamos los distintos mecanismos de defensa que se activan en la planta, así como las estrategias de infección y virulencia del hongo durante la colonización del tejido del musgo. Al comparar los transcriptomas de plantas de *P. patens* tratadas y sin tratar con esporas de *B. cinerea* a 4, 8 y 24 horas post inoculación (hpi), se identificaron 3.072 genes diferencialmente expresados (GDEs). Dentro de los genes vegetales inducidos durante la infección con el hongo, se encontraron genes que codifican para proteínas de función conocida en la inmunidad de plantas vasculares. Estos incluyen genes involucrados en el reconocimiento del patógeno, señalización, transcripción, señalización hormonal, vías metabólicas como ser la de shiquimato y fenilpropanoides, y proteínas con funciones diversas frente al estrés biótico. De forma similar a como ocurre en otras plantas, la infección por *B. cinerea* dio lugar a la represión de genes involucrados en la fotosíntesis y progresión del ciclo celular. Estos resultados demuestran una conservación evolutiva de respuestas de defensa a patógenos en plantas vasculares y no vasculares. Además, identificamos un número significativo de genes vegetales inducidos durante la interacción que fueron adquiridos por transferencia horizontal de procariotas y hongos, y genes huérfanos que sólo se encuentran en *P. patens*, lo que sugiere la existencia de mecanismos de defensa específicos de *P. patens* que cumplen un importante rol en la respuesta inmune a la infección por *B. cinerea*.

Se analizaron los transcriptomas de *B. cinerea* durante el proceso de infección a los mismos tiempos y se identificaron un total de 1.105 GDEs. Mediante estudios del patrón de expresión de los genes sobreexpresados y el análisis de ontología de genes, se demostró que la colonización de los tejidos de *P. patens* por *B. cinerea* depende de la generación de especies reactivas de oxígeno y detoxificación, actividad de transportadores, modificación y degradación de la pared celular de la planta, producción de toxinas y la probable evasión de la defensa de la planta mediante el uso de efectores. Este estudio del proceso de infección de *B. cinerea* se amplió a distintos hospederos, incluyendo, *Arabidopsis thaliana*, *Solanum lycopersicum* y *Lactuca sativa* mediante comparaciones de nuestros transcriptomas con datos de RNA-Seq disponibles en la base de datos del NCBI. Como resultado se identificaron genes de *B. cinerea* involucrados en procesos de

infección y virulencia utilizados frente a todos los hospederos estudiados, mientras que otros fueron más específicos de *P. patens* o angiospermas.

Uno de los genes de *P. patens* inducido por *B. cinerea* codifica para un posible factor de transcripción del tipo "APETALA2/ETHYLENE RESPONSIVE FACTOR" (AP2/ERF), al que denominamos PpERF24. Mediante la expresión transitoria de PpERF24 fusionado a la proteína verde fluorescente (PpERF24:GFP) en *Nicotiana tabacum*, confirmamos que PpERF24 se localiza en el núcleo. Dado el alto nivel de expresión de PpERF24 en respuesta a varios patógenos, se generaron plantas de *P. patens* sobreexpresantes en PpERF24. Se obtuvieron varias líneas transformantes y los estudios funcionales evidenciaron una menor susceptibilidad de plantas con altos niveles de sobreexpresión de PpERF24 al filtrado de cultivo acelular de *Pectobacterium carotovorum* subsp. *carotovorum*, a los hongos *B. cinerea* y *Colletotrichum gloeosporioides* y al oomicete *Pythium irregulare* en comparación a plantas salvajes. Con el objetivo de estudiar los distintos mecanismos moleculares involucrados en la diferencia de susceptibilidad observada ante los diferentes tipos de patógenos, analizamos los transcriptomas de una línea sobreexpresante y plantas salvajes, tratadas y sin tratar con esporas de *B. cinerea*. Los resultados mostraron un aumento de expresión de genes relacionados con la defensa en las plantas que sobreexpresan PpERF24, indicando que PpERF24 activa mecanismos de defensa en *P. patens*.

Los resultados obtenidos durante este trabajo de tesis permitieron extender significativamente la información disponible sobre la activación de mecanismos de defensa de *P. patens* en respuesta al estrés biótico e identificar genes con funciones importantes en la inmunidad durante la evolución de las plantas terrestres.

1. Introducción

Todas las plantas terrestres que existen hoy en día provienen del clado de las estreptofitas, más precisamente a partir de un alga estreptofita como ancestro común, la cual probablemente vivía en agua dulce (de Vries and Archibald, 2018). Fue a partir de la evolución de esta alga que surgió lo que hoy en día son los dos grupos principales de plantas, las briofitas y las traqueofitas. El primer grupo se compone por plantas no vasculares y lo conforman los musgos, hepáticas y antoceros, mientras que dentro del grupo de las traqueofitas se encuentran las plantas vasculares como ser los helechos, licofitas, gimnospermas y angiospermas (Delaux et al., 2019; Fürst-Jansen et al., 2020). La conquista de la tierra por parte de las primeras plantas terrestres fue posible gracias a su adaptación al nuevo ambiente, el cual era más hostil y más variable que el medio acuático. Esto significó crear nuevas estrategias para hacer frente a estreses abióticos como ser la sequía, la radiación UV y la variación en la temperatura (Fürst-Jansen et al., 2020). Estas primeras plantas terrestres, también se vieron desafiadas por microorganismos que ya habitaban la superficie de la tierra, por lo que tuvieron que generar mecanismos de reconocimiento y de defensa efectivos. Algunas de estas interacciones lograron ser benéficas para ambas partes, transformándose por lo tanto en interacciones mutualistas (Field et al., 2015; de Vries and Archibald, 2018). Mediante registros fósiles que datan de aproximadamente 400 millones de años, fue posible descubrir que también existieron interacciones no benéficas entre las primeras plantas terrestres y algunos microorganismos como ser oomicetes y hongos, identificándose así las primeras interacciones planta-microorganismo patógeno (Krings et al., 2007; Strullu-Derrien, 2018). Para tratar de entender los procesos evolutivos que ocurrieron a partir de las primeras plantas terrestres hasta las plantas actuales y conocer cuáles fueron los mecanismos desarrollados para hacer frente a los distintos tipos de estrés al pasar al medio terrestre, se han comparado respuestas de defensa entre plantas briofitas y plantas angiospermas (Delaux et al., 2019; Fürst-Jansen et al., 2020). Estos estudios han permitido identificar y diferenciar aquellas estrategias conservadas a lo largo de todo el linaje de las plantas verdes de aquellas que son especie-específicas. Sin embargo, la mayoría de estos estudios comparativos se han centrado en estreses abióticos y poco se sabe sobre la respuesta de defensa frente a estreses bióticos en briofitas.

1.1. Señales inmunogénicas y percepción del patógeno

Las plantas están permanentemente en contacto con microorganismos presentes en el ambiente. Sin embargo, solo un porcentaje menor de éstos logra establecer una interacción con la planta, ya sea mutualista o patogénica. Como forma de evitar que los microorganismos patógenos colonicen los tejidos de la planta, estas poseen como primera medida de defensa a las barreras físicas preformadas como son la cutícula o la pared celular, y compuestos con actividad antimicrobiana. En la mayoría de los casos estas barreras son suficientes para que no se lleve a cabo la infección de la planta. Sin embargo, cuando los patógenos logran atravesarlas, las células

de la planta perciben al patógeno y activan varias capas más de defensa las cuales van aumentando en especificidad y amplitud de respuesta según sea necesario.

Los microorganismos patógenos que atacan las plantas incluyen virus, bacterias, hongos y oomicetes (Teixeira et al., 2019). Las estrategias que estos utilizan para lograr ingresar en la planta son variadas. En bacterias el ingreso es principalmente por heridas o aberturas naturales de la planta, tales como los estomas y los hidátodos. Una vez dentro, las bacterias comienzan a colonizar los espacios intercelulares y los tejidos llegando a crear biofilms. Los hongos y oomicetes, si bien pueden usar los mismos puntos de entrada que las bacterias, también son capaces de romper mecánicamente las barreras físicas preformadas de la planta y de esta forma ingresar a los tejidos vegetales. Todos estos microorganismos patógenos secretan enzimas que degradan la pared celular, logrando debilitar las barreras físicas de la planta.

1.1.1. Receptores de superficie celular y señalización

El reconocimiento de señales provenientes de los patógenos se da en primera instancia a nivel de la superficie celular vegetal en la membrana plasmática por medio de receptores transmembrana conocidos como receptores de reconocimiento de patrones (PRRs, *pattern recognition receptors*). Dichos receptores reconocen ciertos patrones moleculares asociados a patógenos o microbios (PAMPs/MAMPs, *Pathogen/Microbe-Associated Molecular Patterns*), o al daño que éstos han realizado en los tejidos de la planta (DAMPs, *Damage-Associated Molecular Patterns*). Los ligandos que los PRRs censan se conocen más genéricamente con el nombre de elicitores (Boller and Felix, 2009; Lee et al., 2021). Ejemplos de elicitores exógenos tipo PAMPs/MAMPs son la flagelina bacteriana y el EF-Tu (factor de elongación-Tu) o la quitina presente en la pared celular de los hongos. Entre los elicitores endógenos tipo DAMPs se encuentran los péptidos de sistemina y péptidos moduladores de la inmunidad que actúan como fitocitoquinas como ser los PEPs (*plant elicitor peptide*) (Boller and Felix, 2009; Gust et al., 2017; Lee et al., 2021). Los PRRs identificados hasta el momento pueden dividirse en dos subfamilias. Los receptores quinasa (RK, *receptor kinase*), los cuales son conceptualmente análogos a los receptores del tipo Toll en animales (Tang et al. 2017), y las proteínas del tipo receptor (RLP, *receptor-like protein*). La diferencia radica principalmente en que los receptores RK poseen tres dominios, un dominio extracelular, un dominio transmembrana y un dominio quinasa citosólico. En cambio, los receptores RLP si bien presentan un dominio extracelular y un dominio transmembrana, carecen del dominio quinasa citosólico y en su lugar poseen una cola citosólica corta (Dievart et al., 2020; DeFalco and Zipfel, 2021). La diversidad de dominios extracelulares les permite la interacción con distintos tipos de ligando como ser péptidos, glicanos o pequeñas moléculas, ampliando así la capacidad de reconocimiento de elicitores (Lehti-Shiu et al., 2009; Boutrot and Zipfel, 2017). Algunos ejemplos de PRRs y PAMPs/DAMPs más estudiados y mejor caracterizados se encuentran en la **Figura 1**. El reconocimiento directo de los PAMPs y DAMPs por los receptores PRRs, desencadena lo que se conoce como inmunidad gatillada por patrones o PAMPs (**PTI**, *Pattern-Triggered Immunity*). La activación de los complejos PRRs inicia las cascadas de proteínas quinasas activadas por mitógenos (MAPK, *mitogen-activated protein*

kinases) y las proteínas quinasas dependientes del calcio (CDPK). Esto lleva a una rápida reprogramación de la expresión de genes que regulan los cambios transcripcionales y otras respuestas celulares. La respuesta de defensa por PTI se considera de amplio espectro y es lo suficientemente eficaz como para frenar a aquellos patógenos no especializados y evitar su colonización en la planta. Este tipo de respuesta comprende el incremento de Ca^{2+} citosólico, despolarización de la membrana plasmática y alcalinización extracelular, estallido de especies reactivas del oxígeno (ROS), estallido de óxido nítrico (NO), producción de ácido fosfatídico, cierre de estomas, remodelación de filamentos de actina, producción de compuestos antimicrobianos y fitohormonas, deposición de calosa en el sitio de entrada del patógeno y cierre de plasmodesmos (Yu et al., 2017; DeFalco and Zipfel, 2021).

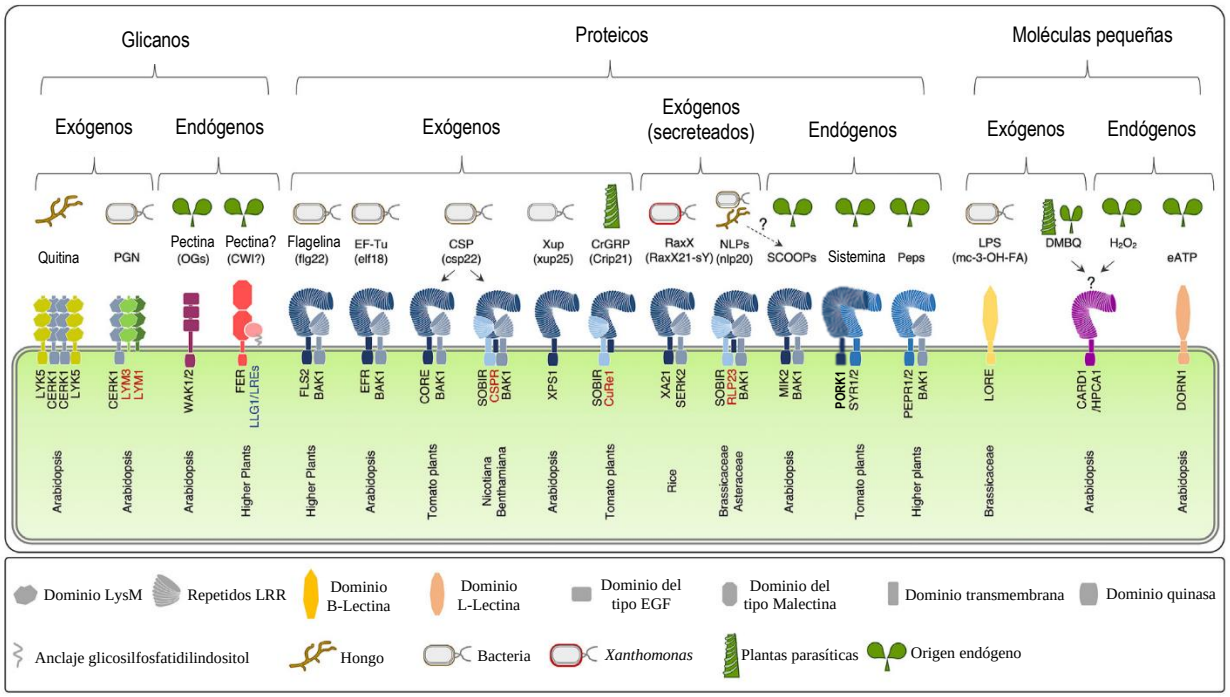

Figura 1. **Ligandos de PRRs.** De izquierda a derecha. **Glicanos:** los oligómeros de quitina son reconocidos por LYK5, que recluta a CERK1, para formar un complejo hetero-tetramérico de forma dependiente del ligando. Los PGNs son detectados por LYM1 y LYM3 con CERK1. Los glicanos endógenos y los OGs (oligogaracturonidos) son reconocidos por el WAK1/2. La integridad de la pared celular (CWI, *cell wall integrity*) puede ser monitorizada por FER y las proteínas ancladas a GPI LLG1/LREs. **Elicitores proteicos:** La flagelina bacteriana y el EF-Tu son detectados respectivamente por FLS2 y EFR mediante el reconocimiento de flg22 y elf18. El epítopo csp22 de las proteínas bacterianas de shock frío (CSP, *cold-shocks proteins*) es detectado por CORE y CSPR. La xantina/uracilo permeasa (XUP, *xanthine/uracil permease*) bacteriana es detectada por XPS1 mediante el reconocimiento del epítope xup25. La proteína de la pared celular de la planta parásita *Cuscuta reflexa*, CrGRP, es detectada por CuRe1/SOBIR1 a través del reconocimiento del epítopo Crip21. Se desconoce si BAK1 es necesaria para la señalización de XPS1 y CuRe1. La proteína bacteriana RaxX es detectada por XA21 y su correceptor SERK2 a través del péptido sulfatado RaxX21-sY. Tanto los PNL fúngicos como los bacterianos son reconocidos por el heterómero RLP23-SOBIR, que posteriormente recluta a BAK1 para la señalización. Durante el daño, los PEPs endógenos y los péptidos de sistemina son liberados por proteasas y detectados por PEPR1/2 y SYR1/2-PORK1, respectivamente. Los sistemas de señalización de PEP también requieren el correceptor BAK1. **Moléculas pequeñas:** El mc-3-OH-FA del LPS es detectado por el Lec-RK LORE de tipo B mientras que el eATP es detectado por el LecRK DORN1 de tipo L. El LRR-RK CARD1/HPCA1 percibe tanto el DMBQ exógeno de las plantas parásitas de la raíz como el eH2O2 (peróxido de hidrógeno extracelular) endógeno. Los nombres de los receptores de la clase RLP y RK se indican en rojo y negro, respectivamente. Imagen obtenida y modificada de Lee et al. 2021.

1.1.1.1. Percepción de Elicitores

Los receptores PRRs mejor estudiados y caracterizados hasta el momento son aquellos que poseen repetidos ricos en leucina (LRR, *leucine-rich repeat*) en su dominio extracelular. Dentro de este grupo se encuentran receptores del tipo RK y RLP (LRR-RK y LRR-RLP, respectivamente). Los LRR-RK mejor caracterizados son de *Arabidopsis thaliana* (Arabidopsis), como FLS2 (*flagelin-sensing 2*), el cual reconoce el epítope flg22 proveniente de bacterias flageladas, y el receptor EFR (*elongation factor-tu receptor*), que reconoce el epítope elf18 encontrado en el factor de elongación Tu de bacterias (Albert et al., 2020) (**Figura 1**). Recientemente se ha reportado en otras especies la existencia de receptores diferentes para flagelina y el factor de elongación Tu demostrando que a lo largo de la evolución de las plantas, múltiples receptores han evolucionado independientemente para la detección de distintos epítopes (Albert et al., 2020).

Para que el reconocimiento de ligandos y activación de receptores PRRs pueda darse, se requiere, casi en la totalidad de los casos, de la interacción del dominio extracelular del PRR con el dominio extracelular de los llamados co-receptores. Estos co-receptores, también pertenecientes a la familia de los LRR-RKs, presentan un dominio extracelular más pequeño (Zhou and Zhang, 2020; Lee et al., 2021). Todos los PRRs del tipo LRR-RK estudiados hasta el momento, usan como co-receptor a un LRR-RK perteneciente a la familia SERK (*somatic embryogenesis receptor kinase*). El dominio quinasa en los receptores es esencial para iniciar la transducción de señales cuando se da el reconocimiento del ligando. Sin embargo, los receptores RLP no poseen dicho dominio. Como forma de compensarlo, estos receptores se asocian con otro tipo de receptor conocido como adaptador, el cual es del tipo LRR-RK. A partir de esta asociación se logra conformar un receptor bipartito. La formación de estos complejos de receptores, desencadenan la transducción de señal y respuesta, más o menos específica dependiendo del estímulo reconocido (Fritz-Laylin et al., 2005; DeFalco and Zipfel, 2021; Lee et al., 2021).

Aunque la mayoría de los receptores PRRs caracterizados hasta el momento presentan en el dominio extracelular el motivo LRR, también se han identificado otros motivos responsables del reconocimiento de elicitores no proteicos. Tal es el caso de aquellos receptores que poseen en su dominio extracelular motivos de lisina (LysM, *lysine motifs*). Estos LysM-PRRs, mayoritariamente detectan glicanos provenientes de la pared celular del patógeno y plantas. Al igual que sucede con los elicitores proteicos, los glicanos reconocidos por los PRRs suelen ser esenciales para los patógenos y su supervivencia. Este es el caso de los peptidoglicanos (PGNs), convirtiéndose en una buena diana de reconocimiento por parte de la planta (Albert et al., 2020; Lee et al., 2021). En Arabidopsis, las moléculas de PGNs son liberadas por la acción de la enzima glicosil hidrolasa LYS1 (*lysozyme 1*). Los PGNs liberados son reconocidas por un complejo formado por tres receptores, dos receptores del tipo LysM-RLPs (LYM1 y LYM3, *LysM domain GPI-anchored protein 1* y 3 respectivamente) y uno del tipo LysM-RK (CERK1, *chitin elicitor receptor kinase 1*) (Willmann et al., 2011). A su vez, en Arabidopsis, CERK1 al asociarse con LYK5 (*LysM-containing receptor-like kinase 5*) forma un complejo dependiente del ligando

quitina, componente principal de la pared celular de los hongos, con el fin de regular la inmunidad antifúngica (Cao et al., 2014; Albert et al., 2020; DeFalco and Zipfel, 2021; Lee et al., 2021).

Otros receptores PRRs descubiertos, distintos a los tipos LRR y LysM, son los pertenecientes a la familia Lec RKs (*Lectin RKs*). Estos receptores, al igual que los anteriores, pueden detectar ligandos de procedencia exógena o endógena. En el caso del reconocimiento de ligandos exógenos, se encuentra el receptor L-LecRK LORE (*G-lectin RK lipooligosaccharide-specific reduced elicitation*) de Arabidopsis el cual reconoce el mc3-OH-FA (*medium-chain 3-hydroxy fatty acid*) de bacterias derivado de lipopolisacáridos (Kutschera et al., 2019; Luo et al., 2020; DeFalco and Zipfel, 2021; Lee et al., 2021). En cuanto a los elicitores de origen endógeno, las plantas apuntan a detectar en la superficie celular aquellas moléculas que suelen estar intracelularmente, pero que por algún motivo o estrés causado se encuentran extracelularmente. Tal es el caso de las moléculas eATP (*extracellular adenosine 5'-triphosphate*) y NAD^+ (*nicotinamide adenine dinucleotide*) las cuales son reconocidas como DAMPs por los receptores B-LecRK DORN1 (*does not respond to nucleotides 1*) y LecRK-I.8 respectivamente (Choi et al., 2014; Wang et al., 2017; Albert et al., 2020; DeFalco and Zipfel, 2021; Lee et al., 2021).

1.1.2. Receptores citosólicos

Cuando los receptores PRRs de la membrana plasmática perciben la presencia de PAMPs o DAMPs, se activa la respuesta PTI. Este tipo de respuesta es útil para la defensa contra patógenos no especializados, sin embargo, existen patógenos capaces de interferir con la respuesta de defensa de la planta por medio de moléculas llamadas efectores. Estos efectores, generalmente liberados en el interior celular, tienen como blanco específico puntos clave en las vías de señalización y de respuesta de la planta para poder apagar, modular o usar a su favor la respuesta de defensa de la misma. La planta por su lado, para frenar a estos patógenos ha adquirido lo que se conoce como receptores intracelulares o NLR (*nucleotide-binding/leucine-rich-repeat*) polimórficos. Estos receptores interceptan a los efectores e inducen una respuesta de defensa robusta llamada inmunidad gatillada por efectores (ETI, *Effector Triggered Immunity*). La ETI consiste básicamente en el mismo tipo de respuesta que PTI solo que la ETI se caracteriza por ser de mayor duración, amplitud y robustez. A su vez, en la ETI se da la resistencia sistémica adquirida (SAR, *systemic aquaried resistance*), lo cual prepara tejidos distantes para enfrentar al patógeno, y presenta como marcador de respuesta, un tipo de muerte celular programada conocida como respuesta hipersensible (HR, *hypersensitive response*) en el sitio de la infección (Fu and Dong 2013; Jones and Dangl 2006).

1.1.2.1. Tipos de receptores citosólicos

Los NLRs presentan una estructura multidominio, dos de los cuales son conservados mientras que el tercero es polimórfico, de ubicación N-terminal y responsable de la activación de la inmunidad. Los dominios compartidos son el dominio central NB-ARC (*Nucleotide-Binding adaptor shared with* APAF-1, *plant resistance proteins, and* CED-4) y el dominio LRR (*leucine-rich repeat*) en el extremo C-terminal respectivamente. Dado el polimorfismo existente en el extremo N-terminal, el mismo es utilizado para clasificar a los NLRs en tres tipos principales: **TNL** (TIR-type NLR, *toll and interleukin-1 receptor* NLR), **CNL** (CC-type NLR, *coiled-coil* NLR) y **RNL** (RPW8-like CC-type NLR, *resistance to powdery mildew-8* NLR) (**Figura 2**). Además, algunos NLRs presentan lo que se denomina dominio integrado (ID, *integrated domain*), pasándose a conocer como **NLR-ID** (NLR-*integrated domain*). Este ID suele presentar similitud con la molécula blanco de efectores y se cree que evolucionaron a partir de la integración del blanco del efector en la arquitectura clásica de dominios del NLR (Adachi et al., 2019; Andolfo et al., 2019). Se cree que los NLRs oscilan entre los estados inactivo y activo, lo cual es controlado por la presencia de ADP (estado inactivo) o ATP (estado activo) en el dominio NBS (*nucleotide-binding site*) del NLR. Este pasaje de un estado a otro puede deberse a la actividad ATPasa del propio dominio NB-ARC o por la acción de proteínas que, interactuando con el NLR, funcionan como factores de intercambio de nucleótidos (Bernoux et al. 2016; J. Wang, Hu, et al. 2019; J. Wang, Wang, et al. 2019). Los NLRs también pueden subclasificarse en *sensor* NLRs (sNLRs) o *helpers* (hNLRs) según reconozcan directa o indirectamente la presencia del efector, o según sean requeridos por otros NLRs para la activación de la respuesta inmune, respectivamente (Bonardi et al., 2011; Tamborski and Krasileva, 2020).

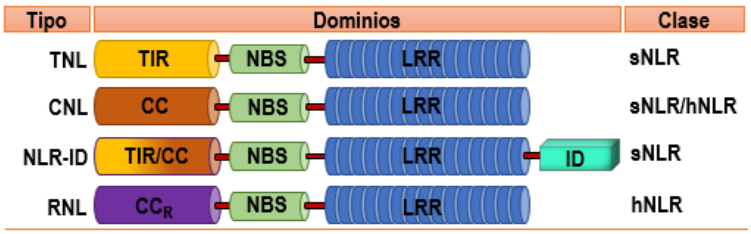

Figura 2. **Arquitectura, clasificación y tipos de NLRs.** Generalmente los receptores NLRs presentan tres dominios, dos de los cuales son compartidos como ser el **NBS** (*nucleotide-binding site*) y el **LRR** (*leucine-rich repeat*) en el centro y el extremo C-terminal respectivamente. El domino ubicado en el extremo N-terminal es polimórfico y puede, a grandes rasgos, ser de tres tipos: **TIR** (*toll and interleukin-1*, **TNL**), **CC** (*coiled-coil*, **CNL**) o **CCR/RPW8** (*resistance to powdery mildew-8 CC-type*, **RNL**). Algunos NLRs con dominios N-terminal del tipo TIR o CC, pueden presentar un cuarto dominio, conocido como dominio integrado o **ID** (*integrated domain*), posible blanco falso de efectores. A este tipo de NLR se le conoce como **NLR-ID**. Por último, los NLRs pueden subclasificarse según su actividad como NLRs de clase sensor (**sNLR**) o clase "*helper*" (**hNLR**) según reconozcan directa/indirectamente al efector o interactúen con el sNLR activado por el efector o esté involucrado en la señalización post reconocimiento del mismo, respectivamente.

1.1.2.2. Evolución de NLRs

Los NLRs son de las familias de receptores inmunes más grande y expandida en plantas. La principal localización subcelular de estos receptores es en el citoplasma celular, aunque también se pueden encontrar en el núcleo o anclados a la membrana plasmática. Su función es detectar efectores del patógeno secretados al interior celular y posterior señalización para dar comienzo a la respuesta inmune. Anteriormente, se pensaba que para cada efector existía un único gen de resistencia (R) que lo reconociese y activara la defensa en la planta (teoría de gen para gen; Flor 1971). Décadas de investigación junto con la posibilidad del clonado de genes y la edición genética de plantas, ampliaron enormemente nuestro conocimiento sobre el funcionamiento del sistema inmune de las plantas. Hoy en día se sabe que la mayoría de estos genes R, son en realidad NLRs y que el dogma central de "gen a gen" que reinó por décadas ya no es tan así. Si bien hay casos de reconocimiento directo entre NLRs y efectores, existen más casos de reconocimiento de un efector mediado por dos o más NLRs. Es así que estos conceptos nuevos dejan entrever una red de interconexiones entre NLRs mucho más compleja, robusta y plástica de lo que se creía. Para explicar cómo surgió esta conectividad entre NLRs se crearon varios modelos evolutivos. El predominante y el de mayor aceptación es aquel que plantea los conceptos de *singleton*, *pairs* (pares) y *network* (red) (Adachi et al., 2019). En la **Figura 3** se esquematiza este modelo, el cual explica la aparición de la red como resultado de la evolución de NLRs *singleton*. Estos NLRs son capaces por sí mismos de percibir directa o indirectamente al efector y activar lo que se conoce como respuesta inmune hipersensible (HR) en la planta. Un ejemplo de NLR de tipo *singleton*, es el NLR ZAR1 el cual tiene funciones de tipo sensor y de señalización, y cuya activación lleva al ensamblado del resistosoma o complejo de NLRs (**Figura 3.c**). Se postula que los NLRs del tipo *singleton* pasaron por un proceso evolutivo que permitió duplicaciones y especialización de funciones dando lugar a los sNLRs (*sensor* NLR) y hNLRs (*helper* NLR, también conocido como ejecutor) generando así, nuevas conexiones entre NLRs que van desde pares a redes más complejas. A partir de este evento de duplicación y especialización algunos NLRs pasaron a funcionar de a pares (**Figura 3.b**), donde el sNLR especializado en reconocer el patógeno se empareja con el hNLR involucrado en la inicialización de la señalización inmunitaria. Una característica en los NLRs que trabajan de a pares, es que en muchos de los casos se encuentran ubicados bidireccionalmente (*"head-to-head*") en el genoma compartiendo el mismo promotor. A su vez, uno de los NLRs presenta un dominio integrado (NLR-ID) que por lo general funcionan como señuelo al simular ser el verdadero blanco del efector (Césari et al., 2014; Chiang and Coaker, 2015; Le Roux et al., 2015; Sarris et al., 2015). Es así que la unión del efector al señuelo integrado facilita la activación del otro NLR con arquitectura clásica de NLRs, dando paso a la activación de la respuesta ETI (Cesari et al., 2014). Además de los modelos evolutivos *singleton* y de a pares de NLRs existe la hipótesis de que ciertos NLRs trabajan conjuntamente con más de un NLR para lograr la señalización y posterior activación de la respuesta inmune (**Figura 3.a**). Evidencia reciente revela que la relación entre NLRs es más compleja de lo que se pensaba validando la idea de una red de NLRs (Wu et al. 2018).

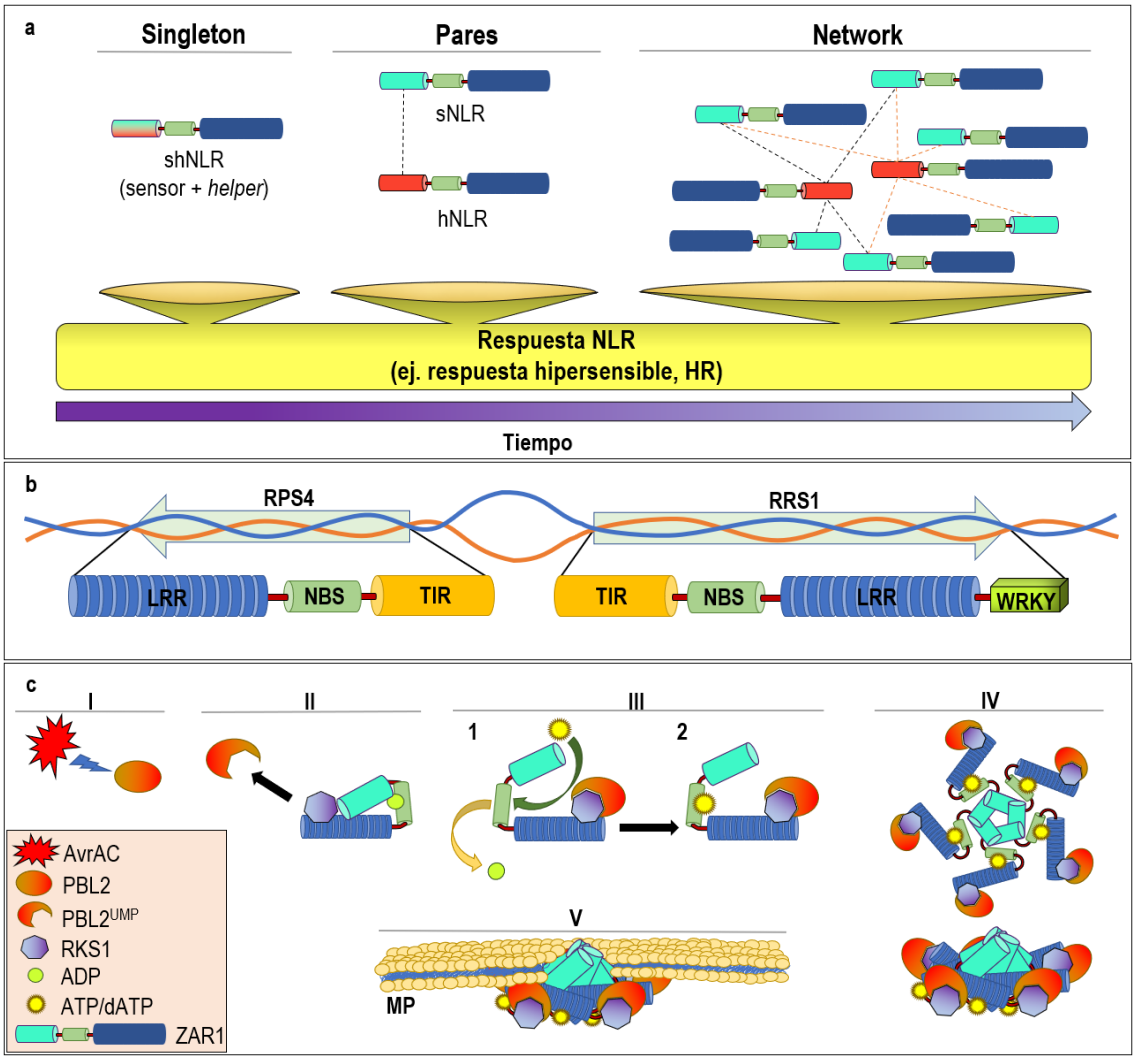

Figura 3. **Evolución y mecanismos de activación de NLRs. a) Evolución de NLRs y respuesta NLR.** Adachi y colaboradores, al analizar la evolución de los NLRs, sostienen que éstos podrían haber evolucionado a partir de receptores singleton multifuncionales los cuales poseían ambas funciones, la de detección y la de señalización (shNLR, NLR con actividad censora y "*helper*"). Posteriormente, en la evolución, estos singletones pudieron haberse duplicado y especializado funcionalmente para dar lugar a los sNLR y hNLRs creando conexiones que van desde pares a redes (*network*) más complejas. **b) Mecanismo de acción por pares de NLRs**. En este ejemplo se observan los genes RPS4 y RRS1, del tipo TNL y NLR-ID respectivamente, los cuales se encuentran con orientación bidireccional en el genoma para asegurar la co-regulación de ambos genes. RRS1 es del tipo sNLR (*sensor* NLR) y presenta un dominio integrado del tipo WRKY, que actúa como señuelo para efectores (ej. Pop2 y AvrRps4). También puede verse la arquitectura de los NLRs, ambos comparten los dominios TIR (*toll and interleukin-1*), NBS (*nucleotide-binding site*) y LRR (*leucine-rich repeat*). El bucle entre flechas simboliza el sitio donde se encuentra el promotor compartido. **c) Ensamblaje del resistosoma.** Otro mecanismo de acción de los NLRs es el ensamblado de lo que se conoce como resistosoma o complejo de NLRs. En Arabidopsis, cuando el efector AvrAC de *Xanthomonas*, es inyectado en la célula, éste uridila a PBL2 (I). El PBL2 uridilado ($PBL2^{UMP}$), puede ser detectado y reclutado por el complejo ZAR1-RSK1 el cual se encontraba en su estado inactivo (II). Una vez formado el complejo ZAR1-RSK1-$PBL2^{UMP}$, ZAR1 sufre un cambio conformacional que permite la liberación de ADP (estado intermedio, III.1) para permitir la unión de ATP/dATP y pasar al estado activo (III.2). Posteriormente se da la oligomerización entre complejos ZAR1-RSK1-$PBL2^{UMP}$ activados para formar un pentámero, el resistosoma (IV). El resistosoma presenta una estructura semejante a la de un poro. Lo anterior, sumado a la afinidad por la membrana plasmática (MP) y a la α hélice presente en el dominio CC de los NLRs ZAR1, hace que el resistosoma se localice en la MP formando un poro (V). Se sabe que esta estructura es un canal calcio-permeable que gatilla la señalización inmune en plantas (Bi et al., 2021).

1.1.2.3. Percepción de Efectores y activación de NLRs

El reconocimiento de los efectores a partir de NLRs puede darse por distintos mecanismos, los cuales inicialmente se diferencian en directos o indirectos. A su vez, los mecanismos indirectos pueden subdividirse en los modelos de guardia, señuelo y señuelo integrado (Cesari, 2018). El mecanismo de reconocimiento directo es aquel en el cual no hay un intermediario entre el efector y el receptor, por lo que el efector es reconocido directamente por el NLR. Ejemplos de este tipo de reconocimiento lo son el NLR Pi-Ta en arroz, RPP1 en Arabidopsis y N en tabaco para los efectores AvrPi-Ta, ATR1 y P50, respectivamente. En cuanto al sistema de reconocimiento indirecto, la primera evidencia surgió en 1998 al estudiar la relación entre el efector AvrPto, la quinasa Pto y el NLR Prf (Van Der Biezen and Jones, 1998). Van Der Biezen y Jones, postularon que el efector AvrPto tiene como blanco a Pto debido a su rol en la inmunidad no gatillada por efectores, y que Prf puede sensar esta interferencia y activar una respuesta inmune más fuerte en la planta. Este postulado maduró y fue lo que luego pasó a conocerse como modelo de guardia (*the guard model*), surgiendo así los llamados mecanismos de reconocimiento indirecto (Dangl and Jones, 2001; van Wersch et al., 2020). Estos mecanismos comprenden el reconocimiento de alteraciones o modificaciones postraduccionales de proteínas de la planta hospedera. Como ejemplo reciente se encuentra el NLR SUMM2 el cual vigila el producto de fosforilación de la cascada por MAPK (*mitogen-activated protein kinase*) y por lo tanto es capaz de detectar modificaciones causadas por efectores en cualquiera de estas MAPK que conforman la cascada (Zhang et al., 2017; van Wersch et al., 2020). Por lo anterior, el modelo de guardia parece sugerir un escenario evolutivo bastante real en el cual los patógenos evolucionan para que sus efectores apunten a proteínas de defensa en la planta mientras que la planta hospedera evoluciona para que sus proteínas R puedan detectar la amenaza y activar una defensa más poderosa (van Wersch et al., 2020). Además del modelo de guardia, existen los de señuelo y señuelo integrado. La diferencia entre el modelo de guardia y los que usan señuelo es que en el primero la proteína que se modifica por el efector tiene una función inmune establecida, mientras que en el modelo de señuelo, el único propósito de la proteína modificada por el efector es la de ser una trampa para éste, sin otra función conocida. Un ejemplo reciente y caracterizado que emplea el modelo de señuelo (*decoy*) es el del CNL ZAR1 (**Figura 3.c**). Como es de esperar el beneficio que se le atribuye a este modelo es que se ve sujeto a una menor presión evolutiva que el modelo de guardia. Esto es así porque el señuelo, al no tener otra función más que la de ser blanco del efector, podría estar más libre para evolucionar y por ejemplo permitir su reconocimiento por otros NLRs (van Wersch et al., 2020). Una variante del modelo de señuelo fue propuesto en el año 2014 luego de haber encontrado, en un pequeño porcentaje de NLRs de plantas, lo que denominaron como dominios integrados o IDs (Cesari et al., 2014; Kroj et al., 2016). Estos IDs tenían cierta similitud con dominios de proteínas blanco de efectores de patógenos lo que hizo suponer que dichos dominios tal vez tuviesen un rol como señuelo, interactuando con los efectores y activando el NLR-ID. Se observó que estos NLR-ID trabajaban de a pares, interactuando con un NLR de arquitectura clásica. Esto tiene sentido desde el punto de vista de la co-regulación y co-expresión.

1.2. Respuesta de defensa compartida y comunicación PTI-ETI

Luego del reconocimiento del patógeno, una de las primeras respuestas compartidas que ocurre entre la PTI y la ETI es la variación de la concentración de Ca^{2+} citosólico. Este cambio se caracteriza por ser rápido y transitorio, siendo crucial en la transducción de señales para poder generar una respuesta adecuada (Reddy et al., 2011; Iqbal et al., 2021). Aunque este tipo de respuesta se da tanto en la PTI como en la ETI, en la primera el Ca^{2+} regresa a los niveles basales unos minutos luego de la activación de la PTI, mientras que en la activación por ETI, esta respuesta puede durar varias horas (Grant et al., 2000; Lecourieux et al., 2005). El influjo de Ca^{2+} es importante para la posterior producción de ROS y la inmunidad estomatal (Yuan et al., 2021b). En los mutantes *dnd1* y *dnd2* (*defense, no death*) de Arabidopsis, con mutaciones en los canales permeables al Ca^{2+} CNGC2 (*cyclic nucleotide-gated channels* 2) y CNGC4, se ha podido evidenciar una acumulación del ácido salicílico (SA; *salicylic acid*) elevada y constitutiva junto con un aumento en la resistencia a bacterias. Sin embargo, estos mutantes también presentaron una HR mediada por AvrRpt2/RPS2 (par de efector y receptor NLR) fuertemente comprometida. Al introducir el gen *NahG*, el cual metaboliza el SA convirtiéndolo en catecol, en el mutante *dnd2*, se eliminó la acumulación elevada de SA constitutivo y la resistencia mejorada, pero tuvo poco impacto en el fenotipo HR. Esta observación sugiere un relacionamiento de CNGC2 y CNGC4 con la HR asociada a la ETI (Jurkowski et al., 2004; Yuan et al., 2021b). Además de este tipo de canales, estudios recientes evidenciaron la formación de la estructura conocida como resistosoma (**Figura 3.c**). La misma está compuesta por complejos CNLs ZAR1 activados, los cuales forman un pentámero con similitud a un canal, y es permeable al Ca^{2+} (Bi et al., 2021).

Muchas proteínas quinasas asociadas a la PTI, incluyendo BIK1/PBLs, CPKs, SIK1 y CRK2, son capaces de fosforilar directamente a RBOHD (*Respiratory Burst Oxidase Homologue* D) para gatillar la producción de ROS extracelular en Arabidopsis (Dubiella et al., 2013; Kadota et al., 2014; Li et al., 2014; Zhang et al., 2018; Kimura et al., 2020; Lee et al., 2020; Yuan et al., 2021b). RBOHD también media la producción de ROS durante la ETI iniciada por los NLR RPS2 y RPM1.Esto sugiere que la segunda fase del ROS asociado a la ETI es dependiente de la señalización por PRR. A su vez, la señalización por PRR es requerida para la máxima fosforilación de RBOHD durante la ETI, mientras que la señalización por NLR aumenta los niveles de RBOHD. Esto evidencia la necesidad de la señalización por PRR y NLR para lograr una producción de ROS robusta durante la ETI (Ngou et al., 2021; Yuan et al., 2021a, 2021b).

La rápida activación de la cascada de MAPK es una característica conocida dentro de la señalización por PRR diferenciándose de su activación por NLR donde la misma es más lenta, pero de mayor duración (Asai et al., 2002; Tsuda et al., 2013; Su et al., 2018). Las quinasas del tipo receptor citoplásmicas (RLCKs por sus siglas en inglés, *receptor-like cytoplasmic kinases*) fosforilan directamente las MAPKKKs luego de la identificación de PAMPs durante la PTI (Yamada et al., 2016; Bi et al., 2018; Yan et al., 2018). Sin embargo, poco se sabe cómo la señalización por NLR activa la cascada MAPK. Estudios en líneas transgénicas de Arabidopsis donde se expresan los efectores AvrRps4 o AvrRpp4 en ausencia de señalización por PRR

demostraron que aunque estén presentes los NLRs tipo TNLs RRS1/RPS4 y RPP4 no ocurre la activación de MAPK (Ngou et al., 2020, 2021). Esto sugiere que las señales de fosforilación de MAPK asociadas a TNL dependen de la vía PTI. En cambio, la activación de la cascada de MAPKs por los NLRs tipo CNLs como RPS2, RPS5 y RPM1 parecen ser independientes de la señalización por PRR, lo que sugiere que PRRs y CNLs podrían activar la cascada MAPK por diferentes mecanismos (Ngou et al., 2021; Yuan et al., 2021a).

El hecho de que las vías PTI y ETI compartan ciertas estrategias para impedir el avance del patógeno, produjo en los últimos años la idea de que en realidad la PTI y la ETI están más relacionadas de lo que solía pensarse. Estudios recientes han mostrado que en realidad existe cierto solapamiento y retroalimentación entre ambas, difuminando su separación e individualidad, ya que se ha evidenciado que para una completa y eficaz respuesta inmune es necesario el solapamiento y la comunicación entre ambos mecanismos (Yuan et al., 2021b). En base a esto, a continuación, se mostrarán otras respuestas de defensa solapadas y con incidencia mutua entre estas vías.

1.2.1. Influencia recíproca entre PTI y ETI

Debido a que en estudios realizados hasta el momento para inferir la relación entre PTI y ETI se usaron patógenos para ingresar los efectores al interior celular de plantas (Roux et al., 2011; Ngou et al., 2021; Yuan et al., 2021b), lo observado correspondía a la resolución de una cascada de señalización causada por la interacción entre la PTI y la ETI, dado que también estarían presentes los PAMPs. Para profundizar en esto, diferentes autores también evaluaron la respuesta PTI y ETI por separado, utilizando tratamientos únicamente con PAMPs, expresión condicional en planta de efectores o ambas. Lo que se demostró es que la señalización por PRRs es importante para la respuesta asociada a la ETI (Ngou et al., 2021; Yuan et al., 2021a, 2021b). Algo que también se observó, fue que la HR, marca de la respuesta ETI, también se afecta cuando se enfrenta los mutantes de Arabidopsis *fls2*, *pepr1/2*, *fls2/efr/cerk1* y *bak1-5/bkk1-1/cerk1* con el efector AvrRpt2 reconocido por el NLR RPS2 (Yuan et al., 2021a). Sin embargo, al activar la señalización de PRRs por PAMPs o por cepas de bacterias no patogénicas, se puede propiciar la HR al expresar de forma heteróloga efectores reconocidos por sus respectivos NLRs (Ngou et al., 2021; Yuan et al., 2021a). Además, se vio que la expresión de los efectores AvrRps4 y AvrRpp4 reconocidos por los NLRs RPS4 y RPP4, respectivamente, y en ausencia de señalización por PRR, no desarrolla una HR macroscópica (Ngou et al., 2021). En adición a la HR, también se vio que las respuestas de ETI vinculadas a la producción de ROS y activación de la cascada de MAPK son también moduladas por la señalización de PRRs. Hay evidencias de que el segundo estallido de ROS durante la ETI es dependiente de la señalización por PRR ya que requiere de la activación de PRRs por PAMPs para que pueda darse (Ngou et al., 2021; Yuan et al., 2021a).También se observó que la colaboración entre las señalizaciones por PRRs y NLRs son necesarias para asegurar una producción robusta de ROS durante la ETI, ya que la señalización por PRRs asegura la correcta fosforilación de RBOHD durante la ETI, mientras que la señalización por NLRs aumenta los niveles de RBOHD (Ngou et al., 2021; Yuan et al., 2021a). Algo parecido a lo que sucede con las ROS pasa con la activación de MPAK, donde se da una activación rápida durante la señalización

por PRRs y una activación más lenta, pero de mayor duración cuando se da por activación de la señalización de NLRs (Yuan et al., 2021b). Así mismo, cuando se expresa en plantas transgénicas efectores, AvrRps4 o AvrRpp4, reconocidos por los NLRs de tipo TNL RRS1/RPS4 y RPP4, y en ausencia de señalización por PRR, no se logra activar la cascada de MAPK.

No solo la señalización de PRRs durante la PTI influye en la ETI, sino que esta relación es bidireccional. Algunos receptores NLRs, al activarse (independientemente de la PTI) provocan un cambio en la expresión de genes que lleva a la acumulación de transcriptos y proteínas de componentes de la señalización por PRR como lo son BAK1, SOBIR1, BIK1/PBLs, RBOHD y MPK3 (Ngou et al., 2021; Yuan et al., 2021a, 2021b). Otra información que ayuda al entendimiento de la acción de la ETI sobre la PTI, es la obtenida a partir de los traductomas mediante *ribosome footprinting* (Xu et al., 2017; Yoo et al., 2019). En estos estudios se resalta la poca correlación que hay entre el transcriptoma y el traductoma durante la PTI, la cual presenta una traducción fuertemente regulada, en comparación con la ETI que muestra una correlación transcripción-traducción bastante fuerte. Esto implicaría que la mayoría de los cambios a nivel traduccional durante la ETI fuesen coordinados con cambios en la transcripción, debido probablemente a que la PTI regula negativamente su respuesta inmune para controlar su amplitud y duración en el tiempo, y asegurar de esta manera la homeostasis inmune (Couto and Zipfel, 2016). Dadas estas observaciones, podría ser que la activación de la PTI durante la ETI, sea una forma de regular positivamente y compensar la propia regulación negativa de la PTI, durante una infección por patógenos, incrementando así la amplitud y el tiempo de respuesta del sistema inmune.

1.2.2. Modelo integrador del sistema inmune de plantas

El tradicional modelo de "*zig-zag*" (Jones and Dangl, 2006) donde se representaba las interacciones entre receptores PRR y R con los PAMPs y distintos efectores, respectivamente, para dar paso primero a la PTI, luego a la ETS y por último a la ETI (de una forma secuencial y cíclica, donde cada respuesta inmune se tomaba por separado e independiente de otra) fue recientemente reevaluado. Si bien falta entender mucho de lo que pasa luego de la activación de las vías PTI y ETI, los avances antes mencionados permiten clarificar algunos puntos. Por ejemplo, la relación entre ambas vías debe considerarse como respuestas que suceden casi en simultáneo, con la activación inicial vía PTI y posterior ETI, con una regulación recíproca de gran importancia para el resultado de la inmunidad en la planta. Si se analiza desde el punto de vista de la interacción entre la planta y el patógeno, dicha regulación recíproca tiene bastante sentido, ya que los patógenos mediante efectores, comprometen componentes principales de la vía PTI para lograr una ventaja en la infección. Esto sumado a la propia regulación negativa de la PTI, hace que su regulación por parte de la ETI funcione de forma compensatoria para lograr una respuesta inmune adecuada. Es así que en el modelo planteado por Yuan et al., 2021b (**Figura 4**), la ETI no es una vía inmune separada, sino un módulo de amplificación que depende de la maquinara de PTI para funcionar de forma efectiva.

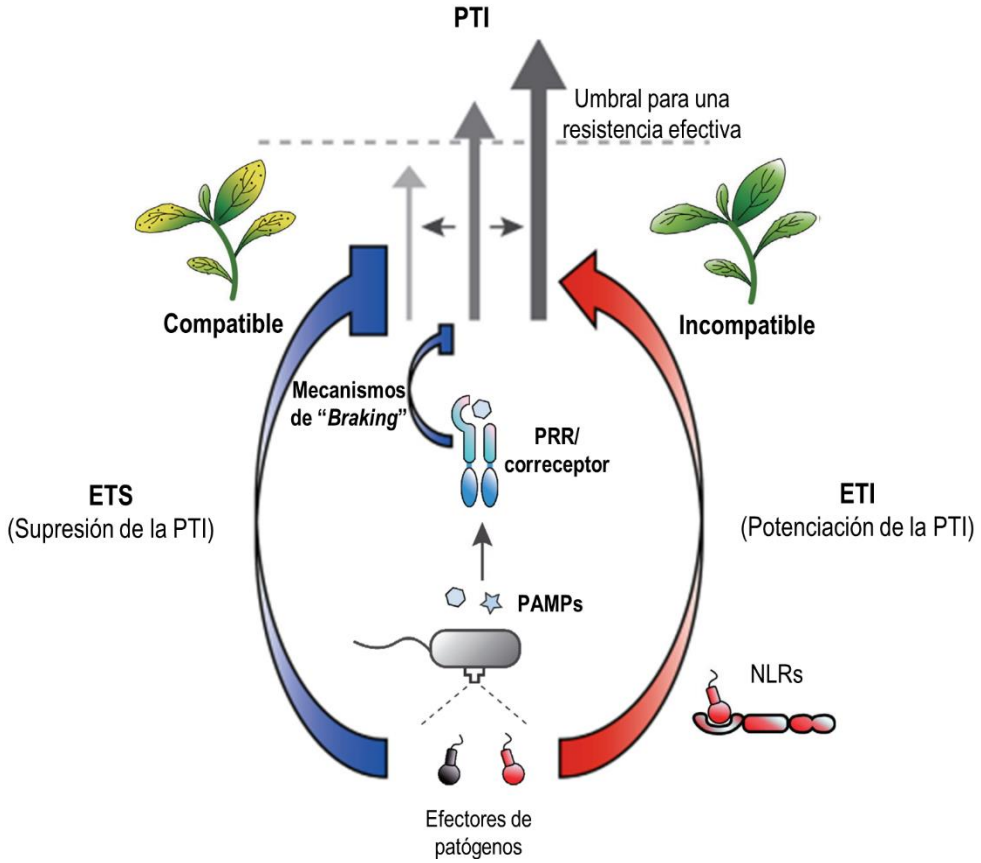

Figura 4. **Modelo actualizado del sistema inmune de plantas.** La PTI actúa como el principal mecanismo de defensa contra patógenos y comensales microbianos. Los componentes de la PTI están bajo control negativo por el mecanismo de "*braking*" endógeno de la planta para prevenir sobreactivación y, fuertemente, por efectores secretados por patógenos (flechas azules sin punta). Los NLRs activados disparan la ETI, la cual potencia y restaura la PTI a través de la sobrerregulación de los componentes de la PTI (flecha roja). Ambas vías inmunes funcionan en conjunto para proveer una resistencia robusta contra los patógenos. El resultado final de la resistencia es la combinación de i) inhibición de la PTI por la ETS (*effector triggered susceptibility*) o por los mecanismos endógenos de "*braking*" y ii) potenciación de la PTI debido a la ETI. "PTI + ETS" es usualmente asociada con interacciones compatibles (en la izquierda) y "PTI + ETI" como interacciones no compatibles (sobre la derecha). Figura obtenida y modificada de Yuan et al., 2021b.

1.2.3. Principales fitohormonas involucradas en el estrés biótico

Las hormonas son factores importantes en la señalización de la respuesta inmune, poseen roles en la activación de la expresión de genes vinculados a la defensa y la regulación fina de las vías de señalización. Las hormonas trabajan en una red muy compleja y cumplen un papel importante en el balance de la respuesta a estímulos ambientales y de desarrollo. Cuando se mencionan las hormonas relacionadas al estrés biótico, hay tres hormonas que tienen un rol crucial en las vías de señalización inducidas por PTI y ETI. Estas hormonas son el SA, el ácido jasmónico (JA) y el etileno (ET). Otras hormonas como las auxinas, el ácido abscísico (ABA), citoquininas (CKs), ácido giberélico (GA) y brasinoesterioides (BRs), principalmente relacionadas al desarrollo

y crecimiento de las plantas, también han emergido como reguladores de inmunidad en plantas (Denancé et al., 2013). Por lo tanto, para poder sobrevivir a los distintos patógenos, las plantas necesitan una correcta comunicación entre las diferentes vías de señalización hormonales (Zhao and Li, 2021). El SA, JA y el ET, son las hormonas más estudiadas en cuanto a su función y comunicación entre sus vías de señalización y dependiendo del tipo de patógeno, serán las vías que se activen. Así por ejemplo, se observó que para aquellos patógenos biótrofos y hemibiótrofos la hormona relacionada es el SA (Glazebrook, 2005; Halim et al., 2007; Spoel et al., 2007), mientras que las hormonas ET y JA, las cuales mayoritariamente trabajan juntas, aunque no siempre, se asocian a las vías de defensa de la planta contra patógenos necrótrofos y herbívoros (Glazebrook, 2005; Spoel et al., 2007). Las hormonas son reguladoras esenciales de las distintas vías como ser la SAR regulada por el SA, y la resistencia sistémica inducida por rizobacterias (ISR, *rhizobacteria-mediated induced systemic resistance*) donde el JA y el ET son indispensables (Yang et al., 2015).

El SA es un compuesto fenólico que posee dos vías biosintéticas (**Figura 5**), una es la vía del isocorismato mediada por la isocorismato sintasa (ICS/SID2, *isochorismate synthase*) y la otra la vía de la fenilalanina mediada por la enzima fenilalanina amonia liasa (PAL, *phenylalanine ammonia lyase*). El SA es necesario para una resistencia tanto local como sistémica así como también en la muerte celular programada (PCD, *programmed cell death*) que ocurre durante la HR (Wildermuth et al., 2001). Esta hormona es sensada por uno o más receptores activando así las vías de señalización y llevando a la producción de proteínas relacionados a la patogénesis (PR, *pathogenesis-related*) con actividad contra microorganismos patógenos. El SA, es un regulador central de la inmunidad, interactúa con otras vías de señalización hormonal como las del ET y JA, como estrategia para afinar la respuesta de resistencia (Corina Vlot et al., 2009; Thaler et al., 2012; Denancé et al., 2013). Recientemente Ding et al.(2018) propusieron un nuevo modelo sobre la forma en que la hormona SA es sensada por la planta a partir de los receptores NPR1 (*non-expressor of PR genes 1*), NPR3 y NPR4. El receptor NPR1 y los receptores NPR3/NPR4 actúan de forma antagónica para regular la expresión de genes de defensa de respuesta al SA. Según este modelo, en la ausencia de patógeno, los niveles de SA son bajos y la expresión de genes de defensa se ve reprimida por NPR3 y NPR4 al actuar como represores de factores de transcripción (FTs) TGA (TGACG *sequence-specific binding protein*), los cuales regulan otros reguladores transcripcionales de respuesta al SA. Sin embargo, cuando la presencia del patógeno es detectada aumenta rápidamente la producción de SA, el cual es sensado tanto por el receptor NPR1 como por los receptores NPR3 y NPR4. NPR3 y NPR4 al unirse al SA disminuyen la supresión que ejercen sobre las proteínas TGA, liberándolas para que regulen la expresión de FTs de respuesta al SA como por ejemplo lo son las proteínas WRKY70, SARD1 (SAR DEFICIENT1), CBP60g (CAM-BINDING PROTEIN 60-LIKE g) y proteínas PR. Las proteínas PR marcadores de respuesta al SA son la PR-1 (*small cysteine-rich secreted protein*), PR-2 (*β-1,3 glucanases*) y PR-5 (*thaumatin*). Paralelamente los niveles altos en SA promueven la disociación del oligómero formado por proteínas NPR1 ubicado en el citosol y posterior traslocación de NPR1 al núcleo, donde funciona como un coactivador transcripcional de genes de respuesta al SA al interaccionar con FTs del tipo TGA. En este modelo no se plantea que NPR3 y NPR4 regulen la inmunidad en la planta mediante el control de los niveles de la proteína NPR1 (Fu et al., 2012), sino que NPR3 y NPR4 funcionan independientemente de NPR1 (Ding et al., 2018).

El JA, implicado en respuestas de estrés biótico y abiótico, también tiene incidencia a partir de la cooperación con otras hormonas, en el desarrollo de la planta. Tanto el JA como sus metabolitos, incluyendo el metil jasmonato (MeJA, *methyl jasmonate*) son componentes derivados del ácido α-linolénico (α-LeA, **Figura 5**), el cual es liberado a partir de lípidos presentes en la membrana tilacoide del cloroplasto por la fosfolipasa 1 (Schaller and Stintzi, 2009; Guan et al., 2019). El α-LeA es luego oxigenado por una lipooxigenasa (LOX, *lipoxygenase*). Posteriormente la enzima 13-aleno óxido sintasa (AOS, 13-*allene oxide synthase*) y 13-aleno óxido ciclasa introducen dioxígeno y ciclan a las moléculas de ácido graso para dar lugar al ácido 12-oxofitodienoico (OPDA, 12-*oxophytodienoic acid*). El OPDA es exportado desde cloroplasto al citosol a partir de la proteína JASSY ubicada en la membrana exterior del cloroplasto (Guan et al., 2019). Una vez en el citosol el OPDA es luego importado a los peroxisomas donde será reducido por la OPDA reductasa (OPR3). Este intermediario es luego procesado por la maquinaria de β-oxidación de ácidos grasos peroxisomal, produciendo el JA. Este JA es exportado al citosol para obtener la forma bioactiva de la hormona a partir de la enzima JAR1 que conjuga la isoleucina a la hormona, dando como producto el JA-Ile ((+)-7-*iso-jasmonoyl-L-isoleucine*) (Li et al., 2017; Guan et al., 2019). La proteína JAZ (*JASMONATE-ZIM-DOMAIN*) se encuentra unida a varios FTs, funcionando como un represor cuando los niveles endógenos de JA-Ile son bajos (Chung et al., 2008). Cuando el nivel de JA-Ile aumenta, se genera la unión de la proteína JAZ con la proteína F-Box conocida como COI1 (*CORONATINE INSENSITIVE* 1), receptor de la hormona. COI1 es parte de la maquinaria de degradación de la ubiquitina proteasoma y forma un complejo con Skp1/Cullin/F-box (SCF^{COI1}) con actividad E3 ubiquitina ligasa. La formación de este complejo resulta en la ubiquitinación y degradación por el proteosoma 26S del represor JAZ. Al degradarse JAZ, se libera el factor de transcripción que estaba secuestrado permitiendo que el mismo encuentre las secuencias blanco y active los genes de respuesta al JA. Algunos de los FTs que sufren represión por JAZ son MYC2, ERF1 y ORA59 (*octadecanoid-responsive Arabidopsis*) (Lorenzo and Solano, 2005; Pré et al., 2008; Guan et al., 2019).

El ET es la molécula de gas hidrocarburo insaturado más simple (**Figura 5**), y es un regulador importante de la PTI contra patógenos biotróficos y regulador central de la red de señalización inmunitaria de las plantas (Yang et al., 2015; Zhao and Li, 2021). En la biosíntesis del ET el punto de inicio es la transformación del aminoácido metionina a S-adenosilmetionina (SAM), el cual es convertido en ácido 1-aminociclopropano-1-carboxilico (ACC) por la ACC sintasa (ACS). Por último, el ACC es utilizado por la enzima 2-oxoglutarato ACC oxidasa (ACO) para dar ET. Los niveles de las enzimas ACS y ACO son determinados por el mismo ET en un bucle de retroalimentación positiva conocido como el ciclo de Yang (Wang et al., 2002; Yang et al., 2015). Esta hormona es reconocida por el receptor de membrana ETR1 (Kendrick and Chang, 2008) el cual está asociado con CTR1 (CONSTITUTIVE TRIPLE RESPONSE 1) en el citosol y funcionan como reguladores negativos de la respuesta al ET. Cuando esta hormona no está presente se mantiene el rol regulatorio negativo de CTR1 sobre EIN2, reprimiendo así la regulación positiva de EIN2 sobre la vía de señalización del ET. Sin embargo, cuando el ET es percibido por ETR1, la represión de la señalización del ET por CTR1 es liberada, lo que permite la continuación de la señalización a través de EIN2. Posteriormente reguladores positivos críticos de la expresión de genes de respuesta al ET, como por ejemplo EIN3, se vuelven activos cuando EIN2 inhibe su degradación por el proteasoma 26S dependiente de la E3 ubiquitina ligasa $SCF^{BF1/2}$.

Gracias a esto, FTs del tipo EIN3 activan la transcripción de FTs como ser ERF1, resultando en la expresión de genes de respuesta al ET (Pieterse et al., 2009).

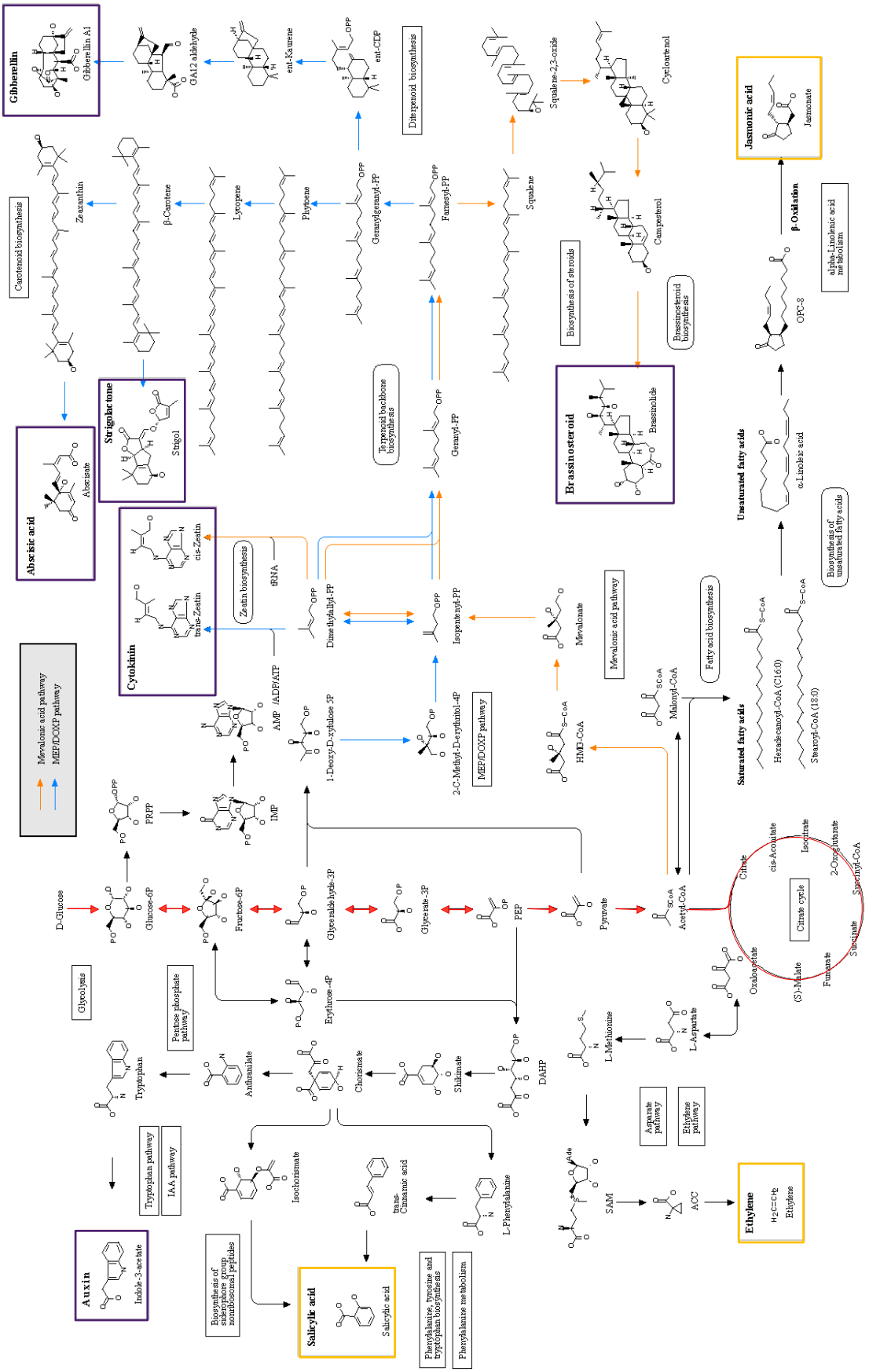

Figura 5. Esquema representativo de las distintas vías biosintéticas de hormonas vegetales. Las hormonas presentes en el esquema son el ácido salicílico, ácido jasmónico, etileno, ácido abscísico, citoquininas, ácido giberélico, stringolactona y brasinoesterioides. El producto final de cada vía biosintética para cada hormona se muestra dentro de un recuadro de color amarillo o violeta según cumplan un rol más importante o no frente a estrés biótico, respectivamente. Las vías del ácido mevalónico y del MEP/DOXP, se marcan con flechas naranja o celeste, respectivamente. La vía de la glucólisis a partir de la cual se inician las demás vías, se encuentra resaltada en rojo. Esquema modificado a partir del generado por *Kyoto Encyclopedia of Genes and Genomes* (KEGG), https://www.genome.jp/kegg/ (Kanehisa et al., 2022).

1.2.4. Factores de transcripción involucrados en la defensa vegetal

Los FTs son una parte importante de la respuesta inmune de la planta, ya que cuando se establece contacto entre la planta y el patógeno, y éste es reconocido por receptores PRRs y/o NLRs se desencadenan los mecanismos de inmunidad por PTI y ETI. Esta activación termina en la reprogramación de la expresión de genes para hacer frente a la amenaza. Los FTs de plantas se caracterizan por tener un gran número de genes que los codifican y variedad de familias en comparación con los de *Drosophila melanogaster* o *Caenorhabditis elegas*. Mientras que en estas otras especies se estima que hay aproximadamente 600 FTs, en Arabidopsis (aun teniendo un genoma similar en tamaño a ellos) es significativamente mayor, existiendo alrededor de 2000 FTs (Riechmann et al., 2000). A su vez, Arabidopsis también posee una gran variedad de FTs, con una mayor diversidad de especificidad de unión al ADN comparado con *D. melanogaster* o *C. elegans*. Esto sugiere que posiblemente la regulación transcripcional en plantas sea más compleja y diversificada que en animales. En Arabidopsis se observa que aproximadamente la mitad de los FTs son específicos de plantas y poseen DBDs (*DNA-binding domains*) que se encuentran únicamente en éstas. Como ejemplos se encuentran a las familias AP2/ERF, NAC, Dof, YABBY, WRKY, GARP, TCP, SBP, ABI3-VP1 (B3), EIL y LFY de FTs (Hong, 2015**, Figura 6**).

Arabidopsis ha sido una planta modelo esencial para el estudio de los FTs (estudios genéticos y moleculares), proveyendo de información valiosa en cuanto a una gran variedad de respuestas planta-específica como ser la defensa de la planta ante la infección por patógenos, respuesta a la luz, y distintos tipos de estrés abiótico como ser frío, sequía, alta salinidad, o desarrollo de la planta (Hong, 2015). Así como hay familias de FTs específicas de plantas, también hay familias de FTs mayoritariamente vinculadas al tipo de respuesta que se requiera, por ejemplo, a la inmunidad de la planta. Se ha visto que estas familias son críticas al momento de regular una respuesta transcripcional cuando las plantas son confrontadas por fitopatógenos (Tsuda and Somssich, 2015). Esto significa que ciertas familias de FTs se dedican particularmente, pero no exclusivamente, a regular la respuesta inmune de la planta. Algunos ejemplos son las familias de FTs conocidas como bHLH (*basic hélix-loop-helix*), MYB (*myeloblastosis related*), NAC (*no apical meristem* (NAM)), WRKY y AP2/ERF (APETALA2/*ethylene responsive factor*) (Tsuda and Somssich, 2015; Jin et al., 2017; Erpen et al., 2018; Baillo et al., 2019).

Se estima que la familia de FTs bHLH en Arabidopsis está compuesta por 162 miembros, con un dominio de unión al ADN de 50-60 aa que permite homo o heterodimerización a la secuencia blanco (Tsuda and Somssich, 2015). Pocos miembros de esta familia se han identificado como críticos para la inmunidad de plantas. Sin embargo, algunos se han visto que son reguladores principales de la coordinación de respuestas de defensa mediadas por JA (*At*MYC2/JAI 1/JIN 1, *At*MYC3 y *At*MYC4) y en la comunicación con otras vías hormonales como ser SA, ABA, GA y auxinas (Kazan and Manners, 2013; Tsuda and Somssich, 2015).

La familia MYB de FTs está compuesta por más de 160 genes según los genomas de Arabidopsis y arroz (Dubos et al., 2010). En plantas, la familia MYB posee una subfamilia de proteínas caracterizadas por el dominio R2R3 las cuales se separan en dos grupos capaces de unirse a secuencias blanco diferentes ((T/C)AAC(T/G)G o G(G/T)T(A/T)G(G/T)T) (Stracke et al., 2001; Tsuda and Somssich, 2015). Varios de estos FTs del tipo MYB tienen función conocida en la inmunidad de plantas siendo los más conocidos *At*MYB30, *At*MYB44, *At*MYB108/BOSI1 de Arabidopsis, y *Hv*MYB6 de cebada (Buscaill and Rivas, 2014; Tsuda and Somssich, 2015).

Las proteínas pertenecientes a la familia NAC de FTs comprenden a 100 y 150 miembros en Arabidopsis y arroz, respectivamente. El dominio de unión al ADN se une a la secuencia blanco CATGTG (Nakashima et al., 2012). Si bien a esta familia de FTs se le atribuye como rol principal funciones en diferentes tipos de estrés abióticos (sequía y alta salinidad) el factor *Hv*ATAF1 de la cebada y varios miembros presentes en Arabidopsis (*At*ANAC019, *At*ANAC055 y *At*ANAC072) han demostrado ser importantes para la inmunidad en plantas (Jensen et al., 2008; Nuruzzaman et al., 2013; Tsuda and Somssich, 2015).

La familia WRKY de FTs consta de más de 70 miembros en Arabidopsis y de 100 aproximadamente en arroz. Todos los integrantes de esta familia comparten el dominio WRKY de 60 aa de extensión que se une al motivo C/TTGAC/T del ADN llamado W-box. El estudio de esta familia en cuanto a su rol en la defensa de plantas ha dado como resultado la identificación de numerosos y distintos miembros de esta familia vinculados a la defensa contra patógenos en Arabidopsis, cebada y arroz (Pandey and Somssich, 2009; Tsuda and Somssich, 2015).

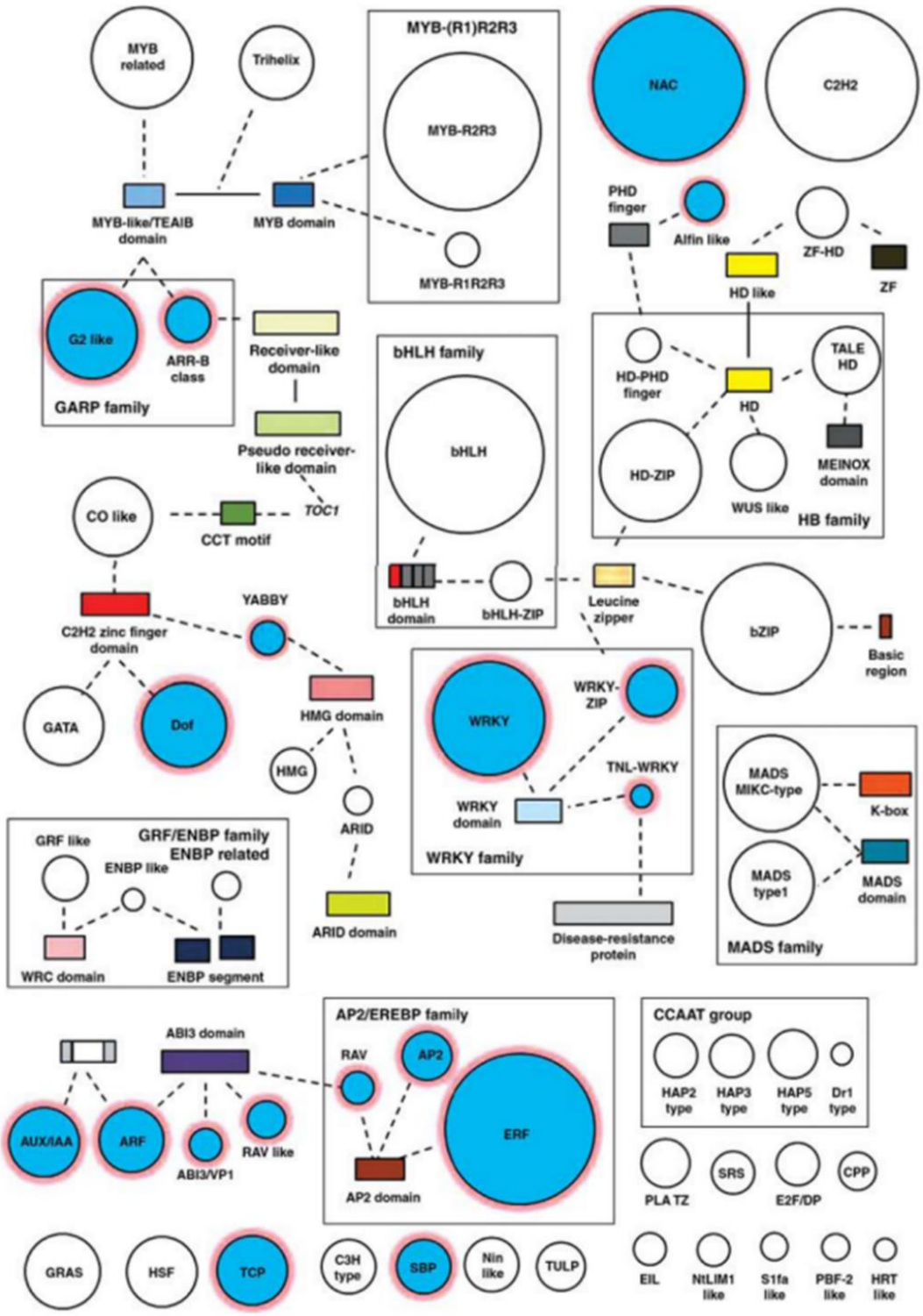

Figura 6. **Familias de FTs en Arabidopsis.** Las familias de FTs se encuentran representadas por círculos cuyo tamaño es proporcional al número de miembros en dicha familia. Dominios que presentan características estructurales similares y que conectan diferentes grupos de FTs se indican con rectángulos. Las familias de FTs específicas de plantas están representadas con círculos azules. Las líneas punteadas indican que un dominio dado es característico de la familia o subfamilia a la cual está conectado. En este esquema, no se representa la familia "*soloist*" perteneciente a la superfamilia AP2/ERF. Ilustración adaptada por Hong, 2015 a partir de Riechmann et al., 2000.

1.2.5. AP2/ERF, superfamilia de factores de transcripción

La superfamilia de FTs AP2/ERF fue inicialmente ubicada en plantas y por un tiempo se pensó era específica de estas. Con el advenimiento de nuevas tecnologías y nuevas bases de datos fue posible encontrarlas también en protistas, cianobacterias y fagos (Wessler, 2005). Se cree que aparecieron en plantas debido a una transferencia horizontal de genes de origen bacteriano o viral, que codificaban para proteínas con dominio AP2 (Licausi et al., 2010). Algo a tener en cuenta es que, si bien se ha mantenido el acrónimo ERF dentro de la superfamilia AP2/ERF, la respuesta ante el ET como regulador del crecimiento no es una característica compartida por todos los integrantes de la superfamilia. Además, su elemento conservado de unión al ADN no se ve directamente afectado por la señalización por etileno.

La clasificación de esta superfamilia se basa en las diferencias existentes entre los dominios AP2, de entre 60-70 residuos aminoacídicos aproximadamente (Okamuro et al. 1997; Riechmann and Meyerowitz 1998), cantidad de intrones, cantidad de dominios AP2 y si existen o no otros dominios presentes (Nakano et al., 2006). Por lo anterior, se ha dividido a la superfamilia AP2/ERF en cuatro familias (**Figura 7**): AP2 (APETALA2), RAV (*related to* ABI3/VP), ERF (*ethylene-responsive-element-binding*) y *Soloist* (grupo de baja homología con el resto de los dominios AP2/ERFs) (Shigyo and Ito, 2004; Nakano et al., 2006; Zhuang et al., 2008; Licausi et al., 2010). Si bien hay alguna excepción, generalmente se conoce a la familia AP2 por poseer dos dominios AP2, a los miembros de la familias ERF y RAV por tener únicamente un dominio AP2 (con excepción de RAV que generalmente posee un dominio adicional del tipo B3 de unión al ADN) (El Ouakfaoui et al., 2010; Licausi et al., 2010). Generalmente, aquellas proteínas que contienen un único domino AP2 y cuyos genes codificantes contienen una pequeña cantidad de intrones, son asignadas a la familia ERF (Nakano et al., 2006).

A la clasificación anterior en familias debe agregársele, para algunas de ellas, nuevas divisiones. Por ejemplo, la familia AP2 se caracteriza por estar compuesta por dos grupos, el primer grupo contiene a las subfamilias AP2 y ANT (AINTEGUMENTA) cuya clasificación dependerá de la secuencia aminoacídica del dominio AP2 doble y de la señal de localización nuclear cerca del primer repetido AP2. El segundo grupo está compuesto por aquellos miembros con un único dominio AP2, y se le conoce como la familia ERF. Esta familia puede subdividirse según la similitud de los dominios AP2 en dos subfamilias, la subfamilia DREB (*dehydratation-responsive-element-binding*) y la subfamilia ERF (Sakuma et al., 2002). Las subfamilias DREB y ERF pueden a su vez subclasificarse en 6 grupos cada una, grupos A1 a A6 y B1 a B6, respectivamente (Sakuma et al., 2002). Estas clasificaciones se siguieron analizando y poco tiempo después se propuso otra clasificación basándose en la estructura intrón-exón de genes de la familia ERF y la aparición de motivos adicionales (Nakano et al., 2006). Bajo esta nueva clasificación la familia ERF quedó dividida en doce grupos, pero estos coincidían substancialmente con la clasificación en subfamilias realizada por Sakuma et al. 2002. Por lo anterior, dentro de esta nueva clasificación, la familia ERF estaría compuesta de las subfamilias ERF I a X, XI-L y Xb-L (Nakano et al., 2006), donde la subfamilia ERF estaría comprendida en las subfamilias ERF V a X, XI-L y Xb-L, mientras que la subfamilia DREB estaría comprendida en las subfamilias ERF I a IV . La

principal diferencia entre las subfamilias DREB y ERF, radica en los aminoácidos presentes en el catorceavo y decimonoveno lugar de la secuencia aminoacídica del dominio AP2. Para la subfamilia ERF los aminoácidos alanina y aspartato estarían en los lugares catorce y diecinueve respectivamente, mientras que para la subfamilia DREB cambiarían a valina en el sitio 14 y ácido glutámico en el sitio 19 (Sakuma et al., 2002; Cui et al., 2021).

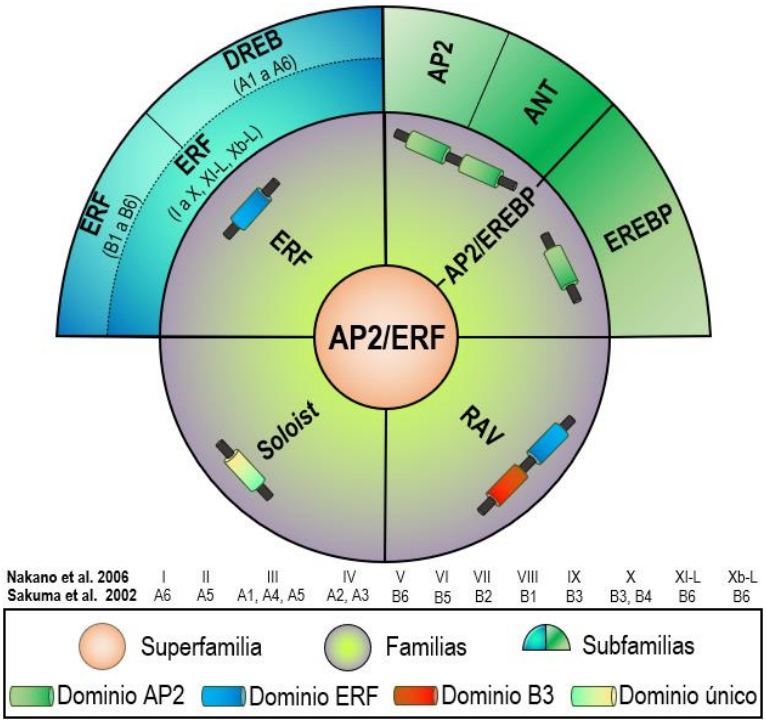

Figura 7. **Estructura y composición de los FTs pertenecientes a la superfamilia AP2/ERF.** En el esquema puede observarse la clasificación de la superfamilia AP2/ERF en las familias ERF (*ethylene-responsive-element-binding*), AP2/EREBP (APETALA2/ *Ethylene Responsive Element Binding Protein*), RAV (*related to* ABI3/VP) y Soloist. También se representan las subfamilias AP2, ANT (AINTEGUMENTA) y EREBP pertenecientes a la familia AP2/EREBP, así como también la familia ERF según Sakuna et al. 2002 (con subfamilias ERF y DREB, divididas en los grupos B1 a B6 y A1 a A6, respectivamente) y según Nakano et al. 2006 (con subfamilias ERFs que comprenden los grupos I a X, XI-L y Xb-L). Dentro de cada familia se muestra la arquitectura tipo de los miembros que la componen, distinguiendo entre tipo de dominio (AP2, ERF, B3 o dominio único), repetición y disposición génica. El dominio único está presente solamente en la familia *Soloist* y refiere a un dominio del tipo AP2/ERF, pero de una estructura fuertemente divergente de aquellas presentes en el resto de genes AP2/ERF. Se muestra la correlación entre las clasificaciones realizada por Sakuna et al. 2002 y Nakano et al. 2006.

Debido a la cantidad de genomas secuenciados y transcriptomas almacenados en bases de datos públicas, es que se ha podido indagar un poco más sobre las funciones de algunas de estas familias de FTs. Por ejemplo, los FTs pertenecientes a la familia AP2, se han asociado a la regulación de procesos de desarrollo, como por ejemplo el desarrollo del órgano floral y el crecimiento del embrión y de la semilla (Cui et al., 2021). En cambio, las subfamilias ERF y DREB se vinculan más a la resistencia ante distintos tipos de estrés, incluyendo los estreses biótico o abiótico (Feng et al., 2020). Por otro lado, se ha asociado a la familia de proteínas RAV como crucial contra las respuestas a estreses biótico y abiótico respondiendo a las señales de las

hormonas ET y brasinoesteroides de las plantas (Alonso et al., 2003; Hu et al., 2004; Sohn et al., 2006; Li et al., 2011; Fu et al., 2014).

La superfamilia AP2/ERF tiene una gran capacidad de unirse a un amplio rango de elementos regulatorios en *cis* en los promotores de genes blanco (Sasaki et al., 2007). Hay dos elementos principales a los cuales se unen estos FTs, GCC-box (elemento AGCCGCC) y DRE/CRT (*dehydration responsive element*/C-*repeat*, elemento RCCGCC) (Gu et al., 2017). La mayoría de las proteínas AP2/ERF pueden unirse a promotores que contengan el elemento GCC-box, sin embargo, el grado de activación diferirá entre miembros de distintos grupos (Pirrello et al., 2012; Gu et al., 2017). Además, aquellos FTs del tipo ERF, también pueden unirse a elementos VWRE (*vascular wounding responsive element*, GAAAAGAAAATTTC) y CE1 (*coupling element*, CACCG) en tabaco, siendo capaces de interactuar directamente con promotores que no contienen elementos GCC (Chakravarthy et al., 2003; Sasaki et al., 2007; Wu et al., 2008).

El conocimiento más detallado de los FTs del tipo AP2/ERF es importante por su potencial biotecnológico, ya que podrían emplearse con el propósito de generar plantas más resistentes a distintos tipos de estrés. Algunos ejemplos de esto, la sobreexpresión de algunos FTs del tipo ERF incrementaron la resistencia a *Stemphylium lycopersici* en tomate, *Fusarium solani* en papa, *Botryosphaeria dothidea* en manzana y *Rhizoctonia cerealis* en trigo (Chen et al., 2008; Charfeddine et al., 2019; Wang et al., 2020; Yang et al., 2020).

1.3. Modelos de estudio

Los organismos modelo se encuentran ampliamente estudiados y son elegidos dada la facilidad para investigar fenómenos biológicos. El uso de organismos modelo permite además comparar hallazgos y estudios entre diferentes laboratorios, dando robustez a los resultados obtenidos. Además, la investigación con plantas modelo proporciona conocimiento relevante para otros organismos en áreas como la biotecnología, la genética, fisiología, ecología, evolución y desarrollo. En la presente tesis se usaron como organismos modelo al musgo *Physcomitrium patens* (*P. patens*), planta no vascular anteriormente conocido como *Physcomitrella patens*, y al hongo *B. cinerea* como patógeno para estudiar los mecanismos de defensa y de infección.

1.3.1. Physcomitrium patens

P. patens pertenece al filo de las briofitas que se cree divergieron hace unos 475 millones de años a partir de un alga verde como ancestro común (Medina et al., 2019; Rensing et al., 2020). Luego, hace unos 420 millones de años aparecieron las primeras plantas vasculares (traqueofitas) a partir de las cuales surgieron cuatro *subphylums* siendo el *Pteropsida* el más conocido por representar al grupo más grande del reino vegetal. Este *subphylum* está comprendido por tres

clases, las Filicineas (helechos), las Gimnospermas (coníferas) y las Angiospermas (plantas con flor) (**Figura 8**).

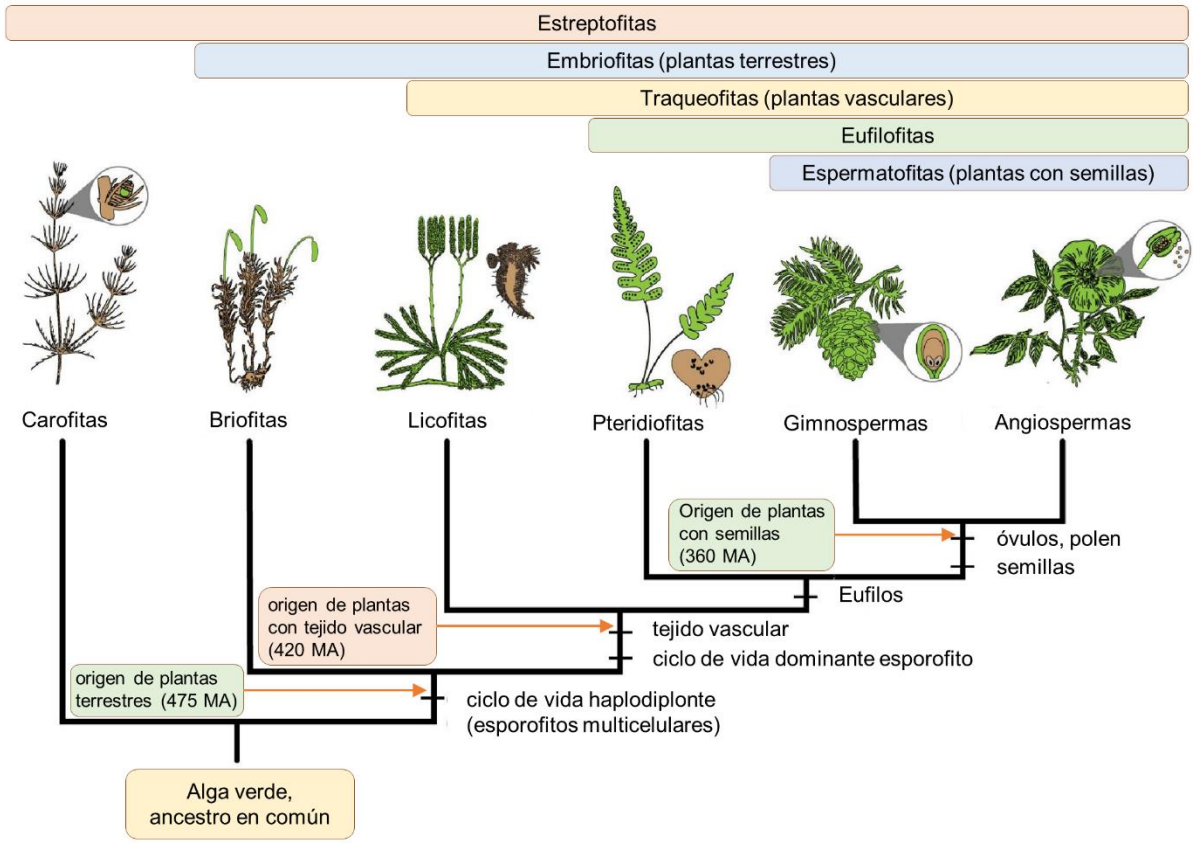

Figura 8. Filogenia simplificada de los principales clados de plantas estreptofitas. En marrón se muestra la fase gametófito (haploide) y en verde la fase esporófito (diploide o poliploide). El alga carofita posee un gametófito multicelular y una única célula llamada esporófito. Todas las embriofitas, o plantas terrestres, tienen un gametofito y esporofitos multicelulares. MA; millones de años atrás. Figura modificada de Sigel et al. 2018.

Como todas las plantas terrestres, los musgos poseen un ciclo de vida haplodiploide donde ambas generaciones, el gametofito haploide y el esporofito diploide, son multicelulares (Rensing, 2016) (**Figura 9**). Sin embargo, al contrario que las licofitas, pteridiofitas, gimnospermas y angiospermas, la fase dominante en los musgos es la del gametofito haploide. Los gametóforos presentan fototropismo positivo, lo que significa que crecen en dirección a la luz. Los esporófitos son la segunda fase de crecimiento y es donde se producen las esporas. En el caso de *P. patens*, tanto los gametófitos masculinos como femeninos son producidos por la misma planta (Cove et al., 1997).

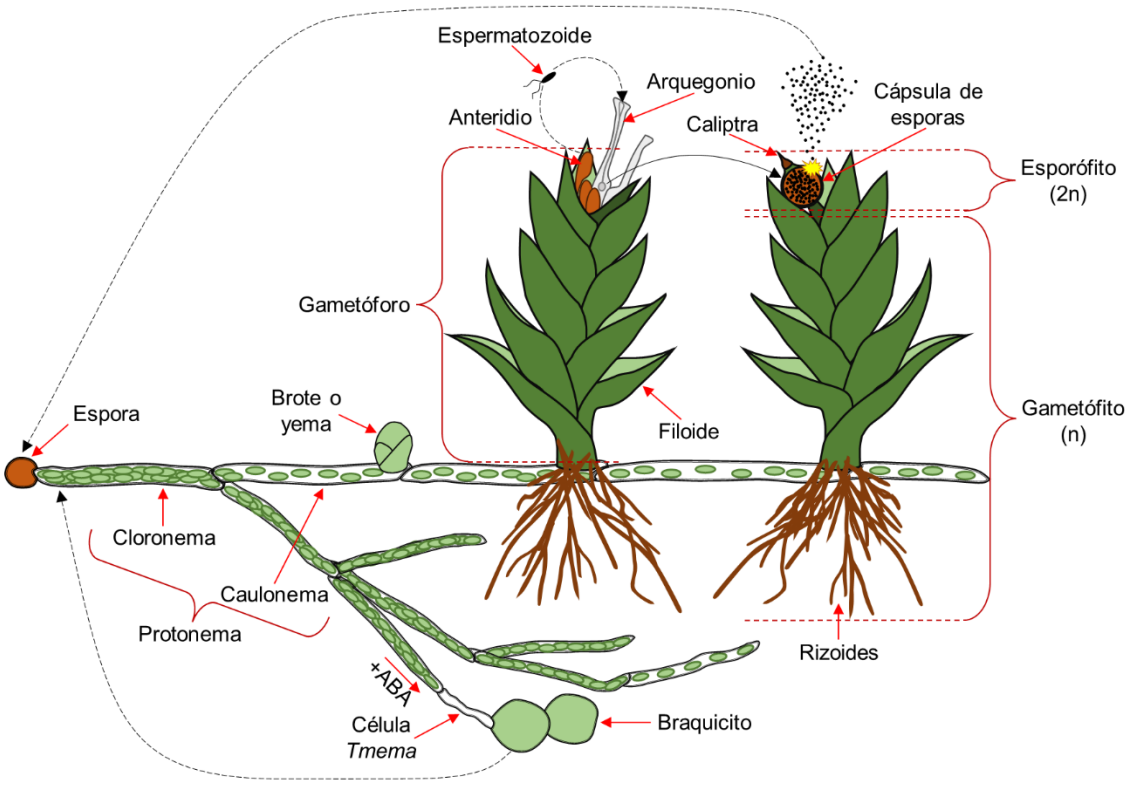

Figura 9. Ciclo de vida de *Physcomitrium patens*. La fase juvenil del gametofito comienza con la germinación de la espora, y es en este momento donde comienza a generarse el protonema. El protonema está compuesto por filamentos de células que se dividen y ramifican por crecimiento apical, y presenta dos tipos celulares, el cloronema y el caulonema. El cloronema, es el tipo celular que emerge primero al germinar la espora, es rico en cloroplastos y tiene los tabiques celulares transversales al eje longitudinal de la célula. Recientemente se observó que al aplicar la hormona ABA, se formaban diásporas vegetativas conocidas como braquicitos (Arif et al., 2019). Luego de unos días de que el cloronema sigue su crecimiento apical, ocurre la transición a células del caulonema, con tabiques ya oblicuos, con menos cantidad de cloroplastos, y un crecimiento más rápido que el cloronema. Al pasar los días se empiezan a generar ramificaciones laterales especializadas llamadas "buds" o yemas, momento en que comenzará la transición a la fase de crecimiento tridimensional. Este tipo de crecimiento conduce al desarrollo controlado por hormonas de los gametóforos, los cuales se encuentran formados por tallos con hojas no vasculares en forma de monocapa y rizoides (Reski and Abel, 1985; Harrison et al., 2009; Coudert et al., 2015). Esquema modificado y reproducido a partir de Strotbek et al., 2013 y Rensing et al., 2020.

Esta planta posee una serie de ventajas que la hacen una excelente planta modelo. Presenta un patrón relativamente sencillo de desarrollo, lo cual facilita el seguimiento de linajes celulares, y presenta mecanismos de respuesta similares ante factores de crecimiento y estímulos ambientales con respecto a plantas vasculares (Schaefer, 2002). Además, debido al pequeño porte de la planta, y su capacidad de propagación vegetativa *in vitro* a partir de una o más células (protoplastos o trozos de tejido), en un lugar reducido puedan realizarse ensayos con un gran número de plantas (Ishikawa et al., 2011; Sugimoto et al., 2011). A su vez, para el año 2008 se contaba con el genoma nuclear, mitocondrial y cloroplástico secuenciados, completando el recurso genómico de esta planta (Sugiura et al., 2003; Terasawa et al., 2007; Rensing et al., 2008). Recientemente, se actualizaron los genomas mitocondrial y cloroplástico, y se realizó un nuevo ensamblado del genoma nuclear que mostró la presencia de 27 pseudocromosomas (con 1% de gaps remanentes)

(Lang et al., 2018). En los últimos años se han generado datos de expresión de genes de *P. patens* sometida a distintos estreses abióticos (sequía, calor, alta intensidad lumínica, UV-B, frío y deficiencia en PO_4), interacciones con microorganismos mediante perfiles de expresión obtenidos por *microarrays* y RNA-Seq a partir de exudados de *Gigaspora margarita* y *Rhizophagus irregularis*, tratamientos con hormonas (OPDA, auxinas y ABA), de sus distintos tejidos para estudiar su crecimiento y desarrollo, y en los últimos años RNA-Seq de estrés biótico frente al hongo *Colletotrichum gloeosporioides (C. gloeosporioides*) (Hiss et al., 2014; Beike et al., 2015; Ortiz-Ramírez et al., 2016; Perroud et al., 2018; Fernandez-Pozo et al., 2020; Otero-Blanca et al., 2021).

1.3.1.1. Interacciones de Physcomitrium patens y microorganismos patógenos

Nuestro grupo de investigación se ha enfocado en los últimos 15 años en la identificación de patógenos que infectan *P. patens* y en los mecanismos de defensa que esta planta activa luego de la colonización de estos microorganismos. Se identificaron varios patógenos de amplio rango de hospedero que infectan importantes cultivos, los cuales colonizan los tejidos de *P. patens*, incluyendo los hongos *C. gloeosporioides* y *B. cinerea*, los oomicetes *Pythium irregulare* (*P. irregulare*) y *Pythium debaryanum* (*P. debaryanum*), y la bacteria *Pectobacterium carotovorum* subsp. *carotovorum* (*P. c. carotovorum*) (Ponce de León et al., 2007, 2012; Oliver et al., 2009; Reboledo et al., 2015; Alvarez et al., 2016). Todos estos patógenos son necrótrofos, y provocan síntomas de enfermedad como amarronamiento, necrosis y maceración del tejido de *P. patens*.

Al estudiar la activación de mecanismos de defensa durante la colonización de estos patógenos, se observó que varias de ellos son similares a los de las plantas vasculares, incluyendo la acumulación de ROS, la activación de una respuesta tipo HR, el fortalecimiento de pared celular y la activación de la expresión de genes de defensa, incluyendo genes PR (Ponce de León et al., 2007; Lawton and Saidasan, 2009; Oliver et al., 2009; Reboledo et al., 2015; Alvarez et al., 2016). En todos estos patosistemas estudiados se induce la expresión de genes involucrados en la defensa de la planta como ser las LOXs (síntesis de ácidos grasos oxigenados), PALs (central en la síntesis de fenilpropanoides y producción de SA), CHSs (primera enzima en la síntesis de flavonoides, Dixon and Paiva 1995) y la proteína PR-1 (Ponce de León et al., 2007, 2012; Oliver et al., 2009; Reboledo et al., 2015; Alvarez et al., 2016). También se observó el aumento en la expresión de genes que codifican para proteínas del tipo dirigentes (DIR), luego de la infección con *B. cinerea* y *C. gloeosporioides* y el tratamiento con el filtrado acelular de *P. c. carotovorum*. detectándose a su vez la acumulación de compuestos fenólicos en los tejidos infectados (Ponce de León et al., 2012; Reboledo et al., 2015; Alvarez et al., 2016). Las proteínas DIR median la unión de monolignoles para formar lignanos y ligninas (Davin and Lewis, 2000), las cuales participan en el reforzamiento de la pared celular durante la respuesta de defensa frente a patógenos (Coram et al., 2008; Chakravarthy et al., 2010). Sin embargo, se observó que *P. patens* no sintetiza lignina, por

lo que probablemente DIR esté involucrada en el acoplamiento de monolignoles que dará lugar a compuestos del tipo lignina (Ponce de León et al., 2012) (**Figura 10**).

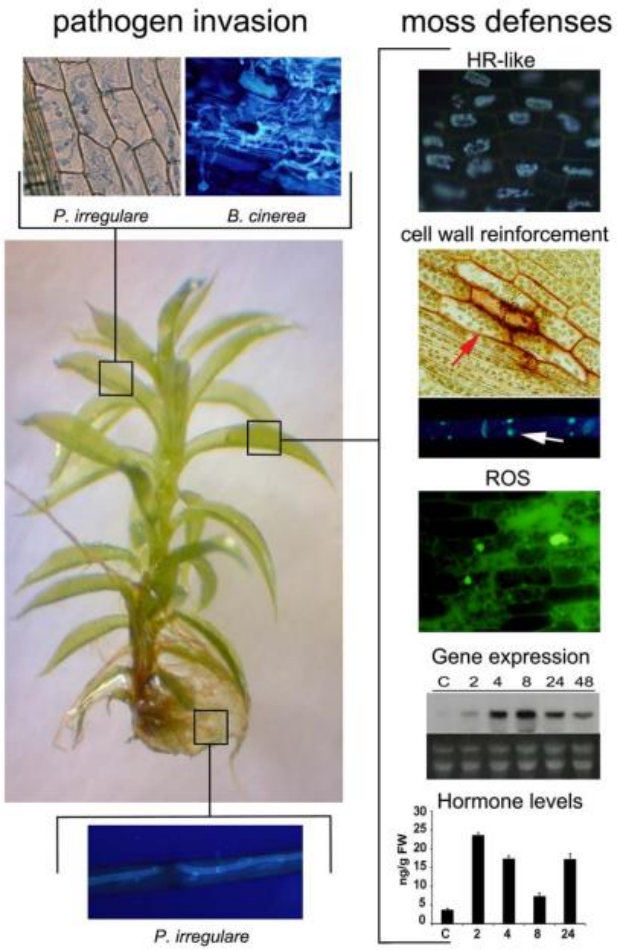

Figura 10. Invasión por patógenos y respuesta de defensa de *P. patens*. Las hojas y rizoides son colonizados por diferentes patógenos, los cuales pueden verse fácilmente mediante diferentes técnicas de tinción (hoja; *trypan blue* y *solophenyl flavine*, rizoides: *solophenyl flavine*) (Ponce de León and Montesano, 2013). Se muestran imágenes representativas de tejidos infectados con el oomicete *P. irregulare* y el hongo *B. cinerea*. Las defensas de la planta son activadas luego de la infección por patógeno, estas incluyen una respuesta del tipo HR, fortificación de pared y reorientación de cloroplastos (flechas rojas), acumulación de ROS, expresión de genes de defensa y aumento en los niveles de hormona (Ponce de León and Montesano, 2013). Imágenes representativas de la respuesta de defensa; respuesta HR, fortificación de la pared celular (acumulación de compuestos fenólicos, evidenciado por paredes celulares teñidas) y producción de ROS en hojas infectadas por *B. cinerea*, deposición de calosa en células de protonema tratadas con elicitores de *P. c. carotovorum* (flechas blancas), y patrón de expresión del gen de defensa *Ppalpha-DOX* y niveles de auxina en respuesta a elicitores de *P. c. carotovorum* a distintas horas luego del tratamiento. La respuesta HR se visualiza mediante compuestos autofluorescentes, fortificación de la pared celular por tinción con *safranin-O*, deposición de calosa por tinción con *methyl blue*, y ROS intracelular con 20,70-*dichlorodihydrofluorescein diacetate*. Figura tomada de Ponce de León and Montesano, 2017.

Varias hormonas relacionadas con la defensa frente al estrés biótico se acumulan en *P. patens* tras la infección con patógenos como *B. cinerea*, *C. gloeosporioides*, *P. irregulare* y *P. debaryanum* siendo algunas de ellas el SA, ABA y OPDA (Ponce de León et al., 2012; Reboledo et al., 2015; Otero-Blanca et al., 2021). También se mostró la inducción de *LOXs*, *AOS* y *OPR*, así como un incremento en los niveles de OPDA durante la infección por *B. cinerea* de *P. patens* (Ponce de León et al., 2012). En las briofitas la vía del JA no se encuentra conservada y en la

hepática *Marchantia polymorpha* (*M. polymorpha*), el dinor-OPDA (dn-OPDA), un homólogo del OPDA con dos carbonos menos, y su isómero dn-iso-OPDA se acumulan después de las heridas y son reconocidos por COI1 para activar la señalización por debajo de este receptor (Monte et al., 2018). Si bien en *P. patens* aún no se sabe cuál es la molécula biológicamente activa para esta vía, en el musgo *Calohypnum plumiforme* se vio que el OPDA y su isómero iso-OPDA se acumularon en mayores cantidades que el dn-OPDA y el dn-iso-OPDA después de la herida. Además, la aplicación exógena de OPDA, dn-OPDA o dn-iso-OPDA indujo la transcripción de los genes JAZ (Inagaki et al., 2021). Esto implicaría que el OPDA, el dn-OPDA, y/o sus isómeros actúan potencialmente como moléculas biológicamente activas para inducir la señalización post-COI1-JAZ. En *P. patens* se ha observado que a las dos horas de tratar la planta con OPDA, se da un pico en la expresión del gen de defensa PAL (*Pp3c2_32410*) diferente a la PAL inducida por SA (*Pp3c1_18830*), y esta diferencia en la expresión podría llevar a la producción de diferentes metabolitos con roles distintos en la defensa (Oliver et al., 2009; Ponce de León et al., 2012).

Otras respuestas inducidas por el tratamiento con patógenos de *P. patens* son el colapso citoplasmático, la acumulación de compuestos auto-fluorescentes y desintegración de cloroplastos, los cuales están asociados a la repuesta HR (Ponce de León et al., 2007, 2012).

El conocimiento generado hasta la fecha sobre las respuestas de defensa que se activan en *P. patens* luego de la infección por patógenos, demuestra que hay respuestas conservadas a lo largo del linaje de las plantas verdes y otras que son específicas de este musgo, por lo que es de interés seguir estudiando esta planta y sus interacciones con patógenos.

1.3.2. *Botrytis cinerea*

La importancia del estudio del hongo *B. cinerea* en diferentes patosistemas, incluyendo *P. patens*, es debido a su incidencia como agente patógeno en la agricultura. Es un hongo necrotrófico causante del moho gris y capaz de infectar más de 1000 especies de plantas, entre las cuales están tanto plantas modelo como de cultivo, y distintos tipos de tejidos, no solo los vegetativos (ej. flores y frutos) (Van Kan, 2006; Williamson et al., 2007; Dean et al., 2012). *B. cinerea* fue ranqueado como el segundo hongo patógeno de plantas más importante, basado en significancia científica y económica (Dean et al., 2012) y se ha convertido en uno de los patógenos necrotróficos de plantas más extensamente estudiado. Actualmente, se utiliza la aplicación de fungicida para controlar a este patógeno, y existe una preocupación creciente sobre el desarrollo de resistencia a estos funguicidas en las poblaciones de *B. cinerea* (Leroch et al., 2013; Hahn, 2014). Hay muchos estudios en cuanto al rol funcional de los genes de virulencia, desarrollo, metabolismo, señalización y resistencia a funguicida. Estos estudios se basan en modelos de genes e información de expresión accesibles gracias a la disponibilidad del genoma secuenciado (Van Kan et al., 2017). Otras características interesantes de *B. cinerea* que lo hacen un buen patógeno modelo son el fácil crecimiento en condiciones *in vitro*, la posibilidad de transformación para la obtención de cepas de interés (Ish-Shalom et al., 2011), la existencia de bases de datos dedicadas a este hongo, y que también pueden obtenerse altas concentraciones de esporas para realizar ensayos de infección.

Las principales características del proceso de infección de *B. cinerea* podrían describirse en las siguientes etapas: 1) penetración de la superficie del hospedero, 2) muerte de tejido del hospedero y formación de la lesión primaria, 3) expansión de la lesión y maceración del tejido, y 4) esporulación (Van Kan, 2006; Choquer et al., 2007). Estas etapas son mediadas por numerosas enzimas extracelulares, proteínas y metabolitos (Nakajima and Akutsu, 2014). Una vez que la espora llega a la superficie de la planta, esta germina produciendo lo que se conoce como tubo germinativo, para luego formar una estructura especializada llamada apresorio. Esta estructura facilita la entrada del hongo por medio de lo que se conoce como gancho de penetración (*penetration peg*) (Gourgues et al., 2004). Generalmente, el daño físico o la penetración mecánica de la cutícula por *B. cinerea* no suele darse, indicando que la actividad enzimática está involucrada en la penetración de las superficies intactas del hospedero (Nakajima and Akutsu, 2014). Estas enzimas se conocen como enzimas degradadoras de la pared celular (CWDE, *cell wall-degrading enzymes*), algunos ejemplos son las pectinasas, incluyendo a las poligalacturonasas (PGs) y pectato y pectina liasas, celulasas, lipasas y proteasas. Además, las CWDEs contribuyen a la conversión del tejido del hospedero en biomasa del hongo al proporcionar el sustrato para ello (Van Kan, 2006; Nakajima and Akutsu, 2014). En *B. cinerea* se encontraron dos enzimas extracelulares capaces de penetrar la superficie del hospedero, una lipasa y una cutinasa (*lip1* y *cutA*, respectivamente) (Nakajima and Akutsu, 2014). Se observó que *lip1* degrada ésteres del tipo ácido graso no saturado de cadena larga presentes por ejemplo en la cutina y ceras, mientras que *cutA* rompe las moléculas de cutina liberando monómeros y oligómeros componentes derivados de ácidos grasos del polímero de cutina insoluble (Comménil et al., 1995; Nakajima and Akutsu, 2014). Sin embargo, se vio que tanto *lip1* como *cutA* no son esenciales para una penetración exitosa de superficies intactas, lo cual se debe a que la mayoría de las CWDEs y cutinasas son codificadas por familias multigénicas (Van Kan et al., 1997; Reis et al., 2005; Choquer et al., 2007). Una vez dentro del tejido y a medida que avanza la invasión de la hifa de infección, *B. cinerea* mata las células de la epidermis y el mesófilo (Clark and Lorbeer, 1976). Una de las estrategias que usa es la secreción de varios metabolitos y proteínas que causan muerte celular cuando se aplican a tejidos de la planta, y algunos inducen síntomas de PCD. La inducción de la PCD facilita la invasión por parte de *B. cinerea* y podría de hecho, ser esencial para una infección exitosa (Govrin and Levine, 2000). A su vez, las toxinas (ej. ácido botridial y botcínico como principales toxinas) y el ácido oxálico (el cual acidifica el tejido de la planta), contribuyen en el proceso de muerte celular en los tejidos del hospedero (Colmenares et al., 2002; Manteau et al., 2003; Van Kan et al., 2017). Otro factor que contribuye a la PCD son las ROS generadas tanto por el patógeno como por el hospedero (Govrin and Levine, 2000; Van Kan, 2006; Choquer et al., 2007).

Las plantas reconocen a *B. cinerea* y activan rápidamente sus mecanismos de defensa para frenar el avance del patógeno. Estos mecanismos suelen comprender la producción de compuestos antimicrobianos y proteínas PRs, y la acumulación de fitohormonas importantes en la defensa ante estrés biótico como ser SA, JA, ET y BR entre otras (AbuQamar et al., 2017). Otra respuesta temprana para intentar detener al patógeno es la generación del estallido oxidativo (*oxidative burst*), el cual puede gatillar la muerte celular por HR. Dicha respuesta se considera la de mayor importancia en la resistencia a enfermedades en plantas. Sin embargo, al ser *B. cinerea* un patógeno necrotrófico, se alimenta de tejido muerto, no sería frenado por esta estrategia (Hutcheson, 1998; Greenberg and Yao, 2004).

2. Hipótesis

La planta *Physcomitrium patens* activa mecanismos de defensa frente a *Botrytis cinerea*, algunos de los cuales son compartidos por plantas angiospermas, mientras que otros son específicos de musgos e incluso de *P. patens*.

B. cinerea activa la expresión de genes involucrados en la patogenicidad y mecanismos de colonización de los tejidos vegetales algunos de los cuales también se expresan frente a angiospermas, mientras que otros genes se inducen solamente frente a *P. patens*.

El factor de transcripción PpERF24 está involucrado en la activación de la defensa frente a patógenos en *P. patens*.

3. Objetivos generales y específicos

Como objetivo general se propone conocer los distintos mecanismos de defensa, conservados y novedosos, de la planta *P. patens* en respuesta al hongo nectrótrofo *B. cinerea*, por medio de un abordaje transcriptómico y funcional. También se espera generar conocimiento original sobre el proceso de infección y diferentes estrategias de virulencia de este hongo al infectar plantas no vasculares o vasculares.

Los objetivos específicos comprenden:

1) Obtener información sobre los distintos mecanismos de defensa de la planta *Physcomitrium patens* durante la infección con el hongo necrótrofo *Botrytis cinerea* mediante un acercamiento transcriptómico.

2) Ahondar en los mecanismos de infección y virulencia del hongo patógeno *Botrytis cinerea* a partir de análisis de RNA-Seq comparativos entre procesos de infección a *Physcomitrium patens* y angiospermas.

3) Realizar una caracterización funcional del factor de transcripción con dominio AP2/ERF (PpERF24) de *Physcomitrium patens* a partir de líneas sobreexpresantes y el análisis de sus transcriptomas.

4. Resultados y discusión

4.1. Capítulo I_- Perfiles transcripcionales revelan respuestas de defensa vegetal conservadas y especie específicas durante la interacción de *Physcomitrium patens* con *Botrytis cinerea*

En el presente capítulo nos planteamos la hipótesis que la planta *Physcomitrium patens* (*P. patens*) activa mecanismos de defensa frente a *Botrytis cinerea* (*B. cinerea*), algunos de los cuales son compartidos por plantas angiospermas, mientras que otros son específicos de musgos e incluso de *P. patens*. Para abordar esta hipótesis nos propusimos como objetivo específico obtener información sobre los distintos mecanismos de defensa de la planta *Physcomitrium patens* durante la infección con el hongo necrótrofo *Botrytis cinerea* mediante un acercamiento transcriptómico. Para lograr esto, se realizaron infecciones de la planta *P. patens* evaluándose el proceso de infección a distintos tiempos. Los tiempos seleccionados fueron elegidos luego de evaluar los síntomas de la planta y la colonización de los tejidos de la misma por parte del hongo mediante microscopía. Los tres tiempos seleccionados fueron 4, 8 y 24 horas post inoculación (identificados como etapas de respuesta temprana, media y tardía, respectivamente). Posteriormente, se extrajo el ARN y se obtuvieron los transcriptomas de dichas muestras mediante RNA-Seq. Luego de filtrar los genomas de los organelos de la planta y quedarnos con el genoma nuclear, se analizó la expresión de genes diferencialmente expresados (GDEs) en cada etapa y se realizó una validación de un conjunto de genes mediante RT-qPCR. Con la lista de GDEs se realizó un análisis de ontología de genes (GO, gene ontology) para observar la respuesta biológica de *P. patens* a la inoculación por *B. cinerea*.

A partir de esta aproximación transcriptómica analizamos los mecanismos moleculares relacionados con la respuesta de defensa de *P. patens* frente a *B. cinerea*. Como resultado observamos un total de 3.702 genes diferencialmente expresados en la planta durante el proceso de infección. Se encontraron genes que codifican para proteínas de función conocida vinculadas a la defensa en angiospermas e involucradas en la percepción de patógenos, señalización, transcripción y señalización hormonal. También se encontraron gran cantidad de GDEs involucrados en vías metabólicas de gran importancia para la respuesta de defensa de la planta, como ser las vías de shikimato y fenilpropanoides. Además, se observó que al igual que ocurre en plantas angiospermas, un alto número de genes involucrados en la fotosíntesis, la progresión del ciclo celular y la división celular estaban reprimidos durante el proceso de infección (Bilgin et al., 2010; Windram et al., 2012). Estos hallazgos, junto con resultados recientes de otros grupos de investigación que muestran que la quitina y el tratamiento con extractos crudos de *Pseudomonas* patogénicas y *Plectosphaerella cucumerina* inhiben el crecimiento de *P. patens* y *M. polymorpha*, respectivamente, indican que como en angiospermas, la detección de PAMPs también provoca la inhibición del crecimiento en briofitas (Ranf et al., 2011; Gimenez-Ibanez et al., 2019; Galotto et

al., 2020). Observamos que cuando *B. cinerea* es reconocido por *P. patens*, se activa la expresión de múltiples genes de defensa asociados al reconocimiento de patógenos por proteínas PRRs y NLRs al igual que ocurre en angiospermas, lo que sugiere una conservación del rol de estas proteínas en la defensa a través del linaje de las plantas verdes. El gran número de GDEs sobreexpresados que codifican para RLKs resalta la importancia de expresar varios receptores que podrían detectar diferentes componentes moleculares del patógeno y así montar una respuesta efectiva de defensa del musgo. Por ejemplo, *P. patens* tiene el receptor CERK1 el cual percibe la quitina de hongos y peptidil glicanos bacterianos, lo que lleva a la inmunidad en la planta. En angiospermas, este receptor actúa en conjunto con LYK5 que funciona como un receptor de quitina (Cao et al., 2014). *P. patens*, presenta tres miembros de la familia LYK5 que cuando se silencian se obtienen plantas insensibles a quitina (Orr et al., 2020). Nuestros datos mostraron un aumento significativo en la expresión de uno de estos LYK5 en *P. patens* durante la infección por *B. cinerea*, reforzando así su importancia en la inmunidad del musgo. Observamos que aunque *P. patens* presenta un gran número de genes NLR, la infección con *B. cinerea* solo provocó la expresión diferencial de tres de estos genes. Esto es algo inesperado ya que varios de estos genes se expresan diferencialmente en otras interacciones entre plantas y *B. cinerea* (Windram et al., 2012; Haile et al., 2019). Aun así, *P. patens* es capaz de activar una respuesta del tipo HR durante la infección por *B. cinerea* (Ponce de León et al., 2012), lo cual se ve respaldado por nuestro análisis al haberse encontrado inducción de varios genes involucrados en la PCD. Además, nuestros datos mostraron un incremento en la expresión de genes relacionados al estrés oxidativo que codifican para peroxidasas, tiorredoxinas, ferredoxinas y GSTs (*glutathione S-transferase*s), al igual que algunos genes TSPO (*translocator protein*s, formalmente conocidos como *peripheral-type benzodiazepine receptors*) involucrados en el transporte de tetrapirrol y control de los niveles de ROS en *P. patens* (Lehtonen et al., 2012). Esto sugiere que el mantenimiento de un balance redox a partir de la generación y eliminación de ROS en los tejidos del musgo es importante. Durante el proceso de infección por *B. cinerea* se encontraron GDEs de *P. patens* involucrados en vías de transducción de señales del sistema inmune, como por ejemplo genes codificantes para MAPKKs y MAPKs, los cuales son esenciales para activar la respuesta de defensa luego de la percepción de la quitina de hongos (Bressendorff et al., 2016).

Una vez que se da el reconocimiento del patógeno por parte de la planta se activa la respuesta de defensa para contener al patógeno mediante la reprogramación de la expresión de genes a cargo de distintas familias de FTs. Se postula que la adaptación al medio terrestre puede estar vinculada al aumento en la cantidad de miembros pertenecientes a las distintas familias de FTs más que en la aparición de familias nuevas. Ejemplo de ellos son las familias MYB, WRKY y AP2/ERF, las cuales se encuentran expandidas significativamente en plantas terrestres en comparación a las algas (Rensing et al., 2008; Rinerson et al., 2015; Pu et al., 2020). En cuanto a la acumulación de hormonas, al igual que ocurre en angiospermas (AbuQamar et al., 2017), observamos que probablemente los jasmonatos, ET y SA tengan un rol en la respuesta de defensa de *P. patens* ante *B. cinerea*. En el caso de los jasmonatos, observamos la sobreexpresión de varios genes vinculados a su síntesis y señalización, como las LOXs, AOCs, OPRs, TIFY (*JAZ;JASMONATE ZIM DOMAIN*) y OPCL1 (*OPC-8:0 CoA ligase 1*), así como proteínas reguladoras como JAZs y FTs bHLH, luego de la inoculación con *B. cinerea*. El ET se ve involucrado en la respuesta adaptativa de *P. patens* a sequía y sumersión a través de la acción del

receptor de ET (ETR) (Yasumura et al., 2012), el cual junto con algunos genes codificantes para AP2/ERF aumentan su expresión durante la infección por *B. cinerea*, indicando que al igual que en angiospermas, el ET se encuentra probablemente involucrado en la respuesta de defensa contra el estrés biótico. El SA se acumula en los tejidos de *P. patens* luego de la infección con *B. cinerea* (Ponce de León et al., 2012), lo que lleva a la inducción de la expresión de PALs. Esto se pudo observar en los datos obtenidos, donde la gran mayoría de los genes *PAL* (17 genes en total) se encontraban inducidos. Además de estas hormonas, también se encontraron GDEs relacionados a la señalización por auxinas, CK, ABA y BR, indicando la presencia de una red hormonal compleja que regula la defensa de *P. patens* contra *B. cinerea*.

Las vías de shikimato y fenilpropanoides fueron cruciales en la adaptación y el pasaje de plantas al medio terrestre logrando así hacer frente a los nuevos tipos de estreses bióticos y abióticos (Emiliani et al., 2009). Esto se ve respaldado por los resultados obtenidos en nuestros análisis, donde observamos la importancia de estas vías en la defensa contra el hongo al encontrar un alto número de genes biosintéticos y regulatorios con alta expresión durante el proceso de infección. El hecho de haberse encontrado actividades diferentes de CHSs en *P. patens* (Li et al., 2018) y de que la mayoría de las *PALs* y *CHSs* se encontraran inducidas durante la infección por *B. cinerea*, sugiere que la plasticidad del metabolismo secundario podría haber permitido a los musgos adaptarse más fácilmente a los patógenos. Por otro lado, se observó la expresión diferencial de genes adquiridos por transferencia horizontal a partir de procariotas y hongos. También encontramos un gran número de GDEs específicos de *P. patens*, conocidos como genes huérfanos (599 genes, 19% del total de GDEs), de los cuales 376 eran genes creados "*de novo*" sugiriendo que podrían representar estrategias adaptativas innovadoras al estrés biótico. En conjunto, estos resultados revelan que el sistema inmune de *P. patens* presenta mecanismos de defensa conservados entre briofitas y angiospermas, así como también defensas específicas del musgo.

Plant Molecular Biology
https://doi.org/10.1007/s11103-021-01116-0

Transcriptional profiling reveals conserved and species-specific plant defense responses during the interaction of *Physcomitrium patens* with *Botrytis cinerea*

Guillermo Reboledo[1] · Astri d Agorio[1] · Lucía Vignale[1] · Ramón Alberto Batista-García[2] · Inés Ponce De León[1]

Received: 3 August 2020 / Accepted: 3 January 2021

Abstract

Key message **Evolutionary conserved defense mechanisms present in extant bryophytes and angiosperms, as well as moss-specific defenses are part of the immune response of *Physcomitrium patens*.**

Abstract Bryophytes and tracheophytes are descendants of early land plants that evolved adaptation mechanisms to cope with different kinds of terrestrial stresses, including drought, variations in temperature and UV radiation, as well as defense mechanisms against microorganisms present in the air and soil. Although great advances have been made on pathogen perception and subsequent defense activation in angiosperms, limited information is available in bryophytes. In this study, a transcriptomic approach uncovered the molecular mechanisms underlying the defense response of the bryophyte *Physcomitrium patens* (previously *Physcomitrella patens*) against the important plant pathogen *Botrytis cinerea*. A total of 3.072 differentially expressed genes were significantly affected during *B. cinerea* infection, including genes encoding proteins with known functions in angiosperm immunity and involved in pathogen perception, signaling, transcription, hormonal signaling, metabolic pathways such as shikimate and phenylpropanoid, and proteins with diverse role in defense against biotic stress. Similarly as in other plants, *B. cinerea* infection leads to downregulation of genes involved in photosynthesis and cell cycle progression. These results highlight the existence of evolutionary conserved defense responses to pathogens throughout the green plant lineage, suggesting that they were probably present in the common ancestors of land plants. Moreover, several genes acquired by horizontal transfer from prokaryotes and fungi, and a high number of *P. patens*-specific orphan genes were differentially expressed during *B. cinerea* infection, suggesting that they are important players in the moss immune response.

Keywords *Physcomitrium patens* · *Botrytis cinerea* · Transcriptome · Defense genes · Orphan genes

Introduction

Land plants (embryohytes) evolved from a streptophyte algal progenitor that probably lived in freshwater environments (de Vries and Archibald 2018). The now extinct early land plants adapted to the new terrestrial environment and associated stresses, including drought, variations in temperature and UV radiation (Fürst-Jansen et al. 2020). From these ancestors the two main groups of living plants evolved, bryophytes (non-vascular plants; mosses, liverworts and hornworts) and tracheophytes (vascular plants; lycophytes, ferns, gymnosperms and angiosperms) (Delaux et al. 2019; Fürst-Jansen et al. 2020). Plant fossil evidence suggests that fungal beneficial associations probably facilitated land colonization by plants improving the capture of nutrients (Delaux et al. 2015; Redecker et al. 2000; Strullu-Derrien et al.

Supplementary Information The online version contains supplementary material available at https://doi.org/10.1007/s11103-021-01116-0.

✉ Inés Ponce De León
iponce@iibce.edu.uy

[1] Departamento de Biología Molecular, Instituto de Investigaciones Biológicas Clemente Estable, Montevideo, Uruguay

[2] Centro de Investigación en Dinámica Celular, Universidad Autónoma del Estado de Morelos, Cuernavaca, México

Published online: 01 February 2021

2014). Moreover, the presence of thickened cell walls in plant fossils, as well as features resembling oomycetes-like microorganisms, suggest the existence of pathogenic fungi interacting with plants 400 million years ago (Mya) (Taylor et al. 2006; Krings et al. 2007; Strullu-Derrien 2018). Comparative analyses of bryophytes and angiosperms (flowering plants) such as *Arabidopsis thaliana* have been very useful to determine the evolution of the biological role played by certain genes during abiotic stress and development, and their possible conservation in the most recent common ancestor of land plants (Delaux et al. 2019; Fürst-Jansen et al. 2020). However, in contrast to the vast information available in angiosperm-pathogen interactions, relatively little is known about the recognition of pathogens and subsequent activation of defense responses in bryophytes.

Plants are in permanent contact with microbial pathogens, including fungi, bacteria, viruses and oomycetes. In order to detect the presence of the pathogen, angiosperms have evolved complex perception and signaling pathways that rely on two interconnected layers of the innate immune system (de Vries et al. 2018a; Han 2019; Wang et al. 2019). One layer uses plasma membrane localized pattern recognition receptors (PRRs), including receptor-like kinases (RLKs), to recognize pathogen-associated molecular patterns (PAMPs) that are essential for microbial survival, for example flagellin or chitin, and host-derived damage-associated molecular patterns (DAMPs) (Boller and Felix 2009; Jones and Dangl 2006). The other layer uses intracellular receptors encoded by disease resistance (R) genes to detect directly or indirectly pathogen-secreted effectors that help to establish successful infections and interfere and suppress plant immunity (Boller and Felix 2009). PRRs can also recognize apoplastic effectors, and during PAMP-triggered immunity (PTI) and effector-triggered immunity (ETI) signaling networks and downstream responses are activated, including mitogen-activated protein kinases (MPKs) cascades, increase in hormone synthesis and reactive oxygen species (ROS) production, and transcriptional regulation of genes with different roles in plant defense (Wang et al. 2019). In addition, the hypersensitive response (HR), a type of programmed cell death (PCD) that restricts the pathogen to the site of infection, is generally activated after intracellular effector recognition, although some PAMPs and apoplastic effectors can also trigger PCD (Wang et al. 2019). A more recent classification of the plant immune system proposes three layers; a recognition layer that involves both PRRs and R proteins, a signal-integration layer that involves signals from the recognition layer, as well as signals from neighboring cells and distant tissues, and a defense action layer that involves diverse defense mechanisms (Wang et al. 2019).

In bryophytes, most of the knowledge related to defense activation has been generated during the interaction of microbial pathogens with the moss *Physcomitrella patens* (Ponce de León and Montesano 2017), which has been recently renamed as *Physcomitrium patens* (*P. patens*) (Rensing et al. 2020). Pathogenic bacteria, fungi and oomycetes infect *P. patens* tissues leading to maceration, necrosis and cell death (Ponce de León 2011). *P. patens* senses the presence of fungal pathogens by perceiving chitin through the receptor CERK1 and consequently activates a MPKs signaling cascade, which is necessary for plant immunity (Bressendorff et al. 2016). Genes of the LYK5 chitin receptor family, which encode lysin-motif-containing protein (LysM), are also functional in *P. patens*, supporting a conserved mechanism for chitin sensing in *P. patens* and angiosperms (Orr et al. 2020). Interestingly, RLKs have been found in algae that diverged 550–750 Mya from land plants (Nishiyama et al. 2018), suggesting that perception of microbes is an ancestral trait that has been retained in the plant lineage. Moreover, the algae *Chara braunii* have several LysM-RLKs that expanded independently of land plant LysM-RLKs, suggesting adaptation mechanisms to an extended range of interacting microorganisms (Nishiyama et al. 2018).

Hormonal levels increase in *P. patens* tissues after pathogen colonization, including salicylic acid (SA), abscisic acid (ABA) and auxin (Ponce de León et al. 2012; Mittag et al. 2015). However, jasmonic acid (JA) is not synthesized in *P. patens* and the liverwort *Marchantia polymorpha* (*M. polymorpha*) (Stumpe et al. 2010; Ponce de León et al. 2012; Yamamoto et al. 2015; Monte et al. 2018), and instead the precursor, cis-oxophytodienoic acid (OPDA), accumulates after pathogen infection in moss tissues (Oliver et al. 2009; Ponce de León et al. 2012). Similarly, JA was not detected in other mosses, algae and lichens (Gachet et al. 2017), and the fern *Azolla filiculoides* seems not to rely on JA signaling (de Vries et al. 2018b). Expression levels of several genes encoding proteins with different roles in defense are induced in *P. patens*-infected tissues, including pathogenesis-related proteins (PRs) with putative antimicrobial activities such as PR-1 and PR-10 (Ponce de León et al. 2007; Castro et al 2016). After pathogen colonization, *P. patens* activates cell wall reinforcement by incorporation of phenolic compounds, callose deposition and induction of genes encoding Dirigent (DIR) proteins involved in the synthesis of lignin-like compounds (Ponce de León et al. 2012; Reboledo et al. 2015; Alvarez et al. 2016). Recent studies in *M. polymorpha* have shown that infection with the oomycete *Phytophthora palmivora* (*P. palmivora*) induces a defense response leading to increased expression of transcription factors (TFs), PRs and genes related to the phenylpropanoid pathway, indicating the several plant defense mechanisms are conserved between liverwort and angiosperms (Carella et al. 2019).

Botrytis cinerea (*B. cinerea*) is a necrotrophic fungus that infects over 200 different plant species including *P. patens*, and causes maceration and necrosis of the plant

tissues (Ponce de León et al. 2007). Several virulence factors, including toxins and cell wall degrading enzymes such as endopolygalacturonases and xylanases are important to cause disease (van Kan 2006). In response to *B. cinerea*, *P. patens* induces ROS production, activates an HR-like response, reinforces the cell wall, increases SA and OPDA synthesis and induces the expression of several genes with known defense functions (Ponce de León et al. 2007, 2012). To get more insights into *P. patens*-pathogen interactions, and since large scale transcriptional studies during pathogen infection are not available for mosses, we performed RNAseq profiling of *P. patens* during *B. cinerea* infection. Our results demonstrate the existence of an evolutionary conserved immune system among the plant lineage, where genes involved in perception, signaling, transcription, secondary metabolism and genes with diverse roles in defense against biotic stress, participate in the response of this plant to *B. cinerea* infection. Moreover, species-specific orphan genes participate in defenses against this pathogen, suggesting that they are important players in the moss immune response.

Material and methods

Plant material and pathogen inoculation

Physcomitrium patens Gransden wild type colonies were cultivated on solid BCDAT medium (Ashton and Cove 1977) under standard long-day conditions (22 °C, 16-h light/8-h dark regime under 60–80 µmol m^2 s^{-1} white light) for 3 weeks before spray inoculation with a *B. cinerea* 2×10^5 spores/mL suspension or water (mock). Three time points corresponding to spore germination (4 h post inoculation; hpi), germ tubes elongation (8 hpi), and moss cells colonization (24 hpi) were analyzed. Three independent biological replicates of tissue were harvested at each time point and treatment for RNA extraction, immediately frozen in liquid nitrogen, and stored at − 80 °C.

Botrytis cinerea staining

Botrytis cinerea tissues were stained with 0.1% solophenyl flavine 7GFE 500 according to Ponce de Leon et al. (2012). Tissues were visualized with an Olympus IX-81 inverted epifluorescence microscope (Shinjuku-ku, Japan) and DPController Software. The solophenyl flavine signal was imaged with a DAPI filter (U-MWU2 Ex: 330-385 nm Em: 420 nm), using 1/60 s exposure time with the IPLANFL N 20 × NA 0.5 and LUCPLANFL 40 × NA 0.6 objectives. Pictures were taken with a CCD camera DP71 at 4, 8 and 24 hpi.

RNA extraction, cDNA library preparation and sequencing

Frozen samples were pulverized with a mortar and pestle and 100 mg were used to extract total RNA using the RNeasy Plant Mini Kit (Qiagen, Germany), including a RNase-Free DNase treatment in column (Qiagen, Germany), according to manufacturer's protocol. RNA quality control, library preparation, and sequencing were performed at Macrogen Inc. (Seoul, Korea). RNA integrity was checked before library preparation using an Agilent Technologies 2100 Bioanalyzer (Agilent Technologies). Libraries for each biological replicate were prepared for paired-end sequencing by TruSeq Stranded Total RNA LT Sample Prep Kit (Plant) with 1 µg input RNA, following the TruSeq Stranded Total RNA Sample Prep Guide, Part # 15031048 Rev. E. Sequencing was performed on Illumina platform (Illumina, California, USA) by Macrogen Inc. (Seoul, Korea) to generate paired-end 101 bp reads, obtaining 41 to 64 M reads per sample with Q20 > 98.31%.

RNA-seq processing

RNA-seq processing steps were done through Galaxy platform (https://usegalaxy.org/). Raw reads quality was revised by FastQC software ver. 0.11.2 (http://www.bioinformatics.babraham.ac.uk/projects/fastqc/) and then preprocessed for both quality and adapter trimmings using Trimmomatic Version 0.38.0 software (Bolger et al. 2014). Additionally to default options, the following parameters were set: adapter sequence TruSeq3 (paired-ended, for MiSeq and HiSeq), always keep both reads of PE True, SLIDINGWINDOW: 4:15 HEADCROP:12 MINLEN:50. Trimmed reads were mapped to reference genomes of *P. patens* using Hisat2 software (Kim et al. 2015). All reads were mapped first against *P. patens* organelle genomes and rRNA sequences (mitochondrial NC_007945.1; chloroplast NC_005087.1; ribosomal HM751653.1, X80986.1 and X98013.1). The remaining reads were mapped against *P. patens* nuclear genome v3 (Lang et al. 2018), using Ppatens_318_v3.fa as the reference genome file and Ppatens_318_v3.3.gene_exons.gff3 as a reference file for gene models (https://phytozome.jgi.doe.gov/pz/portal.html), and concordant mapped read pairs were retained. The BAM files with read mapped in proper pair were obtained with Samtools View software ver. 1.9 and then sorted by name with Samtools Sort software ver. 2.0.3 (Li et al. 2009), for further analysis.

Differential expression analysis

The reads were counted by the FeatureCounts software ver. 1.6.4 (Liao et al. 2013). Additionally, for default options, the following parameters were set: Stranded (Reverse), Count

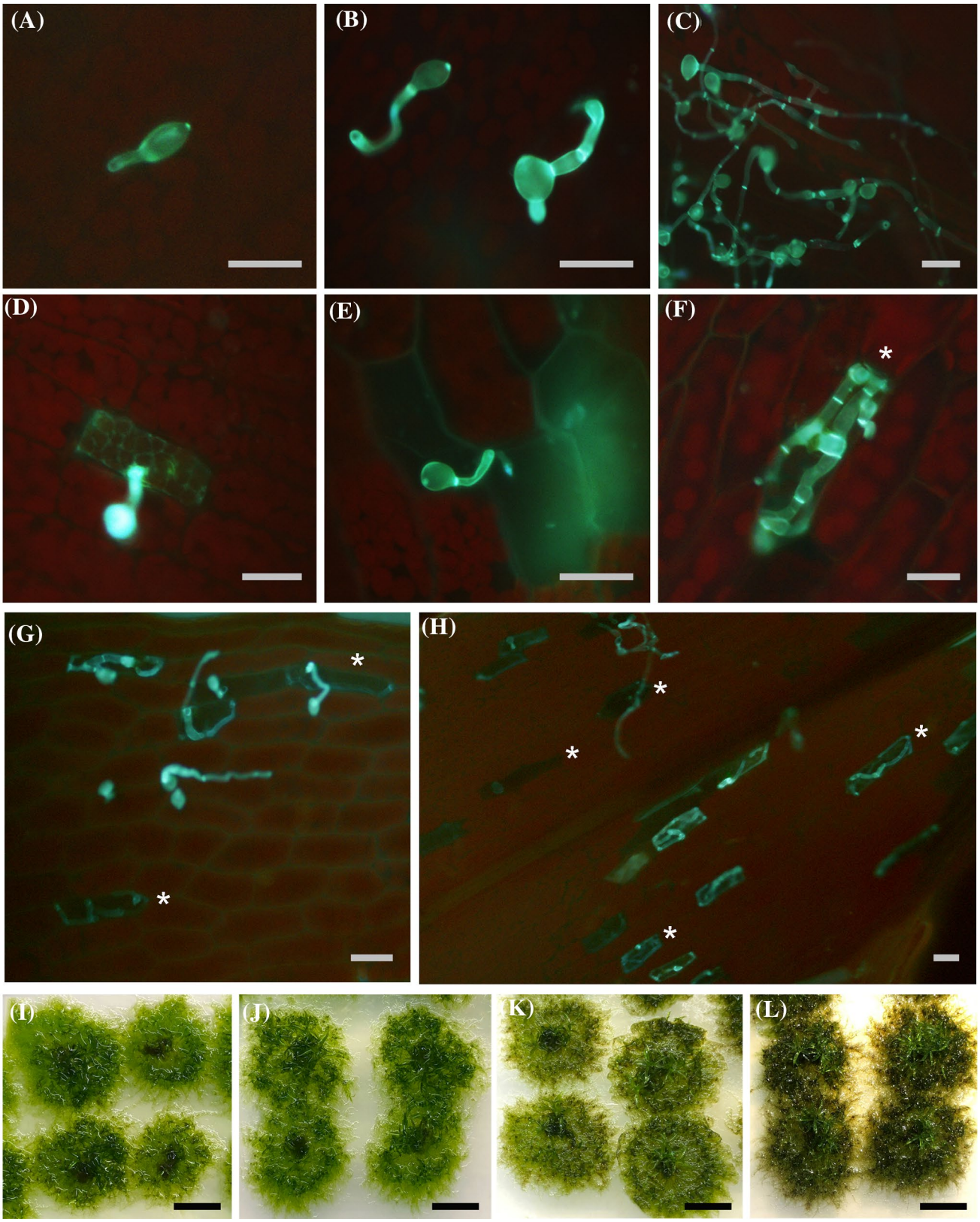
(A)
(B)
(C)
(D)
(E)
(F)
(G)
(H)
(I)
(J)
(K)
(L)

◂**Fig. 1** *B. cinerea* colonization and symptom development in *P. patens*. Infection progress during time is shown; **A** spore germination at 4 hpi, **B** Germ tubes elongation at 8 hpi, **C** proliferation of mycelium at 24 hpi. **D** Hyphal tip approaching a moss cell at 8 hpi, **E** initial penetration of infectious hypha, and **F**–**H** Hyphae growing within moss cell at 24 hpi. Asterisks indicate infected cells. In **G** and **H** only few infected cell are marked as examples. Living cells surrounding infected cells are clearly visible in **F**–**H**. Symptom development at 8 hpi (**J**), 24 hpi (**K**), 48 hpi (**L**), and 24 h water-treated moss colonies (**I**) are shown. The scale bar in **A**–**H** represents 10 µm and 0.5 cm in **I**–**L**

fragments instead of reads—p, Allow read to contribute to multiple features True, Count multi-mapping reads/fragments—M and Reference sequence file *P. patens* v3.3. Differential expression analyses were performed using EdgeR software ver. 3.24.1 (Robinson et al. 2010; Liu et al. 2015a, b) with p-value adjusted threshold 0.05, p-value adjusted method Benjamini and Hochberg (1995) and Minimum log2 Fold Change 2. Counts were normalized to counts per million (cpm) with TMM method and low expressed genes filtered for count values ≥ 5 in three or more samples. In this study, a false discovery rate (FDR) ≤ 0.05 was used to determine significant differentially expressed genes (DEGs) between *B. cinerea* inoculated plants and mock, and expression values were represented by log2 ratio. Heatmaps with DEG data were constructed in GraphPad Prism software ver. 8.0.2.

Quantitative real-time PCR validation of RNA-Seq Data

The expression level of twelve selected genes was analyzed to validate RNA-Seq results via quantitative reverse transcription PCR (RT-qPCR). cDNA was generated from 1 µg of RNA using RevertAid Reverse transcriptase (Thermo Scientific) and oligo (dT) according to the manufacturer's protocol. RT-qPCR was performed in an Applied Biosystems QuantStudio 3 thermocycler using the QuantiNova Probe SYBR Green PCR Kit (Qiagen, Germany); mix proportions and cycling parameters were used as described in manufacturer's instructions. Relative expression of each gene was normalized to the quantity of constitutively expressed Ubi2 gene (Le Bail et al. 2013), using the $2^{-\Delta\Delta Ct}$ method (Livak and Schmittgen 2001). Gene expression of *P. patens* inoculated tissues was expressed relative to the corresponding water-treated samples at the indicated time points, with its expression level set to one. Each data point is the mean value of three biological replicates. Student's t-test was performed to determine the significance for quantitative gene expression analysis using GraphPad Prism software ver. 8.0.2. P-values < 0.01 were considered statistically significant. Primer pairs used for qPCR analyses are provided in Supplementary Table S1, in all cases amplification efficiencies was greater than 95%.

GO enrichment analysis and orphan genes identification

Gene ontology (GO) and functional annotations were assigned based on *P. patens* v3.3 gene models (https://phytozome.jgi.doe.gov/pz/portal.html) and Blast2GO 5.2.5 software (Götz et al. 2008), through Blast and Interpro searches of homologs and protein domains. Additionally, to default options, for every step, the following parameters were set for Blast: e-value ≤ 1.0E−3 and species viridiplantae. Functional enrichment analysis of DEGs obtained previously with EdgeR ver. 3.24.1 was performed using OmicsBox tools (https://www.biobam.com/omicsbox/). GO terms with a FDR ≤ 0.05 were considered for our analysis. To summarize the long list of GO terms, redundant GO terms were removed with REViGO (reduce and visualize gene ontology) (Supek et al. 2011).

Physcomitrium patens differentially expressed orphan genes were identified by selecting in our DEG list those genes described as with no gene ancestry in the phytozome database (this means that no homolog gene was found in viridiplantae). The resulting genes were further analyzed by looking for genes with no Blast (tblastn) hits in viridiplantae (e-value > 1.0E−3) (Wilson el al. 2005).

Results

Global gene expression analysis of *P. patens* plants during *B. cinerea* infection

In previous studies, we have shown that *B. cinerea* infects *P. patens* tissues and that fungal biomass starts to increase after 8 h post-inoculation (hpi), reaching high levels at 24 hpi (Ponce de León et al. 2012). To have more insights into *P. patens* defense response to *B. cinerea* infection, RNAseq profiling was performed at three different stages of the colonization event; spore germination (4 hpi), germ tubes elongation (8 hpi), and hyphae proliferation and tissue colonization (24 hpi) (Fig. 1). At 8 hpi, some plant cells start to respond to *B. cinerea*, evidenced by cell wall modifications detected with solophenyl flavine, and initial penetration attempts of some cells by infectious hyphae were visible (Fig. 1D, E). At 24 hpi, hyphae colonized *P. patens* cells and fungal structures could be clearly distinguished within *P. patens* cells (Fig. 1F–H). In our working conditions, disease symptoms were visible at 24 hpi evidenced by darkening of the tissues and heavy maceration at 48 hpi (Fig. 1K, L), which are typical symptoms caused by this pathogen in angiosperms.

The transcriptomes of water-treated and *B. cinerea*-inoculated *P. patens* tissues were analyzed in three biological replicates. A total of 86.8–96.5% of the reads in the libraries mapped successfully to the genomes of *P. patens* (nuclear, chloroplast and mitochondria). Reads mapped uniquely to the *P. patens* nuclear genome (approximately 208 million reads) were used for further analyses (Supplementary Table S2). During the entire time course, 3.072 DEGs were identified, which represent 9.3% of the 32.926 *P. patens* gene models (Supplementary Table S3). The three selected time points showed a clear distinguishable transcriptional profile in response to *B. cinerea* inoculation (Fig. 2A). Only 17 DEGs were identified at 4 hpi (all upregulated), while a massive transcriptional shift towards upregulation was observed at 8 hpi (1.032 upregulated versus 150 downregulated genes). At 24 hpi, transcriptional changes included a high number of upregulated genes (1.208) as well as downregulated genes (1.482). For this work, we defined the three time points as Early Response (ER; 4 hpi), Middle Response (MR; 8 hpi) and Late Response (LR; 24 hpi). Transcriptional dynamics show an overlap of DEGs in ER, MR and LR, and increased expression levels over time was evident. Of the 17 DEGs induced at ER, 16 and 9 were also upregulated at MR and LR, respectively (Fig. 2B). At MR and LR, 693 upregulated and 91 downregulated DEGs were in common, being the rest specific for each time point.

DEGs present at ER encoded proteins related to stress such as Late Embryogenesis Abundant proteins (LEAs), Hydrophobic protein RCI2, Low Temperature and Salt responsive protein (LTI), DNAJ protein, early light-induced protein (ELIP), transcription factor with an AP2 domain, peripheral-type benzodiazepine receptor (TSPO) and phenylalanine-ammonia lyase (PALs) (Supplementary Table S4). Genes encoding enzymes involved in signaling and synthesis of phosphatidic acid (PA) and sphingolipids, which are lipid messengers involved in plant response to biotic and abiotic stress, were also upregulated during ER, including lipid phosphate phosphatase and glucosylceramidase. The high proportion of ER-inducible genes during MR, and to a less extent during LR, accompanied by increased expression levels, indicate that these genes play a role in moss defense during initial stages of infection.

Biological responses of *P. patens* to *B. cinerea* inoculation

Enrichment of Gene Ontology (GO) terms was performed to identify the biological processes mostly affected by *B. cinerea* infection (Supplementary Table S5). Many different GO terms were enriched underlining the wide extent of the plant response to this pathogen. Most of the top ten significantly enriched GO terms for the upregulated genes were similar at MR and LR, and included metabolic processes such as secondary metabolic process, phenylpropanoid, erythrose 4-phosphate/phosphoenolpyruvate family amino acid, L-phenylalanine and aromatic amino acid family metabolic process, and response to fungus, defense response and response to chemical (Fig. 3). Other upregulated defense-related GO terms present at MR and LR included response to abiotic stimulus, external stimulus, wounding, UV-B, and salt, as well as regulation of hormone levels and jasmonic acid biosynthetic process. Moreover, at LR, cell wall metabolic processes were enriched, including cell wall organization or biogenesis and regulation of cell wall macromolecule. Collectively, biotic, abiotic related processes and phenylpropanoids metabolism, accounted for more than 70%

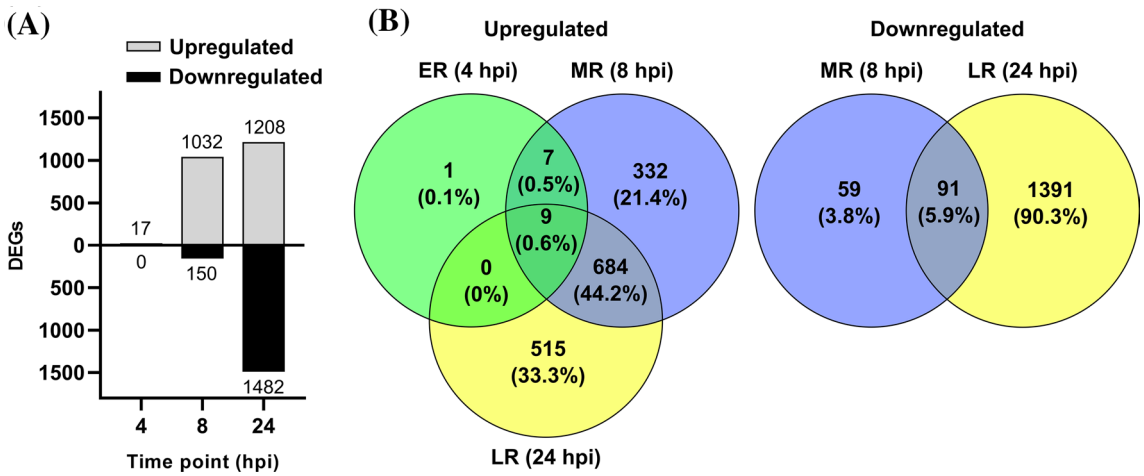

Fig. 2 Differentially expressed *P. patens* genes during *B. cinerea* infection. **A** Number of differentially expressed genes (DEGs), up- and downregulated, in *P. patens* tissues inoculated with *B. cinerea* versus water-treated tissues at 4 hpi, 8 hpi and 24 hpi. **B** Venn diagram of *B. cinerea*-responsive *P. patens* genes at Early Response (ER; 4 hpi), Middle Response (MR; 8 hpi), and Late Response (LR; 24 hpi) showing overlap of expressed *P. patens* genes

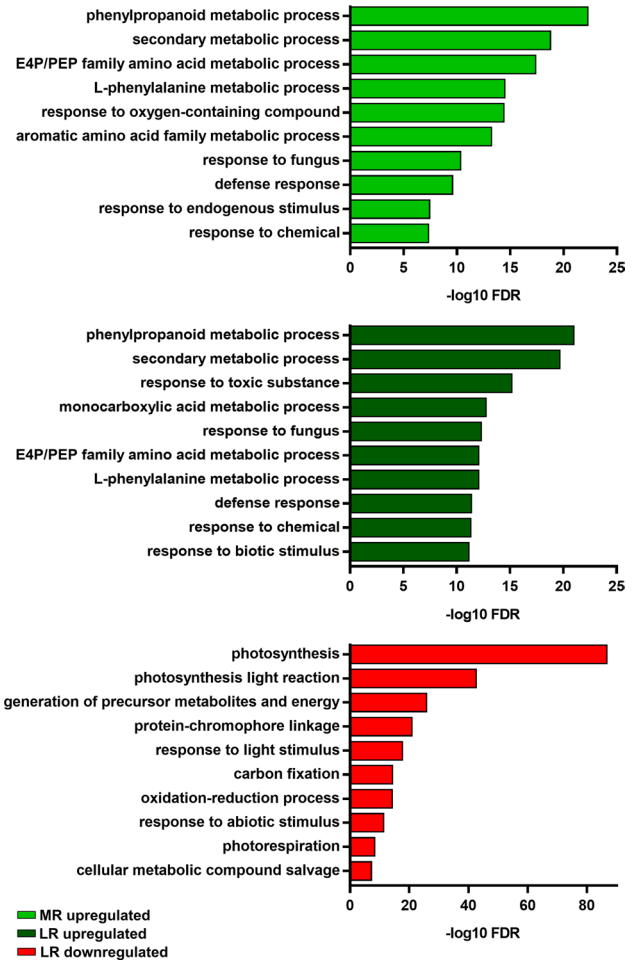

Fig. 3 Enriched gene ontology (GO) biological process terms. The top 10 enrichment GO terms obtained by REViGO at MR and LR are shown and significance is expressed as −log10 FDR. *E4P/PEP*: erythrose 4-phosphate/phosphoenolpyruvate. See Supplementary Table S6 for complete information

and 50% of the GO biological process (BP) terms identified in the up-regulated genes at MR and LR, respectively.

Significant enriched GO terms for downregulated genes were only identified at LR and were related to photosynthesis, including photosynthesis light reaction, generation of precursor metabolites and energy, protein-chromophore linkage, response to light stimulus, carbon fixation, photorespiration and chlorophyll metabolic process. Overrepresented downregulated DEGs included genes encoding chlorophyll binding proteins, proteins related to photosystem I and II, as well as many other proteins related to photosynthesis. Other significantly enriched GO terms were cell cycle process, cell cycle, nuclear division, cell division, chromosome segregation, and anaphase-promoting complex-dependent catabolic process. Within these overrepresented downregulated DEGs, genes encoded cyclins, cyclin-dependent kinases, centromeric proteins, cell division control proteins, kinesins, as well as other proteins involved in cell cycle progression and cell division (Supplementary Tables S5, S6). Taken together, these results indicate that during MR, *P. patens* activates a general respond that encompasses several defense pathways that are maintained during LR, while at LR important processes such as photosynthesis, cell division and cell cycle progression are downregulated.

Activation of the shikimate and phenylpropanoid pathways during *P. patens* defense against *B. cinerea*

GO term enrichment analysis (BP and Molecular Function; MF) and manual inspection of the identified *P. patens* DEGs showed a remarkable overrepresentation of genes involved in the shikimate and phenylpropanoid pathways (Supplementary Tables S5–S7). Several of these genes were amongst the highest induced transcripts at MR and LR. In angiosperms, these pathways contribute with a vast array of metabolites with different roles in defense against invading pathogens, such as preformed chemical and physical barriers (cuticle and lignin), antimicrobial activities (lignans, coumarins, isoflavonoids and flavonoids), as well as signaling molecules (like SA) involved in expression of defense genes in local and systemic tissues (Dixon et al. 2002; Vogt 2010). In total, 12 and 13 genes of the shikimate pathway were upregulated at MR and LR, including gene members encoding eight different enzymes of the pathway (Fig. 4A; Supplementary Table S7). In addition, alteration of the phenylpropanoid pathway by *B. cinerea* starts at ER with increased expression of two *PALs* and continued during MR and LR with upregulation of 93 of 108 DEGs. DEGs encode PALs, cinnamic acid 4-hydroxylases (C4Hs) and 4-hydroxycinnamoyl-CoA ligases (4CLs), which play a crucial role in the formation of the substrate p-coumaroyl-CoA for both monolignol and flavanone biosynthesis. Other DEGs encode CHSs and chalcone isomerases (CHIs), as well as flavonol synthases (FLSs) and flavanone 3-hydroxylases (F3Hs), which are responsible for the production of flavonols in angiosperms. Several other DEGs encode enzymes involved in the biosynthesis of monolignols and lignin-like compounds such as hydroxycinnamoyl-CoA reductases (CCRs), caffeate O-methyltransferases (COMTs), and shikimate O-hydroxycinnamoyl transferases (HCTs). *B. cinerea* inoculation also led to significant increase in six DIR transcripts abundance, some of which were also upregulated *P. patens* tissues infected with other pathogens, and the encoded proteins are probably involved in coupling of monolignols to produce lignin-like compounds (Ponce de León and Montesano 2017). During *B. cinerea* infection, transcript levels of several genes encoding polyphenol oxidases (PPO) such as catechol oxidases and laccases, as well as peroxidases (Prx), increased significantly, which have a role in radical

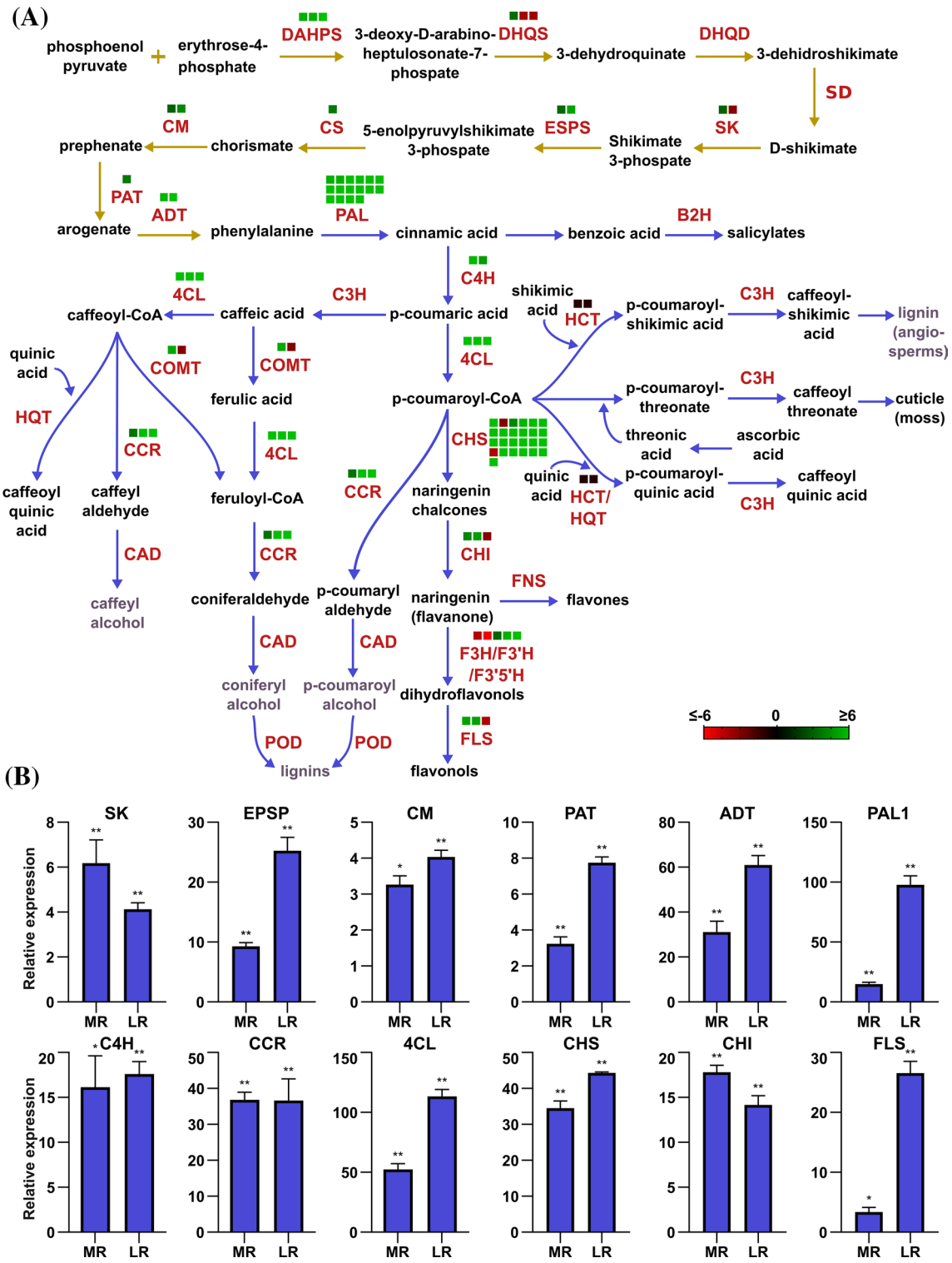

coupling of monolignols to form lignin and other phenolic compounds (Wang et al. 2013). Upregulation of *B. cinerea*-responsive genes encoding TFs TT2 (MYB), TT8 (bHLB), EGL1 and bHLH27 that are involved in flavonoid biosynthesis in other plants (Liu et al. 2015a, b), were also observed. Gene expression values obtained from RNA-seq were validated using qPCR assay for 12 genes of these pathways. The results showed a strong correlation (MR; $R2 = 0.9648$ and LR: $R2 = 0.9465$) between the results obtained with the two techniques (Fig. 4B; Supplementary

◂**Fig. 4** Activation of shikimate and phenylpropanoid pathways during *B. cinerea* infection. **A** Scheme of the shikimate and phenylpropanoid pathways. Heatmaps indicate log2 FC at LR. Abbreviations for the shikimate pathway: DAHPS, 3-deoxy-D-arabino-heptulosonate 7-phosphate synthase; DHQS, 3-dehydroquinate synthase; DHQD/SD, 3-dehydroquinate dehydratase/shikimate dehydrogenase; SK, shikimate kinase; ESPS, 3-phosphoshikimate 1-carboxyvinyltransferase; CS, chorismate synthase; CM, chorismate mutase; PAT, prephenate aminotransferase; ADT, arogenate dehydratase. Abbreviations for the phenylpropanoid pathway: PAL, phenylalanine ammonia-lyase; B2H, benzoic acid-2-hydroxylase; C4H, cinnamate-4-hydroxylase; 4CL, 4-coumarate CoA ligase; CHS, chalcone synthase; CHI, chalcone isomerase; F3H, flavanone 3-hydroxylase; F3´H, flavonoid 3′-hydroxylase; F3′5′H, flavonoid 3′,5′-hydroxylase, FLS, flavonol synthase; FNS, flavone synthase; C3H, coumarate 3-hydroxylase; COMT, caffeoyl/CoA-3-O-methyltransferase; CCR, cinnamoyl-CoA reductase; HQT, hydroxycinnamoyl-CoA quinate transferase; CAD, cinnamoyl-alcohol dehydrogenase; POD, peroxidase, HCT, hydroxycinnamoyl-Coenzyme A shikimate/quinate hydroxycinnamoyltransferase. Metabolites know to be absent in *P. patens* are in grey. Metabolic steps in the shikimate and phenylpropanoid pathways are indicated with yellow and blue arrows, respectively. Adapted from Tohge et al (2013) and Yeh et al. (2014). **B** Validation of differentially expressed genes by RT-qPCR at MR and LR. The expression levels in *B. cinerea*-inoculated plants are relative to the corresponding level of expression in water-treated plants at the indicated time points. Ubi was used as the reference gene. Results are reported as means ± standard deviation (SD) of three samples for each treatment. Asterisks indicate a statistically significant difference between *B. cinerea*-inoculated and the water-treated plants (Students t-test, *P < 0.01; **P < 0.001)

Table S8). Taken together, these findings highlight the important role played by the shikimate and phenylpropanoid pathways in moss defense against *B. cinerea*.

Physcomitrium patens induces the expression of genes involved in pathogen perception, signaling and transcriptional regulation during *B. cinerea* infection

Pathogen perception by membrane-localized RLKs is essential for proper activation of plant defense mechanisms. In total, 55 *RLK* genes were differentially expressed in *B. cinerea*-inoculated tissues compared to control plants, mainly Leucine rich repeat (LRR) containing proteins (including interleukin-1 receptor-associated kinases), as well as putative LysM-containing receptors, lectin receptor kinases and a proline-rich receptor-like protein kinase (Fig. 5; Supplementary Table S9). Upregulation of 21 *RLKs* at MR and 24 *RLKs* at LR was observed, which corresponded to 91% and 49% of the differentially expressed RLKs at each time point, respectively. Interestingly, one gene member of the *P. patens* LYK5 chitin receptor family (Pp3c1_6050) (Orr et al. 2020), was highly induced during *B. cinerea* infection at MR and LR. *CERK1* expression levels did not increase at our time points, which is consistent with chitin-inducible expression of *CERK1* before 4 h (Bressendorff et al. 2016). In addition, genes encoding proteins known to associate to RLKs in angiosperms, such as PTI1-like tyrosine-protein kinase, Mildew resistance Locus (MLO), and putative U-BOX E3 ubiquitin ligases involved in modulating FLS2-mediated angiosperm immune signaling (García et al. 2014; Zhou and Zeng 2018), were all upregulated in response to *B. cinerea* inoculation. Moreover, expression of three putative R protein-encoding genes was affected by *B. cinerea*, including a Toll/interleukin-1 like Receptor (TIR) domain, a NBS-LRR containing proteins and a broad-spectrum mildew resistance protein.

In angiosperms, recognition of pathogens triggers Ca^{2+} fluxes, a rapid production of ROS via consumption of oxygen in a so-called oxidative burst, phosphorylation events by MPKs or Ca^{2+} dependent protein kinases (CDPKs), and transcriptional reprogramming (Knogge et al. 2009). In our transcriptomic analysis, *B. cinerea*-responsive DEGs related to Ca^{2+} signaling encode 24 proteins (17 upregulated), including calmodulin, calcium-binding protein (CML) and calcium dependent protein kinases. ROS are rapidly produced in moss cells after *B. cinerea* infection (Ponce de Leon et al. 2012), and here we show that transcript levels of genes involved in oxidative burst such as respiratory burst oxidase (*RBOH*) and NAD(P)H oxidase are highly induced during *B. cinerea* infection. In addition, *B. cinerea* inoculation led to differential expression of genes encoding calcium-dependent protein kinase (CDPK), MPK and mitogen-activated protein kinase kinase kinase (MEKK). Moreover, transcript levels of all 18 *P. patens* DEGs encoding enzymes involved in signaling and synthesis of PA and sphingolipids increased at MR, including lipid phosphate phosphatase, phosphatidylinositol phospholipase C, phospholipase D and A, diacylglycerol kinase and glucosylceramidase. At LR, of the 28 DEGs related to these lipid messengers, almost 50% were upregulated, suggesting their involvement in moss defense against *B. cinerea* (Fig. 5; Supplementary Table S9).

TFs play a central role in the activation or suppression of gene expression during plant immunity. Consistently, TF activity was a MF GO term overrepresented in upregulated genes at MR and LR (Supplementary Table S6). In total, 192 *P. patens* genes encoding TFs and proteins related to transcription were differentially expressed during *B. cinerea* infection (Fig. 5; Supplementary Table S9). Apetala2/Ethylene Responsive Factor (AP2/ERF) was the largest family in both MR and LR. In total, 46 *AP2/ERF* were responsive to *B. cinerea*; 56% and 65% were upregulated at MR and LR, respectively. Moreover, almost all WRKYs, 17 of 19 DEGs, were upregulated during *B. cinerea* infection, as well as 9 VQ motif-containing protein encoding genes, which are transcription regulators that interact with WRKYs to modulate downstream gene expression involved in plant immunity and response to abiotic stress (Jing and Lin 2015). The other *B. cinerea*-responsive *P. patens* DEGs encoded for TFs know

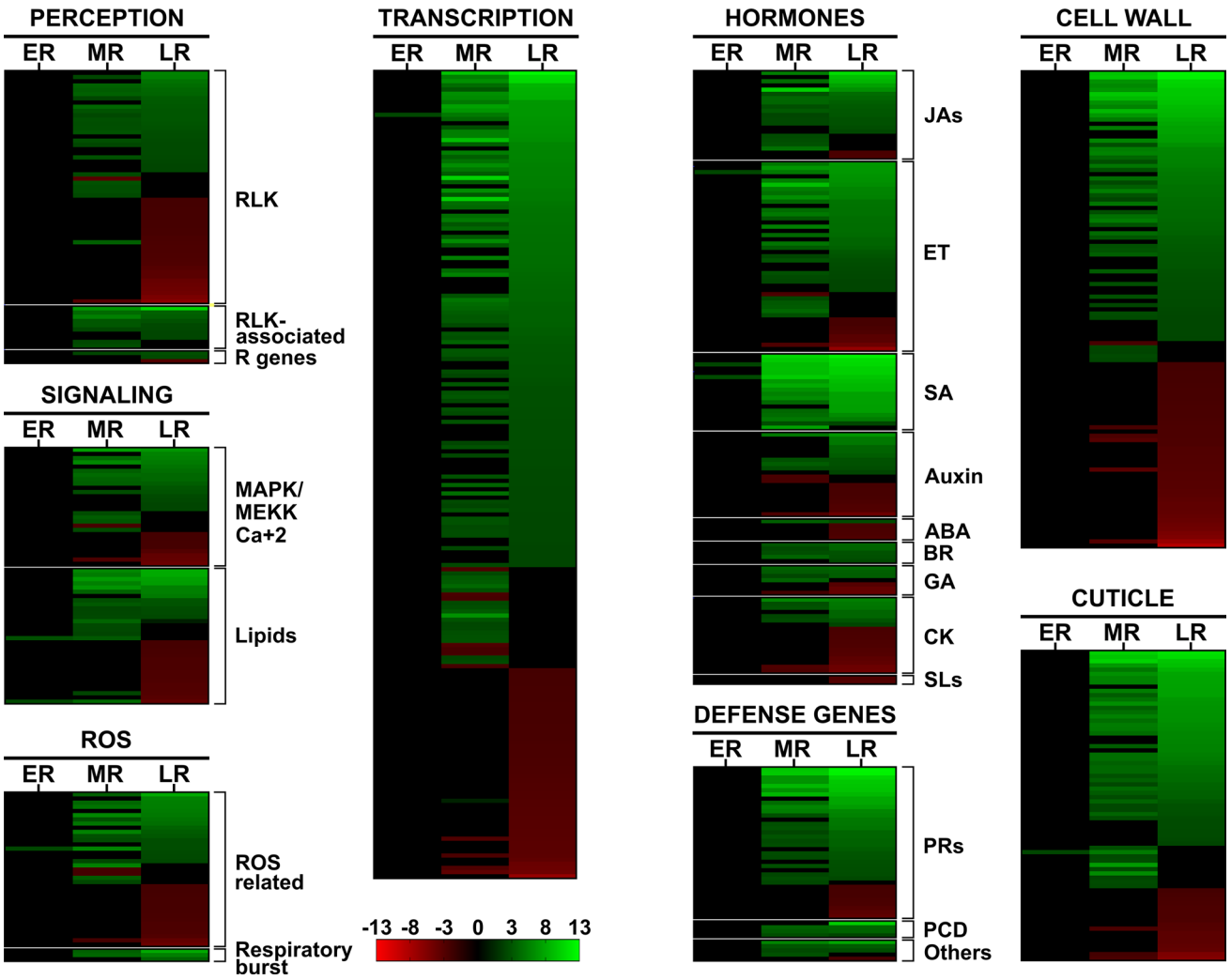

Fig. 5 Heatmap representations of differentially expressed *P. patens* genes during *B. cinerea* infection at ER, MR and LR. *P. patens* DEGs values with $\log_2$ FC ≥ 2.0 or ≤ -2.0 and FDR ≤ 0.05 were used for heatmap construction and grouped according to their role in defense. Normalized values relative to control and ordered according to LR $\log_2$ FC (up to downregulated), are shown in a green–red scale. Abbreviations: RLKs, receptor like kinases; R, resistance; MAPK, Mitogen-activated protein kinase; MEKK, Mitogen-activated protein kinase kinase kinase; ROS, reactive oxygen species; JAs, jasmonates; ET, ethylene; SA, salicylic acid; ABA, abscisc acid; BR, brassinosteroids; GA, gibberellic acid; CK, cytokinin; SLs, stringolactones, PR, pathogenesis-related; PCD, programmed cell death. See Supplementary Table S9-S11 for complete information

to regulate angiosperm responses to biotic stress comprised MYB, bHLH, B3, NAC, GRAS, and PLATZ, as well as other TFs. Taken together, these results indicate that pathogen perception, signaling and activation of TFs leading to defense mechanisms in *P. patens* and angiosperms are in general conserved.

Involvement of hormonal pathways in the *P. patens* defense response against *B. cinerea*

In angiosperms, the plant hormones SA, JA, ethylene (ET), ABA, auxins, cytokinins (CK), gibberellins (GA), and brassinosteroids (BR) function in complex networks to regulate plant resistance against pathogens (Denancé et al. 2013). In this study, the involvement of derivatives of jasmonates and ET during the defense response of *P. patens* to *B. cinerea* infection was highlighted by overrepresented DEGs (Fig. 5; Supplementary Table S10). In total, 19 of 21 DEGs related to jasmonates synthesis and signaling were upregulated during MR and LR, including lipoxygenases (LOXs), allene oxide synthase (AOS), allene oxide cyclases (AOC), OPDA reductase (OPR), OPC-8:0 CoA ligase 1 (OPCL1), TIFY (JAZ;JASMONATE ZIM DOMAIN), and TFs bHLH (bHLH27 and EGL1). This finding is consistent with previous results showing induced expression of *LOXs*, *AOS* and *OPR*, and increased OPDA

levels during infection of *P. patens* tissues with *B. cinerea* (Ponce de León et al. 2012). In addition, 34 of 44 DEGs belonging to the *AP2/ERF* transcription factor family, as well as a putative ET receptor (ETR; two-component sensor histidine kinase) gene, were upregulated in response to *B. cinerea* inoculation.

SA is synthesized in plants from cinnamic acid via PAL or from chorismate via isochorismate synthase (ICS) catalyzed steps (Wildermuth et al. 2001; Vogt 2010; Huang et al. 2010). Here, we show that expression of 17 PAL-encoding genes and a gene encoding a putative SIZ1 protein involved in SA signaling during angiosperm innate immunity (Lee et al. 2007), increases during *B. cinerea* infection. Consistently, SA levels rise in *P. patens* during *B. cinerea* infection, suggesting that this hormone participate in moss defense against biotic stress (Ponce de León et al. 2012). Other DEGs related to auxin, CK, ABA, BR, stringolactones and GA biosynthesis and signaling were differentially expressed (Fig. 5; Supplementary Table S10), although their role in defense against *B. cinerea* was uncertain since some genes were upregulated by the fungus, while others were downregulated. For example, genes encoding GH3 that conjugate amino acids to auxin and other hormones, and several auxin responsive genes were downregulated after *B. cinerea* infection, which is consistent with reduced levels of auxin in *B. cinerea*-infected *P. patens* tissues (Ponce de León et al. 2012). However, auxin inducible proteins and auxin transporters encoding genes were also upregulated by *B. cinerea*. Collectively, these results indicate that like in angiosperms complex hormonal pathways operate during moss defense response against *B. cinerea*.

Physcomitrium patens activates expression of genes with conserved functions in plant defense against pathogens

Induced expression of PRs, which are small proteins with antimicrobial activities, is one of the typical hallmarks of defense response activation against pathogens (van Loon et al. 2006). In total, 23 and 27 of 36 DEGs encoding PR, were upregulated at MR and LR, respectively, including genes encoding PR-1 (small cysteine-rich secreted protein), PR-2 (β-1,3 glucanases), PR-3 (chitinase), *PR-5* (thaumatin), PR-9 (peroxidases), and PR-10 (Bet v I), (Fig. 5; Supplementary Table S11). Peroxidases were among the family with most *B. cinerea*-inducible gene members, including Prx34 (Pp3c4_14530), which participates in *P. patens* defense against pathogens (Lehtonen et al. 2009). Other *B.* cinerea-responsive DEGs related to oxidative stress, encoded glutathione S-transferase (GST), peroxiredoxin, thioredoxin, ferredoxins, catalase and superoxide dismutase. Three TSPO genes were upregulated in *B. cinerea*-infected *P. patens* tissues, including Pp3c24_14170, which is involved in redox homeostasis in moss cells (Lehtonen et al. 2012). Similarly, a gene encoding a tocopherol cyclase, which is involved in production of tocopherol in plastids where it protects membranes from oxidative degradation by ROS (Stahl et al. 2019), and a chloroquine-resistance transporter-like involved in glutathione homeostasis during defense against pathogens (Maughan et al. 2010), were also upregulated during *B. cinerea* infection. ROS accumulation can lead to an HR response, which is a type of programmed cell death (PCD) (Lamb and Dixon 1997). We have previously observed that an HR-like response is triggered in *B. cinerea* infected *P. patens* tissues, which probably facilitates colonization of moss tissues (Ponce de León et al. 2012). Here we show that several genes involved in PCD were upregulated in *P. patens* during *B. cinerea* colonization, including genes encoding subtilisin-like proteases, metacaspase, and a E3 ubiquitin-protein ligase BOI that was previously shown to suppress pathogen-induced cell death in angiosperms (Luo et al. 2010) (Fig. 5; Supplementary Table S11).

Plant cuticle and cell walls serve as the first line of defense against *B. cinerea* limiting the advancement of growing hyphae in angiosperms (AbuQamar et al. 2016). We observed by microscopic analysis that at MR plant cells start to modify their cell walls in response to *B. cinerea* colonization (Fig. 1D). Consistently, 113 *B. cinerea*-responsive DEGs were associated to cell wall biosynthesis or modification. Several genes encoding enzymes involved in cellulose, hemicellulose, arabinose and pectin biosynthesis were induced after *B. cinerea* infection, including cellulose synthase, glucuronosyl transferase, UDP-glucuronate 4-epimerase, UDP-glucuronate decarboxylase and UDP-arabinose 4-epimerase. Other DEGs encode enzymes that participate in endogenous cell wall degradation such as endo-glucanases, endo-xylanase, pectin esterases and pectate lyases, and cell wall modifications such as pectin methylesterase inhibitor and expansins (Fig. 5; Supplementary Table S11). In addition, a high number of genes involved in cuticle lipid biosynthetic pathways (Lee et al. 2020), were differentially regulated in response to this pathogen. Most genes were upregulated, including several genes encoding ATP citrate synthases, acetyl-CoA carboxylases, Long Chain Acyl CoA synthetase, Ketoacyl CoA synthases, and other enzymes involved in very-long-chain fatty acids (VLCFA) and cutin synthesis (Fig. 5; Supplementary Table S11). Moreover, other *B. cinerea*-responsive DEGs encode proteins with known functions in angiosperm defense against pathogens, including proteins that recognize or modify chitin from the pathogen, an α-dioxygenase (α-DOX), and different types of transporters (Supplementary Table S3). Thus, our results suggest that conserved defense mechanisms were likely present in the common ancestor of land plants.

Genes acquired by horizontal transfer and orphan genes participate in moss defense against *B. cinerea*

P. patens has nuclear genes acquired by horizontal gene transfer from bacteria, viruses and fungi (Yue et al. 2012). The acquired functions probably played a role in adaptation mechanisms to different terrestrial environments as well as defense mechanisms against pathogens. Of the 128 horizontal transferred genes identified in Yue et al. (2012), 18 were present in our RNAseq analysis, including DEGs encoding acyl-activating enzyme, glutamate-cysteine ligase, acid phosphatase, allantoate deiminase, methionine-gamma-lyases, oleoyl-[acyl-carrier-protein] hydrolase and beta-glucosidases (Supplementary Table S12). Several of these genes could contribute to defense against *B. cinerea* since they are involved in defense processes such as synthesis of auxin, glutathione, as well as degradation of purine, cellulose and methionine. While these genes were probably acquired from bacteria and have homologs in *Arabidopsis*, other DEGs such as genes encoding a UBIA prenyltransferase and phosphoglycerate kinase, involved in menaquinone biosynthesis and glycolysis respectively, were probably obtained from δ-proteobacteria and do not have homologs in *Arabidopsis*. A gene encoding a MFS transporter involved in sugar transport and two heterokaryon incompatibility proteins (HET), which are only present in fungi and moss, were upregulated during *B. cinerea* infection. Interestingly, a sea anemone cytotoxic protein-coding gene acquired probably by cnidarian and involved in dehydration stress responses of *P. patens* (Hoang et al. 2009), was also upregulated with *B. cinerea*. This gene is JA, SA, ET and ABA inducible, and although the exact function is at present unknown, it could have cytotoxic properties against pathogens (Hoang et al. 2009).

Since almost 50% of the *B. cinerea*-responsive genes obtained by horizontal transfer have no homologues in *Arabidopsis* according to Yue et al. (2012), we looked in more detail at DEGs with no homologues in other plant species. A high number of *B. cinerea*-responsive DEGs, 599 genes representing 19% of the total DEGs, encode putative proteins that do not have significant sequence similarity to any other Viridiplantae proteins/peptides and were considered orphan genes (Wilson et al. 2005). Among the total orphan genes, three, 198 and 236 were upregulated at ER, MR and LR, respectively, while 50 were downregulated at MR and 274 at LR (Fig. 6; Supplementary Table S12). Most of these *B. cinerea*-responsive species-specific genes (92%) are described as with unknown functions in the Phytozome database. Of the 599 orphan genes, 376 showed no blast hits (e-value > $1.0E^{-3}$), meaning that they do not have any homologs and were de novo created genes. In addition, 137 orphan genes belong to multimember gene families, and 12 were not expressed in the *P. patens* Atlas project (Perroud et al. 2018) (Fig. 6). Two *B. cinerea* inducible orphan genes were secreted from moss tissues after chitosan treatment (Lehtonen et al. 2014), including Pp3c19_19780, Pp3c18_6260, suggesting that they play a role in moss defense. Taken together, the acquisition of horizontal transferred gene as well as orphan genes could have provided adaptive advantages to encounter microbial colonization in mosses.

Discussion

With the conquest of land, plants developed adaptation mechanisms to cope with new pathogens present in the air and soil. The identification of the genetic basis of such innovations is relevant for understanding how plant defense responses evolved during the interaction with microbial pathogens across the green lineage. In the present study, we show that the moss *P. patens*, responds to the fungal pathogen *B. cinerea* via a complex and integrated set of defenses encompassing both induced responses and downregulation of specific pathways. Major shifts in gene expression patterns start at MR and precede cell invasion by fungal hyphae and the onset of disease symptoms. Most *P. patens* DEGs were upregulated at MR and included genes encoding proteins involved in pathogen perception, signaling, transcription, hormonal signaling, metabolic pathways and genes with diverse role in defense against biotic stress. In contrast, while almost 70% of the MR inducible DEGs were also upregulated at LR, a high number of genes were downregulated at this later time point, including those related to photosynthesis, cell cycle and cell division. Downregulation of photosynthesis and associated processes in response to *B. cinerea* infection and other plant pathogens is a common phenomenon in angiosperms (Bilgin et al. 2010; Windram et al. 2012). *P. patens* could reallocate nitrogen resources for synthesis of new defense proteins as has been observed in angiosperms (Windram et al. 2012). Moreover, *B. cinerea* infection produced browning of chloroplasts, followed by the breakdown of these organelles (Ponce de León et al. 2007). Besides, plants balance cell cycle regulation and immune response through manipulating the level of cyclins and cyclin-dependent kinase (Qi and Zhang 2020), which is consistent with downregulation of genes encoding these type of proteins in our transcriptomic data during *P. patens*-*B. cinerea* interaction. This finding together with the fact that chitin and crude extracts of pathogenic *Pseudomonas* and *Plectosphaerella cucumerina* treatments inhibited *P. patens* and *M. polymporha* growth, respectively (Galotto et al. 2020; Gimenez-Ibanez et al. 2019), indicate that like in angiosperms (Ranf et al. 2011), PAMPs also trigger growth inhibition in bryophytes.

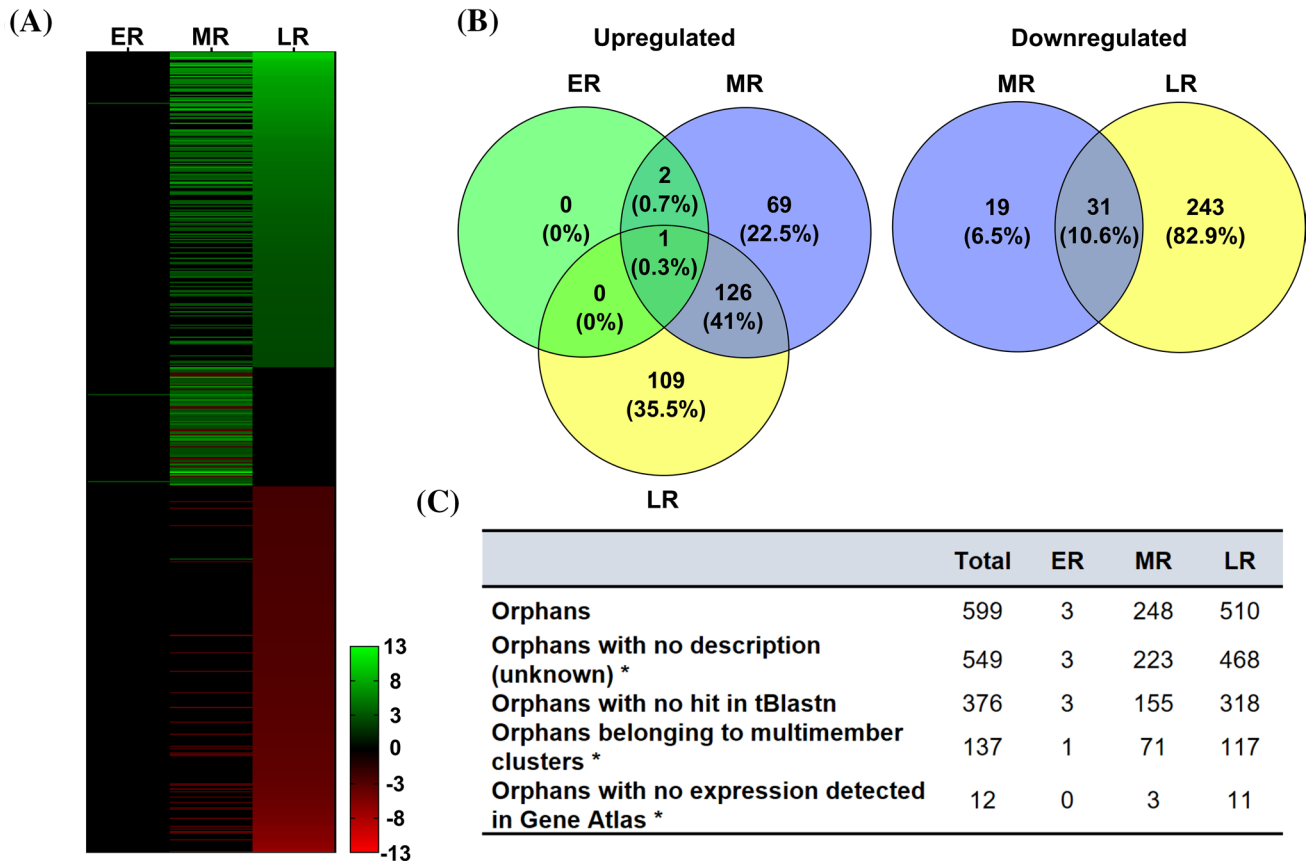

(C)

	Total	ER	MR	LR
Orphans	599	3	248	510
Orphans with no description (unknown) *	549	3	223	468
Orphans with no hit in tBlastn	376	3	155	318
Orphans belonging to multimember clusters *	137	1	71	117
Orphans with no expression detected in Gene Atlas *	12	0	3	11

Fig. 6 *Physcomitrium patens* orphan genes expression in response to *B. cinerea*. **A** Heatmap showing the distribution of *P. patens* orphan DEGs with $\log_2$ FC ≥ 2.0 or ≤ −2.0 and FDR ≤ 0.05 during *B. cinerea* infection at ER, MR and LR. Normalized values relative to control and ordered according to LR $\log_2$ FC (up to downregulated), are shown in a green–red scale. **B** Venn diagrams showing overlap of expressed orphan genes (upregulated and downregulated) at ER, MR and LR. **C** Distribution of identified *B. cinerea*-responsive *P. patens* orphan genes and some orphan sequence characteristics. Asterisks indicate information extracted from phytozome.org. See Supplementary Table S12 for complete information

Our results show that *P. patens* perceives *B. cinerea* and activates the expression of multiple defense genes associated to pathogen recognition by both PRRs and R proteins in angiosperms, suggesting a conserved role of the encoded proteins in defense throughout the green plant lineage. The high number of upregulated DEGs encoding RLKs, mainly proteins with LRR domains, highlight the importance to express many receptors that may detect molecular components of the pathogen in order to mount an effective moss defense response. Consistently, RLK families expanded with the establishment of land plants as an adaptation mechanism to fast-evolving pathogens (Lehti-Shiu et al. 2009). Interestingly, while *P. patens* has a CERK1 receptor that perceives fungal chitin and bacterial peptidyl glycan leading to plant immunity (Bressendorff et al. 2016), flagellin-derived peptide flg22 and the elongation factor Tu are not sensed by moss cells since *P. patens* lacks FLS2 and EFR orthologues receptors (Boller and Felix 2009). Similarly, *M. polymorpha* does not have a FLS2 orthologue and does not respond to flg22 (Gimenez-Ibanez et al. 2019). In *A. thaliana*, LYK5 functions as chitin receptor, likely in concert with CERK1 (Cao et al. 2014). *P. patens* has three LYK5 members and silencing this gene family renders chitin insensitive plants (Orr et al. 2020). Our data show that the expression levels of one *PpLYK5* gene increased significantly during *B. cinerea* infection, supporting its role in moss immunity. Genes encoding proteins known to associate with RLKs in angiosperms were also upregulated in *P. patens*, suggesting that the common ancestor of land plants likely possessed a perception mechanism of PAMPs through different types of RLKs and associated proteins that modulate immune responses to pathogens. Although mosses have a high number of R genes (Gao et al. 2018), *B. cinerea* infection only altered the expression of three R genes in *P. patens*. This result was unexpected since many R genes were differentially regulated in other plant-*B. cinerea* interactions (Windram et al. 2012; Haile et al. 2019).

However, *P. patens* activates an HR-like response during *B. cinerea* infection (Ponce de León et al. 2012), and our transcriptomic analysis shows that several genes involved in plant PCD are induced. Thus, further research is needed to understand the role played by R genes in moss immunity and how pathogen effectors interfere with defense.

Alterations in the *P. patens* transcriptome due to *B. cinerea* colonization comprised gene members related to signaling pathways in angiosperms, including lipid messengers such as inositol 1,4,5-trisphosphate (IP3), PA, sphingolipids, and calcium. Consistently, chitin triggers cytosolic calcium increase in *P. patens* cells that leads to induced expression of defense genes (Galotto et al. 2020). Moreover, ROS level rises quickly in *P. patens* cells during *B. cinerea* infection (Ponce de León et al. 2012), acting probably as second messengers during moss immunity. Upregulation of *B. cinerea*-responsive genes encoding peroxidases, including Prx34 known to be responsible for the oxidative burst in *P. patens* after chitin treatment (Lehtonen et al. 2012), as well as a RBOH and NADPH oxidases, highlighted the role played by ROS in moss defense. In fact, mutants lacking the secreted Prx34 are more susceptible to fungal pathogens (Lehtonen et al. 2009). Our data showed increased expression of oxidative stress related genes encoding peroxiredoxins, thioredoxins, ferredoxins and GSTs, as well as several *TSPO* genes, which are involved in mitochondrial tetrapyrrole transport and control ROS levels in *P. patens* (Lehtonen et al. 2012), supporting the importance to maintain a redox balance through generation and elimination of ROS in moss tissues. This result is in accordance with increased ROS production upon pathogen recognition in *tpso1* mutants that may result in severe damage, cell death and disease symptoms after fungal infection (Lehtonen et al. 2012). Genes encoding MEKKs and MPK were differentially expressed during *B. cinerea* infection, indicating that they are involved in immune responses and may promote defense gene expression. *P. patens* has components of an immune pathway that include MEKK, MAP kinase kinase (MKK), and two MPKs that are required for defense responses to fungal chitin (Bressendorff et al. 2016). MPK moss mutants result in loss of basal resistance to pathogens, evidenced by reduced defense gene expression and cell wall associated defenses (Bressendorff et al. 2016). TFs with known functions in angiosperm defenses against *B. cinerea*, including AP2/ERF, WRKY, MYB, bHLH, PLATZ and NAC (Mengiste et al. 2003; Berrocal-Lobo et al. 2002; Zhao et al. 2012; AbuQamar et al. 2017), were also differentially expressed in fungal-infected moss tissues. Compared with algae, the numbers of members of TFs families including MYB, WRKY, and AP2/ERF have expanded significantly in land plants and might be associated to terrestrial adaptation (Rensing et al. 2008; Rinerson et al. 2015; Pu et al. 2020). The high number of AP2/ERF TFs, as well as WRKYs and associated regulatory proteins with VQ motif, upregulated during *B. cinerea* infection, suggest their involvement in defenses to counteract pathogens among these adaptation mechanisms. Previous work also showed induced expression of AP2/ERF family members by other biotic stresses such as elicitors of *P. carotovorum*, chitosan and *Phytophthora capsici* (Alvarez et al. 2016; Bressendorff et al. 2016; Overdijk et al. 2016). This result is consistent with a central regulatory role played by the AP2/ERF family during different stress conditions in *P. patens* (Hiss et al. 2014). Interestingly, three *B. cinerea*-inducible NAC TFs (Pp3c13_20650, Pp3c3_12890 and Pp3c4_20430), that are involved in *P. patens* water-conducting cell development, showed cell wall thickening and PCD when overexpressed in *P. patens* (Xu et al. 2014). Collectively, these findings indicate that mosses and angiosperms have similar defense signaling pathways and that TFs have an important role in orchestrating moss defense responses during pathogen infection.

Like in angiosperms (AbuQamar et al. 2017), our findings suggest that jasmonates, ET and SA play a role in *P. patens* defense responses against *B. cinerea*. Bryophytes have conserved sequences for all jasmonoyl-isoleucine (JA-Ile) signaling pathway components but lack the hormone JA-Ile (Stumpe et al. 2010; Gachet et al. 2017; Ponce de León et al. 2012; Monte et al. 2018). Instead, dinor-OPDA is the ligand for the functionally conserved JA-Ile receptor (COI1) in bryophytes (Monte et al. 2018). In the present study, we showed upregulation of several genes encoding enzymes involved in jasmonate production, as well as JAZs and bHLH TFs upon *B. cinerea* inoculation. Moreover, OPDA levels increased in *B. cinerea*-infected *P. patens* tissues and wounded *M. polymorpha*, and OPDA treatment induces the expression of defense genes in both bryophytes (Ponce de León et al. 2012; Perroud et al. 2018; Gimenez-Ibanez et al. 2019). Additionally, *M. polymorpha coi-1* mutants displayed reduced resistance against the generalist herbivore *Spodoptera littoralis* and the fungal pathogen *Irpex lacteus* (Monte et al. 2018; Matsui et al. 2020). These findings demonstrate that in spite of the difference in the identity of the bioactive hormone, their role in defense against pathogens is conserved among angiosperms and bryophytes.

ET is synthesized in *P. patens*, although the key enzyme 1-aminocyclopropane-1-carboxylate (ACC) synthase (ACS) encoded by two genes, have no ACS activity (Sun et al. 2016). This finding together with evidence showing that *P. patens* and *M. polymorpha* are unable to convert exogenously added ACC to ET, indicate that a different ethylene biosynthetic pathway may exist in bryophytes (Sun et al. 2016). ET is involved in *P. patens* adaptive responses to drought and submergence through the action of ET receptor (ETR) (Yasumura et al. 2012). In our analysis, transcript levels of an ETR and several AP2/ERFs encoding genes increased during *B. cinerea* infection, indicating that as in

angiosperms, ET is probably involved in defense responses against biotic stress. However, further research is required to determine the role played by this hormone during bryophyte-pathogen interactions.

SA increases in *P. patens* tissues after *B. cinerea* inoculation leading to induced expression of *PAL* (Ponce de León et al. 2012). Similarly, SA levels rise in *M. polymorpha* after *Pseudomonas* extracts treatment, leading to activation of typical SA markers such as *PR-1*, *PR-2*, and *PR-5* (Gimenez-Ibanez et al. 2019). Thus, bryophytes perceive microbial pathogens and activate SA signaling to restrict pathogen colonization similarly as in angiosperms. *P. patens* has only one SA receptor, NPR1-like protein, which partially rescue *Arabidopsis npr1* mutant, suggesting the presence of a NPR1-like positive regulator of SA-mediated defense responses in mosses (Peng et al. 2017). The SA pathway was probably present in the common ancestor of land plants since all genes of this pathway are present in bryophytes but not in algae (Wang et al. 2015). However, the recent finding that *P. patens* NPR1-like receptor did not complement *Arabidopsis npr3-4* double mutant suggests that fine-tuning of SA-induced defense responses probably evolved later in angiosperms (Peng et al. 2017).

Other DEGs related to auxin, CK, ABA, and BR signaling show that a complex hormonal network regulate *P. patens* defense against *B. cinerea*. Auxin levels decreased in *P. patens* after *B. cinerea* infection, while ABA levels increases at 24 hpi, although this hormone could be of fungal origin used as a mechanism to contribute to infection (Ponce de León et al. 2012). BR are important for rose defense against *B. cinerea* (Liu et al. 2018), and here we show that all fungal-responsive DEGs of this pathway are upregulated in *P. patens*. However, the BR receptor and the key regulator BKI1 (Brassinosteroid Insensitive1 Kinase Inhibitor) are not present in *P. patens* and moss cells do not respond to BR (Prigge et al. 2010; Wang et al. 2015). In addition, *P. patens* lacks a GA biosynthetic pathway downstream of ent-kaurenoic acid (KA), indicating that KA metabolites instead of GA may play physiological roles (Miyazaki et al. 2018). The observation that genes encoding ent-kaurene synthases and a KA 2-oxidase (PpKA2ox; Pp3c17_7090; Miyazaki et al. 2018) were upregulated during *B. cinerea* infection, suggests a possible involvement of KA metabolites in plant defense to pathogen invasion. Collectively, these results show that hormonal signaling, several of which have different features with angiosperms, are involved in *P. patens* defense responses against pathogens.

The shikimate and phenylpropanoid pathways played a crucial role in adaptation mechanisms of land plants to cope with abiotic stresses such as UV radiation and desiccation, as well as microbial attack (Emiliani et al. 2009). Several lines of evidence show that components of the phenylpropanoid pathway were already present in streptophyte algae, including lignin-like compounds and flavonoids, suggesting pre-adaptation mechanisms that assisted successful transition from freshwater to land (Sørensen et al. 2011; de Vries et al. 2017; Jiao et al. 2020). This also reinforces the idea that the role of phenylpropanoids in plant defenses against abiotic and biotic stress originated prior to the ancestral land plant (de Vries et al. 2017; Jiao et al. 2020). Our data highlight the importance of the shikimate and phenylpropanoid pathways in moss defense against pathogens since a very high number of biosynthetic and regulatory genes were upregulated during *B. cinerea* infection. Similar results were obtained during angiosperms-*B. cinerea* interactions (Windram et al. 2012; Haile et al. 2019, 2020). The contribution of phenylpropanoids to bryophyte defense against pathogens was evidenced in several other *P. patens*-pathogen interactions (Oliver et al. 2009; Reboledo et al. 2015; Alvarez et al. 2016), and during infection of the liverwort *M. polymorpha* with the oomycete *P. palmivora* (Carella et al. 2019). *P. patens* genome duplicated 45 Mya and several gene families expanded, including *PALs* and *CHSs* (Koduri et al. 2010; Wolf et al. 2010). The presence of different CHSs activities in *P. patens* (Li et al. 2018), and the fact that most *PALs* and *CHSs* are induced during *B. cinerea* infection, suggest that plasticity of secondary metabolism could have allowed mosses to adapt more easily to pathogens. Cinnamic acid levels increases after *P. carotovorum* elicitor treatment (Alvarez et al. 2016), and caffeic acid, coumaric acid, 4-hydroxybenzoic acid and caffeoyl quinic acid have been detected in *P. patens* tissues, some of which have antimicrobial properties (Erxleben et al. 2012; Richter et al. 2012). The encoded proteins of several *B. cinerea*-responsive DEGs have sequence similarities to CHI, F3H and FLS. However, enzymatic activities have been characterized only for *P. patens* C4H, 4CL, CHS, CHI, HCT and C3H/CYP98, and functional studies have been performed for few of these enzymes (Jiang et al. 2006; Silber et al. 2008; Ngaki et al. 2012; Eudes et al. 2016; Renault et al. 2017; Alber et al. 2019; Wohl and Petersen 2020). Both CHIs are enhancers of flavonoid production genes encoding type IV CHI proteins with no CHI activity (Ngaki et al. 2012; Waki et al. 2020). However, no apparent orthologs for F3H and FLS have been found by phylogenetic analysis in *P. patens* (Kawai et al. 2014; Yonekura-Sakakibara et al. 2019). Thus, while hornworts seem to lack flavonoids, and some mosses accumulate biflavonoids in response to UVB exposure (Davies et al. 2020), the presence of the later steps in flavonoid biosynthesis have not been demonstrated in *P. patens*. In contrast, *M. polymorpha* and other liverworts accumulate different types of flavonoids (Albert et al. 2018; Davies et al. 2020). *P. patens* has a pre-lignin pathway instead of true lignin (Weng and Chapple 2010), and we showed previously that polyphenolic compounds reinforce the cell wall upon *B. cinerea* infection (Ponce de León et al. 2012). Upregulation

of DIR, PPO and Prx encoding genes, which are involved in monolignols coupling, may contribute to strengthen the polyphenolic cell walls. This finding together with the fact that SA levels rises upon *B. cinerea* inoculation (Ponce de León et al. 2012), suggest that cinnamic acid-derived metabolites and monolignol-containing compounds are important for moss defense against pathogens. Recently, Renault et al. (2017) showed that the pre-lignin pathway of *P. patens* involves the formation of caffeic acid coupled to the hexose-derived ascorbate pathway, rather than the shikimate pathway, as is reported for angiosperms. This leads to the formation of soluble caffeoyl-threonic acids, which are essential for the synthesis of the moss cuticle. In addition, transcript levels of several *B. cinerea*-responsive MYB, belonging to R2R3 MYB (Pu et al. 2020), and bHLB TFs are involved in phenylpropanoid biosynthesis in angiosperms (Xu et al. 2013). Consistently, a functional analysis demonstrated that a R2R3-MYB TF activates flavonoids biosynthesis in *M. polymorpha*, and the expression of members of this pathway is necessary for liverwort defense against *P. palmivora* (Carella et al. 2019). Collectively, these observations indicate that like in angiosperms, phenylpropanoids play important roles in bryophyte defense, suggesting that the emergence of specialized secondary metabolites in early land plants was probably important to protect plant tissues from invading microorganisms.

PRs belong to a protein family with demonstrated roles in defense responses of angiosperms to pathogens (van Loon et al. 2006). Homologs of most PR gene members are present in bryophytes with the exception of *PR-12* (defensin) and *PR-13* (thionin) that probably evolved later in angiosperms (Visser et al. 2018). In our transcriptomic analysis, *PR-1*, *PR-2*, *PR-3*, *PR-5*, *PR-9* and *PR-10* were upregulated during *B. cinerea* infection, indicating their contribution to moss defense. Consistently, constitutive expression of PR-10 (Pp3c2_27350) increased resistance to the oomycete *P. irregulare* in *P. patens*, where cell wall reinforcement probably contributes to halt pathogen colonization (Castro et al. 2016). Peroxidases encoding DEGs were among the highest *B. cinerea*-inducible members of the moss PR family, similarly as in *P. palmivora*-infected *M. polymorpha* tissues (Carella et al. 2018, 2019). In addition, *B. cinerea*-inducible Prx34, *PR-5* and a thioredoxin (Pp3c6_10090), were secreted to the apoplast in chitosan-treated moss tissues (Lehtonen et al. 2014). These apoplastic proteins could contribute to moss defense by regulating cellular redox status or exerting antifungal activities, and/or through cell wall reinforcement by catalyzing H_2O_2-dependent cross-linking of cell wall components. The importance of cell wall defenses in *P. patens* response to *B. cinerea* colonization was evidenced by differential expression of a high number of genes involved in cell wall synthesis and modifications. Two genes encoding pectin methylesterase inhibitor were upregulated at MR and LR, which are involve in making the wall more resistant to degradation by fungal enzymes by increasing methylated pectin in the cell wall (Lionetti et al. 2007). Moreover, several downregulated genes encoded expansins, known to influence cell wall extensibility and *B. cinerea* susceptibility in *Arabidopsis* (AbuQamar et al. 2013). In addition, genes involved in cuticle biosynthetic pathways, including those related to fatty acid, VLCFA, cutin and wax synthesis (Lee et al. 2020), were mostly upregulated during *B. cinerea* infection. Cell wall reinforcement and cuticle associated defenses probably serve as the first line of defense to limit the advancement of growing hyphae, like in angiosperms (AbuQamar et al. 2016). Several LOXs and an α-Dioxygenase encoding genes were upregulated upon *B. cinerea* inoculation, and similarly as in angiosperms they produce oxylipins with different roles in plant defense against pathogens (Ponce de León et al. 2015). α-DOX-derived oxylipins increases after pathogen infection in *P. patens* and *Arabidopsis* and protect plant tissues against cellular damage caused by pathogens (Ponce de León et al. 2002; Machado et al. 2015). Collectively, these findings suggest a conserved role for a high number of DEGs in mediating defense responses to fungal pathogens throughout the land plant lineage.

Several genes present in our *P. patens–B. cinerea* transcriptomes and associated to defense were acquired by horizontal gene transfer from prokaryotes and fungi. Upregulated DEGs included genes involves in auxin, glutathione, fatty acid biosynthesis, glycolysis and sugar transport (Yue et al. 2012), which participate in plant disease resistance. Moreover, a UBIA prenyltransferase encoding gene from proteobacterial origin was upregulated by *B. cinerea* infection, which could be involved in ubiquinone synthesis that has antioxidant activity (Li 2016). Interestingly, two *B. cinerea* inducible genes encoded heterokaryon incompatibility proteins (HET) obtained probably from fungi, which participate in innate immune response by protecting the fungus from pathogens and serve as damaged self-recognition system by inducing PCD (Medina-Castellanos et al 2018). The possible contribution of HET genes in moss immunity was further supported by Sun et al. (2020), which demonstrated that several HET genes are upregulated by fungal elicitor, SA and MeJA. Fungal colonization played a fundamental role in land colonization by plants (Remy et al. 1994), and gene acquisition following fungal interaction might have represented adaptive benefits for resistance to pathogen colonization. In addition, 13% of the total *P. patens* genes are orphan genes, which are species-specific genes with no homologs in other plants (Zimmer et al. 2013). Our findings show that a large proportion of *B. cinerea*-responsive *P. patens* DEGs (599 genes: 19%) correspond to orphan genes, from which 376 were de novo created genes, suggesting that they could represent innovative adaptive strategies to biotic

stress. The involvement of orphan genes in cold acclimation (Beike et al. 2015), indicate that they also participate in abiotic stress tolerance. Moreover, twelve *B. cinerea*-responsive *P. patens* orphan genes were not expressed in any condition present in the large-scale RNA-seq *P. patens* Altlas project (Perroud et al. 2018), suggesting that they could represent pathogen-specific orphans. Deciphering the roles played by orphan genes, most of which have no annotations, during biotic and abiotic stress in *P. patens*, will help to understand how they contributed to stress adaptation mechanisms of this moss. In conclusion, our results reveal that conserved defense mechanisms between extant bryophytes and angiosperms, as well as moss-specific defenses are part of the *P. patens* immune system. Further studies on *P. patens*-pathogen interactions will contribute to uncover the molecular mechanisms underlying moss-specific defenses and their involvement during coevolution of land plants and pathogens.

Acknowledgements This work was supported by "Fondo Conjunto" Uruguay-México (AUCI-AMEXCID), "Agencia Nacional de Investigación e Innovación (ANII) (graduate fellowships)" Uruguay, "Programa de Desarrollo de las Ciencias Básicas (PEDECIBA)" Uruguay, and "Programa para Grupo de I+D Comisión Sectorial de Investigación Científica, Universidad de la República", Uruguay. The authors thank Héctor Romero and Andrea Zimmers for bioinformatics advice.

Author contributions GR performed the experiments; GR, AA and IPDL analyzed and interpreted the data and participated in discussions; GR and AA helped to write the article; LV participated in the interpretation of the data, artwork, discussions and drafting of the work; RM participated in the drafting of this work; all the authors revised and contributed to the final version of the manuscript; IPDL wrote the manuscript. All authors read and approved the final version of the manuscript.

Data availability The sequencing raw data from the RNA-Seq libraries were deposited on the Sequence Read Archive from NCBI under SRA accession: PRJNA647932. Data are available through https://www.ncbi.nlm.nih.gov/bioproject/647932. In addition, data sets supporting the results of this article are included in Additional files.

Compliance with ethical standards

Conflict of interest Authors declare no conflict of interest.

References

AbuQamar S, Ajeb S, Sham A, Enan MR, Iratni R (2013) A mutation in the expansin-like A2 gene enhances resistance to necrotrophic fungi and hypersensitivity to abiotic stress in *Arabidopsis thaliana*. Mol Plant Pathol 14(8):813–827. https://doi.org/10.1111/mpp.12049

AbuQamar S, Moustafa K, Tran LS (2016) Omics' and plant responses to *Botrytis cinerea*. Front Plant Sci 7:1658. https://doi.org/10.3389/fpls.2016.01658

AbuQamar S, Moustafa K, Tran LS (2017) Mechanisms and strategies of plant defense against *Botrytis cinerea*. Crit Rev Biotechnol 37(2):262–274. https://doi.org/10.1080/07388551.2016.1271767

Alber AV, Renault H, Basilio-Lopes A, Bassard JE, Liu Z, Ullmann P, Lesot A, Bihel F, Schmitt M, Werck-Reichhart D, Ehlting J (2019) Evolution of coumaroyl conjugate 3-hydroxylases in land plants: lignin biosynthesis and defense. Plant J 99:924–936. https://doi.org/10.1111/tpj.14373

Albert NW, Thrimawithana AH, McGhie TK, Clayton WA, Deroles SC, Schwinn KE, Bowman JL, Jordan BR, Davies KM (2018) Genetic analysis of the liverwort *Marchantia polymorpha* reveals that R2R3MYB activation of flavonoid production in response to abiotic stress is an ancient character in land plants. New Phytol 218(2):554–566. https://doi.org/10.1111/nph.15002

Alvarez A, Montesano M, Schmelz E, Ponce de León I (2016) Activation of shikimate, phenylpropanoid, oxylipins, and auxin pathways in *Pectobacterium carotovorum* elicitors-treated moss. Front Plant Sci 7:328. https://doi.org/10.3389/fpls.2016.00328

Ashton NW, Cove D (1977) The isolation and preliminary characterization of auxotrophic and analogue resistant mutants of the moss, *Physcomitrella patens*. Mol Genet Genomics 154:87–95. https://doi.org/10.1007/BF00265581

Beike AK, Lang D, Zimmer AD, Wüst F, Trautmann D, Wiedemann G, Beyer P, Decker EL, Reski R (2015) Insights from the cold transcriptome of *Physcomitrella patens*: global specialization pattern of conserved transcriptional regulators and identification of orphan genes involved in cold acclimation. New Phytol 205(2):869–881. https://doi.org/10.1111/nph.13004

Benjamini Y, Hochberg Y (1995) Controlling the false discovery rate - a practical and powerful approach to multiple testing. J R Stat Soc Ser B Methodol 57(1):289–300. https://doi.org/10.2307/2346101

Berrocal-Lobo M, Molina A, Solano R (2002) Constitutive expression of ETHYLENE-RESPONSE-FACTOR1 in *Arabidopsis* confers resistance to several necrotrophic fungi. Plant J 29:23–32. https://doi.org/10.1046/j.1365-313x.2002.01191.x

Bilgin DD, Zavala JA, Zhu J, Clough SJ, Ort DR, DeLucia EH (2010) Biotic stress globally downregulates photosynthesis genes. Plant Cell Environ 33:1597–1613. https://doi.org/10.1111/j.1365-3040.2010.02167.x

Bolger AM, Lohse M, Usadel B (2014) Trimmomatic: a flexible trimmer for Illumina sequence data. Bioinformatics 30(15):2114–2120. https://doi.org/10.1093/bioinformatics/btu170

Boller T, Felix G (2009) A renaissance of elicitors: perception of microbe associated molecular patterns and danger signals by pattern-recognition receptors. Annu Rev Plant Biol 60:379–406. https://doi.org/10.1146/annurev.arplant.57.032905.105346

Bressendorff S, Azevedo R, Kenchappa CS, Ponce de León I, Olsen JV, Rasmussen MW, Erbs G, Newman MA, Petersen M, Mundy J (2016) An innate immunity pathway in the moss *Physcomitrella patens*. Plant Cell 28(6):1328–1342. https://doi.org/10.1105/tpc.15.00774

Cao Y, Liang Y, Tanaka K, Nguyen CT, Jedrzejczak RP, Joachimiak A, Stacey G (2014) The kinase LYK5 is a major chitin receptor in Arabidopsis and forms a chitin-induced complex with related kinase CERK1. eLife 3:e3766. https://doi.org/10.7554/eLife.03766.001

Carella P, Gogleva A, Tomaselli M, Alfs C, Schornack S (2018) *Phytophthora palmivora* establishes tissue-specific intracellular infection structures in the earliest divergent land plant lineage. Proc Natl Acad Sci USA 115(16):E3846–E3855. https://doi.org/10.1073/pnas.1717900115

Carella P, Gogleva A, Hoey DJ, Bridgen AJ, Stolze SC, Nakagami H, Schornack S (2019) Conserved biochemical defenses underpin host responses to oomycete infection in an early-divergent

land plant lineage. Curr Biol 29(14):2282-2294.e5. https://doi.org/10.1016/j.cub.2019.05.078

Castro A, Vidal S, Ponce de León I (2016) Moss Pathogenesis-Related-10 protein enhances resistance to *Pythium irregulare* in *Physcomitrella patens* and *Arabidopsis thaliana*. Front Plant Sci 7:580. https://doi.org/10.3389/fpls.2016.00580

Davies KM, Jibran R, Zhou Y, Albert NW, Brummell DA, Jordan BR, Bowman JL, Schwinn KE (2020) The evolution of flavonoid biosynthesis: a bryophyte perspective. Front Plant Sci 11:7. https://doi.org/10.3389/fpls.2020.00007

de Vries J, Archibald JM (2018) Plant evolution: landmarks on the path to terrestrial life. New Phytol 217:1428–1434. https://doi.org/10.1111/nph.14975

de Vries J, de Vries S, Slamovits CH, Rose LE, Archibald JM (2017) How embryophytic is the biosynthesis of phenylpropanoids and their derivatives in streptophyte algae. Plant Cell Physiol 58:934–945. https://doi.org/10.1093/pcp/pcx037

de Vries A, de Vries J, von Dahlen JK, Gould SB, Archibald JM, Rose LE, Slamovits CH (2018a) On plant defense signaling networks and early land plant evolution. Commun Integr Biol 11(3):1–14. https://doi.org/10.1080/19420889.2018.1486168

de Vries S, de Vries J, Teschke H, von Dahlen JK, Rose LE, Gould SB (2018b) Jasmonic and salicylic acid response in the fern *Azolla filiculoides* and its cyanobiont. Plant Cell Environ 41(11):2530–2548. https://doi.org/10.1111/pce.13131

Delaux PM, Radhakrishnan GV, Jayaraman D, Cheema J, Malbreil M, Volkening JD et al (2015) Algal ancestor of land plants was preadapted for symbiosis. Proc Natl Acad Sci USA 112:13390–13395. https://doi.org/10.1073/pnas.1515426112

Delaux P-M, Hetherington AJ, Coudert Y, Delwiche C, Dunand C, Gould S, Kenrick P, Li F-W, Philippe H, Rensing SA, Rich M, Strullu-Derrien C, de Vries J (2019) Reconstructing trait evolution in plant evo-devo studies. Curr Biol 29(21):R1110–R1118. https://doi.org/10.1016/j.cub.2019.09.044

Denancé N, Sánchez-Vallet A, Goffner D, Molina A (2013) Disease resistance or growth: the role of plant hormones in balancing immune responses and fitness costs. Front Plant Sci 4:155. https://doi.org/10.3389/fpls.2013.00155

Dixon RA, Achnine L, Kota P, Liu CJ et al (2002) The phenylpropanoid pathway and plant defence-a genomics perspective. Mol Plant Pathol 5:371–390. https://doi.org/10.1046/j.1364-3703.2002.00131.x

Emiliani G, Fondi M, Fani R, Gribaldo S (2009) A horizontal gene transfer at the origin of phenylpropanoid metabolism: a key adaptation of plants to land. Biol Direct 4:7. https://doi.org/10.1186/1745-6150-4-7

Erxleben A, Gessler A, Vervliet-Scheebaum M, Reski R (2012) Metabolite profiling of the moss *Physcomitrella patens* reveals evolutionary conservation of osmoprotective substances. Plant Cell Rep 31:427–436. https://doi.org/10.1007/s00299-011-1177-9

Eudes A, Pereira JH, Yogiswara S, Wang G, Teixeira Benites V, Baidoo EEK et al (2016) Exploiting the substrate promiscuity of hydroxycinnamoyl-CoA: shikimate hydroxycinnamoyl transferase to reduce lignin. Plant Cell Physiol 57(3):568–579. https://doi.org/10.1093/pcp/pcw016

Fürst-Jansen JMR, de Vries S, de Vries J (2020) Evo-physio: on stress responses and the earliest land plants. J Exp Bot 71(11):3254–3269. https://doi.org/10.1093/jxb/eraa007

Gachet MS, Schubert A, Calarco S, Boccard J, Gertsch J (2017) Targeted metabolomics shows plasticity in the evolution of signaling lipids and uncovers old and new endocannabinoids in the plant kingdom. Sci Rep 7:41177. https://doi.org/10.1038/srep41177

Galotto G, Abreu I, Sherman CA, Liu B, Gonzalez-Guerrero M, Vidali L (2020) Chitin triggers calcium-mediated immune response in the plant model *Physcomitrella patens*. Mol Plant Microbe Interact 33(7):911–920. https://doi.org/10.1094/MPMI-03-20-0064-R

Gao Y, Wang W, Zhang T, Gong Z, Zhao H, Han GZ (2018) Out of water: the origin and early diversification of plant R-genes. Plant Physiol 177(1):82–89. https://doi.org/10.1104/pp.18.00185

García J, Kusch S, Panstruga R (2014) Magical mystery tour: MLO proteins in plant immunity and beyond. New Phytol 204(2):273–281. https://doi.org/10.1111/nph.12889

Gimenez-Ibanez S, Zamarreño AM, García-Mina JM, Solano R (2019) An evolutionarily ancient immune system governs the interactions between *Pseudomonas syringae* and an early-diverging land plant lineage. Curr Biol 29(14):2270-2281.e4. https://doi.org/10.1016/j.cub.2019.05.079

Götz S, Garcia-Gomez JM, Terol J, Williams TD, Nagaraj SH, Nueda MJ, Robles M, Talon M, Dopazo J, Conesa A (2008) High-throughput functional annotation and data mining with the Blast2GO suite. Nucleic Acids Res 36(10):3420–3435. https://doi.org/10.1093/nar/gkn176

Haile ZM, Nagpala-De Guzman EG, Moretto M, Sonego P, Engelen K, Zoli L, Moser C, Baraldi E (2019) Transcriptome profiles of strawberry (*Fragaria vesca*) fruit interacting with *Botrytis cinerea* at different ripening stages. Front Plant Sci 10:1131. https://doi.org/10.3389/fpls.2019.01131

Haile ZM, Malacarne G, Pilati S, Sonego P, Moretto M, Masuero D, Vrhovsek U, Engelen K, Baraldi E, Moser C (2020) Dual transcriptome and metabolic analysis of *Vitis vinifera* cv. Pinot Noir berry and *Botrytis cinerea* during quiescence and egressed infection. Front Plant Sci 10:1704. https://doi.org/10.3389/fpls.2019.01704

Han G-Z (2019) Origin and evolution of the plant immune system. New Phytol 222(1):70–83. https://doi.org/10.1111/nph.15596

Hiss M, Laule O, Meskauskiene RM, Arif MA, Decker EL, Erxleben A, Frank W et al (2014) Large-scale gene expression profiling data for the model moss *Physcomitrella patens* aid understanding of developmental progression, culture and stress conditions. Plant J 79(3):530–539. https://doi.org/10.1111/tpj.12572

Hoang QT, Cho SH, McDaniel SF, Ok SH, Quatrano RS, Shin JS (2009) An actinoporin plays a key role in water stress in the moss *Physcomitrella patens*. New Phytol 184:502–510. https://doi.org/10.1111/j.1469-8137.2009.02975.x

Huang J, Gu M, Lai L, Fan B, Shi K, Zhou Y-H, Yu JQ, Chen Z (2010) Functional analysis of the *Arabidopsis* PAL gene family in plant growth, development, and response to environmental stress. Plant Physiol 153:1526–1538. https://doi.org/10.1104/pp.110.157370

Jiang C, Schommer C, Kim SY, Suh DY (2006) Cloning and characterization of chalcone synthase from the moss *Physcomitrella patens*. Phytochemistry 67(23):2531–2540. https://doi.org/10.1016/j.phytochem.2006.09.030

Jiao C, Sørensen I, Sun X, Sun H, Behar H, Alseekh S, Philippe G, Palacio Lopez K et al (2020) The *Penium margaritaceum* genome: Hallmarks of the origins of land plants. Cell 181:1097-1111.e12. https://doi.org/10.1016/j.cell.2020.04.019

Jing Y, Lin R (2015) The VQ motif-containing protein family of plant-specific transcriptional regulators. Plant Physiol 169(1):371–378. https://doi.org/10.1104/pp.15.00788

Jones JDG, Dangl JL (2006) The plant immune system. Nature 444:323–329. https://doi.org/10.1038/nature05286

Kawai Y, Ono E, Mizutani M (2014) Evolution and diversity of the 2-oxoglutarate-dependent dioxygenase superfamily in plants. Plant J 78(2):328–343. https://doi.org/10.1111/tpj.12479

Kim D, Langmead B, Salzberg S (2015) HISAT: a fast spliced aligner with low memory requirements. Nat Methods 12:357–360. https://doi.org/10.1038/nmeth.3317

Knogge W, Lee J, Rosahl S, Scheel D (2009) Signal perception and transduction in plants. In: Deising HB (ed) Plant relationships. The Mycota (A Comprehensive Treatise on Fungi as Experimental Systems for Basic and Applied Research), vol 5. Springer, Berlin, pp 337–361

Koduri PK, Gordon GS, Barker EI, Colpitts CC, Ashton NW, Suh DY (2010) Genome-wide analysis of the chalcone synthase superfamily genes of *Physcomitrella patens*. Plant Mol Biol 72:247–263. https://doi.org/10.1007/s11103-009-9565-z

Krings M, Taylor TN, Hass H, Kerp H, Dotzler N, Hermsen EJ (2007) Fungal endophytes in a 400-million-yr-old land plant: infection pathways, spatial distribution, and host responses. New Phytol 174:648–657

Lamb C, Dixon RA (1997) The oxidative burst in plant disease resistance. Annu Rev Plant Physiol Plant Mol Biol 48:251–275. https://doi.org/10.1146/annurev.arplant.48.1.251

Lang D, Ullrich KK, Murat F, Fuchs J, Jenkins J, Haas FB, Piednoel M, Gundlach H, Van Bel M, Meyberg R et al (2018) The *Physcomitrella patens* chromosome-scale assembly reveals moss genome structure and evolution. Plant J 93:515–533

Le Bail A, Scholz S, Kost B (2013) Evaluation of reference genes for RT qPCR analyses of structure-specific and hormone regulated gene expression in *Physcomitrella patens* gametophytes. PLoS ONE 8(8):e70998. https://doi.org/10.1371/journal.pone.0070998

Lee J, Nam J, Park HC, Na G, Miura K, Jin JB et al (2007) Salicylic Acid-Mediated innate immunity in *Arabidopsis* is regulated by SIZ1 SUMO E3 ligase. Plant J 49(1):79–90. https://doi.org/10.1111/j.1365-313X.2006.02947.x

Lee SB, Yang SU, Pandey G, Kim MS, Hyoung S, Choi D, Shin JS, Suh MC (2020) Occurrence of land-plant-specific glycerol-3-phosphate acyltransferases is essential for cuticle formation and gametophore development in *Physcomitrella patens*. New Phytol 225(6):2468–2483. https://doi.org/10.1111/nph.16311

Lehti-Shiu MD, Zou C, Hanada K, Shiu SH (2009) Evolutionary history and stress regulation of plant receptor-like kinase/pelle genes. Plant Physiol 150:12–26. https://doi.org/10.1104/pp.108.134353

Lehtonen MT, Akita M, Kalkkinen N, Ahola-Iivarinen E, Rönnholm G, Somervuo P et al (2009) Quickly-released peroxidase of moss in defense against fungal invaders. New Phytol 183:432–443. https://doi.org/10.1111/j.1469-8137.2009.02864.x

Lehtonen MT, Akita M, Frank W, Reski R, Valkonen JP (2012) Involvement of a class III peroxidase and the mitochondrial protein TSPO in oxidative burst upon treatment of moss plants with a fungal elicitor. Mol Plant Microbe Interact 25(3):363–371. https://doi.org/10.1094/MPMI-10-11-0265

Lehtonen MT, Takikawa Y, Rönnholm G, Akita M, Kalkkinen N, Ahola-Iivarinen E et al (2014) Protein secretome of moss plants (*Physcomitrella patens*) with emphasis on changes induced by a fungal elicitor. J Proteome Res 13:447–459. https://doi.org/10.1021/pr400827a

Li W (2016) Bringing bioactive compounds into membranes: the UbiA superfamily of intramembrane aromatic prenyltransferases. Trends Biochem Sci 41(4):356–370. https://doi.org/10.1016/j.tibs.2016.01.007

Li H, Handsaker B, Wysoker A, Fennell T, Ruan J, Homer N, Marth G, Abecasis G, Durbin R (2009) The sequence alignment/map format and SAMtools. Bioinformatics 25(16):2078–2079. https://doi.org/10.1093/bioinformatics/btp352

Li L, Aslam M, Rabbi F, Vanderwel MC, Ashton NW, Suh DY (2018) PpORS, an ancient type III polyketide synthase, is required for integrity of leaf cuticle and resistance to dehydration in the moss *Physcomitrella patens*. Planta 247(2):527–541. https://doi.org/10.1007/s00425-017-2806-5

Liao Y, Smyth GK, Shi W (2014) FeatureCounts: an efficient general purpose program for assigning sequence reads to genomic features. Bioinformatics 30(7):923–930. https://doi.org/10.1093/bioinformatics/btt656

Lionetti V, Raiola A, Camardella L, Giovane A, Obel N, Pauly M, Favaron F, Cervone F, Bellincampi D (2007) Overexpression of pectin methylesterase inhibitors in *Arabidopsis* restricts fungal infection by *Botrytis cinerea*. Plant Physiol 143(4):1871–1880. https://doi.org/10.1104/pp.106.090803

Liu R, Holik AZ, Su S, Jansz N, Chen K, Leong HS, Blewitt ME, Asselin-Labat ML, Smyth GK, Ritchie ME (2015a) Why weight? Modelling sample and observational level variability improves power in RNA-seq analyses. Nucleic Acids Res 43(15):e97. https://doi.org/10.1093/nar/gkv412

Liu J, Osbourn A, Ma P (2015b) MYB transcription factors as regulators of phenylpropanoid metabolism in plants. Mol Plant 8:689–708. https://doi.org/10.1016/j.molp.2015.03.012

Liu X, Cao X, Shi S, Zhao N, Li D, Fang P, Chen X, Qi W, Zhang Z (2018) Comparative RNA-Seq analysis reveals a critical role for brassinosteroids in rose (Rosa Hybrida) petal defense against *Botrytis cinerea* infection. BMC Genet 19(1):62. https://doi.org/10.1186/s12863-018-0668-x

Livak KJ, Schmittgen TD (2001) Analysis of relative gene expression data using real-time quantitative PCR and the $2-\Delta\Delta CT$ Method. Methods 25(4):402–408. https://doi.org/10.1006/meth.2001.1262

Luo H, Laluk K, Lai Z, Veronese P, Song F, Mengiste T (2010) The Arabidopsis Botrytis Susceptible1 interactor defines a subclass of RING E3 ligases that regulate pathogen and stress responses. Plant Physiol 154(4):1766–1782. https://doi.org/10.1104/pp.110.163915

Machado L, Castro A, Hamberg M, Bannenberg G, Gaggero C, Castresana C et al (2015) The *Physcomitrella patens* unique alpha-dioxygenase participates in both developmental processes and defense responses. BMC Plant Biol 15:439. https://doi.org/10.1186/s12870-015-0439-z

Matsui H, Iwakawa H, Hyon GS, Yotsui I, Katou S, Monte I et al (2020) Isolation of natural fungal pathogens from *Marchantia polymorpha* reveals antagonism between salicylic acid and jasmonate during liverwort–fungus interactions. Plant Cell Physiol 61:265–275. https://doi.org/10.1093/pcp/pcz187

Maughan SC, Pasternak M, Cairns N, Kiddle G, Brach T, Jarvis R, Haas F et al (2010) Plant homologs of the plasmodium falciparum chloroquine-resistance transporter, PfCRT, are required for glutathione homeostasis and stress responses. Proc Natl Acad Sci USA 107(5):2331–2336

Medina-Castellanos E, Villalobos-Escobedo JM, Riquelme M, Read ND, Abreu-Goodger C, Herrera-Estrella A (2018) Danger signals activate a putative innate immune system during regeneration in a filamentous fungus. PLoS Genet 14(11):e1007390. https://doi.org/10.1371/journal.pgen.1007390

Mengiste T, Chen X, Salmeron J, Dietrich R (2003) The BOTRYTIS SUSCEPTIBLE1 Gene encodes an R2R3MYB transcription factor protein that is required for biotic and abiotic stress responses in *Arabidopsis*. Plant Cell 15(11):2551–2565. https://doi.org/10.1105/tpc.014167

Mittag J, Šola I, Rusak G, Ludwig-Müller J (2015) *Physcomitrella patens* auxin conjugate synthetase (GH3) double knockout mutants are more resistant to *Pythium* infection than wild type. J Plant Physiol 183:75–83. https://doi.org/10.1016/j.jplph.2015.05.015

Miyazaki S, Hara M, Ito S, Tanaka K, Asami T, Hayashi KI, Kawaide H, Nakajima M (2018) An ancestral gibberellin in a moss *Physcomitrella patens*. Molecular Plant 11(8):1097–1100. https://doi.org/10.1016/j.molp.2018.03.010

Monte I, Ishida S, Zamarreño AM, Hamberg M, Franco-Zorrilla JM, García-Casado G et al (2018) Ligand-receptor co-evolution shaped the jasmonate pathway in land plants. Nat Chem Biol 14(5):480–488. https://doi.org/10.1038/s41589-018-0033-4

Ngaki MN, Louie GV, Philippe RN, Manning G, Pojer F, Bowman ME et al (2012) Evolution of the chalcone-isomerase fold from fatty-acid binding to stereospecific catalysis. Nature 485:530–533. https://doi.org/10.1038/nature11009

Nishiyama T, Sakayama H, de Vries J, Buschmann H, Saint-Marcoux D, Ullrich KK, Haas FB, Vanderstraeten L et al (2018) The Chara Genome: secondary complexity and implications for plant terrestrialization. Cell 174(2):448-464.e24. https://doi.org/10.1016/j.cell.2018.06.033

Oliver JP, Castro A, Gaggero C, Cascón T, Schmelz EA, Castresana C, Ponce de León I (2009) *Pythium* infection activates conserved plant defense responses in mosses. Planta 230(3):569–579. https://doi.org/10.1007/s00425-009-0969-4

Orr RG, Foley SJ, Sherman C, Abreu I, Galotto G, Liu B, González-Guerrero M, Vidali L (2020) Robust survival-based RNA interference of gene families using in tandem silencing of adenine phosphoribosyltransferase. Plant Physiol 184(2):607–619. https://doi.org/10.1104/pp.20.00865

Overdijk EJ, De Keijzer J, De Groot D, Schoina C, Bouwmeester K, Ketelaar T et al (2016) Interaction between the moss *Physcomitrella patens* and *Phytophthora*: a novel pathosystem for live-cell imaging of subcellular defence. J Microsc 263:171–180. https://doi.org/10.1111/jmi.12395

Peng Y, Sun T, Zhang Y (2017) Perception of salicylic acid in *Physcomitrella patens*. Front Plant Sci 8:2145. https://doi.org/10.3389/fpls.2017.02145

Perroud PF, Haas FB, Hiss M, Ullrich KK, Alboresi A, Amirebrahimi M, Barry K et al (2018) The *Physcomitrella patens* gene atlas project: large-scale RNA-seq based expression data. Plant J 95(1):168–182. https://doi.org/10.1111/tpj.13940

Ponce de León I (2011) The moss *Physcomitrella patens* as a model system to study interactions between plants and phytopathogenic fungi and oomycetes. J Pathog 2011:719873. https://doi.org/10.4061/2011/719873

Ponce de León I, Montesano M (2017) Adaptation mechanisms in the evolution of moss defenses to microbes. Front Plant Sci 8:366. https://doi.org/10.3389/fpls.2017.00366

Ponce de León I, Sanz A, Hamberg M, Castresana C (2002) Involvement of the *Arabidopsis* α-DOX1 fatty acid dioxygenase in protection against oxidative stress and cell death. Plant J 29:61–72. https://doi.org/10.1046/j.1365-313x.2002.01195.x

Ponce de León I, Oliver JP, Castro A, Gaggero C, Bentancor M, Vidal S (2007) *Erwinia carotovora* elicitors and *Botrytis cinerea* activate defense responses in *Physcomitrella patens*. BMC Plant Biol 7:52. https://doi.org/10.1186/1471-2229-7-52

Ponce de León I, Hamberg M, Castresana C (2015) Oxylipins in moss development and defense. Front Plant Sci 6:483. https://doi.org/10.3389/fpls.2015.00483

Ponce De León I, Schmelz EA, Gaggero C, Castro A, Álvarez A, Montesano M (2012) *Physcomitrella patens* activates reinforcement of the cell wall, programmed cell death and accumulation of evolutionary conserved defence signals, such as salicylic acid and 12-oxo-phytodienoic acid, but not jasmonic acid, upon *Botrytis cinerea* infection. Mol Plant Pathol 13(8):960–974. https://doi.org/10.1111/j.1364-3703.2012.00806.x

Prigge MJ, Lavy M, Ashton NW, Estelle M (2010) *Physcomitrella patens* auxin-resistant mutants affect conserved elements of an auxin-signaling pathway. Curr Biol 20:1907–1912. https://doi.org/10.1016/j.cub.2010.08.050

Pu X, Yang L, Liu L, Dong X, Chen S, Chen Z, Liu G, Jia Y, Yuan W, Liu L (2020) Genome-wide analysis of the MYB transcription factor superfamily in *Physcomitrella patens*. Int J Mol Sci 21(3):975. https://doi.org/10.3390/ijms21030975

Qi F, Zhang F (2020) Cell cycle regulation in the plant response to stress. Front Plant Sci 10:1765. https://doi.org/10.3389/fpls.2019.01765

Ranf S, Eschen-Lippold L, Pecher P, Lee J, Scheel D (2011) Interplay between calcium signalling and early signalling elements during defence responses to microbe- or damage-associated molecular patterns. Plant J 68:100–113

Reboledo G, Del Campo R, Alvarez A, Montesano M, Mara H, Ponce de León I (2015) *Physcomitrella patens* activates defense responses against the pathogen *Colletotrichum gloeosporioides*. Int J Mol Sci 16(9):22280–22298. https://doi.org/10.3390/ijms160922280

Redecker D, Kodner R, Graham LE (2000) Glomalean fungi from the Ordovician. Science 289:1920–1921. https://doi.org/10.1126/science.289.5486.1920

Remy W, Taylor TN, Hass H, Kerp H (1994) Four hundred million-year-old vesicular arbuscular mycorrhizae. Proc Natl Acad Sci USA 91:11841–11843

Renault H, Alber A, Horst NA, Basilio Lopes A, Fich EA, Kriegshauser L et al (2017) A phenol-enriched cuticle is ancestral to lignin evolution in land plants. Nat Commun 8:14713. https://doi.org/10.1038/ncomms14713

Rensing SA, Lang D, Zimmer AD, Terry A, Salamov A, Shapiro H, Nishiyama T, Perroud PF, Lindquist EA, Kamisugi Y et al (2008) The *Physcomitrella* genome reveals evolutionary insights into the conquest of land by plants. Science 319:64–69. https://doi.org/10.1126/science.1150646

Rensing SA, Goffinet B, Meyberg R, Wu SZ, Bezanilla M (2020) The Moss *Physcomitrium* (*Physcomitrella*) patens: a model organism for non-seed plants. Plant Cell 32(5):1361–1376. https://doi.org/10.1105/tpc.19.00828

Richter H, Lieberei R, Strnad M, Novák O, Gruz J, Rensing SA, von Schwartzenberg K (2012) Polyphenol oxidases in *Physcomitrella*: functional PPO1 knockout modulates cytokinin-dependent development in the moss *Physcomitrella patens*. J Exp Bot 63(14):5121–5135. https://doi.org/10.1093/jxb/ers169

Rinerson CI, Rabara RC, Tripathi P, Shen QJ, Rushton PJ (2015) The evolution of WRKY transcription factors. BMC Plant Biol 15:66. https://doi.org/10.1186/s12870-015-0456-y

Robinson MD, McCarthy DJ, Gordon K (2010) Smyth, edgeR: a Bioconductor package for differential expression analysis of digital gene expression data. Bioinformatics 26(1):139–140. https://doi.org/10.1093/bioinformatics/btp616

Silber MV, Meimberg H, Ebel J (2008) Identification of a 4-coumarate:CoA ligase gene family in the moss Physcomitrella patens. Phytochemistry 69(13):2449–2456. https://doi.org/10.1016/j.phytochem.2008.06.014

Sørensen I, Pettolino FA, Bacic A, Ralph J, Lu F, O'Neill MA, Fei Z, Rose JK, Domozych DS, Willats WG (2011) The charophycean green algae provide insights into the early origins of plant cell walls. Plant J 68(2):201–211. https://doi.org/10.1111/j.1365-313X.2011.04686.x

Stahl E, Hartmann M, Scholten NJ (2019) A role for tocopherol biosynthesis in *Arabidopsis* basal immunity to bacterial infection. Plant Physiol 181(3):1008–1028. https://doi.org/10.1104/pp.19.00618

Strullu-Derrien C (2018) Fossil filamentous microorganisms associated with plants in early terrestrial environments. Curr Opin Plant Biol 44:122–128. https://doi.org/10.1016/j.pbi.2018.04.001

Strullu-Derrien C, Kenrick P, Pressel S, Duckett JG, Rioult J, Strullu DG (2014) Fungal associations in *Horneophyton ligneri* from the Rhynie Chert (c. 407 million year old) closely resemble those in extant lower land plants: novel insights into ancestral plant-fungus symbioses. New Phytol 203:964–979. https://doi.org/10.1111/nph.12805

Stumpe M, Göbel C, Faltin B, Beike AK, Hause B, Himmelsbach K, Bode J, Kramell R, Wasternack C, Frank W, Reski R, Feussner I (2010) The moss *Physcomitrella patens* contains cyclopentenones but no jasmonates: mutations in allene oxide cyclase lead to reduced fertility and altered sporophyte morphology. New Phytol 188:740–749. https://doi.org/10.1111/j.1469-8137.2010.03406.x

Sun L, Dong H, Nasrullah MY, Wang NN (2016) Functional investigation of two 1-aminocyclopropane-1-carboxylate (ACC) synthase-like genes in the moss *Physcomitrella patens*. Plant Cell Rep 35(4):817–830. https://doi.org/10.1007/s00299-015-1923-5

Sun G, Bai S, Guan Y, Wang S, Wang Q, Liu Y, Liu H, Goffinet B et al (2020) Are fungi-derived genomic regions related to antagonism toward fungi in mosses? New Phytol 228(4):1169–1175. https://doi.org/10.1111/nph.16776

Supek F, BoŠsnjak M, Škunca N, Šmuc T (2011) REViGO summarizes and visualizes long lists of gene ontology terms. PLoS ONE 6(7):e21800. https://doi.org/10.1371/journal.pone.0021800

Taylor TN, Krings M, Kerp H (2006) *Hassiella monospora* gen. et sp. nov., a microfungus from the 400 million year old Rhynie chert. Mycol Res 110:628–632. https://doi.org/10.1016/j.mycres.2006.02.009

Tohge T, Watanabe M, Hoefgen R, Fernie AR (2013) Shikimate and phenylalanine biosynthesis in the green lineage. Front Plant Sci 4:62. https://doi.org/10.3389/fpls.2013.00062

Van Kan JA (2006) Licensed to kill: the lifestyle of a necrotrophic plant pathogen. Trends Plant Sci 11:247–253. https://doi.org/10.1016/j.tplants.2006.03.005

Van Loon LC, Rep M, Pietersen CMJ (2006) Significance of inducible defense-related proteins in infected plants. Annu Rev Phytopathol 44:135–162. https://doi.org/10.1146/annurev.phyto.44.070505.143425

Visser EA, Wegrzyn JL, Myburg AA, Naidoo S (2018) Defence transcriptome assembly and pathogenesis related gene family analysis in *Pinus tecunumanii* (low elevation). BMC Genomics 19:632. https://doi.org/10.1186/s12864-018-5015-0

Vogt T (2010) Phenylpropanoid biosynthesis. Mol Plant 3(2):20. https://doi.org/10.1093/mp/ssp106

Waki T, Mameda R, Nakano T, Yamada S, Terashita M, Ito K, Tenma N et al (2020) A conserved strategy of chalcone isomerase-like protein to rectify promiscuous chalcone synthase specificity. Nat Commun 1(1):870. https://doi.org/10.1038/s41467-020-14558-9

Wang Y, Chantreau M, Sibout R, Hawkins S (2013) Plant cell wall lignification and monolignol metabolism. Front Plant Sci 4:220. https://doi.org/10.3389/fpls.2013.00220

Wang C, Liu Y, Li SS, Han GZ (2015) Insights into the origin and evolution of the plant hormone signaling machinery. Plant Physiol 167(3):872–886. https://doi.org/10.1104/pp.114.247403

Wang Y, Tyler BM, Wang Y (2019) Defense and counterdefense during plant-pathogenic oomycete infection. Annu Rev Microbiol 73:667–696. https://doi.org/10.1146/annurev-micro-020518-120022

Weng JK, Chapple C (2010) The origin and evolution of lignin biosynthesis. New Phytol 187:273–285. https://doi.org/10.1111/j.1469-8137.2010.03327.x

Wildermuth MC, Dewdney J, Wu G, Ausubel FM (2001) Isochorismate synthase is required to synthesize salicylic acid for plant defence. Nature 414:562–571. https://doi.org/10.1038/35107108

Wilson GA, Bertrand N, Patel Y, Hughes JB, Feil EJ, Field D (2005) Orphans as taxonomically restricted and ecologically important genes. Microbiology 151:2499–2501. https://doi.org/10.1099/mic.0.28146-0

Windram O, Madhou P, McHattie S, Hill C, Hickman R, Cooke E et al (2012) *Arabidopsis* defense against *Botrytis cinerea*: chronology and regulation deciphered by high-resolution temporal transcriptomic analysis. Plant Cell 24(9):3530–3557. https://doi.org/10.1105/tpc.112.102046

Wolf L, Rizzini L, Stracke R, Ulm R, Rensing SA (2010) The molecular and physiological responses of *Physcomitrella patens* to ultraviolet-B radiation. Plant Physiol 153:1123–1134. https://doi.org/10.1104/pp.110.154658

Xu W, Grain D, Le Gourrierec J, Harscoët E, Berger A, Jauvion V, Scagnelli A, Berger N et al (2013) Regulation of flavonoid biosynthesis involves an unexpected complex transcriptional regulation of TT8 expression *Arabidopsis*. New Phytol 198(1):59–70. https://doi.org/10.1111/nph.12142

Xu B, Ohtani M, Yamaguchi M, Toyooka K, Wakazaki M, Sato M et al (2014) Contribution of NAC transcription factors to plant adaptation to land. Science 343(6178):1505–1508. https://doi.org/10.1126/science.1248417

Yamamoto Y, Ohshika J, Takahshi T, Ishizaki K, Kohchi T, Matusuura H, Takahashi K (2015) Functional analysis of allene oxide cyclase, MpAOC, in the liverwort *Marchantia polymorpha*. Phytochemistry 116:48–56. https://doi.org/10.1016/j.phytochem.2015.03.008

Yasumura Y, Pierik R, Fricker MD, Voesenek LA, Harberd NP (2012) Studies of *Physcomitrella patens* reveal that ethylene-mediated submergence responses arose relatively early in land-plant evolution. Plant J 72(6):947–959. https://doi.org/10.1111/tpj.12005

Yeh SY, Huang FC, Hoffmann T, Mayershofer M, Schwab W (2014) FaPOD27 functions in the metabolism of polyphenols in strawberry fruit (*Fragaria* sp.). Front Plant Sci 5:518. https://doi.org/10.3389/fpls.2014.00518

Yonekura-Sakakibara K, Higashi Y, Nakabayashi R (2019) The origin and evolution of plant flavonoid metabolism. Front Plant Sci 10:943. https://doi.org/10.3389/fpls.2019.00943

Yue J, Hu X, Sun H, Yang Y, Huang J (2012) Widespread impact of horizontal gene transfer on plant colonization of land. Nat Commun 3:1152. https://doi.org/10.1038/ncomms2148

Zhao Y, Wei T, Yin KQ, Chen Z, Gu H, Qu LJ, Qin G (2012) Arabidopsis RAP22 plays an important role in plant resistance to Botrytis cinerea and ethylene responses. New Phytol 195(2):450–460. https://doi.org/10.1111/j.1469-8137.2012.04160.x

Zhou B, Zeng L (2018) The tomato U-Box type E3 Ligase PUB13 acts with group III ubiquitin E2 enzymes to modulate FLS2-mediated immune signaling. Front Plant Sci 9:615. https://doi.org/10.3389/fpls.2018.00615

Zimmer AD, Lang D, Buchta K, Rombauts S, Nishiyama T, Hasebe M et al (2013) Reannotation and extended community resources for the genome of the non-seed plant *Physcomitrella patens* provide insights into the evolution of plant gene structures and functions. BMC Genomics 14:498. https://doi.org/10.1186/1471-2164-14-498

4.2. Capítulo II_-Transcriptoma de *Botrytis cinerea* durante el proceso de infección de la briofita *Physcomitrium patens* y angiospermas

Con el fin de seguir estudiando la interacción *P. patens-B. cinerea*, nos planteamos en este capítulo la siguiente hipótesis: que *B. cinerea* activa la expresión de genes involucrados en la patogenicidad y mecanismos de colonización de los tejidos vegetales algunos de los cuales también se expresan frente a angiospermas, mientras que otros genes se inducen solamente frente a *P. patens*. Para responder esta pregunta, como objetivo específico nos propusimos ahondar en los mecanismos de infección y virulencia de *B. cinerea* a partir de análisis de RNA-Seq comparativos entre procesos de infección en *Physcomitrium patens* y angiospermas. Para ello se realizó en primer lugar un nuevo análisis de los transcriptomas obtenidos en el Capítulo I de la presente tesis enfocándonos en los reads del hongo durante la colonización de *P. patens* en los tres tiempos seleccionados (temprano, mediano y tardío). Posteriormente se analizaron "*de novo*" varios transcriptomas obtenidos por RNA-Seq del hongo *B. cinerea* infectando distintas plantas vasculares. Una vez obtenida la lista de GDEs en el proceso de infección de este hongo en *P. patens*, se realizó su validación por RT-qPCR así como un análisis de GO para estudiar la respuesta biológica del mismo al infectar esta briofita. Luego se compararon las distintas listas de GDEs para encontrar aquellos mecanismos de infección y virulencia del hongo, comunes o no entre la briofita *P. patens* y angiospermas.

Mediante el análisis de los transcriptomas de las diferentes etapas de infección y *B. cinerea* crecido en medio de cultivo, encontramos un total de 1.015 GDEs de *B. cinerea* en los tejidos del musgo. Los patrones de expresión de genes inducidos y el enriquecimiento de GOs indicó que la infección de los tejidos del musgo por *B. cinerea* es dependiente de la generación de ROS y su detoxificación, actividad de transportadores, degradación y modificación de la pared celular, producción de toxinas y probablemente evasión de la defensa de la planta por proteínas efectoras. La producción de ROS es importante para *B. cinerea* ya que permite la colonización acelerada de los tejidos y ayuda en la invasión del hospedero al proveer sustratos para oxidasas que pueden modificar la cutícula de la superficie celular vegetal (Van Kan, 2006). Por otra parte, la generación endógena de ROS es importante para la germinación de los conidios y la penetración del hospedero (Hou et al., 2020; Zhang et al., 2020). En el análisis que realizamos observamos un aumento en la expresión de oxidorreductasas del hongo durante la infección temprana de *P. patens*. Estos genes incluyen *BcniaD* y *BcniiA*, cuya expresión sigue aumentando a lo largo de las etapas de infección analizadas. Estos genes también se encuentran sobreexpresados en las angiospermas Arabidopsis, *Solanum lycopersicum* (tomate) y *Lettuce sativa* (lechuga), pero solo en etapas tardías. En etapa media y tardía en *P. patens* pudimos detectar que los procesos de oxidorreducción continuaban al encontrar genes codificantes para lacasas, quinona reductasa, GMC oxidorreductasa, peroxidasas, glutatión peroxidasa (Bcgpx3), GST, y diferentes tipos de oxidorreductasas. La lacasa, quinona reductasa y la GMC oxidoreductase pueden ser fuente de ROS necesarias para la infección por *B. cinerea*, mientras que las peroxidasas, glutation peroxidasas al igual que otras enzimas de detoxificación pueden cumplir la función de controlar los niveles de ROS (Siegmund and

Viefhues, 2015). Al igual que en *P. patens*, en la colonización de Arabidopsis, *S. lycopersicum* y *L. sativa* por *B. cinerea*, se encontró un gran número de genes sobreexpresados relacionados a ROS, incluyendo peroxidasas, GSTs, catalasas, SODs y diferentes oxidorecutasas. La actividad oxidorreductasa en el secretoma de varias especies de *Botrytis*, representa hasta el 10% del mismo, remarcando la importancia de estas actividades durante la infección por el hongo (Valero-Jiménez et al., 2019). *B. cinerea* facilita la muerte celular del hospedero al producir toxinas como el ácido botrydial y botcínico (Colmenares et al., 2002; Van Kan et al., 2017). Al comparar la infección en *P. patens* a las 24 hpi con 8 hpi logramos observar un aumento en la expresión de genes vinculados a la producción de ácido botcínico, incluyendo *Bcboa3-7* y *Bcboa9*, sugiriendo la participación de esta toxina en la infección de *P. patens*. En cambio, los genes que codifican para las enzimas involucradas en la biosíntesis de botrydial, se encontraron sobreexpresados en Arabidopsis, *S. lycopersicum* y *L. sativa*, mientras que en *P. patens* solo *Bcbot2* codificante para la sesquiterpeno ciclasa mostró una leve inducción. Otros genes del cluster botrydial incluyen a *Bcbot1*, *Bcbot3* y *Bcbot4* que codifican para proteínas citocromo P450, y *Bcbot5* que codifica para una acetil transferasa putativa, no fueron detectadas o fueron reprimidas. El mayor regulador positivo de la síntesis botrydial, *Bcbot6*, que codifica para un FT Zn(II)2Cys6, y la deshidrogenasa Bcbot7 que podría estar relacionada con la conversión de botrydial a dihydrobotrydial (Siewers et al., 2005; Collado and Viaud, 2016), se vieron inducidas frente a angiospermas y no frente a *P. patens*. Estos resultados sugieren que el botrydial no juega un rol relevante en la infección de *P. patens*.

NEP1 y NEP2 son proteínas secretadas con actividad de inducción de necrosis (Arenas et al., 2010) y diferencialmente expresadas por el hongo durante la infección de *P. patens* y la mayoría de las angiospermas analizadas. Como patógeno nectrótrofo, encontramos un gran número de enzimas con actividad hidrolíticas tanto durante la infección de *P. patens* como en angiospermas. La mayor cantidad de GDEs inducidos por el hongo durante la infección en *P. patens* y angiospermas codifican para CAZymes, incluyendo cutinasas y PCWDEs (*Plant Cell Wall Degrading Enzymes*) que causan el colapso de los tejidos del hospedero y la patogénesis. Estas enzimas extracelulares son potenciales factores de virulencia que podrían jugar un rol importante al facilitar el crecimiento de las hifas debido al ablandamiento de los tejidos del hospedero y a convertir materiales complejos de la planta en aptos para su consumo por parte del hongo. Según nuestros análisis transcriptómicos la mayor proporción de genes CAZymes se encontraron inducidos a tiempos tardíos de infección lo cual concuerda con la mayor maceración y muerte celular del tejido de la planta, el cual es necesario para una colonización efectiva. Nuestros resultados revelaron la inducción de genes del hongo que codifican para CAZymes secretadas comunes a todos los procesos de infección de las plantas estudiadas, al igual que la inducción de otros genes CAZymes específicos de algunas de ellas. La infección en *P. patens* fue la que mostró el mayor número de genes fúngicos inducidos codificantes para pectina y pectato liasas (8 genes), seguido por la infección en *S. lycopersicum* (6 genes), y finalmente la infección en Arabidospis y *L. sativa* (4 genes). Algunos GDEs del hongo se encontraron inducidos únicamente durante la infección de *P. patens* pero no fueron detectados en angiospermas, incluyendo genes que codifican para *β-glucoside gluco-hydrolase, BcXyn11C*, a *GPI* proteína de anclaje; *poly(β-D-mannuronate) lyas*e, una exo-PG, una *glycoside hydrolase* y una *cellobiose dehydrogenase*, entre otros. Así mismo, otros GDEs del hongo aparecieron preferencialmente expresados en una o dos angiospermas. Los patógenos de plantas tienen transportadores como ser

los *ATP-binding cassette* (ABC) y los MFS (*major facilitator superfamily transporters*), encargados de la excreción de compuestos tóxicos para el patógeno creados por el hospedero como estrategia de defensa (VanEtten et al., 2001). Observamos que durante la infección en *P. patens*, *B. cinerea* induce la expresión de un gran número de genes que codifican para posibles trasportadores MFS, alguno de los cuales se encuentran fuertemente inducidos (*Bcin07g06720* y *Bcin09g05570*). Resulta interesante que la mayoría de estos genes codificantes para transportadores MFS, solo se encontraron inducidos en la infección de *P. patens* y no en angiospermas, lo que sugiere que los transportadores MFS podrían tener un rol importante en la interacción *P. patens-B. cinerea*.

Nuestro análisis transcripcional de *B. cinerea* al infectar plantas demostró que hay mecanismos moleculares comunes involucrados en la virulencia del hongo y el proceso de infección en *P. patens* y angiospermas. Sin embargo, diferencias en los patrones de expresión de genes CAZymes y genes del hongo que codifican para posibles transportadores MFS revelan que algunas funciones de infección son específicas en *P. patens* o angiospermas.

Journal of *Fungi*

MDPI

Article

Botrytis cinerea Transcriptome during the Infection Process of the Bryophyte *Physcomitrium patens* and Angiosperms

Guillermo Reboledo [1], Astrid Agorio [1], Lucía Vignale [1], Ramón Alberto Batista-García [2] and Inés Ponce De León [1,*]

[1] Departamento de Biología Molecular, Instituto de Investigaciones Biológicas Clemente Estable, Montevideo 11600, Uruguay; greboledo@iibce.edu.uy (G.R.); aagorio@iibce.edu.uy (A.A.); lvignale@iibce.edu.uy (L.V.)

[2] Centro de Investigación en Dinámica Celular, Instituto de Investigación en Ciencias Básicas y Aplicadas, Universidad Autónoma del Estado de Morelos, Cuernavaca 62209, Mexico; rabg@uaem.mx

* Correspondence: iponce@iibce.edu.uy

Abstract: *Botrytis cinerea* is a necrotrophic pathogen that causes grey mold in many plant species, including crops and model plants of angiosperms. *B. cinerea* also infects and colonizes the bryophyte *Physcomitrium patens* (previously *Physcomitrella patens*), which perceives the pathogen and activates defense mechanisms. However, these defenses are not sufficient to stop fungal invasion, leading finally to plant decay. To gain more insights into *B. cinerea* infection and virulence strategies displayed during moss colonization, we performed genome wide transcriptional profiling of *B. cinerea* during different infection stages. We show that, in total, 1015 *B. cinerea* genes were differentially expressed in moss tissues. Expression patterns of upregulated genes and gene ontology enrichment analysis revealed that infection of *P. patens* tissues by *B. cinerea* depends on reactive oxygen species generation and detoxification, transporter activities, plant cell wall degradation and modification, toxin production and probable plant defense evasion by effector proteins. Moreover, a comparison with available RNAseq data during angiosperm infection, including *Arabidopsis thaliana, Solanum lycopersicum and Lactuca sativa*, suggests that *B. cinerea* has virulence and infection functions used in all hosts, while others are more specific to *P. patens* or angiosperms.

Keywords: *Botrytis cinerea*; transcriptome; *P. patens*; angiosperms; ROS; cell wall degrading enzymes; transporters; virulence; secretome

Citation: Reboledo, G.; Agorio, A.; Vignale, L.; Batista-García, R.A.; Ponce De León, I. *Botrytis cinerea* Transcriptome during the Infection Process of the Bryophyte *Physcomitrium patens* and Angiosperms. *J. Fungi* **2021**, *7*, 11. https://doi.org/10.3390/jof7010011

Received: 20 October 2020
Accepted: 22 December 2020
Published: 28 December 2020

1. Introduction

Botrytis cinerea is a necrotrophic fungus that causes grey mold and infects more than 1000 plant species, including model plants and many crops such as tomato, lettuce and berries [1–3]. It is found worldwide causing disease in fruits, flowers and leaves, leading to pre- and post-harvest crop losses [4–6]. *B. cinerea* is considered the second most important plant-pathogenic fungus, based on scientific and economic significance [2], and therefore it is an extensively studied plant pathogen. This fungus mainly enters the plant via direct penetration or through natural openings or wounds [7]. This ascomycete is a necrotrophic pathogen with a broad host range that kills the plant cells and colonizes the dead tissues to acquire nutrients [7]. *B. cinerea* stimulates reactive oxygen species (ROS) production by the plant and exploits the host programmed cell death (PCD) machinery to cause infection [8,9]. The infection strategies are well described and they rely on several virulence factors, including toxins and plant cell wall degrading enzymes (PCWDEs), necrosis-secreted proteins, transporter proteins and enzymes that protect the fungus from oxidative stress [10]. After landing on the plant surface, spores germinate and appresoria-mediated penetration involves the formation of a penetration peg needed to enter into the host cells [11]. CWDEs such as pectinases, including poly-galacturonases (PGs) and pectate and pectin lyases, as well as cellulases, xylanases, cutinases, lipases, and proteases, are

produced to breach the plant surface, allowing plant tissue colonization and release of carbohydrates for consumption [9]. The high capacity for plant cell wall degradation and modification of glycoconjugates and polysaccharides by *B. cinerea* was demonstrated by the presence in its genome of 367 genes encoding putative CAZymes (Carbohydrate-Active enZymes) [12]. Most CWDEs and cutinases are encoded by multigenic families, and mutants in these genes do not always affect fungal virulence, indicating that some of these enzymes may have partly redundant functions [9,13–16]. Host cell death is facilitated by the action of fungal phytotoxins, including the two main toxins: botrydial and botcinic acid [17,18]. *B. cinerea* produces oxalic acid leading to acidification of the plant tissue [19], and mutants unable to produce this metabolite do not colonize the host tissues [20].

Plant cells recognize *B. cinerea* rapidly and mount a defense response activating the production of antimicrobial compounds and antimicrobial Pathogenesis-Related proteins (PRs), increasing the number of hormones such as salicylic acid (SA), jasmonic acid (JA), ethylene (ET) and brassinosteroids (BR), and other genes with different roles in defense [21]. In turn, *B. cinerea* suppresses plant defenses in early stages by producing small RNAs and effector proteins, which enables the fungus to establish inside the host tissues and accumulate biomass prior to the necrotrophic phase [22]. In addition to angiosperms, *B. cinerea* also infects and colonizes mosses in nature (*Polytrichum juniperinum*; [23]), and under axenic laboratory conditions (*Physcomitrium patens* (previously *Physcomitrella patens*); [24]). Mosses, liverworts and hornworts are bryophytes and, due to their key phylogenetic position as members of the sister lineage of vascular plants, they represent ideal organisms to perform evolutionary studies on defense mechanisms activated in plants in response to biotic stress. Fossil records suggest the existence of pathogenic fungi interacting with plants 400 million years ago [25]. These microorganisms might have imposed a selective pressure on early land plants, leading to the development of plant defense mechanisms to respond to microbial infection. Similar as in angiosperms, *B. cinerea* colonization leads to host cell death and necrosis of *P. patens* tissues [24,26]. After landing on the moss surface, spores germinate, germ tubes elongate and appressoria penetrate the plant cell cytoplasm directly through the plant leaf cell walls, or by invasion of the intercellular spaces between leaf cells leading to cytoplasm infection [27]. In response to infection, *P. patens* activates a defense response that includes the production of ROS, SA and the precursor of JA cis-oxophytodienoic acid (OPDA), reinforcement of the cell walls, and induction of genes encoding PRs and enzymes involved in secondary metabolism [24,26]. However, the activation of these defense mechanisms is not sufficient to stop *B. cinerea* growth and colonization, leading to plant decay. Recently, we have shown that *P. patens* responds to this fungal pathogen with transcriptional reprogramming of 3072 plant genes, which encode proteins involved in pathogen perception, signaling, transcription, hormonal signaling, secondary metabolic pathways and proteins with diverse role in defense against biotic stress [28]. To gain more insights into *B. cinerea* infection and virulence strategies displayed during moss colonization, we focused on the transcriptional response of *B. cinerea* genes during the infection process of *P. patens*. The results demonstrate that fungal genes encoding enzymes involved in ROS production and detoxification, CAZymes, and other virulence factors such as transporters, toxins and cell death inducing factors, were upregulated in *P. patens* tissues. Moreover, comparative analysis of *B. cinerea*-upregulated genes during *P. patens* and three angiosperms infections suggests that some genes involved in the infection process and virulence are commonly upregulated in all plant hosts, while other genes with these functions are more specific to *P. patens* or angiosperms.

2. Materials and Methods

2.1. B. cinerea, P. patens Inoculation and Microscopy

A *B. cinerea* strain isolated from lemon plants [24] was cultured on potato dextrose agar (PDA) at 22 °C, with a photoperiod of 16-h light/8-h dark. To inoculate *P. patens*, a spore suspension of *B. cinerea* was prepared from a 12-day-old culture. For this, *P. patens* Gransden wild type colonies were cultivated axenically on cellophane overlaid solid BCDAT medium

(1.6 g L^{-1} Hoagland's, 1 mM $MgSO_4$, 1.8 mM KH_2PO_4 pH 6.5, 10 mM KNO_3, 45 µM $FeSO_4$, 1 mM $CaCl_2$, 5 mM ammonium tartrate, and 10 g L^{-1} agar) as described by Ashton and Cove [29]. Moss colonies were grown at 22 °C under standard long-day conditions (16-h light/8-h dark regime under 60–80 µmol m^2 s^{-1} white light). After 3 weeks of growth, colonies were sprayed with a 2 × 10^5 spores/mL suspension of *B. cinerea* and each colony received approximately 5000 spores. Tissues were inoculated 5 h after the start of photoperiod. Three time points were analyzed; 4 h post inoculation (hpi), 8 hpi and 24 hpi. *B. cinerea* mycelium grown on PDA plates for 12 days was used as a control. Three independent biological replicates, consisting of 3 plates with 16 moss colonies each, at each infection time point, and mycelium grown on PDA plates were harvested for RNA extraction, immediately frozen in liquid nitrogen, and stored at −80 °C.

B. cinerea tissues were stained with 0.1% solophenyl flavine 7GFE 500 according to [26]. Fluorescence microscopy was performed with an Olympus BX61 microscope (Shinjuku-ku, Japan). Photographs were taken at 4 hpi, 8 hpi and 24 hpi.

2.2. RNA Extraction, RNA Sequencing, Data Processing and qPCR Analysis of P. patens-Infected Tissues

RNA was extracted using the RNeasy Plant Mini Kit, including a RNase-Free DNase I digestion in column (Qiagen, Germany). RNA quality control, library preparation, and sequencing were performed at Macrogen Inc. (Seoul, Korea). RNA integrity was checked before library preparation using an Agilent Technologies 2100 Bioanalyzer (Agilent Technologies). Libraries for each biological replicate were prepared for paired-end sequencing by TruSeq Stranded Total RNA LT Sample Prep Kit (Plant) with 1 µg input RNA, following the TruSeq Stranded Total RNA Sample Prep Guide, Part # 15,031,048 Rev. E. Sequencing was performed on Illumina platform (Illumina, CA, USA) by Macrogen Inc. (Seoul, Korea) to generate paired-end 101 bp reads, obtaining 41 to 64 M reads per sample with Q20 > 98.43%. RNA-seq processing steps were done through Galaxy platform (https://usegalaxy.org/). Raw reads quality was revised by FastQC software ver. 0.11.2 (http://www.bioinformatics.babraham.ac.uk/projects/fastqc/) and then preprocessed for both quality and adapter trimmings using Trimmomatic Version 0.38.0 software [30]. Additionally, to the default options, the following parameters were adjusted: adapter sequence TruSeq3 (paired-ended, for MiSeq and HiSeq), always keep both reads of PE, and SLIDINGWINDOW: 4:15 HEADCROP:12 MINLEN:50. Trimmed reads were mapped to the reference genome of *B. cinerea* isolate B05.10 (ASM14353v4) (http://fungi.ensembl.org/Botrytis_cinerea/Info/Index) using Hisat2 software [31]. The BAM files were obtained with Samtools View software ver. 1.9 and then sorted by name with Samtools Sort software ver. 2.0.3 [32], for further analysis. All raw RNA-Seq read data are deposited in the National Center for Biotechnology Information (NCBI) Short Read Archive (http://www.ncbi.nlm.nih.gov/sra/) under the BioProject accession code PRJNA647932.

Reads were counted using FeatureCounts software ver. 1.6.4 [33]. Additionally to default options, parameters were adjusted for: count fragments instead of reads, allow read to map to multiple features, and use reference sequence file GCA_000143535.4_ASM14353v4_genomic. Cluster analysis of replicates from each time point and control samples was performed by Principal Component Analysis (PCA) using pcaExplorer 2.16.0 software [34]. Differential expression analyses were performed using EdgeR software ver. 3.24.1 [35], with *p*-value adjusted threshold 0.05, *p*-value adjusted method of Benjamini and Hochberg [36] and Minimum log2 Fold Change 2. Counts were normalized to counts per million (cpm) with the TMM method and low expressed genes filtered for count values ≥ 3 in all samples. In this study, a false discovery rate (FDR) ≤ 0.05 was used to determine significant differentially expressed genes (DEGs) between *B. cinerea* grown on *P. patens* and *B. cinerea* grown on PDA (control), and expression values were represented by log2 ratio.

Expression level of 16 selected *B. cinerea* genes related to pathogenesis was analyzed to validate RNAseq results via quantitative reverse transcription PCR (RT-qPCR). cDNA was generated from 1 µg of RNA using RevertAid Reverse transcriptase (Thermo Scientific) and oligo (dT) according to the manufacturer's protocol. RT-qPCR was performed using the

QuantiNova Probe SYBR Green PCR Kit (Qiagen, Germany), according to manufacturer's instructions, in an Applied Biosystems QuantStudio 3 thermocycler. Relative expression of each gene was normalized to the quantity of constitutively expressed BctubB, using the $2^{-\Delta\Delta Ct}$ method [37]. Gene expression of *B. cinerea* grown on plant was expressed relative to *B. cinerea* grown on PDA, with its expression level set to one. Each data point is the mean value of three biological replicates. The significance for quantitative gene expression analysis was determined with Student's *t*-test using GraphPad Prism software ver. 8.0.2. *p*-values < 0.05 were considered statistically significant. Primer pairs used for qPCR analyses are provided in Supplementary Table S1. All primer combinations showed amplification efficiencies greater than 95%.

2.3. RNA-seq Data from B. cinerea Grown on A. thaliana, S. lycopersicum, and L. sativa and Comparison with B. cinerea Grown on P. patens

RNA-seq Illumina sequence reads from *B. cinerea* grown in *Arabidopsis thaliana* [38], *Lactuca sativa* (lettuce) [39], and *Solanum lycopersicum* (tomato) [40], were obtained from NCBI. These plant hosts were chosen since *A. thaliana* represents a model plant for angiosperms, and *S. lycopersicum* and *L. sativa* are two important crops affected by *B. cinerea*. In all cases data correspond to plant leaves inoculated with a spore suspension of *B. cinerea* strain B05.10, using 1×10^5 spores/mL for *A. thaliana* (2000 spores per leaf), 2×10^5 spores/mL for *S. lycopersicum* (6000 spores per leaf) and 5×10^5 spores/mL for *L. sativa* (10.000 spores per leaf). The closest available time points after inoculation compared to our *B. cinerea* transcriptomes in *P. patens* were considered; *A. thaliana* 12 and 24 hpi, *S. lycopersicum* 16 and 23 hpi, and *L. sativa* 24 and 48 hpi. Hence, in this study the corresponding RNA-seq were analyzed: *A. thaliana* at 12 hpi (SRR3383472, SRR3383521, SRR3383545) and 24 hpi (SRR3383805, SRR3383815, SRR3383816), *L. sativa* at 24 hpi (SRA059059, split and extract data using barcode 24hpib1 CCGTCC, 24hpib2 GTCCGC and 24hpib3 GTGGCC) and 48 hpi (SRA059059, split and extract data using barcode: 48hpib1 CTTGTA, 48hpib2 TTAGGC and 48hpib3 GATCAG), *S. lycopersicum* at 16 hpi (SRR12676683, SRR12676682, SRR12676681) and 23 hpi (SRR12676681, SRR12676679, SRR12676678). RNA-seq processing steps were done through Galaxy platform (https://usegalaxy.org/) using the same pipeline as described before for *P. patens* RNAseq processing; setting TruSeq3 for single-ended in Trimmomatic 0.38.0 in accordance to Illumina single-end sequencing data available for *A. thaliana*, *L. sativa* and *S. lycopersicum*. Differential expression analyses were performed using EdgeR software ver. 3.24.1, using the same parameters as for *P. patens* analysis (*p*-value adjusted threshold 0.05, *p*-value adjusted by Benjamini and Hochberg method and Minimum log2 Fold Change 2). Counts were normalized to counts per million (cpm) with TMM method and low expressed genes filtered for count values ≥ 3 in all samples; a FDR ≤ 0.05 was used to determine significant differentially expressed genes (DEGs) between *B. cinerea* grown on *A. thaliana*, *L. sativa*, *S. lycopersicum* and *B. cinerea* grown on PDA (control), and expression values were represented by log2 ratio.

To compare DEGs from *P. patens* and the three studied angiosperms, hierarchical clustering analysis of expressed genes were performed on log2 Fold-Change expression values using the "hclust" tool from R package "stats" ver. 3.6.0. To visualize the obtained data, heatmap plots were performed using the "heatmap.2" tool from R package "gplots" ver. 3.1.0.

2.4. Functional Clasification and Comparison with B. cinerea Secretomes

To test for GO terms enrichment in different sets of DEGs, GO and functional annotations were assigned using G: profiler (http://biit.cs.ut.ee/gprofiler/); which use data retrieved from Ensembl database and fungi, plants or metazoa specific versions of Ensembl Genomes [41]. Only annotated genes were used and GO terms with a FDR ≤ 0.05 were considered for our analysis.

B. cinerea DEGs obtained in the different plant species (*P. patens* and angiosperms) were compared with previously published *B. cinerea* secretomes [42,43]. Candidate effectors were searched for among these genes using EffectorP ver 2.0 (http://effectorp.csiro.au/).

3. Results

3.1. B. cinerea Differentially Expressed Genes during P. patens Infection

P. patens consists of juvenile proto-nemal filaments that further develop into leafy gametophores with rhizoids [44]. Proto-nemal filaments and leaves were infected by *B. cinerea*, as can be visualized by solophenyl flavine staining (Figure S1). *B. cinerea* infection process starts with the germination of spores at the plant surface at 4 h post inoculation (hpi), and continues with germ tubes elongation and formation of terminal swollen structures called appressoria at 8 hpi. Finally, hyphae proliferate and protonemal and leaf cells are invaded at 24 hpi. Accordingly, *B. cinerea* starts to enhance biomass production at 8 hpi, reaching high levels at 24 hpi [26]. Symptoms development were visible at 24 hpi with typical browning and maceration of the tissue (Figure S1).

In order to identify *B. cinerea* molecular players involved in virulence and *P. patens* colonization, we performed transcriptional profiling of these three stages. Samples of *B. cinerea* infecting *P. patens* tissues (4, 8 and 24 hpi) and *B. cinerea* grown on PDA medium (control) generated a total of 312,737,769 clean reads after removing adapter sequences and low-quality reads (Table S2). Considering all samples, 0.12% to 92.86% of the reads in the libraries mapped successfully to the genome of *B. cinerea* (nuclear and mitochondria). Reads mapped uniquely to *B. cinerea* nuclear genome were considered for further analyses; 98,929 at 4 hpi, 796,752 at 8 hpi, 4,261,033 at 24 hpi and 53,254,525 for control *B. cinerea* samples. Biological variability within replicates was analyzed by principal component analysis (PCA). As shown in Figure 1, the first principal component (PC1) accounted for 40% of the total variation and separates the three time points (4, 8 and 24 hpi), and the control *B. cinerea* samples. Variability between biological replicates was very low as indicated.

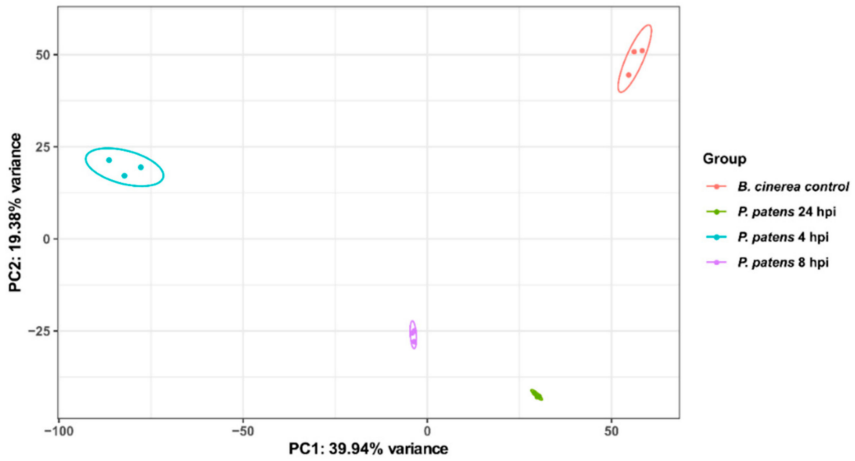

Figure 1. Analysis of *B. cinerea* RNA-Seq data during *P. patens* infection by principal component analysis (PCA). Variation among the three biological replicates per sample (*P. patens* 4 hpi, *P. patens* 8 hpi, *P. patens* 24 hpi and *B. cinerea* control), is shown. Colored dots denote each biological replicate.

Differential expression was first analyzed between *B. cinerea* genes expressed *in planta* during the different infection time points. In total, 184 *B. cinerea* genes were differentially expressed, 106 were upregulated and 78 were downregulated (Figure 2a; Table S3). In the 8 versus 4 hpi comparison, 14 differentially expressed genes (DEGs) were upregulated and 14 DEGs were downregulated. The number of DEGs increased when 24 hpi was compared with 8 hpi; 84 and 52 DEGs were upregulated and downregulated, respectively. Finally, the comparison of 24 versus 4 hpi showed 19 upregulated and 27 downregulated DEGs. Given the low number of *B. cinerea* DEGs, we compared each time point of infection with PDA grown mycelium in order to obtain more information on the infection process. In total, 1015 *B. cinerea* DEGs were obtained and among them 613 were upregulated and 402 downregulated (Figure 2b; Table S3).

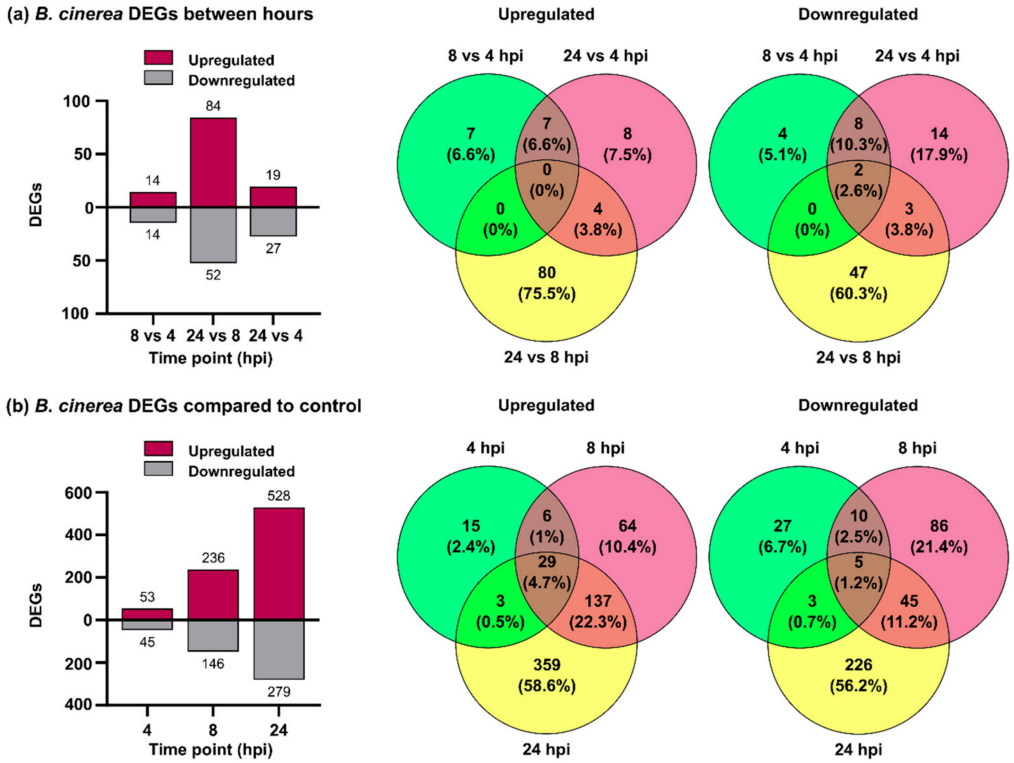

Figure 2. Differentially expressed *B. cinerea* genes during *P. patens* infection. (**a**) Number of differentially expressed genes (DEGs) and Venn diagrams from *B. cinerea* comparisons at 8 vs. 4 hpi, 24 vs. 8 hpi and 24 vs. 4 hpi. (**b**) Number of DEGs and Venn diagrams from *B. cinerea* at 4, 8 and 24 hpi compared with potato dextrose agar (PDA) samples. Log2 FC $\geq$ 2.0 or ≤ -2.0 and false discovery rate (FDR) $\leq$ 0.05 were considered for DEGs identification. In Venn diagrams, the overlap of expressed fungal genes can be observed.

Based on this finding, we decided to consider the 1015 DEGs for further analyses. *B. cinerea* DEGs increased over time and more upregulated genes than downregulated genes were observed at the three time points. The number of upregulated *B. cinerea* genes increased from 53 at 4 hpi, to 236 at 8 hpi, and finally to 528 at 24 hpi. Among downregulated genes, 45, 146 and 279 were identified at 4, 8 and 24 hpi, respectively. A high proportion of upregulated genes present at 4 hpi were also identified at 8 hpi and 24 hpi (71% and 78%), and similarly 70% of upregulated genes at 8 hpi were also upregulated at 24 hpi.

3.2. B. cinerea Genes Encoding Secreted Cell Wall Degrading Enzymes and Other Virulence Factors Are Induced during P. patens Infection

Gene ontology (GO) term enrichment analysis and manual inspection of the identified DEGs were performed to identify the biological processes (BP), molecular function (MF) and cellular compartment (CC) mostly affected in *B. cinerea* during moss infection (Figure S2; Table S4). Enriched downregulated processes include terms related to ribonucleotide and nucleotide binding at 4 hpi, transporter activities at 4 and 8 hpi, and ion binding activities at 8 and 24 hpi. In addition, downregulated genes were also enriched in GO terms such as tetrapyrrole and heme binding, oxidoreduction processes and oxidoreductase activities, and FAD binding and monooxygenase activity at 24 hpi. For upregulated genes, GO terms enrichment at 4 hpi were related to organic acid and oxoacid metabolic processes, amino acids metabolic and biosynthetic processes, oxidoreduction processes such as nicotinamide adenine dinucleotide (NAD) binding, oxidoreductase activities acting on different compounds, and transporter activity. At 8 hpi, the most significantly enriched GO terms for upregulated genes were those involved in degradation of various cell wall components, including hydrolase activities hydrolyzing O-glycosyl compounds

or acting on glycosyl bonds, PG activity, catalytic activity and carbohydrate metabolic process. All these GO terms were also enriched for upregulated genes at 24 hpi, and other GO terms included carbohydrate binding, hydrolase activity, polysaccharide binding, cellulose binding, alpha-L-arabinofuranosidase activity, cutinase activity, pectate lyase activity, carbon-oxygen lyase activity acting on polysaccharides, and arabinose metabolic process. In addition, intrinsic components of membrane were present at all time points, while the extracellular region was a common GO term for upregulated genes at 8 and 24 hpi, which is consistent with secretion of hydrolytic enzymes to degrade the plant cell wall. These results show that GO enrichment analysis also provided insights into temporal characteristics of fungal pathogenesis.

We further focused on upregulated genes since they could encode proteins involved in *B. cinerea* pathogenesis. In total, 29 DEGs were commonly upregulated at all time points, including genes encoding several major facilitator superfamily (MFS) transporters, two sugar transporters (Bchxt19 and Bchxt15), a nitrate reductase (BcniaD), a nitrite reductase (BcniiA), several types of hydrogenases, a common fungal extracellular membrane (CFEM) domain-containing protein (Bcin09g02270), a chitinase, and several hypothetical proteins. In addition, genes involved in the catabolic pathway of D-galacturonic acid [45], which is the major component of pectin polysaccharides [46], were upregulated during the infection process, including those encoding a 2-keto-3-deoxy-L-galactonate aldolase (Bclga1), galactonate dehydratase (Bclgd1) and galacturonate reductase (Bcgar2). To validate the expression profiles of the RNA-Seq data, some of these genes and others related to pathogenesis were selected for analysis using RT-qPCR. The results obtained by the two techniques showed a strong correlation (R2 = 0.9882) (Figure 3; Table S5). Among the common 137 upregulated genes present at 8 and 24 hpi, virulence components such as cutinases and secreted proteins including CAZymes involved in pectin (mainly homogalacturonan), hemicellulose (mainly xyloglucan) and cellulose degradation were identified, as well as Bcnep1 and Bcnep2 (Necrosis- and Ethylene-inducing Proteins), glutathione peroxidase and glutathione S-transferase (GST) (Table S6). At 8 hpi upregulated genes encode PGs (Bcpg2, Bcpg4, Bcpg6, Bcpgx1 and a second exo-PG), pectate lyases, pectin lyases, beta-glucosidases, a xyloglucan endo-β-glucanase (BcXYG1), an endo-beta-1,4-glucanase, a xylanase, cellobiose dehydrogenases, a cello-bio-hydrolase, and arabino-furanosidases (Table S6). At 24 hpi, the number of upregulated genes encoding enzymes for homogalacturonan degradation increased to seven PGs (Bcpg2, Bcpg4, Bcpg5, Bcpg6, Bcpgx1 and two other exo-PGs), four pectate lyases, four pectin lyases and a pectin-esterase. Genes encoding enzymes that target xyloglucan were upregulated at 24 hpi, included β-glucoside gluco-hydrolase, three beta-glucosidases and BcXYG1 (Table S6). In addition, genes encoding enzymes for xylan degradation were also upregulated at 24 hpi, including Bcxyn11A, Bcxyn11C and three other xylanases. Genes encoding secreted enzymes acting on rhamnogalacturonans backbone, xylan backbone, mannans, cellulose, and side-chains were also upregulated at 24 hpi. These DEGs included glycoside hydrolases, rhamnogalacturonases, beta-glucosidase, mannosidases, glucanases and cello-bio-hydrolase, arabino-furanosidase and beta-galactosidases, among others. In addition, several peptidases were upregulated at 8 and 24 hpi. Taken together, these results support the important role played by these fungal enzymes during *P. patens* infection.

Surprisingly, genes encoding enzymes involved in botcinic acid synthesis were downregulated at 8 and 24 hpi, indicating higher expression levels in fungi growing on PDA medium. However, when DEGs expressed *in planta* were compared, several genes involved in botcinic acid production were upregulated at 24 hpi compared to 8 hpi, including Bcboa3, Bcboa4, Bcboa5, Bcboa6, Bcboa7 and Bcboa9 (Table S3; Figure 3). Other genes that increased *in planta* during the progression of infection (24 compared to 8 hpi), included those encoding cutinases, PGs, a pectin lyase, Bcnep2, and MSF transporters, among others (Table S3).

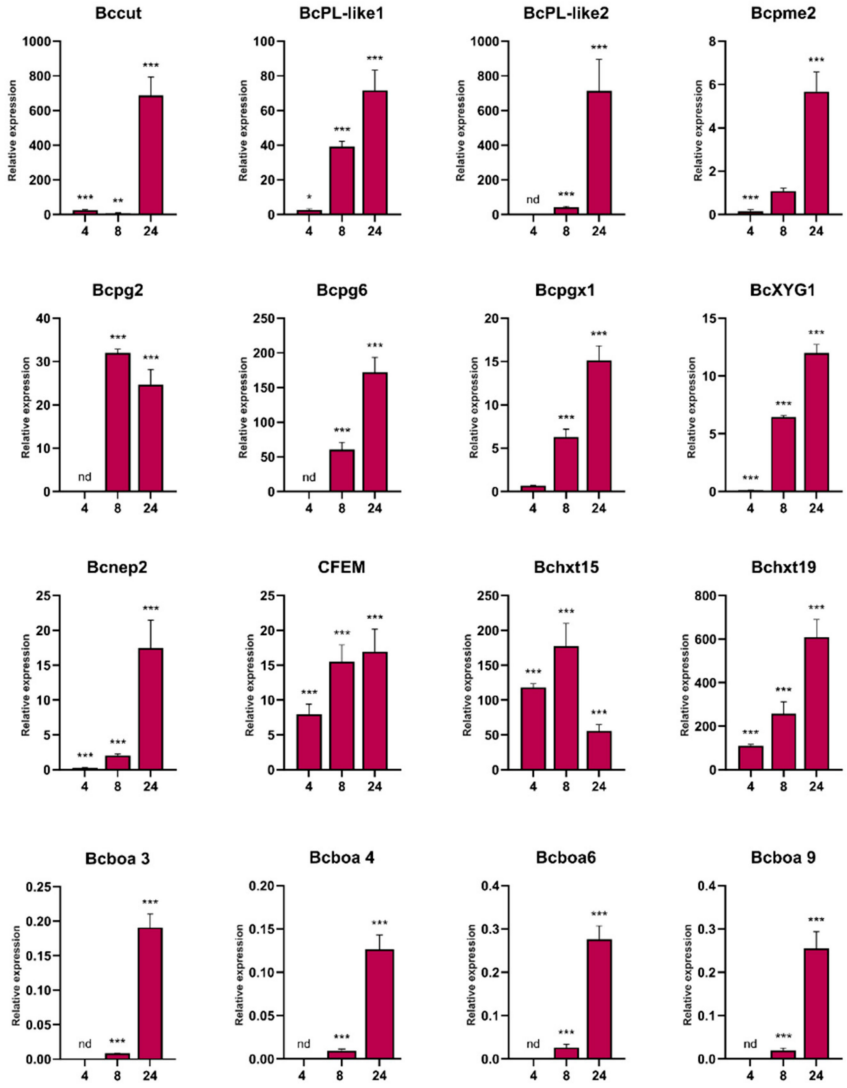

Figure 3. Validation of *B. cinerea* differentially expressed genes during *P. patens* infection by quantity reverse transcription RT-qPCR at 4, 8 and 24 hpi. The expression levels of *B. cinerea* genes infecting *P. patens* at the indicated time points are relative to the level of expression of *B. cinerea* grown in PDA. Genes are represented by the corresponding abbreviation as indicated in Table S1. *BctubB* was used as the reference gene. Results are reported as means ± standard deviation (SD) of three samples for each treatment. Asterisks indicate a statistically significant difference between *B. cinerea* grown in *P. patens* and in PDA (Students *t*-test, * $p < 0.5$, ** $p < 0.01$; *** $p < 0.005$). Abbreviation: nd: no data.

3.3. Genes Encoding B. cinerea Virulence Factors and Candidate Effectors Are Upregulated during Moss Infection

In addition to CWDEs genes, other genes encoding virulence factors and known effectors were present among the upregulated *B. cinerea* genes during *P. patens* infection. These included the cell death inducing factors Bcnep1 and Bcnep2, the necrosis-inducing xylanase Xyn11A and xyloglucanase BcXYG1, as well as the necrosis inducing Bcpg2. Several genes encoding CFEM domain-containing proteins were also upregulated during moss infection, including CFEM1, which is important for pathogenesis (Table S6). Genes encoding two secreted CalciNeurine-Dependant (CND1 and CND3) genes with putative virulence functions, peptidases and proteinases were also upregulated in moss tissues, including secreted aspartic proteinase (Bcap9), peptidases and a metalloproteinase (Deuterolysin; Bcmp1). We searched for effectors among the upregulated *B. cinerea* DEGs encoding secreted fungal proteins, using EffectorP (Table S6). Eight candidate secreted effectors were identified, including Pectin lyase (Bcin04g00470), BcNEP1, the small secreted BcSSP2A, two ribonu-

cleases (Bcin07g03720 and Bcin05g04720), and three hypothetical proteins. One of these hypothetical protein-encoding genes, Bcin04g03920, showed very high expression levels at 8 and 24 hpi. These results indicate the involvement of virulence factors during *P. patens* infection, and suggest that candidate secreted effectors may interfere with plant defenses.

3.4. Comparison of B. cinerea DEGs during the Interaction with P. patens and Three Different Angiosperms

The expression pattern of *B. cinerea* genes encoding virulence factors and other proteins involved in the infection process of *P. patens* was compared with gene expression pattern during angiosperms infection, using available RNAseq data that were reanalyzed in this work. A summary of the number of reads mapped to the *B. cinerea* genome from each biological replicates in the different plant hosts is provided in Table S2. The percentage of reads that uniquely mapped to the *B. cinerea* genome relative to the total number of reads, in each sample, were in general similar between species, except for *P. patens* at 4–8 hpi and *L. sativa* at 24 hpi (lower percentage of reads), and *S. lycopersicum* at 23 hpi (higher percentage of reads). The number of *B. cinerea* genes targeted by these reads and the number of genes that passed FDR ≤ 0.05, for each plant species are shown in Table S7. Based on the low number of reads and DEGs in *L. sativa* 24 hpi, this time point was discarded for further analyses. PCA showed that PC1 accounted for 38% of the total variation and segregated *P. patens* from angiosperms (Figure S3). In addition, PC1 also allows the differentiation between early time point in angiosperms (*A. thaliana* 12 hpi and *S. lycopersicum* 16 hpi) and later time points (*A. thaliana* 24 hpi, *S. lycopersicum* 23 hpi and *L. sativa* 48 hpi). This result suggests that the transcriptome state of *B. cinerea* during early infection of the different angiosperms is comparable, and a similar scenario occurs within the late time points. The number of *B. cinerea* DEGs with $|\log2\ FC| \geq 2$ in *A. thaliana* were 520 upregulated and 369 downregulated genes at 12 hpi, and 772 upregulated and 386 downregulated genes at 24 hpi. *S. lycopersicum* has 841 upregulated and 780 downregulated DEGs at 16 hpi and 1101 upregulated and 988 downregulated genes at 23 hpi, while *L. sativa* has 645 upregulated and 269 downregulated DEGs at 48 hpi (Figure 4a; Tables S8–S10).

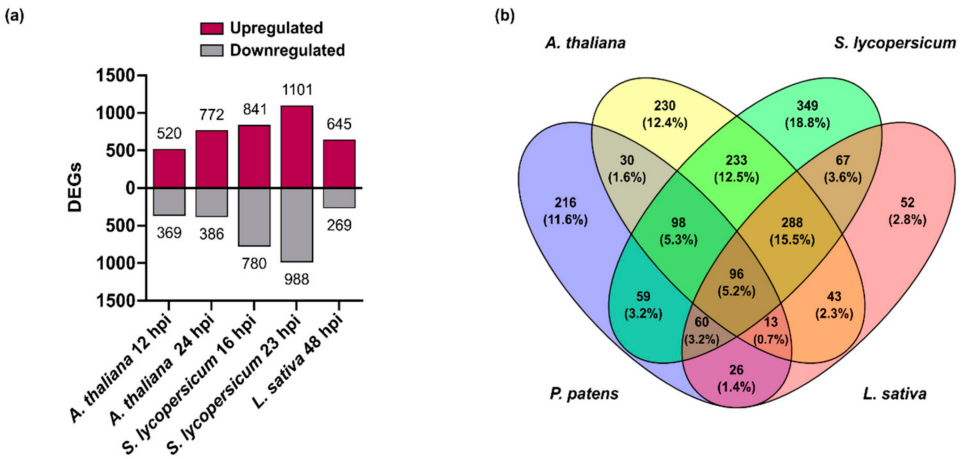

Figure 4. Differentially expressed *B. cinerea* genes during *P. patens* and angiosperms infection. (**a**) Number of differentially expressed genes (DEGs) from *B. cinerea* grown in different plant species at the indicated time points. (**b**) Venn diagram of *B. cinerea* upregulated DEGs in different plant species, showing overlap of upregulated fungal genes. *P. patens*: *B. cinerea* DEGs at 8 and 24 hpi; *A. thaliana*: *B. cinerea* DEGs at 12 and 24 hpi; *S. lycopersicum*: *B. cinerea* DEGs at 16 and 23 hpi; and *L. sativa*: *B. cinerea* DEGs at 48 hpi. For the Venn diagram, DEGs had log2 FC ≥ 2, FDR ≤ 0.05, and were expressed differentially in at least one time point for each plant species condition.

We first centered our analysis in the upregulated *B. cinerea* DEGs and show that 96 DEGs were commonly upregulated in all hosts, while 216 and 288 DEGs were only upregulated in *P. patens* and in the three angiosperms, respectively (Figure 4b). The 96 com-

mon upregulated DEGs showed an expression profile that separated samples into two groups by hierarchical clustering, one comprising the early time points and a second that included the late time points of infection in the different hosts (Figure 5; Table S11).

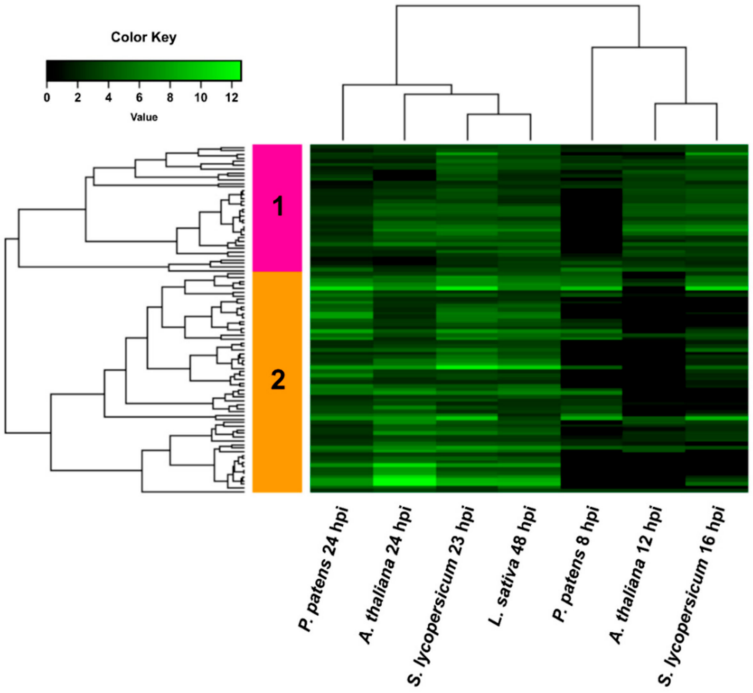

Figure 5. Heatmap of hierarchical clustering of common upregulated *B. cinerea* DEGs during infection of *P. patens* and different angiosperms. DEGs correspond to the 96 common upregulated genes of *B. cinerea* grown in all plant species. Selected DEGs had log2 FC $\geq$ 2, FDR $\leq$ 0.05, and were expressed differentially in at least one time point for each plant species. For samples where no significant difference with control was observed (FDR > 0.05) or no data was available, the log2 FC was assigned as cero. See Table S11 for complete information.

In addition, two gene clusters with different expression patterns were identified; cluster 1 included DEGs that were equally upregulated at early and late time points, while cluster 2 showed a higher number of upregulated DEGs during the late time points of infection compared with early time points. Common upregulated *B. cinerea* genes in all plant species encoded proteins with oxidoreductase activity, virulence factors (NEP2 and CFEM containing protein), transferases, transporters and hypothetical proteins, distributed in both clusters. Cluster 2 included several genes encoding secreted CAZymes such as Bcpg2, Bcpg6, pectin lyases, pectate lyase, rhamnogalacturonan acetyl-esterase, α-L-rhamnosidase, α-galactosidase, β-galactosidase, α-N-arabino-furanosidase, and Bcxyn11A. Based on this result, we looked into more detail to the expression pattern of genes encoding predicted secreted proteins of *B. cinerea* during *P. patens* and angiosperm infection (Figure 6; Table S12). Hierarchical clustering grouped the expression pattern of secretome-encoding genes into a group that included the late time points of angiosperms, and a second group including both time points of *P. patens* and the early time points of angiosperms. In addition, clustering identified genes with three expression patterns, cluster 1 has the highest number of upregulated *B. cinerea* DEGs. We focused in this cluster and observed that *B. cinerea* DEGs were detected in some but not all hosts. Expression patterns of fungal DEGs were similar during infection of *S. lycopersicum* 23 hpi and *L. sativa* 48 hpi, while expression profiles of fungal genes in angiosperms and *P. patens* differ at late infection stages.

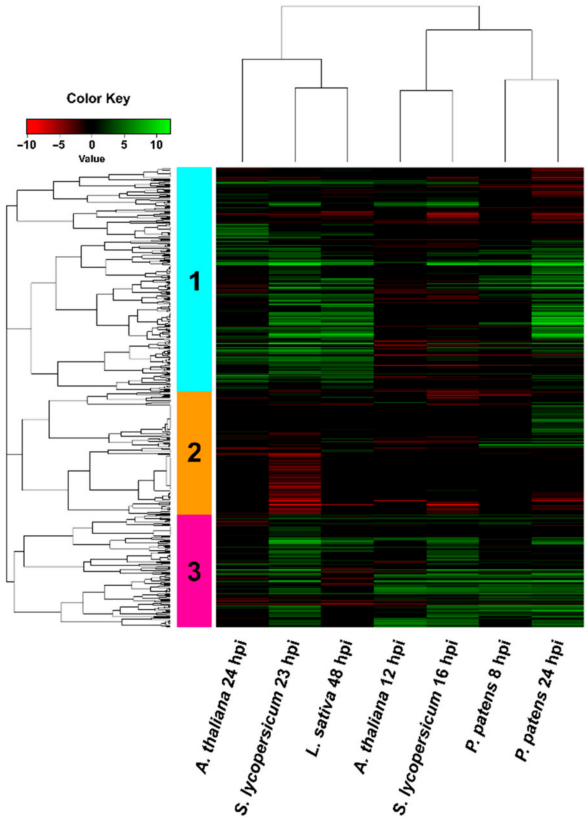

Figure 6. Hierarchical clustering (heat map) showing genes encoding secreted *B. cinerea* proteins during infection of *P. patens* and different angiosperms. Only DEGs that passed FDR $\leq$ 0.05 were considered in the analysis. For samples where no significant difference with control was observed (FDR > 0.05) or no data was available, the log2 FC was assigned as cero. See Table S12 for complete information.

Cluster 1 also included DEGs that are commonly upregulated in all plant species such as the previously mentioned Bcpg2, Bcpg6, pectate lyase, pectin lyase and other CAZymes, which were among the highest upregulated DEGs in all plant species. In addition, several CAZymes genes were only upregulated at late time points in all plant species except *A. thaliana*, including genes encoding endoglucanases, endo-β-mannosidase, rhamnogalacturonase, α-L-arabino-furanosidase, a cellobiohydrolase, a glycoside hydrolase and a xylanase. Finally, a small group of upregulated DEGs that encode putative secreted carboxylic ester hydrolase and hypothetical proteins were present at late time points in angiosperms and not in *P. patens*. Inversely, a group of upregulated DEGs present in *P. patens* at 24 hpi were not differentially expressed in angiosperms, including genes encoding β-glucoside gluco-hydrolase, endo-1,4-beta-xylanase (BcXyn11C), carboxylic ester hydrolase, peroxidase, and an exo-PG, among others.

We further analyzed in more detail the 216 *B. cinerea* DEGs that were only upregulated in *P. patens* and showed very low or no expression in angiosperms. These DEGs were distributed in two clusters (Figure 7, Table S13): cluster 1 contained upregulated *B. cinerea* DEGs at 8 hpi and 24 hpi, while cluster 2 was mainly composed of upregulated DEGs at 24 hpi.

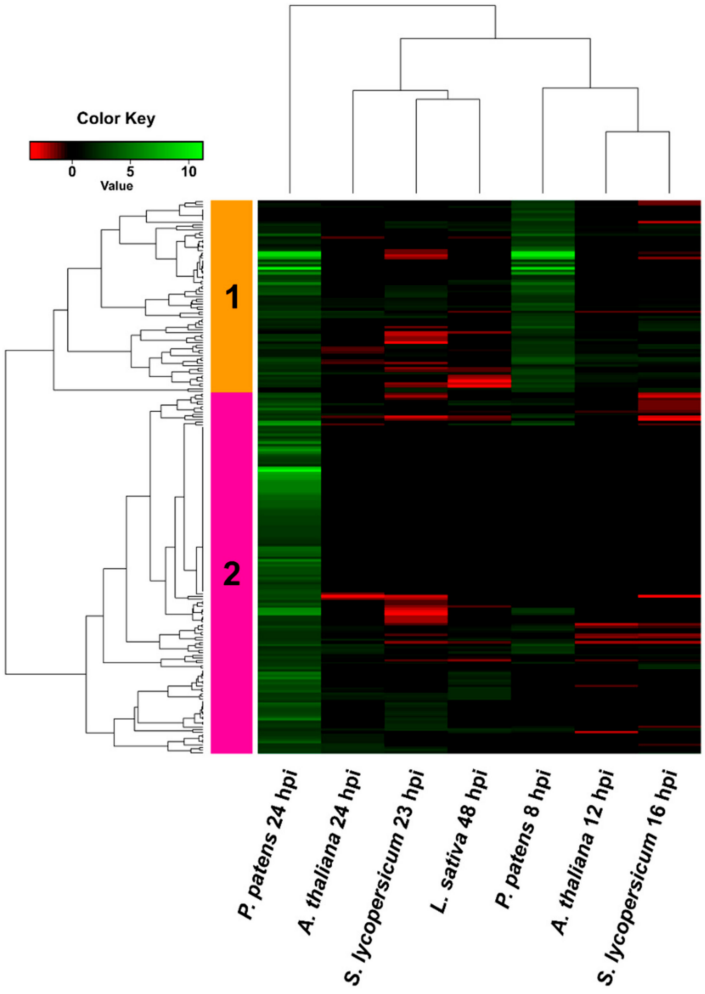

Figure 7. Hierarchical clustering (heat map) showing *B. cinerea* genes only upregulated in *P. patens*. DEGs correspond to the 216 genes that were only upregulated when growing in *P. patens*. Selected DEGs had log2 FC $\geq$ 2, FDR $\leq$ 0.05, and were expressed differentially in at least one time point for each plant species. For samples where no significant difference with control was observed (FDR > 0.05) or no data was available, the log2 FC was assigned as cero. See Table S13 for complete information.

In cluster 1, four upregulated DEGs showed very high expression levels at 8 and 24 hpi, and encoded a D-malate dehydrogenase, a glyceraldehyde-3-phosphate dehydrogenase (GAPDH), a D-glycerate 3-kinase and a MFS transporter. Interestingly, 22 additional genes encoding putative fungal MSF transporters were upregulated in *P. patens* and in almost all cases expression was not detected or was repressed in angiosperms. Among other upregulated *B. cinerea* genes that were only upregulated in *P. patens* we found carboxylic ester hydrolases, cellobiose dehydrogenase, beta-glucosidases, a peroxidase, a polyketide synthase (BcPks8), and a high number of hypothetical proteins. Additionally, six Zn(2)-C6 transcription factors, including the BcGaaR GalA regulator involved in D-galacturonic acid utilization by *B. cinerea* [47], were upregulated during *P. patens* infection and not in angiosperms. Interestingly, Bcaba2 encoding a Cytochrome P450 monooxygenase, which is an ABA biosynthesis cluster protein, was only upregulated at 24 hpi in *P. patens* tissues.

Among the 288 *B. cinerea* DEGs that were only upregulated in angiosperms (Figure 4b), we focused on those that were not detected or showed very low expression levels in *P. patens* (Figure 8; Table S14). Interestingly, among them we detected most genes of the botrydial gene cluster at least at one time point, including Bcbot1, Bcbot3, Bcbot4 and Bcbot5. In addition, Bcbot2 was highly upregulated in all angiosperms, while in *P. patens* an

induction below log2 FC 2 was observed at 24 hpi. The major positive regulator of botrydial synthesis, the transcription factor Bcbot6 (Bcin12g06420), and a dehydrogenase (Bcbot7; Bcin12g06430), were only upregulated in the three angiosperms. Other fungal upregulated DEGs that were only detected in angiosperms included genes encoding glutaredoxins, GSTs, superoxide dis-mutases (SOD), other oxidoreductase related proteins, carboxyl ester hydrolases, transcription factors including Nmra and bZIP, and hypothetical proteins, among others. Taken together, these results reveal that several *B. cinerea* genes that play important roles in host infection have different expression patterns in the plant species analyzed.

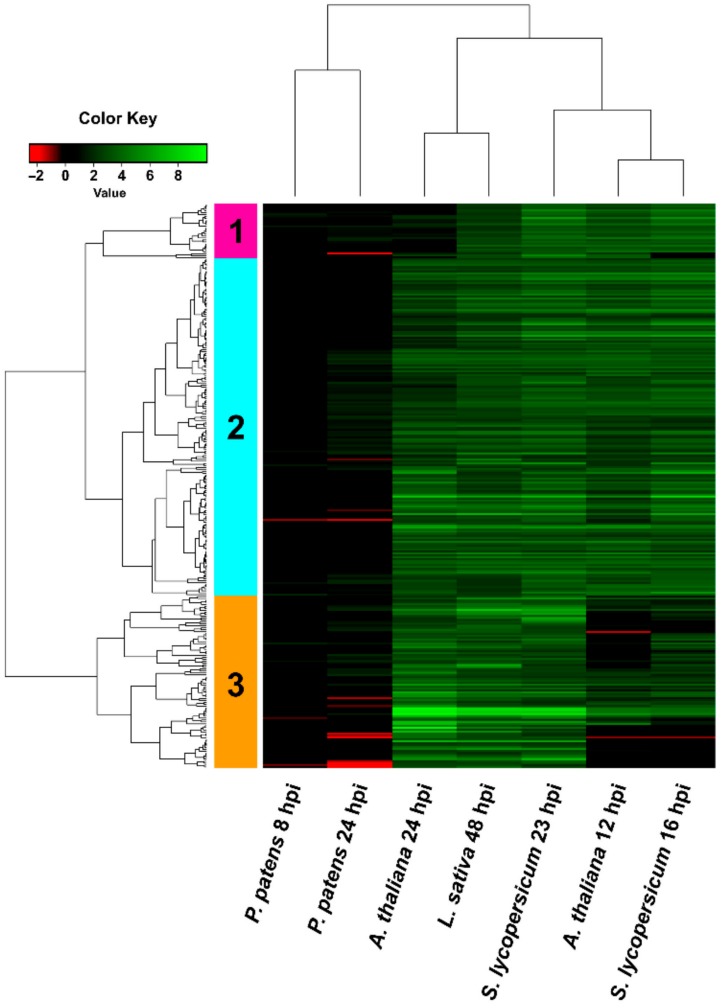

Figure 8. Hierarchical clustering (heat map) showing *B. cinerea* DEGs only upregulated in angiosperms. DEGs correspond to the 288 genes that were upregulated in all angiosperms and not in *P. patens*. Selected DEGs had log2 FC $\geq$ 2, FDR $\leq$ 0.05, and were expressed differentially in at least one time point for each plant species. For samples where no significant difference with control was observed (FDR > 0.05) or no data was available, the log2 FC was assigned as cero. See Table S14 for complete information.

Finally, we looked into *B. cinerea* DEGs that were only downregulated in *P. patens* or in angiosperms (Figure S4, Tables S15 and S16). In total 111 and 93 fungal DEGs were only downregulated in *P. patens* or angiosperms, respectively. From those, only two genes that were downregulated in angiosperms showed increased expression in *P. patens* that was close to Log2 FC=2 (Bcin06g02530: DUF2235 domain-containing protein and Bcin05g05110: hypothetical protein). In contrast, several genes that were downregulated in *P. patens* were upregulated in all angiosperms, including Bcbot4, and two genes encoding a hydrolase

EHN domain-containing protein and a PKS. Other DEGs that were downregulated in *P. patens* and showed increased expression in some of the angiosperms included those encoding the aspartic proteinase Bccap1, two ABC transporters, an acyl transferase and several hypothetical proteins. Finally, Bcboa3-5 were downregulated in *P. patens* and showed no expression in most angiosperms. Taken together, our results show that common and differential expression patterns of genes with roles in virulence and infection exist between *P. patens* and angiosperms.

4. Discussion

Transcriptional profiling during the *B. cinerea* infection process has been performed in several angiosperms [38–40,48–51]. However, no information related to the molecular mechanisms used by *B. cinerea* during moss invasion is available. Mosses interact with a variety of fungal pathogens in nature and under controlled conditions in the laboratory [52,53]. To get insights into *B. cinerea* infection and virulence strategies developed during moss colonization, we performed a global expression profiling of different infection stages. Expression patterns of upregulated genes and GO enrichment analysis indicated that infection of moss tissues by *B. cinerea* depends on ROS generation and detoxification, transporter activities, plant cell wall degradation and modification, toxin production and probable plant defense evasion by effector proteins. Moreover, a comparison with available RNAseq data during angiosperm infection, including *A. thaliana*, *S. lycopersicum* and *L. sativa*, suggests that *B. cinerea* has probably virulence and infection functions that are used in all hosts, while others are more specific to *P. patens* or angiosperms.

ROS production is important for *B. cinerea* virulence during plant invasion and increased levels of ROS in plant cells are beneficial to the pathogen, leading to accelerated colonization of host tissue [8]. We have previously observed that during *P. patens-B. cinerea* interaction, ROS are produced in *P. patens* cells after hyphal contact, probably resembling an oxidative burst response, and also in hyphal tips in contact with moss cells [26]. Similarly, in angiosperms, generation of H_2O_2 in the tip of the penetration pegs that breach the cuticle has been described [54]. ROS might assist in host invasion by providing substrates for oxidases that can modify the cuticle [9]. Moreover, endogenous ROS play crucial roles in *B. cinerea* conidial germination and host penetration [55,56]. Here, we show that oxidoreductase activities are enriched in upregulated fungal genes during early *P. patens* infection (4 hpi), including genes encoding BcniaD and BcniiA, that are further upregulated during the entire time course of infection analyzed. Similarly, *BcniaD* and *BcniiA* are both upregulated during *A. thaliana*, *S. lycopersicum* and *L. sativa* infection, but only at late time points. The relevance of this finding needs further investigation, since the production of nitric oxide (NO) by *B. cinerea* probably promotes fungal colonization of the plant tissue, although nitrate reductase is not the main system responsible for the production of NO in this pathogen [57]. Oxidoreductase processes continued during *P. patens* infection at 8 and 24 hpi, and genes encoding laccase, quinone reductase, GMC oxidoreductase, peroxidases, glutathione peroxidase (Bcgpx3), GST, and different types of oxidoreductases were upregulated. Laccase, quinone reductase and GMC oxidoreductase can be a source of ROS production needed for *B. cinerea* infection, while peroxidases, glutathione peroxidases as well as other detoxification enzymes may act to control ROS levels [58]. In addition, Bcin12g02910 encoding a cellobiose dehydrogenase, that is secreted at early time points of infection and could be responsible for ROS generation by *B. cinerea* [59], was upregulated during *P. patens* infection. Similarly, during *B. cinerea* colonization of *A. thaliana*, *S. lycopersicum* and *L. sativa*, a high number of ROS related genes were upregulated, including peroxidases, GSTs, catalases, SODs and different oxidoreductases. Consistently, oxidoreductase activities in the secretome of several *Botrytis* species, including *B. cinerea*, represented 10% of the total secretome, highlighting the importance of these activities during fungal infection [48].

ROS production contribute to host cell death, favoring invasion and further colonization of *B. cinerea* in the dead host tissue [60]. This pathogen facilitates host cell death by

producing toxins, including botrydial and botcinic acid [17,18]. We only observed increased expression of fungal genes involved in botcinic acid production, including Bcboa3-7 and Bcboa9, during *P. patens* infection when we compared 24 hpi with 8 hpi, suggesting the involvement of this toxin in moss infection. Interestingly, genes encoding the biosynthesis enzymes of botrydial [61], were upregulated in *A. thaliana*, *S. lycopersicum* and *L. sativa*, while in *P. patens* only Bcbot2 encoding the sesquiterpene cyclase showed a slight induction. Other genes of the botrydial cluster, including Bcbot1, Bcbot3 and Bcbot4 that encode cytochrome P450 proteins, and Bcbot5 encoding a putative acetyl transferase, were not detected or were repressed. In addition, the major positive regulator of botrydial synthesis Bcbot6 that encode a putative Zn(II)2Cys6 transcription factor, and the dehydrogenase Bcbot7 that might be involved in the conversion of botrydial to dihydrobotrydial [62,63], were only upregulated in angiosperms and not in *P. patens*. The fact that botrydial related genes were not upregulated during moss infection was not expected. However, it was previously shown that mutations in botrydial biosynthetic genes and the Bcbot6 regulator did not alter the development and virulence of *B. cinerea*, which is in accordance with a redundant role of botcinic acid and botrydial in virulence of this fungal pathogen [64,65]. Other genes encoding secreted fungal proteins with necrosis-inducing activity such as NEP1 and NEP2 [66], were upregulated in *P. patens* and most analyzed angiosperms. An HR-like response with similar features as in angiosperms has been observed in *B. cinerea*-infected *P. patens* tissues [26], and these proteins may contribute to induce PCD in moss for fungi benefit. In addition, upregulation of several hydrolase-encoding genes during *P. patens* infection, such as Bcpg2, Xyn11A and xyloglucanase BcXYG1, with known cell death inducing activities in angiosperms [43,67–69], may contribute to moss cell death and facilitate fungal infection. These three hydrolases are able to induce a necrotic response independent of their catalytic activity, and Bcpg2 and Xyn11A are commonly upregulated genes in all analyzed plant hosts.

As expected for a pathogen with a necrotrophic lifestyle, we show that a large number of *B. cinerea* genes upregulated during *P. patens* and angiosperms infection, encode enzymes with hydrolytic activities. Consistently, hydrolase activity was reported as the most common molecular function of the *B. cinerea* secretome and other *Botrytis* species (approximately 25% of the total secretome) [48]. The production of extracellular proteins is shown to be regulated at the transcriptional level, suggesting a fine-tuning of *B. cinerea* secretome according to conditions that contribute to accomplish successful infection [70]. A high proportion of the upregulated fungal genes in *P. patens* and angiosperms encode CAZymes, including cutinases and PCWDEs with a role in host tissue breakdown and pathogenesis. Many of these enzymes were also detected in different studies of *B. cinerea* secretomes [59,70–73]. These extracellular enzymes are potential virulence factors that could play important roles in facilitating hyphal growth by softening the host tissues and converting complex plant material available for consumption [74]. Our expression profiles showed that the highest proportion of CAZymes genes were upregulated at late time points of infection, which is consistent with higher maceration rates and cell death of plant tissues, which are needed for effective colonization.

The initial interaction between plants and *B. cinerea* occurs at the plant cuticle, and upregulation of three cutinase-encoding genes in moss tissues suggests that as in other plants [9,15,16,75], these enzymes play a role in breaching *P. patens* cuticle for host penetration. Penetration pores were detected on the surface of *P. patens* cell walls and in intercellular spaces that are colonized by infection hyphae that subsequently invaded leaf cells [27]. Cutinases may be involved in gametophore colonization since fungal penetration pegs penetrate the tissues directly through leaf cell walls [53], and protonema cells have no cuticle [76]. In addition, some *B. cinerea* cutinases show high homology to acetylxylanesterases [77], and could be involved in degradation of xylans in moss tissues. Moreover, the expression pattern of cutinases varied among angiosperms infection and while BccutB was only upregulated in *S. lycopersicum*, other cutinases were expressed in more than one plant. Consistently, previous studies have shown that the expression

levels of these enzymes depended on the host tissues [77]. Our results also revealed the presence of common upregulated genes encoding secreted CAZymes in all host plants, as well as CAZymes genes that were detected in some but not all plants hosts. Bcpg2, Bcpg6, two pectin lyases, a pectate lyase, rhamnogalacturonan acetyl-esterase, α-L-rhamnosidase, α-galactosidase, β-galactosidase, α-N-arabino-furanosidase, and Bcxyn11A were upregulated in all plant host. In accordance, PGs, pectin lyases, pectate lyases and Bcxyn11A are essential for virulence and fungal colonization into host tissues [69,75,77,78]. *P. patens* infection showed the highest number of upregulated genes encoding pectin and pectate lyases (8 genes), followed by *S. lycopersicum* infection (6 genes), and finally *A. thaliana* and *L. sativa* infection (4 genes). Moreover, several upregulated DEGs were present in *P. patens* but were not detected in angiosperms, including genes encoding β-glucoside gluco-hydrolase, BcXyn11C, a GPI anchored protein; poly(β-D-mannuronate) lyase, an exo-PG, a glycoside hydrolase and a cellobiose dehydrogenase, among others. In addition, several *B. cinerea* DEGs appeared to be preferentially expressed in one or two specific angiosperms. Remarkably, induced expression of secreted CAZymes could be related to cell wall composition in different plant species [77]. The cell walls of mosses and angiosperms are mainly composed of the same classes of polysaccharides with the exception of xylogalacturonan, which has not been detected in *P. patens*, and some differences exist inside chain composition and structure [79,80]. HG, β-1,4-galactan, α-1,5-arabinan, desterified pectin and RG-I have been identified in *P. patens* and some moss species may contain an RG-II-like polysaccharide [80]. In *P. patens*, the main upregulated *B. cinerea* DEGs were related to pectin homogalacturonan and XyG backbone-degrading enzymes. Furthermore, upregulation of Bclga1, Bclgd1 and Bcgar2 involved in the catabolic pathway of the final product released from pectin degradation, D-galacturonic acid, suggest that pectin depolymerizing and utilization of D-galacturonic acid is important as a carbon nutrient for *B. cinerea*, allowing efficient colonization of *P. patens* tissues. BcGaaR encoding a Zn2Cys6 transcription factor involved in D-galacturonic acid utilization [47], was also upregulated in moss tissues. *B. cinerea* mutants in Bclga1, Bclgd1 and Bcgar2, have affected virulence on *N. benthamiana* and *A. thaliana* leaves, but not on *S. lycopersicum*, indicating host-specific virulence [81]. Interestingly, this difference was correlated with the amount of D-galacturonic acid present in these hosts since *S. lycopersicum* has lower D-galacturonic acid content than *A. thaliana* and *N. benthamiana* leaves. At 24 hpi, upregulated DEGs encoded enzymes involved in HG, XyG backbone, RG-I backbone, xylan backbone, mannans, cellulose, and side-chains/adducts degradation and modification. Upregulation of Bcpme2 in *P. patens* and most angiosperms may facilitate the action of PGs by demethylating pectin to pectate. *B. cinerea* cellulases and hemi-cellulases (xylanases)-encoding genes were also upregulated during *P. patens* and angiosperms colonization. BcAra1 encoding an endo-arabinanase that carries out the breakdown of arabinan [82], was upregulated at late time points during *P. patens*, *A. thaliana* and *S. lycopersicum* infections. Interestingly, BcAra1 plays an important role during infection of *A. thaliana* where mutants provoke smaller lesions, while in *N. benthamiana* lesion size did not differ compared to the wild type strain, indicating that Bcara1 plays a host-dependent role in the virulence of *B. cinerea* [82]. Expression levels of BcAra1 in *N. benthamiana* were much lower than in *A. thaliana* indicating regulation at the transcriptional level that serves as a determinant of disease progression. Taken together, our results are consistent with host-dependent expression of genes related to cell-wall degradation and modification by *B. cinerea*.

Two of the highest expressed *B. cinerea* genes during *P. patens* infection encoded a malate dehydrogenase and GAPDH. Interestingly, malate dehydrogenase catalyzes the reversible conversion of oxalacetate and malate, and oxalacetate is a precursor of the pathogenicity factor oxalic acid [83]. Oxalic acid facilitates *B. cinerea* infection through different mechanisms, including enhancement of PGs activity to promote cell wall degradation, suppression of the plant oxidative burst, induction of HR, inhibition of plant–protection enzymes, and alteration of the cellular redox status in the plant [12]. Consistently, malate dehydrogenase has been identified in the secretome of different *B. cinerea* strains [84].

GAPDH functions in the glycolytic cycle and it may serves as a virulence factor as has been proposed for several pathogenic fungi [85]. In addition, other virulence genes were upregulated during *P. patens* infection, including BcCFEM1, which has a putative GPI modification site and is required for virulence and tolerance to osmotic and cell wall stress [43]. Other genes encoding CFEM domain-containing proteins were upregulated in the different hosts, which is consistent with their potential role in pathogenicity [86,87]. Upregulated genes encoding secreted proteins with putative virulence functions during *P. patens* and angiosperm infection included different CND proteins. The calcium/calcineurin signaling pathway controls the botrydial gene cluster, and calcineurin phosphatase has an essential role in virulence and was shown to be involved in *B. cinerea* appressorium formation [10,88]. Secreted proteinases and peptidases have been reported as virulence factors involved in host-tissue invasion and pathogenicity, and different types of fungal proteases were upregulated in *P. patens* and angiosperms, including aspartic proteinases [89]. Consistently, a high number of proteases were found in different *B. cinerea* secretomes [42,48,59]. Several studies have demonstrated the role of secreted effector genes in the establishment of *B. cinerea* infection via suppression of plant defense [42]. We identified several candidate effectors genes that were upregulated during *P. patens* infection and could interfere with moss defenses. They include known effectors such as BcNEP1 and BcSSP2 [90], two ribonucleases and three hypothetical proteins, including Bcin04g03920, which is highly expressed in *P. patens*, *A. thaliana* and *S. lycopersicum*. Ribonucleases are known effectors in other necrotrophic pathogens, such as *Blumeria graminis*, where they bind to host ribosomes and inhibit the action of plant ribosome-inactivating proteins that are known components of plant immune responses that lead to host cell death [91].

Plants perceive pathogens by detecting pathogen-associated molecular patterns (PAMPs) through pattern recognition receptors [92]. Several secreted enzymes of *B. cinerea* are recognized by plant leucine-rich repeat receptors, including PGs [93], and BcXYG1 [42], leading to activation of plant defense. Interestingly, *P. patens* induces rapidly the expression levels of a high number of genes encoding these type of receptors during *B. cinerea* infection [28]. However, further research is needed to understand if some of these receptors recognize PGs and other fungal PAMPs in moss tissues. Moreover, we observed that two genes encoding putative plant pectin methyl-esterase inhibitor were upregulated in *P. patens* after *B. cinerea* colonization [28]. These inhibitors could be involved in making the wall more resistant to degradation by fungal enzymes by increasing methylated pectin in the cell wall [94]. In response to plant defense activation, *B. cinerea* has developed different strategies to interfere with plant immunity, including secretion of hydrolases to detoxify antifungal secondary metabolites produced by the host. *B. cinerea* is capable of degrading stilbene phytoalexins [95] from grapevines, α- tomatine [96] from *S. lycopersicum*, and metabolize scopoletin from tobacco [97]. Moreover, cruciferous phytoalexins were detoxified by *B. cinerea* via either oxidative degradation or hydrolysis [98]. In addition, upregulation of genes encoding peptidases and proteases during *P. patens* and angiosperms infection, leads to amino acids release for fungal growth, degradation of plant cell wall proteins and defense proteins [59]. Plant pathogens, have transporters, such as ATP-binding cassette (ABC) and MFS transporters, involved in the excretion of plant compounds that are toxic for the pathogen and are produced by the host as a defensive strategy [99]. These transporters contribute to virulence and are especially useful for pathogens with a broad host range [99], including *B. cinerea*. Here, we show that during *P. patens* infection, *B. cinerea* induces the expression of a high number of genes encoding putative MFS transporters, some of which are very highly induced (Bcin07g06720 and Bcin09g05570). Interestingly, most of these MSF-transporter encoding genes were only upregulated during *P. patens* infection and not in angiosperms. The large number of MSF transporters gene members in the *B. cinerea* genome, 286 and 282 genes in strain T4 and strain B05.10, respectively, highlight their importance in counteracting the effect of antimicrobial compounds [100]. Consistently, a MFS and an ABC transporter contribute to virulence in *B. cinerea* and increase tolerance to glucosinolates and camalexin respectively, which are produced by *A. thaliana* as defensive

compounds [100,101]. Moreover, Bcmfs1 is involved in tolerance to antifungal compounds such as camptothecin and cercosporin [102]. Our results suggest that MFS transporters could play an important role in *P. patens*–*B. cinerea* interaction, although further studies are needed to reveal whether these transporters are involved in detoxification of moss specific metabolites. Until now, only few compounds with antifungal activity have been identified in *P. patens* [103], and due to their requirement in improved defenses to biotic challengers during plant colonization, these metabolites are of particular interest.

5. Conclusions

Our transcriptional profiling of *B. cinerea*-infected plants demonstrated that common molecular mechanisms were involved in fungal virulence and the infection process in *P. patens* and angiosperms. However, differences in expression patterns of fungal CAZymes genes and putative MFS transporter genes between hosts revealed that some infection functions are specific to *P. patens* or angiosperms infections. A deeper understanding of the plant cell wall targets, as well as the identity of metabolites with antifungal activities of the encoded proteins by *P. patens*, will certainly increase our knowledge of bryophyte-fungal interactions. In addition, the use of *B. cinerea* mutants will contribute to uncover the molecular pathogenic mechanisms and regulatory network used by this pathogen during moss infection and their involvement during coevolution of pathogens with land plants.

Supplementary Materials: The following are available online at https://www.mdpi.com/2309-608X/7/1/11/s1, Figure S1: *B. cinerea* infection of *P. patens* tissues. Infection progress during time is shown; (a) spore germination at 4 hpi, (b) germ tubes elongation at 8 hpi, (c) proliferation of mycelium at 24 hpi, (d) appresorium formation at 8 hpi, (e) hyphae colonizing a leaf cell, and (f) hyphae colonizing a protonemal cell. Symptom development at 8 hpi (h), 24 hpi (i) and 24 h water-treated moss colonies (g) are shown. The arrow in (d) indicate an appresorium. The scale bar in a-f represents 10 µm and 0.5 cm in g-i. Figure S2: Enriched gene ontology (GO) terms of *B. cinerea* DEGs. The top 15 enrichment GO terms were chosen according to their statistical significance (−log10 FDR). GO enrichment are shown for upregulated and downregulated *B. cinerea* DEGs at 4, 8 and 24 hpi. See Table S5 for complete information. Figure S3: Analysis of *B. cinerea* RNA-Seq data during *P. patens*, *A. thaliana*, *S. lycopersicum* and *L. sativa* infection by principal component analysis (PCA). Colored dots denote each biological replicate. Figure S4: *B. cinerea* downregulated DEGs during *P. patens* and angiosperm infection. (a) Venn diagram of *B. cinerea* downregulated DEGs in different plant species, showing overlap of fungal repressed genes. *P. patens*: sum of *B. cinerea* DEGs at 8 and 24 hpi; *A. thaliana*: sum of *B. cinerea* DEGs at 12 and 24 hpi; *S. lycopersicum*: sum of *B. cinerea* DEGs at 16 and 23 hpi; and *L. sativa*: *B. cinerea* DEGs at 48 hpi. For Venn diagram, DEGs had log2 FC ≤ -2, FDR $\leq$ 0.05, and were expressed differentially in at least one time point for each plant species condition. (b) Hierarchical clustering (heat map) showing *B. cinerea* genes only downregulated in *P. patens*. Fungal DEGs corresponds to the 111 genes that were only downregulated in *P. patens*. (c) Hierarchical clustering showing *B. cinerea* genes only downregulated in angiosperms. Fungal DEGs corresponds to the 93 genes that were only downregulated in angiosperms. Table S1: List of qPCR primers used in this study. Table S2: Summary of mapped reads of *B. cinerea* in the RNA-Seq libraries. 1–3 indicate the three biological replicates of different plants species at the indicated time points. Table S3: List of *B. cinerea* differentially expressed genes (DEGs) during *P. patens* infection at 4, 8 and 24 hpi. Table S4: Enriched gene ontology (GO) terms (over-representation) for biological processes (BP), molecular function (MF) and cell compartment (CC) at 4, 8 and 24 hpi. Table S5: Validation of RNA-Seq data by qPCR assay: correlation of log2 FC values for 16 genes obtained by RNA-Seq and qPCR. Gene name and identification, log2 fold change from RNA-seq and RT-qPCR analysis and description are provided. Table S6: List of *B. cinerea* upregulated DEGs encoding secreted proteins during infection of *P. patens* at 4, 8 and 24 hpi. Table S7: Summary of numbers of *B. cinerea* analyzed genes. Table S8: List of *B. cinerea* differentially expressed genes (DEGs) during *A. thaliana* infection at 12 and 24 hpi. Table S9: List of *B. cinerea* differentially expressed genes (DEGs) during *S. lycopersicum* infection at 16 and 23 hpi. Table S10: List of *B. cinerea* differentially expressed genes (DEGs) during *L. sativa* infection at 48 hpi. Table S11: List of common upregulated genes in all plants species. *B. cinerea* DEGs were included when log2 FC was ≥ 2 and FDR ≤ 0.05 in at least one time point of each plant species. For samples where no significant difference with control was observed (FDR > 0.05) or no data was

available, the log2 FC was assigned as cero. Table S12: List of genes encoding putative secreted *B. cinerea* proteins in *P. patens*, *A. thaliana*, *L. lycopersicum* and *L. sativa* at the indicated time points of infection. DEGs were considered when FDR was $\leq$0.05. For samples where no significant difference with control was observed (FDR > 0.05) or no data was available, the log2 FC was assigned as cero. Table S13: List of 96 *B. cinerea* DEGs that were only upregulated in *P. patens*. DEGs were considered when log2 FC was $\geq$ 2 and FDR $\leq$ 0.05 in at least one time point of each plant species. For samples where no significant difference with control was observed (FDR > 0.05) or no data was available, the log2 FC was assigned as cero. Table S14: List of 288 *B. cinerea* DEGs that were only upregulated in all angiosperms and not in *P. patens*. DEGs were considered when log2 FC was $\geq$ 2 and FDR $\leq$ 0.05 in at least one time point of each plant species. For samples where no significant difference with control was observed (FDR > 0.05) or no data was available, the log2 FC was assigned as cero. Table S15: List of 111 *B. cinerea* DEGs that were only downregulated in *P. patens*. DEGs were considered when log2 FC was ≤ -2 and FDR $\leq$ 0.05 in at least one time point of *P. patens*. For samples where no significant difference with control was observed (FDR > 0.05) or no data was available, the log2 FC was assigned as cero. Table S16: List of 93 *B. cinerea* DEGs that were only downregulated in all angiosperms and not in *P. patens*. DEGs were considered when log2 FC was ≤ -2 and FDR $\leq$ 0.05 in at least one time point of each plant species. For samples where no significant difference with control was observed (FDR > 0.05) or no data was available, the log2 FC was assigned as cero.

Author Contributions: Conceived and designed the experiments: I.P.D.L., A.A., G.R.; Performed the experiments: G.R. and L.V.; Analyzed and interpreted the data: I.P.D.L., A.A., G.R. and L.V.; Wrote the article: I.P.D.L.; participated in the drafting of this work A.A., G.R., L.V. and R.A.B.-G. All authors have read and agreed to the published version of the manuscript.

Funding: This research was funded by "Fondo Conjunto" Uruguay-México (AUCI-AMEXCID), "Agencia Nacional de Investigación e Innovación (ANII) (graduate fellowships)" Uruguay, "Programa de Desarrollo de las Ciencias Básicas (PEDECIBA)" Uruguay, and "Programa para Grupo de I + D Comisión Sectorial de Investigación Científica, Universidad de la República", Uruguay.

Acknowledgments: The authors thank Ricardo Larraya for technical assistance.

Conflicts of Interest: The authors declare no conflict of interest.

References

1. Elad, Y.; Pertot, I.; Cotes Prado, A.M.; Stewart, A. Plant hosts of *Botrytis* spp. In *Botrytis—The Fungus, the Pathogen and Its Management in Agricultural Systems*; Fillinger, S., Elad, Y., Eds.; Springer: Berlin, Germany, 2015; pp. 413–486.
2. Dean, R.; van Kan, J.A.L.; Pretorius, Z.A.; Hammond-Kosack, K.E.; Di Pietro, A.; Spanu, P.D.; Rudd, J.J.; Dickman, M.; Kahmann, R.; Ellis, J. The Top 10 fungal pathogens in molecular plant pathology. *Mol. Plant Pathol.* **2012**, *13*, 414–430. [CrossRef] [PubMed]
3. Williamson, B.; Tudzynski, B.; Tudzynski, P.; Van Kan, J.A.L. *Botrytis cinerea*: The cause of grey mould disease. *Mol. Plant Pathol.* **2007**, *8*, 561–580. [CrossRef] [PubMed]
4. Nicot, P.C.; Baille, A. Integrated Control of *Botrytis cinerea* on Greenhouse Tomatoes. In *Aerial Plant Surface Microbiology*; Springer: Boston, MA, USA, 2007; pp. 169–189.
5. Elad, Y.; Williamson, B.; Tudzynski, P.; Delen, N. *Botrytis* spp. and Diseases They Cause in Agricultural Systems—An Introduction. In *Botrytis: Biology, Pathology and Control*; Springer Science and Business Media LLC: Dordrecht, The Netherlands, 2007; pp. 1–8.
6. Fillinger, S.; Elad, Y. *Botrytis—The Fungus, the Pathogen and Its Management in Agricultural Systems*; Springer: New York, NY, USA, 2016.
7. Holz, G.; Coertze, S.; Williamson, B. The Ecology of Botrytis on Plant Surfaces. In *Botrytis: Biology, Pathology and Control*; Elad, Y., Williamson, B., Tudzynski, P., Delen, N., Eds.; Springer: Dordrecht, The Netherlands, 2007; pp. 9–27.
8. Govrin, E.M.; Levine, A. The hypersensitive response facilitates plant infection by the necrotrophic pathogen *Botrytis cinerea*. *Curr. Biol.* **2000**, *10*, 751–757. [CrossRef]
9. Van Kan, J.A. Licensed to kill: The lifestyle of a necrotrophic plant pathogen. *Trends Plant Sci.* **2006**, *11*, 247–253. [CrossRef] [PubMed]
10. Choquer, M.; Fournier, E.; Kunz, C.; Levis, C.; Pradier, J.-M.; Simon, A.; Viaud, M. *Botrytis cinerea* virulence factors: New insights into a necrotrophic and polyphageous pathogen. *FEMS Microbiol. Lett.* **2007**, *277*, 1–10. [CrossRef]
11. Gourgues, M.; Brunet-Simon, A.; Lebrun, M.-H.; Levis, C. The tetraspanin BcPls1 is required for appressorium-mediated penetration of *Botrytis cinerea* into host plant leaves. *Mol. Microbiol.* **2003**, *51*, 619–629. [CrossRef]
12. Amselem, J.; Cuomo, C.A.; Van Kan, J.A.L.; Viaud, M.; Benito, E.P.; Couloux, A.; Coutinho, P.M.; De Vries, R.P.; Dyer, P.S.; Fillinger, S.; et al. Genomic Analysis of the Necrotrophic Fungal Pathogens *Sclerotinia sclerotiorum* and *Botrytis cinerea*. *PLoS Genet.* **2011**, *7*, e1002230. [CrossRef]

13. Espino, J.; Brito, N.; Noda, J.; González, C. *Botrytis cinerea* endo-ß-1,4-glucanase Cel5A is expressed during infection but is not required for pathogenesis. *Physiol. Mol. Plant Pathol.* **2005**, *66*, 213–221. [CrossRef]
14. Kars, I.; McCalman, M.; Wagemakers, L.; Van Kan, J.A.L. Functional analysis of *Botrytis cinerea* pectin methylesterase genes by PCR-based targeted mutagenesis: Bcpme1 and Bcpme2 are dispensable for virulence of strain B05.10. *Mol. Plant Pathol.* **2005**, *6*, 641–652. [CrossRef]
15. Van Kan, J.A.L.; Klooster, J.W.V.; Wagemakers, C.A.M.; Dees, D.C.T.; Van Der Vlugt-Bergmans, C.J.B. Cutinase A of *Botrytis cinerea* is Expressed, but not Essential, During Penetration of Gerbera and Tomato. *Mol. Plant Microbe Interact.* **1997**, *10*, 30–38. [CrossRef]
16. Reis, H.; Pfiffi, S.; Hahn, M. Molecular and functional characterization of a secreted lipase from *Botrytis cinerea*. *Mol. Plant Pathol.* **2005**, *6*, 257–267. [CrossRef] [PubMed]
17. Colmenares, A.J.; Aleu, J.; Durán-Patrón, R.; Collado, I.G.G.; Hernández-Galán, R. The Putative Role of Botrydial and Related Metabolites in the Infection Mechanism of *Botrytis cinerea*. *J. Chem. Ecol.* **2002**, *28*, 997–1005. [CrossRef] [PubMed]
18. Van Kan, J.A.L.; Stassen, J.H.M.; Mosbach, A.; Van Der Lee, T.A.J.; Faino, L.; Farmer, A.D.; Papasotiriou, D.G.; Zhou, S.; Seidl, M.F.; Cottam, E.; et al. A gapless genome sequence of the fungus *Botrytis cinerea*. *Mol. Plant Pathol.* **2016**, *18*, 75–89. [CrossRef] [PubMed]
19. Manteau, S.; Abouna, S.; Lambert, B.; Legendre, L. Differential regulation by ambient pH of putative virulence factor secretion by the phytopathogenic fungus *Botrytis cinerea*. *FEMS Microbiol. Ecol.* **2003**, *43*, 359–366. [CrossRef] [PubMed]
20. Kunz, C.; Vandelle, E.; Rolland, S.; Poinssot, B.; Bruel, C.; Cimerman, A.; Zotti, C.; Moreau, E.; Vedel, R.; Pugin, A.; et al. Characterization of a new, nonpathogenic mutant of *Botrytis cinerea* with impaired plant colonization capacity. *New Phytol.* **2006**, *170*, 537–550. [CrossRef]
21. AbuQamar, S.F.; Moustafa, K.; Tran, L.S. Mechanisms and strategies of plant defense against *Botrytis cinerea*. *Crit. Rev. Biotechnol.* **2017**, *37*, 262–274. [CrossRef] [PubMed]
22. Veloso, J.; Van Kan, J.A. Many Shades of Grey in Botrytis–Host Plant Interactions. *Trends Plant Sci.* **2018**, *23*, 613–622. [CrossRef]
23. Racovitza, A. Etude systématique et bryologique des champignons bryophiles. In *Muséum National d'Histoire naturelle*; Museum National D'histoire Naturelle: Paris, France, 1959; Volume 10, p. 288.
24. Ponce De León, I.; Oliver, J.P.; Castro, A.; Gaggero, C.; Bentancor, M.; Vidal, S. *Erwinia carotovora* elicitors and *Botrytis cinerea* activate defense responses in *Physcomitrella patens*. *BMC Plant Biol.* **2007**, *7*, 52. [CrossRef]
25. Krings, M.; Taylor, T.N.; Hass, H.; Kerp, H.; Dotzler, N.; Hermsen, E.J. Fungal endophytes in a 400-million-yr-old land plant: Infection pathways, spatial distribution, and host responses. *New Phytol.* **2007**, *174*, 648–657. [CrossRef]
26. Ponce De León, I.; Schmelz, E.A.; Gaggero, C.; Castro, A.; Álvarez, A.; Montesano, M. *Physcomitrella patens* activates reinforcement of the cell wall, programmed cell death and accumulation of evolutionary conserved defence signals, such as salicylic acid and 12-oxo-phytodienoic acid, but not jasmonic acid, upon *Botrytis cinerea* infection. *Mol. Plant Pathol.* **2012**, *13*, 960–974. [CrossRef]
27. Yan, H.Q.; Zhang, T.T.; Lan, S.C.; Jiang, S. Ultrastructural study on the interaction between *Physcomitrella patens* and *Botrytis cinerea*. *Plant Pathol.* **2017**, *67*, 42–50. [CrossRef]
28. Reboledo, G.; Agorio, A.; Vignale, L.; Batista-García, R.; Ponce de León, I. Transcriptional profiling reveals conserved and species-specific plant defense responses during the interaction of *Physcomitrium patens* with *Botrytis cinerea*. *Plant Mol. Biol.* **2020**. under review.
29. Ashton, N.W.; Cove, D.J. The isolation and preliminary characterisation of auxotrophic and analogue resistant mutants of the moss, *Physcomitrella patens*. *Mol. Genet. Genom.* **1977**, *154*, 87–95. [CrossRef]
30. Bolger, A.M.; Lohse, M.; Usadel, B. Trimmomatic: A flexible trimmer for Illumina sequence data. *Bioinformatics* **2014**, *30*, 2114–2120. [CrossRef] [PubMed]
31. Kim, D.; Langmead, B.; Salzberg, S.L. HISAT: A fast spliced aligner with low memory requirements. *Nat. Methods* **2015**, *12*, 357–360. [CrossRef]
32. Li, H.; Handsaker, B.; Wysoker, A.; Fennell, T.; Ruan, J.; Homer, N.; Marth, G.; Abecasis, G.; Durbin, R. 1000 Genome Project Data Processing Subgroup. The Sequence Alignment/Map format and SAMtools. *Bioinformatics* **2009**, *25*, 2078–2079. [CrossRef]
33. Liao, Y.; Smyth, G.K.; Shi, W. featureCounts: An efficient general purpose program for assigning sequence reads to genomic features. *Bioinformatics* **2013**, *30*, 923–930. [CrossRef]
34. Martini, F.; Binder, H. pcaExplorer: An R/Bioconductor package for interacting with RNA-seq principal components. *BMC Bioinform.* **2019**, *20*, 1–8. [CrossRef]
35. Robinson, M.D.; McCarthy, D.J.; Smyth, G.K. edgeR: A Bioconductor package for differential expression analysis of digital gene expression data. *Bioinformatics* **2009**, *26*, 139–140. [CrossRef]
36. Benjamini, Y.; Hochberg, Y. Controlling the false discovery rate: A practical and powerful approach to multiple testing. *J. R. Stat. Soc. Ser. B Stat. Methodol.* **1995**, *57*, 289–300. [CrossRef]
37. Livak, K.J.; Schmittgen, T.D. Analysis of relative gene expression data using real-time quantitative PCR and the $2^{-\Delta\Delta CT}$ Method. *Methods* **2001**, *25*, 402–408. [CrossRef] [PubMed]
38. Coolen, S.; Proietti, S.; Hickman, R.; Olivas, N.H.D.; Huang, P.-P.; Van Verk, M.C.; Van Pelt, J.A.; Wittenberg, A.H.; De Vos, M.; Prins, M.; et al. Transcriptome dynamics of Arabidopsis during sequential biotic and abiotic stresses. *Plant J.* **2016**, *86*, 249–267. [CrossRef]

39. De Cremer, K.; Mathys, J.; Voß, C.; Froenicke, L.; Michelmore, R.; Cammue, B.P.A.; De Coninck, B. RNAseq-based transcriptome analysis of *Lactuca sativa* infected by the fungal necrotroph *Botrytis cinerea*. *Plant Cell Environ.* **2013**, *36*, 1992–2007. [CrossRef] [PubMed]
40. Srivastava, D.A.; Arya, G.C.; Pandaranayaka, E.P.J.; Manasherova, E.; Prusky, D.; Elad, Y.; Frenkel, O.; Harel, A. Transcriptome Profiling Data of *Botrytis cinerea* Infection on Whole Plant *Solanum lycopersicum*. *Mol. Plant Microbe Interact.* **2020**, *33*, 1103–1107. [CrossRef]
41. Raudvere, U.; Kolberg, L.; Kuzmin, I.; Arak, T.; Adler, P.; Peterson, H.; Vilo, J. g:Profiler: A web server for functional enrichment analysis and conversions of gene lists (2019 update). *Nucleic Acids Res.* **2019**, *47*, W191–W198. [CrossRef] [PubMed]
42. Heard, S.; Brown, N.A.; Hammond-Kosack, K. An Interspecies Comparative Analysis of the Predicted Secretomes of the Necrotrophic Plant Pathogens *Sclerotinia sclerotiorum* and *Botrytis cinerea*. *PLoS ONE* **2015**, *10*, e0130534. [CrossRef] [PubMed]
43. Zhu, W.; Ronen, M.; Gur, Y.; Minz-Dub, A.; Masrati, G.; Ben-Tal, N.; Savidor, A.; Sharon, I.; Eizner, E.; Valerius, O.; et al. BcXYG1, a Secreted Xyloglucanase from *Botrytis cinerea*, Triggers Both Cell Death and Plant Immune Responses. *Plant Physiol.* **2017**, *175*, 438–456. [CrossRef] [PubMed]
44. Cove, D.J.; Knight, C.D.; Lamparter, T. Mosses as model systems. *Trends Plant Sci.* **1997**, *2*, 99–105. [CrossRef]
45. Zhang, L.; Thiewes, H.; Van Kan, J.A. The d-galacturonic acid catabolic pathway in *Botrytis cinerea*. *Fungal Genet. Biol.* **2011**, *48*, 990–997. [CrossRef]
46. Mohnen, D. Pectin structure and biosynthesis. *Curr. Opin. Plant Biol.* **2008**, *11*, 266–277. [CrossRef]
47. Zhang, L.; Lubbers, R.J.; Simon, A.; Stassen, J.H.; Ribera, P.R.V.; Viaud, M.; Van Kan, J.A. A novel Zn2Cys6transcription factor BcGaaR regulates D-galacturonic acid utilization in *Botrytis cinerea*. *Mol. Microbiol.* **2016**, *100*, 247–262. [CrossRef] [PubMed]
48. Valero-Jiménez, C.A.; Veloso, J.; Staats, M.; Van Kan, J.A. Comparative genomics of plant pathogenic Botrytis species with distinct host specificity. *BMC Genom.* **2019**, *20*, 1–12. [CrossRef] [PubMed]
49. Kong, W.; Chen, N.; Liu, T.; Zhu, J.; Wang, J.; He, X.; Jingqi, W. Large-Scale Transcriptome Analysis of Cucumber and *Botrytis cinerea* during Infection. *PLoS ONE* **2015**, *10*, e0142221. [CrossRef] [PubMed]
50. Haile, Z.M.; Guzman, E.G.N.-D.; Moretto, M.; Sonego, P.; Engelen, K.; Zoli, L.; Moser, C.; Baraldi, E. Transcriptome Profiles of Strawberry (*Fragaria vesca*) Fruit Interacting With *Botrytis cinerea* at Different Ripening Stages. *Front. Plant Sci.* **2019**, *10*, 1131. [CrossRef]
51. Haile, Z.M.; Malacarne, G.; Pilati, S.; Sonego, P.; Moretto, M.; Masuero, D.; Vrhovsek, U.; Engelen, K.; Baraldi, E.; Moser, C. Dual Transcriptome and Metabolic Analysis of *Vitis vinifera* cv. Pinot Noir Berry and *Botrytis cinerea* During Quiescence and Egressed Infection. *Front. Plant Sci.* **2020**, *10*, 1704. [CrossRef]
52. Davey, M.L.; Currah, R.S. Interactions between mosses (Bryophyta) and fungi. *Can. J. Bot.* **2006**, *84*, 1509–1519. [CrossRef]
53. Ponce De León, I. The Moss *Physcomitrella patens* as a Model System to Study Interactions between Plants and Phytopathogenic Fungi and Oomycetes. *J. Pathog.* **2011**, *2011*, 1–6. [CrossRef]
54. Tenberge, K.B.; Beckedorf, M.; Hoppe, B.; Schouten, A.; Solf, M.; Driesch, M.V.D. In Situ Localization of AOS in Host-Pathogen Interactions. *Microsc. Microanal.* **2002**, *8*, 250–251. [CrossRef]
55. Zhang, M.; Sun, C.; Liu, Y.; Feng, H.; Chang, H.; Cao, S.; Li, G.; Yang, S.; Hou, J.; Zhu-Salzman, K.; et al. Transcriptome analysis and functional validation reveal a novel gene, BcCGF1, that enhances fungal virulence by promoting infection-related development and host penetration. *Mol. Plant Pathol.* **2020**, *21*, 834–853. [CrossRef]
56. Hou, J.; Feng, H.; Chang, H.; Liu, Y.; Li, G.; Yang, S.; Sun, C.; Zhang, M.; Yuan, Y.; Sun, J.; et al. The H3K4 demethylase Jar1 orchestrates ROS production and expression of pathogenesis-related genes to facilitate *Botrytis cinerea* virulence. *New Phytol.* **2019**, *225*, 930–947. [CrossRef]
57. Turrion-Gomez, J.L.; Benito, E.P. Flux of nitric oxide between the necrotrophic pathogen *Botrytis cinerea* and the host plant. *Mol. Plant Pathol.* **2011**, *12*, 606–616. [CrossRef] [PubMed]
58. Siegmund, U.; Viefhues, A. Reactive Oxygen Species in the Botrytis—Host Interaction. In *Botrytis—The Fungus, the Pathogen and Its Management in Agricultural Systems*; Springer: Cham, Germany, 2015; pp. 269–289.
59. Espino, J.J.; Gutiérrez-Sánchez, G.; Brito, N.; Shah, P.; Orlando, R.; González, C. The *Botrytis cinerea* early secretome. *Proteom.* **2010**, *10*, 3020–3034. [CrossRef] [PubMed]
60. Tiedemann, A. Evidence for a primary role of active oxygen species in induction of host cell death during infection of bean leaves with *Botrytis cinerea*. *Physiol. Mol. Plant Pathol.* **1997**, *50*, 151–166. [CrossRef]
61. Pinedo, C.; Wang, C.-M.; Pradier, J.-M.; Dalmais, B.; Choquer, M.; Le Pêcheur, P.; Morgant, G.; Collado, I.G.; Cane, D.E.; Viaud, M. Sesquiterpene Synthase from the Botrydial Biosynthetic Gene Cluster of the Phytopathogen *Botrytis cinerea*. *ACS Chem. Biol.* **2008**, *3*, 791–801. [CrossRef] [PubMed]
62. Siewers, V.; Viaud, M.; Jimenez-Teja, D.; Collado, I.G.; Gronover, C.S.; Pradier, J.-M.; Tudzynski, B.; Tudzynski, P. Functional Analysis of the Cytochrome P450 Monooxygenase Gene bcbot1 of *Botrytis cinerea* Indicates That Botrydial Is a Strain-Specific Virulence Factor. *Mol. Plant Microbe Interact.* **2005**, *18*, 602–612. [CrossRef] [PubMed]
63. Collado, I.G.G.; Viaud, M. Secondary Metabolism in *Botrytis cinerea*: Combining Genomic and Metabolomic Approaches. In *Botrytis—The Fungus, the Pathogen and Its Management in Agricultural Systems*; Springer: Cham, Germany, 2015; pp. 291–313.
64. Porquier, A.; Morgant, G.; Moraga, J.; Dalmais, B.; Luyten, I.; Simon, A.; Pradier, J.-M.; Amselem, J.; Collado, I.G.; Viaud, M. The botrydial biosynthetic gene cluster of *Botrytis cinerea* displays a bipartite genomic structure and is positively regulated by the putative Zn(II)2Cys6 transcription factor BcBot6. *Fungal Genet. Biol.* **2016**, *96*, 33–46. [CrossRef] [PubMed]

65. Dalmais, B.; Schumacher, J.; Moraga, J.; Le Pêcheur, P.; Tudzynski, B.; Collado, I.G.; Viaud, M. The *Botrytis cinerea* phytotoxin botcinic acid requires two polyketide synthases for production and has a redundant role in virulence with botrydial. *Mol. Plant Pathol.* **2011**, *12*, 564–579. [CrossRef]
66. Arenas, Y.C.; Kalkman, E.R.; Schouten, A.; Dieho, M.; Vredenbregt, P.; Uwumukiza, B.; Oses-Ruiz, M.; Van Kan, J.A. Functional analysis and mode of action of phytotoxic Nep1-like proteins of *Botrytis cinerea*. *Physiol. Mol. Plant Pathol.* **2010**, *74*, 376–386. [CrossRef]
67. Noda, J.; Brito, N.; González, C. The *Botrytis cinerea* xylanase Xyn11A contributes to virulence with its necrotizing activity, not with its catalytic activity. *BMC Plant Biol.* **2010**, *10*, 38. [CrossRef]
68. Kars, I.; Krooshof, G.H.; Wagemakers, L.; Joosten, R.; Benen, J.A.E.; Van Kan, J.A.L. Necrotizing activity of five *Botrytis cinerea* endopolygalacturonases produced in *Pichia pastoris*. *Plant J.* **2005**, *43*, 213–225. [CrossRef]
69. Brito, N.; Espino, J.J.; González, C. The Endo-β-1,4-Xylanase Xyn11A Is Required for Virulence in *Botrytis cinerea*. *Mol. Plant Microbe Interact.* **2006**, *19*, 25–32. [CrossRef] [PubMed]
70. Li, B.; Wang, W.; Zong, Y.; Qin, G.; Tian, S. Exploring Pathogenic Mechanisms of *Botrytis cinerea* Secretome under Different Ambient pH Based on Comparative Proteomic Analysis. *J. Proteome Res.* **2012**, *11*, 4249–4260. [CrossRef] [PubMed]
71. Shah, P.; Atwood, J.A.; Orlando, R.; El Mubarek, H.; Podila, G.K.; Davis, M.R. Comparative Proteomic Analysis of *Botrytis cinerea* Secretome. *J. Proteome Res.* **2009**, *8*, 1123–1130. [CrossRef] [PubMed]
72. Fernández-Acero, F.J.; Colby, T.; Harzen, A.; Carbú, M.; Wieneke, U.; Cantoral, J.M.; Schmidt, J. 2-DE proteomic approach to the *Botrytis cinerea* secretome induced with different carbon sources and plant-based elicitors. *Proteomics* **2010**, *10*, 2270–2280. [CrossRef] [PubMed]
73. Shah, P.; Powell, A.L.; Orlando, R.; Bergmann, C.; Gutierrez-Sanchez, G. Proteomic Analysis of Ripening Tomato Fruit Infected by *Botrytis cinerea*. *J. Proteome Res.* **2012**, *11*, 2178–2192. [CrossRef] [PubMed]
74. Staples, R.C.; Mayer, A. Putative virulence factors of *Botrytis cinerea* acting as a wound pathogen. *FEMS Microbiol. Lett.* **1995**, *134*, 1–7. [CrossRef]
75. Leroch, M.; Kleber, A.; Silva, E.; Coenen, T.; Koppenhöfer, D.; Shmaryahu, A.; Valenzuela, P.D.T.; Hahn, M. Transcriptome Profiling of *Botrytis cinerea* Conidial Germination Reveals Upregulation of Infection-Related Genes during the Prepenetration Stage. *Eukaryot. Cell* **2013**, *12*, 614–626. [CrossRef]
76. Lee, S.B.; Yang, S.U.; Pandey, G.; Kim, M.; Hyoung, S.; Choi, D.; Shin, H.-Y.; Suh, M.C. Occurrence of land-plant-specific glycerol-3-phosphate acyltransferases is essential for cuticle formation and gametophore development in *Physcomitrella patens*. *New Phytol.* **2019**, *225*, 2468–2483. [CrossRef]
77. Blanco-Ulate, B.; Morales-Cruz, A.; Amrine, K.C.H.; Labavitch, J.M.; Powell, A.L.T.; Cantu, D. Genome-wide transcriptional profiling of *Botrytis cinerea* genes targeting plant cell walls during infections of different hosts. *Front. Plant Sci.* **2014**, *5*, 435. [CrossRef]
78. Have, A.T.; Breuil, W.O.; Wubben, J.P.; Visserb, J.; Van Kan, J.A. *Botrytis cinerea* Endopolygalacturonase Genes Are Differentially Expressed in Various Plant Tissues. *Fungal Genet. Biol.* **2001**, *33*, 97–105. [CrossRef]
79. Moller, I.; Sørensen, I.; Bernal, A.J.; Blaukopf, C.; Lee, K.; Øbro, J.; Pettolino, F.; Roberts, A.; Mikkelsen, J.D.; Knox, J.P.; et al. High-throughput mapping of cell-wall polymers within and between plants using novel microarrays. *Plant J.* **2007**, *50*, 1118–1128. [CrossRef] [PubMed]
80. Roberts, A.W.; Roberts, E.M.; Haigler, C.H. Moss cell walls: Structure and biosynthesis. *Front. Plant Sci.* **2012**, *3*, 166. [CrossRef] [PubMed]
81. Zhang, L.; van Kan, J.A.L. *Botrytis cinerea* mutants deficient in D-galacturonic acid catabolism have a perturbed virulence on *Nicotiana benthamiana* and Arabidopsis; but not on tomato. *Mol. Plant Pathol.* **2013**, *14*, 19–29. [CrossRef] [PubMed]
82. Nafisi, M.; Stranne, M.; Zhang, L.; Van Kan, J.A.L.; Sakuragi, Y. The Endo-Arabinanase BcAra1 Is a Novel Host-Specific Virulence Factor of the Necrotic Fungal Phytopathogen *Botrytis cinerea*. *Mol. Plant Microbe Interact.* **2014**, *27*, 781–792. [CrossRef] [PubMed]
83. Lyon, G.D.; Goodman, B.A.; Williamson, B. *Botrytis cinerea* Perturbs Redox Processes as an Attack Strategy in Plants. In *Botrytis: Biology, Pathology and Control*; Springer: Dordrecht, The Netherlands, 2007; pp. 119–141.
84. González-Fernández, R.; Aloria, K.; Valero-Galván, J.; Redondo, I.; Arizmendi, J.M.; Jorrín-Novo, J.V. Proteomic analysis of mycelium and secretome of different *Botrytis cinerea* wild-type strains. *J. Proteom.* **2014**, *97*, 195–221. [CrossRef]
85. Pandey, V.; Singh, M.; Pandey, D.; Kumar, A. Integrated proteomics, genomics, metabolomics approaches reveal oxalic acid as pathogenicity factor in *Tilletia indica* inciting Karnal bunt disease of wheat. *Sci. Rep.* **2018**, *8*, 1–14. [CrossRef]
86. Guyon, K.; Balagué, C.; Roby, D.; Raffaele, S. Secretome analysis reveals effector candidates associated with broad host range necrotrophy in the fungal plant pathogen *Sclerotinia sclerotiorum*. *BMC Genom.* **2014**, *15*, 1–19. [CrossRef]
87. Seifbarghi, S.; Borhan, M.H.; Wei, Y.; Coutu, C.; Robinson, S.J.; Hegedus, D.D. Changes in the *Sclerotinia sclerotiorum* transcriptome during infection of *Brassica napus*. *BMC Genom.* **2017**, *18*, 1–37. [CrossRef]
88. Viaud, M.; Brunet-Simon, A.; Brygoo, Y.; Pradier, J.-M.; Levis, C. Cyclophilin A and calcineurin functions investigated by gene inactivation, cyclosporin A inhibition and cDNA arrays approaches in the phytopathogenic fungus *Botrytis cinerea*. *Mol. Microbiol.* **2003**, *50*, 1451–1465. [CrossRef]
89. Have, A.T.; Espino, J.J.; Dekkers, E.; Van Sluyter, S.C.; Brito, N.; Kay, J.; González, C.; Van Kan, J.A. The *Botrytis cinerea* aspartic proteinase family. *Fungal Genet. Biol.* **2010**, *47*, 53–65. [CrossRef]

90. Denton-Giles, M.; McCarthy, H.; Sehrish, T.; Dijkwel, Y.; Mesarich, C.H.; Bradshaw, R.E.; Cox, M.P.; Dijkwel, P.P. Conservation and expansion of a necrosis-inducing small secreted protein family from host-variable phytopathogens of the Sclerotiniaceae. *Mol. Plant Pathol.* **2020**, *21*, 512–526. [CrossRef] [PubMed]
91. Pennington, H.G.; Jones, R.; Kwon, S.; Bonciani, G.; Thieron, H.; Chandler, T.; Luong, P.; Morgan, S.N.; Przydacz, M.; Bozkurt, T.; et al. The fungal ribonuclease-like effector protein CSEP0064/BEC1054 represses plant immunity and interferes with degradation of host ribosomal RNA. *PLoS Pathog.* **2019**, *15*, e1007620. [CrossRef] [PubMed]
92. Boller, T.; Felix, G. A Renaissance of Elicitors: Perception of Microbe-Associated Molecular Patterns and Danger Signals by Pattern-Recognition Receptors. *Annu. Rev. Plant Biol.* **2009**, *60*, 379–406. [CrossRef] [PubMed]
93. Zhang, L.; Kars, I.; Essenstam, B.; Liebrand, T.W.; Wagemakers, L.; Elberse, J.; Tagkalaki, P.; Tjoitang, D.; Ackerveken, G.V.D.; Van Kan, J.A. Fungal Endopolygalacturonases Are Recognized as Microbe-Associated Molecular Patterns by the Arabidopsis Receptor-Like Protein RESPONSIVENESS TO BOTRYTIS POLYGALACTURONASES1. *Plant Physiol.* **2014**, *164*, 352–364. [CrossRef]
94. Lionetti, V.; Raiola, A.; Camardella, L.; Giovane, A.; Obel, N.; Pauly, M.; Favaron, F.; Cervone, F.; Bellincampi, D. Overexpression of Pectin Methylesterase Inhibitors in Arabidopsis Restricts Fungal Infection by *Botrytis cinerea*. *Plant Physiol.* **2007**, *143*, 1871–1880. [CrossRef]
95. Sbaghi, M.; Jeandet, P.; Bessis, R.; Leroux, P. Degradation of stilbene-type phytoalexins in relation to the pathogenicity of *Botrytis cinerea* to grapevines. *Plant Pathol.* **1996**, *45*, 139–144. [CrossRef]
96. Quidde, T.; Osbourn, A.; Tudzynski, P. Detoxification of α-tomatine by *Botrytis cinerea*. *Physiol. Mol. Plant Pathol.* **1998**, *52*, 151–165. [CrossRef]
97. El Oirdi, M.; Trapani, A.; Bouarab, K. The nature of tobacco resistance against *Botrytis cinerea* depends on the infection structures of the pathogen. *Environ. Microbiol.* **2010**, *12*, 239–253. [CrossRef]
98. Pedras, M.S.C.; Hossain, S.; Snitynsky, R.B. Detoxification of cruciferous phytoalexins in *Botrytis cinerea*: Spontaneous dimerization of a camalexin metabolite. *Phytochemistry* **2011**, *72*, 199–206. [CrossRef]
99. VanEtten, H.; Temporini, E.; Wasmann, C. Phytoalexin (and phytoanticipin) tolerance as a virulence trait: Why is it not required by all pathogens? *Physiol. Mol. Plant Pathol.* **2001**, *59*, 83–93. [CrossRef]
100. Vela-Corcía, D.; Srivastava, D.A.; Dafa-Berger, A.; Rotem, N.; Barda, O.; Levy, M. MFS transporter from *Botrytis cinerea* provides tolerance to glucosinolate-breakdown products and is required for pathogenicity. *Nat. Commun.* **2019**, *10*, 1–11. [CrossRef] [PubMed]
101. Stefanato, F.L.; Abou-Mansour, E.; Buchala, A.; Kretschmer, M.; Mosbach, A.; Hahn, M.; Bochet, C.G.; Métraux, J.-P.; Schoonbeek, H.-J. The ABC transporter BcatrB from *Botrytis cinerea* exports camalexin and is a virulence factor on *Arabidopsis thaliana*. *Plant J.* **2009**, *58*, 499–510. [CrossRef] [PubMed]
102. Hayashi, K.; Schoonbeek, H.-J.; De Waard, M.A. Bcmfs1, a Novel Major Facilitator Superfamily Transporter from *Botrytis cinerea*, Provides Tolerance towards the Natural Toxic Compounds Camptothecin and Cercosporin and towards Fungicides. *Appl. Environ. Microbiol.* **2002**, *68*, 4996–5004. [CrossRef] [PubMed]
103. Ponce De León, I.; Montesano, M. Adaptation Mechanisms in the Evolution of Moss Defenses to Microbes. *Front. Plant Sci.* **2017**, *8*, 366. [CrossRef]

4.2.1. Figuras suplementarias Capítulo II

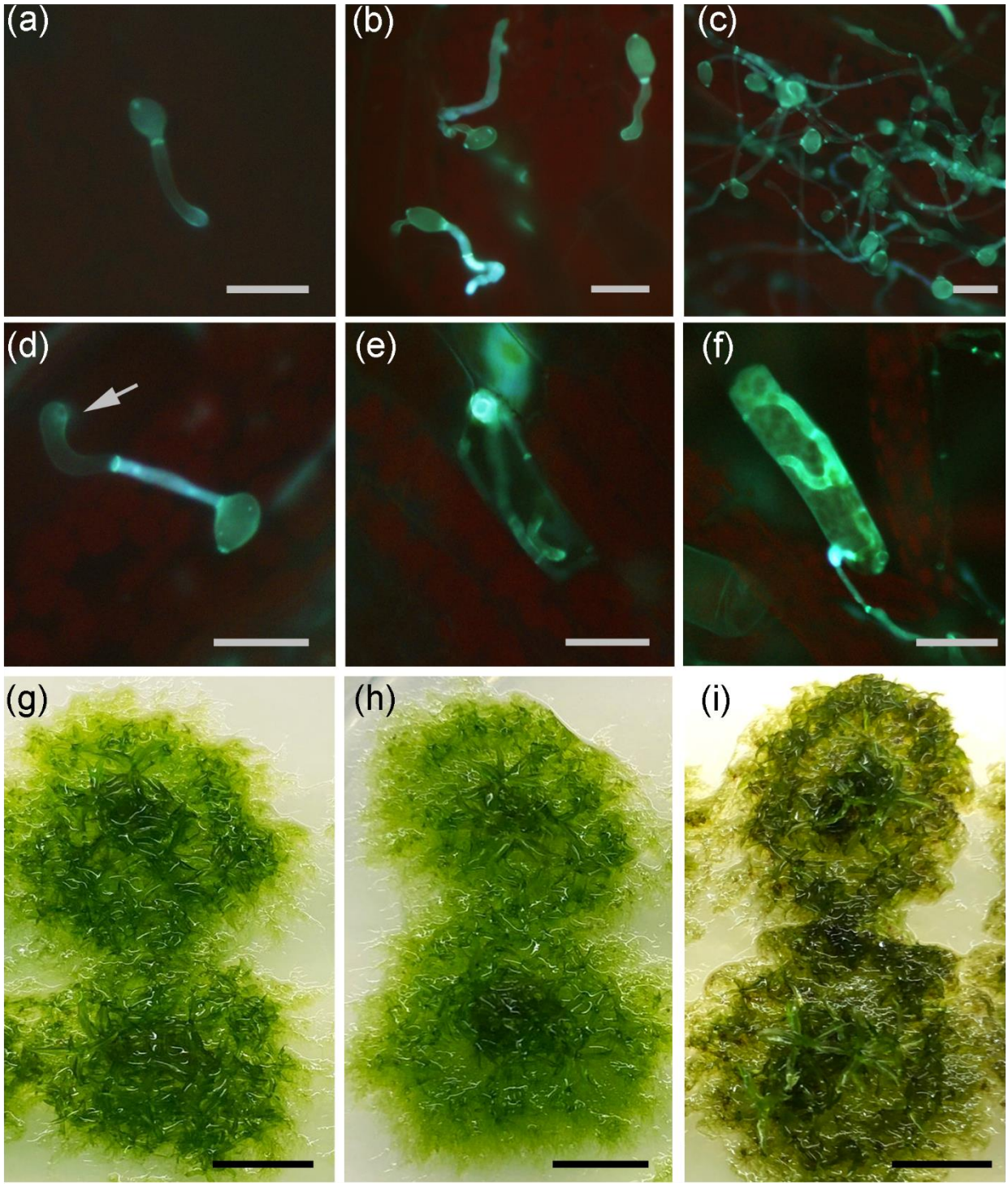

Figure S1: *B. cinerea* infection of *P. patens* tissues. Infection progress during time is shown; (a) spore germination at 4 hpi, (b) germ tubes elongation at 8 hpi, (c) proliferation of mycelium at 24 hpi, (d) appresorium formation at 8 hpi, (e) hyphae colonizing a leaf cell, and (f) hyphae colonizing a protonemal cell. Symptom development at 8 hpi (h), 24 hpi (i) and 24 h water-treated moss colonies (g) are shown. The arrow in (d) indicate an appresorium. The scale bar in a-f represents 10 µm and 0.5 cm in g-i.

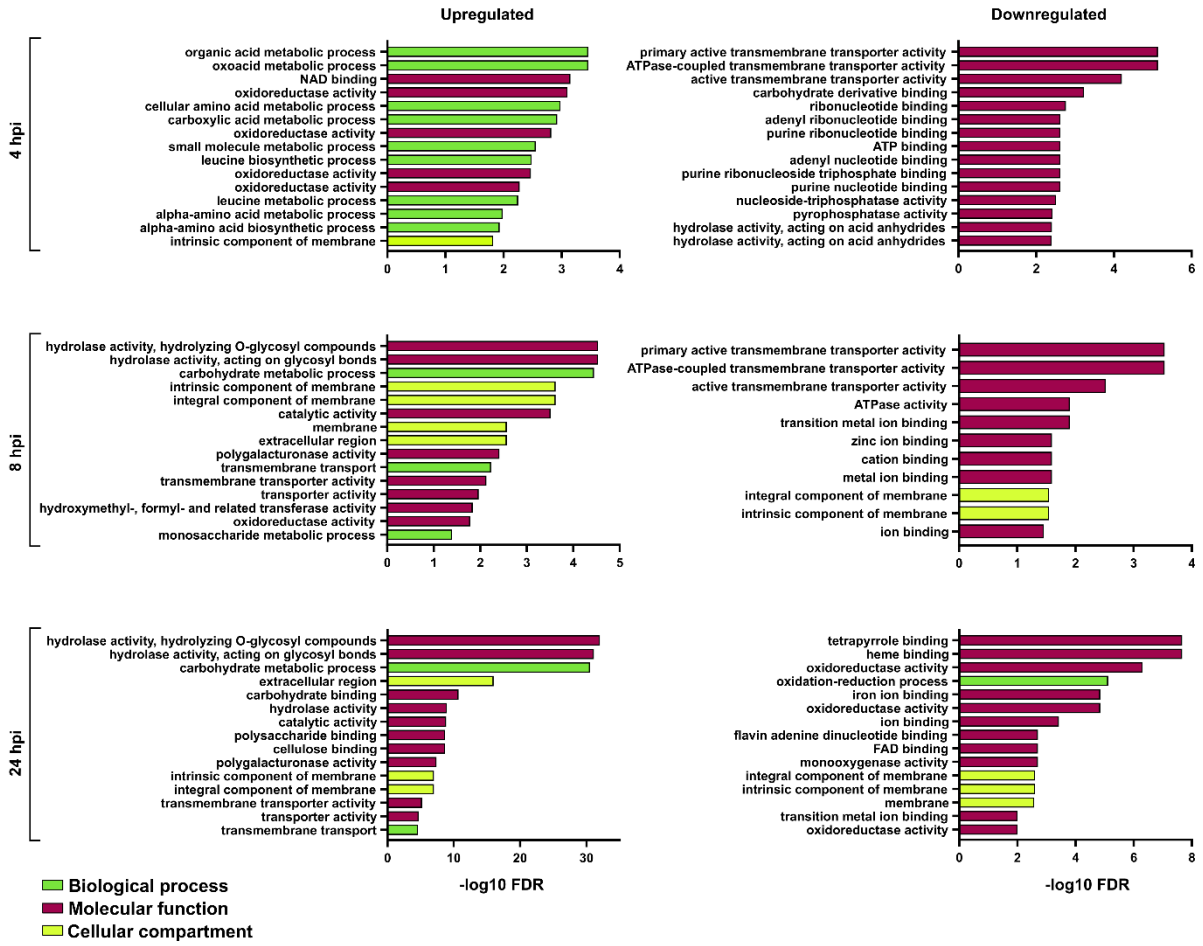

Figure S2: Enriched gene ontology (GO) terms of *B. cinerea* DEGs. The top 15 enrichment GO terms were chosen according to their statistical significance (−log10 FDR). GO enrichment are shown for upregulated and downregulated *B. cinerea* DEGs at 4, 8 and 24 hpi. See Table S5 for complete information.

Figure S3: Analysis of *B. cinerea* RNA-Seq data during *P. patens*, *A. thaliana*, *S. lycopersicum* and *L. sativa* infection by principal component analysis (PCA). Colored dots denote each biological replicate.

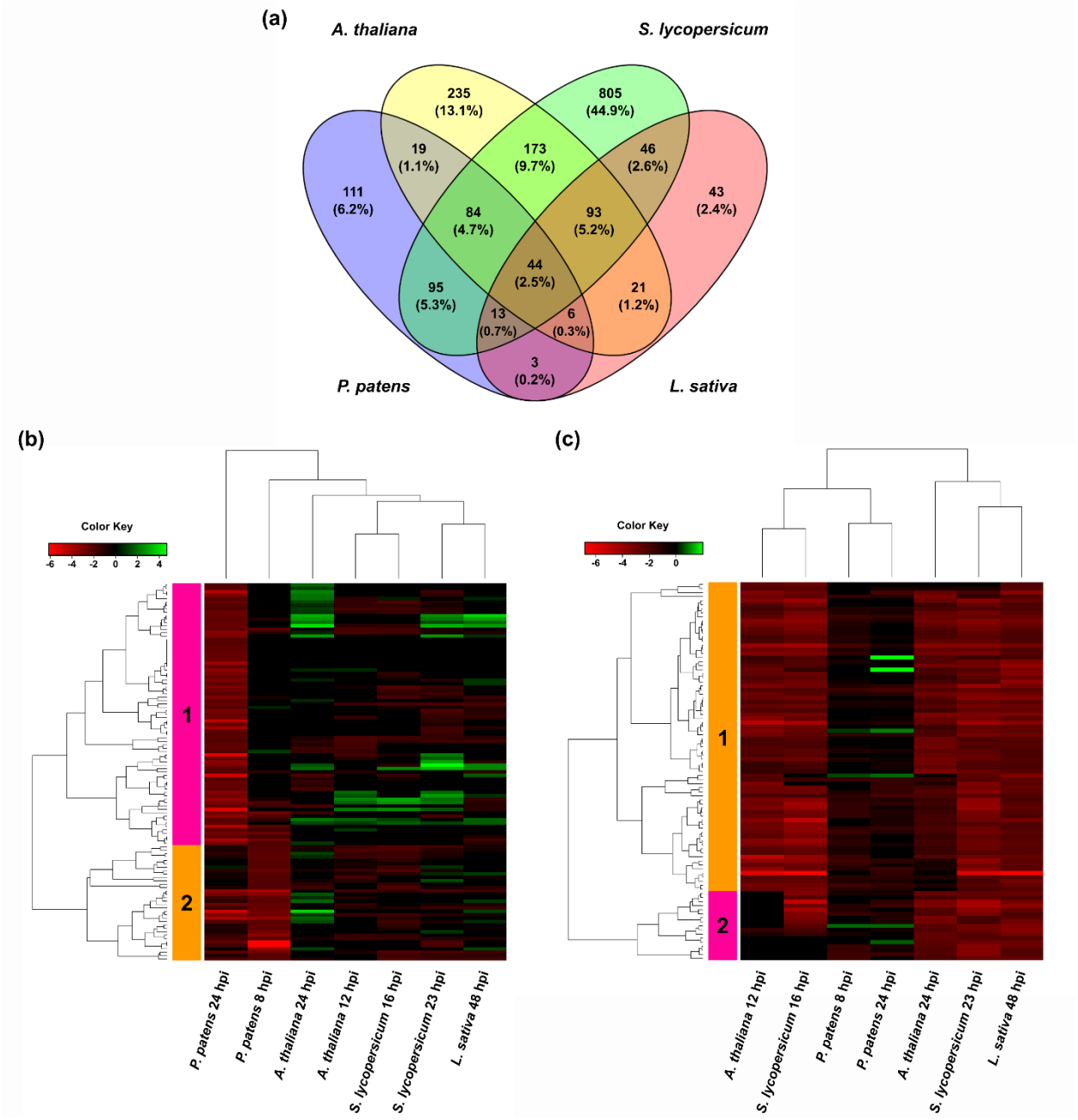

Figure S4: *B. cinerea* downregulated DEGs during *P. patens* and angiosperm infection. (a) Venn diagram of *B. cinerea* downregulated DEGs in different plant species, showing overlap of fungal repressed genes. *P. patens*: sum of *B. cinerea* DEGs at 8 and 24 hpi; *A. thaliana*: sum of *B. cinerea* DEGs at 12 and 24 hpi; *S. lycopersicum*: sum of *B. cinerea* DEGs at 16 and 23 hpi; and *L. sativa*: *B. cinerea* DEGs at 48 hpi. For Venn diagram, DEGs had log2 FC ≤ −2, FDR ≤ 0.05, and were expressed differentially in at least one time point for each plant species condition. (b) Hierarchical clustering (heat map) showing *B. cinerea* genes only downregulated in *P. patens*. Fungal DEGs corresponds to the 111 genes that were only downregulated in *P. patens*. (c) Hierarchical clustering showing *B. cinerea* genes only downregulated in angiosperms. Fungal DEGs corresponds to the 93 genes that were only downregulated in angiosperms.

4.3. Capítulo III- Un factor de transcripción específico de musgos mejora la resistencia a patógenos en *Physcomitrium patens*

En este tercer capítulo estudiamos un factor de transcripción de la familia AP2/ERF y su posible participación en la respuesta de defensa vegetal. Nos planteamos como hipótesis que el factor de transcripción PpERF24 está involucrado en la activación de la defensa frente a patógenos en *P. patens*. Para abordar esta pregunta se propone como objetivo específico realizar una caracterización funcional del factor de transcripción con dominio AP2/ERF (PpERF24) de *P. patens* a partir de líneas sobreexpresantes y el análisis de sus transcriptomas. A partir de la secuencia codificante de PpERF24 se realizó un análisis filogenético de los dominios AP2 de factores de transcripción pertenecientes a la familia ERF de *P. patens* y *Arabidopsis thaliana*. Para la caracterización funcional de PpERF24, se inocularon plantas sobreexpresantes y salvajes con diferentes patógenos, incluyendo los hongos *B. cinerea* y *C. gloeosporioides*, el oomicete *Pythium irregulare* y elicitores de la bacteria fiotpatógena *Pectobacterium carotovorum*, y se evaluó el daño celular generado en la planta. Además se agroinfiltraron hojas de plantas de tabaco con construcciones génicas conteniendo PpERF24 fusionado a GFP para corroborar que su localización subcelular es nuclear. Para la obtención de los transcriptomas se trataron plantas sobreexpresantes en PpERF24 y plantas salvajes con agua o esporas del hongo *B. cinerea* recolectando las muestras 24 horas post inoculación. Una vez obtenidos los transcriptomas por RNA-Seq y analizados se realizaron distintas comparaciones entre las diferentes líneas y tratamientos para identificar aquellos genes que se expresan diferencialmente en la línea sobreexpresante y que pudiesen explicar la mayor resistencia en estas plantas en comparación a plantas salvajes.

Como se mencionó anteriormente, la familia AP2/ERF es una gran superfamilia de FTs específica de plantas que participa en el desarrollo y respuesta de defensa a estrés biótico y abiótico en angiospermas (Xu et al., 2011). La cantidad de FTs de esta superfamilia se encuentra altamente expandida en plantas terrestres comparado con las algas, sugiriendo que tal vez hayan podido contribuir a la colonización de la tierra (Bowman et al., 2017).

Las plantas terrestres, incluyendo los musgos, han evolucionado diferentes mecanismos de defensa para protegerse de patógenos invasores y de estreses abióticos. Uno de estos mecanismos incluye los FTs ERF (ERF y DREB). Mediante una búsqueda en la base de datos PlantTFDB (*Plant Transcription Factor Database*) encontramos que en *P. patens* hay al menos 161 genes AP2/ERF y una proporción muy grande de ellos responden a diferentes tipos de estrés abiótico e interacciones bióticas (Reboledo et al., 2022). De estos 161 genes AP2/ERF, 16 pertenecen a la familia AP2, 143 a la familia ERF (ERF+DREB) y 2 a la familia RAV. En este capítulo nos enfocamos en el estudio de la función de un ERF específico de musgo, que denominamos PpERF24. La familia ERF está dividida en las subfamilias ERF y DREB según la similitud de la secuencia de sus dominios AP2, incluyendo los amino ácidos conservados A14 y D19 en ERFs y V14 y E19 en DREBs (Sakuma et al., 2002). Observamos que de las 143 proteínas pertenecientes

a la familia ERF, 36 de ellas se agrupaban en un clado musgo específico, mientras que 47 proteínas DREBs y 60 ERFs de *P. patens* se agrupaban con las subfamilias DREB y ERF de Arabidopsis. Es interesante observar que tanto PpERF24 como otras proteínas dentro del clado musgo-especifico poseen amino ácidos conservados en las posiciones 15 y 20 del dominio AP2, V15 o I15 e I20, posiciones equivalentes a las 14 y 19 de DREB y ERF (desfasadas debido a un amino ácido adicional en la posición 10, el cual resultó mayormente un E10). En *P. patens* V15 se encontró conservado en 22 miembros (61%) del clado musgo específico, mientras que otros miembros de este clado tienen I15 (5 proteínas), u otro amino ácido en dicha posición (nueve proteínas). La presencia de P20 en 33 de 45 dominios AP2 musgo específico (73%) indica sobre la relevancia de este residuo en el elemento YRG. Observamos que el motivo YKGIR, y RYIS que incluye I15, en el elemento YRG separó el subclado PpERF24 del subclado Pp3c22_20520 y el resto de las proteínas específicas de musgo. Es de destacar que, todos los miembros del subclado de PpERF24 de *P. patens* son inducidos por los patógenos *B. cinerea* y *C. gloeosporioides* (Reboledo et al., 2022). Más estudios son necesarios para entender cómo los motivos encontrados en las proteínas específicas de musgos afectan su unión al ADN.

Se realizaron estudios funcionales con PpERF24 mediante su sobreexpresión en plantas de *P. patens*. Observamos que aquellas plantas que sobreexpresan PpERF24 (PpERF24-OX-2 y PpERF24-OX-4) exhibían un menor daño celular ante la infección por *B. cinerea*, *P. irregulare* y el tratamiento con elicitores de *P. c. carotovorum* al compararles con plantas control. Además, la línea PpERF24-OX-4, con mayor expresión de PpERF24, también mostró un incremento en la resistencia ante el hongo *C. gloeosporiodies*. Esto es consistente con estudios previos que muestran que la sobreexpresión de ERF1 confiere resistencia a varios hongos en Arabidopsis, incluyendo *B. cinerea* (Berrocal-Lobo et al., 2002).

Al analizar los transcriptomas de plantas PpERF24-OX-4 y plantas salvajes, se vio que ante la infección por *B. cinerea* se inducen categorías similares de genes. Entre estos se incluyen genes codificantes para proteínas de vías importantes en la defensa y proteínas con rol de defensa como ser PRRs involucrados en la percepción del patógeno, señalización por quinasas y calcio, regulación de la transcripción, defensas asociadas a la pared celular, vías de fenilpropanoides y hormonales incluyendo la vía del jasmonato al igual que genes codificantes para proteínas relacionadas a la patogenicidad con actividad antimicrobiana. Por otro lado, observamos 391 GDEs en PpERF24-OX-4 al comparar con plantas salvajes en condiciones control. Aproximadamente el 50% de estos genes se encontraron también inducidos en plantas salvajes infectadas con *B. cinerea*, sugiriendo que podrían estar involucrados en reacciones de defensa de la planta y favorecer su respuesta haciéndola más resistente a patógenos. El hecho de que en plantas PpERF24-OX-4 control comparadas con plantas salvajes control, se encontraran inducidos dos genes que codifican para *flavonoid 3'-hydroxylasas* y un FT TT2 (perteneciente a la familia MYB de FTs), sugiere que una rápida producción de compuestos de defensa fenólicos, podrían llevar a un menor daño celular producido por patógenos. Estos hallazgos son consistentes con el reforzamiento de la pared celular de *P. patens* por acumulación de compuestos fenólicos luego de la infección con *B. cinerea* (Ponce de León et al., 2012). Además, la acumulación de compuestos fenólicos en PpERF24-OX-4 proveniente de esta vía podría llevar a la acumulación de compuestos con actividad antimicrobiana, contribuyendo a reducir la colonización por parte del hongo. Sí bien

hay compuestos derivados de la vía de los fenilpropanoides en *P. patens* que presentan actividad antimicrobiana (Erxleben et al., 2012; Richter et al., 2012), son necesarios más estudios para determinar si algunos de ellos se producen en mayor cantidad en la líneas que sobreexpresan *PpERF24*. También fue posible observar una mayor inducción de genes relacionados con la remodelación y mantenimiento de la pared celular y varios FTs pertenecientes a las familias ERFs, MYBs y PLATz al comparar plantas PpERF24-OX-4 control con plantas salvajes control. Los niveles de expresión de varios de estos FTs también se encontraron inducidos en *P. patens* en respuesta a *C. gloeosporioides* (Otero-Blanca et al., 2021). A su vez, observamos en PpERF24-OX-4 la inducción de genes que codifican para peroxidasas y una RBOH, los cuales, al igual que en angiospermas, se encuentran asociadas al estallido oxidativo en *P. patens* luego del tratamiento con quitina (Lehtonen et al., 2012), mientras que mutantes en la peroxidasa PRX34 son más susceptibles a patógenos fúngicos (Lehtonen et al., 2009). Dado que el receptor CERK1, involucrado en el reconocimiento de la quitina de hongos, también está inducido en plantas PpERF24-OX-4 control, en comparación a plantas salvajes control, se infiere que podría estar confiriendo una ventaja al momento de reconocer al patógeno, activando las respuestas de defensa. En el mismo sentido, se ha visto que la sobreexpresión de CERK1 de manzana en plantas de *N. benthamiana* afecta múltiples respuestas de defensa e incrementa la resistencia a patógenos fúngicos (Chen et al., 2020). Otros genes inducidos en PpERF24-OX-4 en comparación a plantas salvajes control, vinculados a la defensa, incluyen a una quitinasa, una β-1,3 glucanasa y una cupina.

Observamos que la vía del jasmonato se encontraba activada en PpERF24-OX-4 al comparar con plantas control, evidenciado por el aumento en la expresión de AOC y OPR. Esta vía participa en la defensa de *P. patens* contra *B. cinerea* (Ponce de León et al., 2012). Es interesante destacar, que se ha propuesto que el ERF ORA59 orquesta las vías de señalización del ET y JA y regula la resistencia a patógenos necrótrofos, incluyendo *B. cinerea* (Pré et al., 2008).

Nuestros resultados revelan que PpERF24 regula positivamente la inmunidad de *P. patens* contra la infección por patógenos mediante la modulación de los niveles de expresión de genes vinculados a respuestas de defensa. Más estudios en los ERFs específicos de musgo contribuirán a entender los mecanismos moleculares subyacentes a su acción, incluyendo elementos de unión al ADN, otras proteínas que interactúen y su contribución a la defensa de la planta.

The moss-specific transcription factor PpERF24 increases resistance against pathogens in *Physcomitrium patens*

Guillermo Reboledo[1], Astrid Agorio[1], Lucía Vignale[1] and Inés Ponce De León[1]*

[1] Departamento de Biología Molecular, Instituto de Investigaciones Biológicas Clemente Estable, Montevideo, Uruguay

***** Corresponding Author

iponce@iibce.edu.uy

Keywords: transcription factor, AP2/ERF, *Physcomitrium patens*, pathogens, defense

Abstract

APETALA2/Ethylene-responsive factors (AP2/ERF) transcription factors have greatly expanded in land plants compared to algae. In angiosperms, AP2/ERFs play important regulatory functions in plant defenses against pathogens and abiotic stress by controlling the expression of target genes. In the moss *Physcomitrium patens*, a high number of members of the ERF family are induced during pathogen infection, suggesting that they are important regulators in bryophyte immunity. In the current study, we analyzed a *P. patens* pathogen-inducible ERF family member designated as PpERF24. Orthologs of PpERF24 were only found in other mosses, while they were absent in *Marchanthia polymorpha*, *Selaginella moellendorffii* and angiosperms. We show that PpERF24 belongs to a moss-specific clade with distinctive amino acids features in the AP2 domain. Interestingly, all *P. patens* members of the PpERF24 subclade are induced by fungal pathogens. The function of PpERF24 during plant immunity was assessed by an overexpression approach and transcriptomic analysis. Overexpressing lines showed increased resistance to infection by the fungal pathogens *Botrytis cinerea* and *Colletotrichum gloeosporioides*, the oomycete *Pythium irregulare*, as well as treatment with elicitors of *Pectobacterium carotovorum*. Transcriptomic analysis revealed that PpERF24 positively modulate the expression levels of defense genes involved in transcriptional regulation, phenylpropanoid and jasmonate pathways, oxidative burst and pathogenesis-related genes. These findings give novel insights into potential mechanism by which PpERF24 increases plant defenses against several pathogens by regulating important players in defense mechanisms.

1 Introduction

Plant transcription factors (TFs) play crucial roles in regulating the expression of target genes that function in developmental processes and responses against environmental stresses. APETALA2/ETHYLENE RESPONSE FACTORS (AP2/ERFs) are a large plant-specific TF superfamily that participates in growth, development and defense responses to abiotic and biotic stress in angiosperms (Xu *et al*., 2011). The number of AP2/ERF TFs have greatly expanded in land plants compared to algae, suggesting that they may have contributed to terrestrialization (Bowman *et al*., 2017). Members of the family are defined by the AP2 domain, which comprises one or two AP2 DNA-binding domains with 60 to 70 conserved amino acid residues that consists of three β-sheet strands and an α-helix motif (Allen *et al*., 1998). The AP2 domain has two important regions, namely YRG and RAYD elements. The YRG element includes 20 amino acids that play a critical role in establishing direct contact with the DNA (Okamuro *et al*., 1997). The RAYD element contains approximately 40 amino acids in the α-helix region that plays an important role in protein-protein interaction, as well as a putative alternative role in DNA binding (Okamuro *et al*., 1997; Jofuku *et al*., 1994). Based on the number of AP2 domains and sequence similarities, AP2/ERFs are classified into three major families, including AP2 (APETALA2), ERF (Ethylene-Responsive-Element Binding protein) and RAV (Related to ABI3/VP) (Licausi *et al*., 2013). A fourth group belonging to the AP2/ERF superfamily is named Soloist, and although it contains a single AP2 domain, sequence and gene structure strongly diverge from those of the AP2/ERF TFs (Sakuma *et al*., 2002). The ERF family is further divided into two major subfamilies, the ERF and the DREB subfamily, which comprises twelve groups in *Arabidopsis thaliana* (Sakuma *et al*., 2002; Nakano *et al*., 2006). AP2 TFs have two tandem AP2 domains, whereas ERF and DREB family members contain a single AP2 domain (Nakano *et al*., 2006). Usually, AP2 members are key factors that regulate development and organ formation (Aukerman and Sakai 2003), while members of the ERF and DREB subfamily are more related to responses to environmental stress (Lata and Prasad, 2011). DREBs bind to the DRE elements in stress-responsive genes and are mainly involved in plant tolerance against different type of abiotic stresses, including drought, freezing, salt and heat (Lata and Prasad, 2011). In contrast, ERFs are involved in defense responses to pathogen attack by binding to a *cis*-acting ethylene response element (GCC box) (Solano *et al*., 1998; Berrocal-Lobo *et al*., 2002). However, more recently it was shown that several ERFs also bind to DRE elements and play regulatory roles in

integrating ethylene, abscisic acid (ABA), jasmonate, and redox signaling in plant responses to abiotic stresses (Müller and Munné-Bosch, 2015).

Several studies have revealed that overexpression of ERF TFs in angiosperms increases resistance against different pathogens as well as tolerance to drought, cold, and salt (Xu *et al*., 2011). For example, overexpression of some ERFs increased resistance to: *Stemphylium lycopersici* in tomato (Yang *et al*. 2020a), *Fusarium solani* in potato (Charfeddine *et al*., 2019), *Botryosphaeria dothidea* in apple (Wang *et al*., 2020), and *Rhizoctonia cerealis* in wheat (Chen *et al*., 2008). Increased resistance was associated with enhanced expression of pathogenesis-related (PR) proteins (Charfeddine *et al*., 2019; Chen *et al*., 2008). Moreover, *DREB DEAR1* expression increased in response to pathogen infection and its overexpression in *A. thaliana* renders plants with improved resistance to the bacterial pathogen *Pseudomonas syringae* (Tsutsui *et al*., 2009).

Mosses, together with liverworts and hornworts, are bryophytes that represent the three major lineages of non-vascular plants. Comparative studies of bryophytes and vascular plants, including angiosperms, allow the identification of evolutionary conserved biological roles of genes during stress and their possible conservation in the most recent common ancestor of land plants. In the algae *Chlamydomonas reinhardtii*, an *AP2/ERF* gene participates in the early response to cold stress (Li *et al.*, 2020), suggesting that the involvement of AP2/ERF members in defense responses to stress occur throughout the green lineages. In contrast to angiosperms, studies on the functional role of moss TFs in stress mechanisms have not been addressed until present. The moss *Physcomitrium patens*, formerly *Physcomitrella patens*, is considered a model plant to study abiotic and biotic stress in mosses (Frank *et al*., 2005; Ponce de León and Montesano, 2017). According to the PlantTFDB v5.0 database (Jin *et al*. 2017), *P. patens* has 161 AP2/ERF genes, divided into 16 AP2, 143 ERF (ERF+DREB) and two RAV. This number is comparable with other plants such as *A. thaliana*, *Solanum lycopersicum* and *Oryza sativa*, which has 146, 167 and 156 members, respectively. Transcriptomic analyses revealed that *P. patens* differentially expresses many members of the AP2/ERF superfamily in response to biotic interactions and abiotic stresses (Reboledo *et al.*, 2022). *Botrytis cinerea* and *Colletotrichum gloeosporioides* inoculation led to differential expression of a high number of AP2/ERFs compared to control tissues, including 90 ERF/DREB (69 induced and 21 repressed), 7 AP2 (6 induced and 1 repressed), and one RAV that was only induced with *B. cinerea* (Reboledo *et al*., 2022). These findings suggest that ERF and DREB TFs are important regulators in *P. patens* defense responses against biotic stress.

In a previous study, we identified a member of the ERF family of *P. patens*, which was induced during treatments with elicitors of the phytopathogenic bacteria *Pectobacterium carotovorum* subsp. *carotovorum* (Alvarez *et al*., 2016). Transcriptomic analysis of *P. patens* tissues during biotic and abiotic stress revealed that this gene is highly induced by fungal pathogens, while it is repressed by ABA and drought (Reboledo *et al*., 2022), highlighting a possible involvement in plant responses to pathogen infection. Here, we assessed the role of this TF, named as PpERF24, during plant immunity by an overexpression approach and transcriptomic analysis. We show that PpERF24 positively regulated plant resistance against several pathogens by regulating expression levels of genes related to defense.

2 MATERIALS AND METHODS

Plant material and growth conditions

P. patens Gransden wild type and PpERF24 overexpressing lines were grown and maintained on solid BCDAT medium (Ashton and Cove 1977) with cellophane disks under standard long-day conditions (22°C, 16-h light/8-h dark regime under 60–80 μmol m^2 s^{-1} white light). Three weeks old colonies were used for all experiments.

Pathogen inoculation and culture filtrate treatments

P.c. carotovorum strain SCC1 (Rantakari *et al.*, 2001) was propagated on Luria-Bertani medium at 28º C. Cell-free culture filtrates (CF) were prepared according to Ponce de León *et al.* (2007). The CF containing *P.c. carotovorum* elicitors was applied on *P. patens* colonies by spray. *B. cinerea* was cultivated on Potato-Dextrose Agar (PDA) at 22º C and 2 x 10^5 spores/mL suspension was used to inoculate *P. patens* colonies by spray (Ponce de León *et al.* 2007). *C. gloeosporioides* was grown on PDA at 22ºC and 2 x 10^5 conidia/mL suspension was used to inoculate *P. patens* colonies by spray (Reboledo *et al.* 2015). Water treated plants were used as control. *P. irregulare* was grown on PDA at 26 ºC and *P. patens* colonies were inoculated with 0.5 cm diameter agar plugs containing *P. irregulare* mycelium, as described by Oliver *et al.* (2009). As control PDA plugs were placed on top of each colony.

PpERF24 overexpression and *P. patens* transformation

To generate *P. patens* lines overexpressing *PpERF24*, the Pp3c11_14690V3.1 coding sequence was amplified from gDNA using primers OXERF24 5’ fw (5´-AGGTAATGCAGTCGAGCATAC-3´)

and OXERF24 3' rv (5´-TCACCTGTCTAAGACAACC-3´). The PCR product was cloned into pGEM-T Easy vector (Promega). PpERF24 coding sequence was subcloned into *EcoRI* site of the pENTR2B vector (Gateway). The obtained pENTR2B:PpERF24 construct was sequenced by Sanger at Macrogen Inc. (Korea), then transferred via LR clonase (Invitrogen) to a pTHUbi destination vector (Perroud *et al*., 2011). The obtained pTHUBi:PpERF24 construct was verified by Sanger sequencing at Macrogen Inc. (Korea). *P. patens* Gransden wild type protoplast were transformed with pTHUBi-PpERF24 linearized with *SwaI*. Polyethyleneglycol-mediated transformation of protoplasts was performed according to Schaefer *et al*. (1991). Tissues of plants showing growth after hygromycin selection were harvested to analyze the incorporation of the transgene. Levels of *PpERF24* transcript accumulation of selected transformants were assayed by Northern blot analysis as described by Castro *et al*. (2016). For this, PpERF24 cDNA probe was labeled with [α32P]-dCTP using the RediprimeII Random Prime labeling system kit (GE Health care). DNA content of different PpERF24 overexpressing lines was measured by flow cytometry according to Castro *et al.* (2016). For this, 5000 nuclei from each colony were analyzed. Haploid PpERF24 overexpressing lines were considered for further experiments.

Subcellular localization of PpERF24-GFP

PpERF24 coding sequence without the stop codon was amplified from *pMDC7:PpERF24* using primers mPpERF24BamHI_fw (5´- CTGGATGGATCCCCGAATTCACTAGTG -3´) and mPpERF24NotI_rv (5´- AATTCGCGGCCGCCTGTCTAAGA -3´) which contained restriction sites for *BamHI* and *NotI* restriction enzymes, respectively. The corresponding fragment was cloned into *BamHI* and *NotI* sites of the pENTR2B vector (Gateway), and transferred via LR clonase (Invitrogen) to vector pMDC83 (Curtis *et al.*, 2003) containing the GFP coding sequence and 2x35S promoter regulation. The obtained 2x35S:PpERF24-GFP construct was sequenced by Sanger at Macrogen Inc. (Korea). For free GFP control, a pMDC83:ΔccdB construct, without ccdB gene, was generated. For this, pMDC83 was digested with *KpnI*, purified and ligated. The obtained pMDC83:ΔccdB construct was sequenced by Sanger at Macrogen Inc. (Korea). The 2x35S:PpERF24-GFP and pMDC83:ΔccdB constructs were introduced in *Agrobacterium tumefaciens* strain C58C1, and *Nicotiana tabacum* leaves were agroinfiltrated as described by Yang *et al*. (2000b). The fluorescence signals of the tobacco leaves were captured with a LSM Zeiss 800 confocal microscope (Carl Zeiss Microscopy) two days after agroinfiltration. Excitation laser line 488 and 640 were used for GFP and chloroplast signal detection, respectively. The acquisition

software used was ZEN Blue 2.6 (Carl Zeiss Microscopy). Image processing was done with ImageJ 1.52p (Schindelin *et al*., 2012).

Sequence analysis of PpERF24 and comparison with other ERF and DREB proteins

The analysis of conserved domains in PpERF24 protein was performed using the Simple Modular Architecture Research Tool (SMART) (Letunic *et al.* 2021) at http://smart.embl-heidelberg.de/. Secondary structure prediction was performed using JPred4 (Drozdetskiy *et al.* 2015) at http://www.compbio.dundee.ac.uk/jpred4/. The subcellular localization of PpERF24 proteins was predicted using Plant-mSubP (Sahu *et al.*, 2020) at http://bioinfo.usu.edu/Plant-mSubP/. *PpERF24* orthologues and closest genes were identified by blast search on genomes available at phyotozome.org (https://phytozome-next.jgi.doe.gov/blast-search), including all moss genomes available at the moment (*P. patens*, *Ceratodon purpureus*, *Sphagnum fallax* and *Sphagnum magellanicum*), the liverwort *Marchantia polymorpha*, the lycophyte *Selaginella moellendorffii* and representative genomes of angiosperms (*A. thaliana*, *Glycine max*, *S. lycopersicum*, *Vitis vinifera* and *O. sativa*); in all cases the best blast hits were considered. To complete the search, a tblastn analysis using Pp3c7_10780V3.1 protein as query sequence was performed at NCBI (https://blast.ncbi.nlm.nih.gov/), excluding *P. patens*; other species best blast hits obtained in this analysis with an e-value <1.0E-10 were retrieved and the corresponding protein sequence downloaded. To further analyze these proteins and two *PpERF24* orthologues reported in *Funaria hygrometrica* (Kirbis *et al*. 2020), a blast search on the *P. patens* genome using these proteins as query sequences was performed at phyotozome.org and NCBI, and sequence identity percentage with Pp3c7_10780V3.1 was obtained.

Phylogenetic analysis

For phylogenetic analysis, multiple alignments of the full-length amino acid sequences derived from the AP2 domain of *P. patens* and *A. thaliana* ERF family, retrieved from PlantTFDB v5 database (Jin *et al*. 2017), as well as from moss and liverwort proteins obtained in this work (Fh_17935, Fh_23703, CepurR40.9G091300.1.p, CepurR40.11G133100.1.p, TR55251, TR125756, DREB5-9 , Sphfalx11G110500.1.p, Sphmag11G113800.1.p, and Mapoly0166s0010.2.p) were performed with MAFFT (Katoh *et al*., 2019). The AP2 domain of PpERF24 was used as a reference and amino acids flanking it were trimmed from all proteins. These sequences were realigned and the resulting alignment was used to create an unrooted phylogenetic tree by Maximum likelihood using iqtree

1.3.11.1 software (Nguyen *et al*. 2015). The following parameters were used: ultrafast bootstrap (Minh *et al*. 2013) with 1,000 bootstrap replicates, and standard model selection followed by tree construction. The best-fit model LG+G4 was chosen according to Bayesian information criterion. The phylogenetic tree was visualized with iTOL6.5.2 (Letunic and Bork 2021). The AP2 domains of the different clades were retrieved and sequences logos for conserved motifs were obtained from multiple sequence alignments of *A. thaliana*, *P. patens* and other mosses AP2 domains using CLC Main Workbench ver 21.0.4 (Qiagen).

Cell Death Measurements

For cell death measurements, *P. patens* colonies treated with CF were incubated with 0.1 % Evans blue during 1 h whereas *P. patens* colonies inoculated with fungi and *P. irregulare* were incubated with 0.05 % Evans blue during 2 h. After incubation, tissues were washed four times with deionized water to remove excess and unbound dye. Dye bound to dead cells was solubilized in 50% methanol with 1% SDS for 45 min at 60 ºC and the absorbance measured at 600 nm (Oliver *et al.*, 2009; Levine *et al*., 1994). Samples were dried at 60 ºC during 16 h and results are expressed as Abs600nm/mg dry weight (DW). Eight samples containing four colonies were analyzed for each genotype and treatment, and each experiment was repeated at least three times. Data from each experiment was tested for normality and further compared using a two-way ANOVA where P-values <0.05 were considered statistically significant. Statistical analysis was performed with GraphPad Prism software ver. 8.0.2.

RNA extraction, cDNA library preparation and sequencing

For RNA extraction of *B. cinerea*-infected plants, three independent biological replicates of tissue were harvested from each genotype and treatment at 24 hpi, immediately frozen in liquid nitrogen, and stored at -80˚C. Frozen samples were pulverized with a mortar and pestle and total RNA was extracted using the RNeasy Plant Mini Kit (Qiagen, Germany), including an RNase-Free DNase treatment in column (Qiagen), according to manufacturer's protocol. RNA quality control, library preparation, and sequencing were performed at Macrogen Inc. (Korea). RNA integrity was checked before library preparation using an Agilent Technologies 2100 Bioanalyzer (Agilent Technologies). Libraries for each biological replicate were prepared for paired-end sequencing by TruSeq Stranded Total RNA LT Sample Prep Kit (Plant) with 1 μg input RNA, following the TruSeq Stranded Total RNA Sample Prep Guide, Part # 15031048 Rev. E. Sequencing was performed on Illumina platform

by Macrogen Inc. (Korea) to generate paired-end 101 bp reads, obtaining 46 to 66 M reads per sample with Q20 >97,85 %.

RNA-seq processing and differential expression analysis

RNA-seq processing steps were done through Galaxy platform (Afgan *et al.*, 2018) at https://usegalaxy.org/, following Reboledo *et al.* (2021) pipeline. Trimmed reads were mapped to reference genomes of *P. patens* using Hisat2 software (Kim *et al.*, 2015). All reads were mapped first against *P. patens* organelle genomes and rRNA sequences (mitochondrial NC_007945.1; chloroplast NC_005087.1; ribosomal HM751653.1, X80986.1 and X98013.1). The remaining reads were mapped against *P. patens* nuclear genome v3 (Lang *et al.*, 2018), using Ppatens_318_v3.fa as the reference genome file and Ppatens_318_v3.3.gene_exons.gff3 as a reference file for gene models (https://phytozome.jgi.doe.gov/pz/portal.html), and concordant mapped read pairs were retained. The BAM files with reads mapped in proper pairs were obtained with Samtools View software ver. 1.9 and then sorted by name with Samtools Sort software ver. 2.0.3 (Li *et al.*, 2009).

Reads were counted by the FeatureCounts software ver. 1.6.4 (Liao *et al.*, 2014) as in Reboledo *et al.* (2021). Differential expression analyzes were performed using EdgeR software ver. 3.24.1 (Robinson *et al.*, 2010; Liu *et al.*, 2015) with p-value adjusted threshold 0.05, p-value adjusted method Benjamini and Hochberg (1995) and Minimum log2 Fold Change 1. For comparison, counts were normalized with TMM method. Low expressed genes were filtered for count values ≥5 in three or more samples. In this study, a false discovery rate (FDR) ≤0.05 was used to determine significant differentially expressed genes (DEGs) between samples, and expression values were represented by log2 ratio. Hierarchical clustering, and heatmaps plots, of expressed genes were performed on log2 Fold Change expression values using the R package “gplots” ver. 3.1.0.

GO enrichment analysis

Gene ontology (GO) and functional annotations were assigned based on *P. patens* v3.3 gene models (https://phytozome.jgi.doe.gov/pz/portal.html) and Blast2GO ver. 5.2.5 software (Götz *et al.*, 2008), through Blast and Interpro searches of homologs and protein domains (Reboledo *et al.* 2021). DEG functional enrichment analysis was performed using OmicsBox tools (https://www.biobam.com/omicsbox/). GO terms with a FDR ≤0.05 were considered for our analysis.

3 RESULTS

3.1. *PpERF24* is a moss-specific pathogen inducible gene

In a previous study, we identified a member of the AP2/ERF superfamily (Pp3c11_14690) that was induced during treatment with elicitors of *P.c. carotovorum* (Alvarez *et al*., 2016). This gene has an open reading frame of 534 nucleotides and encodes a protein of 177 amino acids referred as *PpERF24* according to AP2/ERF members at PlantTFDB v5.0 database (**Supplementary Table 1**). The predicted AP2 domain consists of 63 amino acids with three-stranded anti-parallel β-sheet (β1–β3) and an α-helix according to SMART. We searched for proteins with high identity to PpERF24 at NCBI and Phytozome database and identified three *P. patens* genes that covered amino acids 20 to 177 and exhibited 58 and 67% of identity, including Pp3c7_10780, Pp3c2_25760 and Pp3c1_14230 (**Table 1**). Other *P. patens* genes showed 69 % identity only in the AP2 domain (39-99 aa). Putative orthologs were only identified in other moss species; CepurR40.9G091300 of *C. purpureus* shared 68% identity with PpERF24 in amino acids 38-177 and TR55251_c0_g3_i1 of *Bryum argenteum* shared 66% identity in amino acids 31-177 (**Table 1**). Two additional orthologs were identified in the moss *F. hygrometrica* (Fh_17935 and Fh_23703) (Kirbis *et al*., 2020). Interestingly, the liverwort *M. polymorpha*, the lycophyte *S. moellendorffii*, and angiosperms did not have orthologs (**Table 1**). To further analyze the characteristics of these proteins in the ERF family of *P. patens* (143 ERF+DREB), the deduced amino acid sequences of the AP2 domains were aligned with 123 ERF family members of *A. thaliana* obtained from the PlantTFDB v5.0 database, and the moss proteins identified by blast analysis (**Table 1**). An unrooted phylogenetic tree was constructed, showing well-supported clades that separated a moss-specific clade with *P. patens* and other moss proteins, and several clades including *A. thaliana* DREBs and ERFs groups described by Nakano *et al.* (2006), as well as *P. patens* proteins (**Figure 1**). Based on the tree and the ERF family classification in *A. thaliana*, *P. patens* has 36 moss-specific proteins, 47 DREBs and 60 ERFs. Interestingly, PpERF24 was included in the moss-specific clade, forming a subclade with the three *P. patens* homologs Pp3c7_10780, Pp3c2_25760 and Pp3c1 14230, the orthologs CepurR40.9G091300, TR55251, Fh_23703, Fh_17935 and two additional sequences Sphfalx11G110500 and Sphmag11G113800.

Multiple alignment of the AP2 domain of the DREB and ERF clades showed highly conserved signatures in the YRG and RAYD elements between *P. patens* and *A. thaliana* (**Supplementary Figure 1, 2**). The motifs YRG or YKG and WLG involved in DNA binding were present in most AP2 domains of *P. patens* ERFs and DREBs (**Figure 2A**). The AYD signature of the RAYD motif

involved in protein-protein interactions and DNA binding was highly conserved in *P. patens* ERFs and DREBs, while the R residue changed to other amino acid in several members of both species (**Figure 2A**). Furthermore, the amino acids valine at position 14 and glutamic acid at position 19 (V14 and E19) that are typical of DREBs (Zhuang *et al*., 2008; Duan *et al*., 2013), were present in most *P. patens* DREBs (**Figure 2A, Supplementary Figure 1**). Similarly, alanine at position 14 (A14) and aspartic acid at position 19 (D19) that define ERFs, were found in most *P. patens* ERFs (**Figure 2A, Supplementary Figure 2**). In contrast, alignment of the AP2 domains of the moss-specific clade showed less conserved signatures in the YRG and RAYD elements (**Figure 2A, Supplementary Figure 3**). For example, a high number of moss-specific AP2 domains have an additional E at position 10 (E10), resulting in an RxRPELG/NK/R signature, which changed in ERF and DREB to RxRxWGK/R. Due to the additional E10, the conserved amino acids at position 14 and 19 changed to 15 and 20 in those moss-specific AP2 domains. Moreover, whereas the WLG motif was conserved in almost all moss-specific AP2 domains, other motifs such as FKG, and RAFD were more frequent in moss-specific proteins than *P. patens* and *A. thaliana* DREBs and ERFs. Furthermore, moss-specific clade AP2 domains have in most cases a V15 or an isoleucine at position 15 (I15) and a proline at position 20 (P20), corresponding to position 14 and 19 in members of the DREB and ERF clades (**Figure 2A**). Based on these findings, we looked into more detail to sequence alignment of the PpERF24 subclade and the Pp3c22_20520 subclade (**Figure 1, Figure 2B**). We found clear differences in amino acid composition in the YRG and RAYD elements of both subclades. The most remarkably change is the presence of an I15 in the PpERF24 subclade and a V15 in the Pp3c22_20520 subclade. Changes in other signatures include; YKGIR and RYIS in the YRG element of the PpERF24 subclade that is converted to FRGVR and KWVT in the Pp3c22_20520 subclade. Interestingly, all *P. patens* members of the PpERF24 subclade are induced by the fungal pathogens *B. cinerea* and *C. gloeosporioides* (Reboledo *et al.*, 2022), suggesting a possible role in moss defense against biotic stress. Based on these findings, we further characterized PpERF24 and evaluated its role in moss defenses against pathogen infection.

3.2. Subcellular localization of PpERF24

According to subcellular localization prediction using Plant-mSubP (Sahu *et al*., 2020), PpERF24 goes to the nucleus. To confirm this prediction, the intracellular localization of PpERF24 was determined by transient expression of the PpERF24:GFP fusion protein in *N. tabacum* leaves (**Figure 3**). Consistent with the function of a TF, confocal microscopy showed that PpERF24:GFP fusion

protein was located in the nucleus and the fluorescent signals of the control were observed in whole cells.

3.3. Overexpression of *PpERF24* increases resistance against pathogens in *P. patens*

P. patens lines overexpressing *PpERF24* were generated and two transformants designated PpERF24-OX-2 and PpERF24-OX-4 exhibiting high constitutive levels of *PpERF24* were selected for further studies (**Supplementary Figure 4A**). No variation in the phenotype of overexpressing lines compared to wild type plants was observed during gametophytic growth under normal growth conditions (**Supplementary Figure 4B**). The possible role of PpERF24 during defense responses against pathogens was evaluated by inoculating moss colonies with *B. cinerea*, *C. gloeosporioides*, *P. irregulare*, or treated with elicitors of *P.c. carotovorum*, and measuring cellular damage. Symptom development between genotypes did not show visible differences after treatments with pathogens (data not shown). However, cell death decreased significantly in PpERF24-OX-2 and PpERF24-OX-4 compared to wild type tissues, after inoculation with *B. cinerea*, *P. irregulare* and treatment with elicitor of *P.c. carotovorum*, while only PpERF24-OX-4 exhibited increased resistance against *C. gloeosporioides* (**Figure 4**). These findings indicate that PpERF24 contributed to increased resistance against pathogens, evidenced by less cellular damage.

To get more insights into the function of PpERF24 in resistance mechanisms, we performed a transcriptional profiling analysis of wild type and PpERF24-OX-4 plants after 24 hours of control treatment or *B. cinerea* inoculation. RNA-seq generated a total of 268 million reads that mapped to the nuclear genome (**Supplementary Table 2**). A total of 391 differentially expressed genes (DEGs) were identified when PpERF24-OX-4 control plants were compared with control wild type plants (242 were upregulated and 149 were downregulated) (**Figure 5, Supplementary Table 3**). Interestingly, 51 % (124) of the upregulated DEGs were also induced during *B. cinerea* infection in wild type plants, and 54% (80) of the downregulated DEGs were also repressed in wild type infected plants. In total, 2652 and 3371 genes were induced and repressed, respectively, in wild type *B. cinerea* inoculated plants compared to control plants. Similarly, 2208 induced and 2697 repressed genes were present in the comparison between *B. cinerea*-inoculated PpERF24-OX-4 and the corresponding control tissue (**Figure 5A**). Furthermore, 1923 genes were commonly upregulated during *B. cinerea* inoculation in PpERF24-OX-4 and wild type plants compared to the corresponding controls (**Figure 5B**). Similarly, a high number of DEGs (2349) were downregulated in both genotypes when *B. cinerea* and control treatments were compared (**Figure 5B**).

Enrichment of Gene Ontology (GO) terms was performed to identify the biological processes (BP) and molecular functions (MF) mostly affected by *B. cinerea* infection in wild type and PpERF24-OX-4 (**Supplementary Table 4**). A high number of the top 15 significantly enriched GO terms for upregulated and downregulated genes were similar in *B. cinerea* infected wild type and PpERF24-OX-4 plants. For upregulated DEGs, enriched GOs BP terms included, phenylpropanoid metabolic process, secondary metabolic process, cinnamic acid biosynthetic process, response to fungus, defense response, response to oxygen-containing compound, and defense response to fungus. Similarly, enriched MF GOs were related to naringenin-chalcone synthase activity, DNA-binding transcription factor activity, transcription regulator activity, phenylalanine ammonia-lyase activity, heme binding, ammonia-lyase activity, catalytic activity, tetrapyrrole binding, carbon-nitrogen lyase activity, oxidoreductase activity, active transmembrane transporter activity, and nutrient reservoir activity. For downregulated DEGs, enriched GOs included terms related to photosynthesis, responses to different types of lights and response to abiotic stimulus (**Supplementary Table 4**). When PpERF24-OX-4 and wild type control plants were compared, only upregulated genes showed enriched GO terms, including DNA-binding transcription factor activity and transcription regulator activity.

3.4. Increased resistance in PpERF24 overexpressing lines correlates with induced expression of defense related genes

Since PpERF24-OX-4 under control treatment showed differential expression of genes with possible roles in defense, such as TFs, compared to wild type plants, we focused on the group of 391 DEGs. Hierarchical clustering identified a group of upregulated DEGs in PpERF24-OX-4 control tissues, which did not show differential expression during *B. cinerea* inoculation in PpERF-OX-4 and wild type plants (clusters 3 and 4). This result could be due to higher expression levels in PpERF-OX-4 that did not increased significantly during *B. cinerea* inoculation and were therefore not considered as DEGs. However, several groups of genes that showed increased expression in PpERF-OX-4 control samples compared to wild type control samples, were also induced by *B. cinerea* in both genotypes (clusters 2 and 3) (**Figure 6**). Within these upregulated DEGs, genes encoded five ERFs, five MYBs including TT2, one PLATZ and other proteins involved in defense against biotic stress, including chitin elicitor receptor kinase 1 (CERK1), chitinase, respiratory burst oxidase (RBOH), beta-1,3 glucanase, cupin, peroxidase and flavonoid 3'-hydroxylases (**Supplementary Table 5**). Furthermore, genes encoding a lipase, an allene oxide cyclase (AOC) and a 12-oxophytodienoic acid reductase

(OPR) involved in the jasmonate pathway were upregulated. Additionally, in PpERF24-OX-4 genes involved in cell wall remodeling and integrity maintenance were upregulated compared to wild type plants under control conditions, including xyloglucan 6-xylosyltransferases, protein trichome birefringence, mannan polymerase II complex, galacturonosyl transferase, and cobra-like protein. Taken together, these findings suggest that PpERF24 positively regulates the expression of defense genes, leading to increased resistance to pathogens.

4 DISCUSSION

Land plants, including mosses, have evolved different defense mechanisms to protect themselves against invading pathogens and abiotic stresses. One of these defense mechanisms include AP2/ERF TFs (Reboledo *et al*., 2022). In *P. patens,* at least 161 AP2/ERF genes have been identified and a high proportion of them respond to different types of abiotic stresses and biotic interactions (Reboledo *et al*., 2022). ERF family is divided into ERF and DREB subfamilies based on the sequence similarity of their AP2 domain, including the conserved A14 and D19 for ERFs, and the V14 and E19 for DREBs (Sakuma *et al*., 2002). According to our phylogenetic tree and *A. thaliana* classification, 36 *P. patens* proteins belong to a moss-specific clade, while 47 *P. patens* DREBs and 60 *P. patens* ERFs are grouped with *A. thaliana* DREB and ERF subfamilies. Interestingly, while most *P. patens* and *A. thaliana* proteins in the ERF and DREB clades have these conserved amino acids, PpERF24 and other *P. patens* proteins within the moss-specific clade have a conserved V15 or I15 and P20 due to an additional amino acid at position 10, which was in most cases an E10. Consistently, several members of a *B. argenteum*-specific ERF clade have a V15 and a P20 in the AP2 domain (Li *et al*., 2018). It has been shown previously that while DREB V14 is generally conserved in different plant species, several angiosperms have a leucine or a valine instead of E19 (Wang *et al*., 2011; Dubouzet *et al*., 2003), suggesting that the function of the 14th amino acid is likely more important than the 19th for specific DNA-binding activity (Wang *et al*., 2011). In *P. patens*, V15 was conserved in 22 members (61%) of the moss-specific clade, while other members of this clade have I15 (five proteins), or other amino acids in that position (nine proteins). The presence of P20 in 33 of 45 moss-specific AP2 domains (73%) suggests the relevance of this residue in the YRG element. Remarkably, the signatures YKGIR, and RYIS that includes I15, in the YRG element separated PpERF24 subclade from Pp3c22_20520 subclade and the rest of the moss-specific proteins. Conserved amino acids within the YRG element are important for DNA binding, including amino acid 14 and 19 that bind to promoter regions of the target genes and modulate their expression (Allen *et al*., 1998; Sakuma *et al*., 2002). How the PpERF24 subclade signatures within the YRG

element affect DNA binding to specific elements needs further investigation. Interestingly, all *P. patens* members of the PpERF24 subclade are induced by the pathogens *B. cinerea* and *C. gloeosporioides* (Reboledo *et al*., 2022).

Overexpression of *PpERF24* generated moss plants that exhibited less damage to *B. cinerea*, *P. irregulare* and treatment with elicitors of *P. c. carotovorum* compared to wild type plants, while the line that exhibited the highest expression level of PpERF24 also showed increased resistance to *C. gloeosporioides*. This is consistent with previous studies showing that overexpression of ERF1 confers resistance in *A. thaliana* to several fungi, including *B. cinerea* (Berrocal-Lobo *et al*., 2002). Moreover, overexpression of ERF TF ORA59 (octadecanoid-responsive Arabidopsis) increases resistance against *P. c. carotovorum*, while mutant ora59 plants were more susceptible to this pathogen (Kim *et al*. 2018). ORA59 interacts in the nucleus with another ERF (RAP2.3) and play a positive role in ethylene-regulated responses (Kim *et al*., 2018).

Transcriptional profiling and GO enrichment analysis of PpERF24-OX-4 and wild type plants revealed that in response to *B. cinerea* similar categories of genes were upregulated. These include genes encoding proteins of important defense pathways and proteins with diverse roles in defense, such as receptors involved in perception of the pathogen, kinases and calcium signaling, transcriptional regulation, cell wall associated defenses, phenylpropanoid pathway and hormonal pathways including the jasmonate pathway. Furthermore, genes encoding pathogenesis-related proteins with antimicrobial activities were upregulated in response to *B. cinerea* inoculation in wild type and PpERF24-OX-4, including *PR-1* (small cysteine-rich secreted protein), *PR-2* (β-1,3 glucanases), *PR-3* (chitinase), *PR-5* (thaumatin), *PR-9* (peroxidases), and *PR-10* (Bet v I). Similarly, photosynthesis related processes were downregulated in both genotypes after fungal infection, which could be related to browning and breakdown of chloroplasts (Ponce de León *et al*. 2007), and reallocation of nitrogen resources for synthesis of proteins involved in defense as has been observed in angiosperms (Windram *et al*. 2012). In total, 391 genes were differentially expressed in PpERF24-OX-4 compared to wild type under control conditions. Interestingly, approximately 50% of these upregulated genes were also upregulated during *B. cinerea* inoculation in wild type plants, suggesting their involvement in defense reactions that could favor the plants response making it more resistant to pathogens. The fact that transcript levels of two genes encoding flavonoid 3'-hydroxylases and a TF TT2 were higher in PpERF24-OX-4 compared to wild type under control conditions, suggest that rapid production of phenolic defense compounds could lead to less cellular damage produced by the

pathogen. These findings are consistent with reinforcement of *P. patens* cell walls by accumulation of phenolic and lignin-like compounds after *B. cinerea* infection (Ponce de León *et al*., 2012). Moreover, in PpERF24-OX-4 the accumulation of phenolic compounds derived from this pathway could lead to the accumulation of compounds with antimicrobial activities, contributing to reduce fungal colonization. Several compounds derived from the phenylpropanoid pathway have been detected in *P. patens*, including cafeic acid, coumaric acid, 4-hydroxybenzoic acid and cafeoyl quinic acid, some of which have antimicrobial activities (Erxleben *et al*. 2012; Richter *et al*. 2012). The possibility that PpERF24 overexpressing lines produce higher amounts of some of these molecules needs further investigation.

Several genes involved in cell wall remodeling and integrity maintenance were upregulated in PpERF24-OX-4 compared to wild type plants under control conditions, which could have an impact on cell wall composition and disease susceptibility. Deposition of heteroxylan near the fungal penetration sites in the epidermal cell wall is believed to enhance physical resistance to fungal penetration pegs and hence to improve pre-invasion resistance (Chowdhury *et al*., 2017). Moreover, cell wall polymer cross-linking could increase through association with phenolic compounds, and fungal colonization could be delayed so that other defense strategies can be activated (Huckelhoven, 2005).

Several TFs genes such as *ERFs*, *MYBs*, and *PLATZ* are more highly expressed in PpERF24-OX-4 compared to wild type control plants, and transcript levels of these TFs increased in both genotypes after *B. cinerea* inoculation. Expression levels of several of these type of TFs also increased in *P. patens* tissues in response to *C. gloeosporioides* (Otero-Blanca *et al*., 2021). Among the upregulated DEGs we found genes encoding a peroxidase and a respiratory burst oxidase (RBOH). Like in angiosperms, RBOH and peroxidases are associated to the oxidative burst in *P. patens* after chitin treatment (Lehtonen *et al*. 2012), and mutants in peroxidase PRX34 are more susceptible to fungal pathogens (Lehtonen *et al*. 2009). Interestingly, *CERK1* involved in chitin sensing was upregulated in PpERF24-OX-4 control compared to wild type control plants. Consistently, overexpression of apple *CERK1* affects multiple defense responses in *Nicotiana benthamiana* plants and increased their resistance to fungal pathogens (Chen *et al*., 2020). The expression levels of other genes related to defense was higher in PpERF24-OX-4 compared to wild type control plants, including chitinase, β-1,3 glucanase and cupin. Similarly, overexpression of *AtERF1*, *AtERF2* and *AtERF14*, activates

expression levels of a chitinase (*ChiB*) and a defensin 1.2 (*PDF1.2*) in *A. thaliana* (Solano *et al*., 1998; Brown *et al*., 2003; McGrath *et al*., 2005; Oñate-Sánchez *et al*., 2007).

The jasmonate pathway was activated in PpERF24-OX-4 compared to control plants, evidenced by increased expression of *AOC* and *OPR*. This pathway participates in *P. patens* defense against *B. cinerea* (Ponce de León *et al*., 2012). Interestingly, ERF ORA59 has been suggested to integrate ethylene and jasmonic acid signaling and regulate resistance to necrotrophic pathogens, including *B. cinerea* (Pré *et al*., 2008). In conclusion, like in angiosperms, our results reveal that PpERF24 positively regulates moss immunity against pathogen infection by modulating the expression levels of genes involved in defense responses, demonstrating a functionally conservation that suggests that ERF function probably existed in the common ancestor. Further studies on moss-specific ERFs, including PpERF24, will contribute to reveal the molecular mechanisms underlying their action, including DNA binding elements, other interacting proteins and target genes and their contribution to moss defense.

5 Conflict of Interest

The authors declare that the research was conducted in the absence of any commercial or financial relationships that could be construed as a potential conflict of interest.

6 Data Availability Statement

The original contributions presented in the study are publicly available in NCBI under accession number PRJNA821520.

7 Author Contributions

GR made the overexpressing lines, performed all the experiments and analyzed the transcriptomic data. AA and LV participated in phylogenetic analysis. GR, AA, LV and IPDL analyzed and interpreted the data and participated in discussions. IPDL wrote the manuscript and GR, LV and AA helped to write the article. All authors read and approved the final version of the manuscript.

8 Funding

This work was supported by “Fondo Conjunto” Uruguay-México (AUCI-AMEXCID), “Agencia Nacional de Investigación e Innovación (ANII) (graduate fellowships)” Uruguay, “Programa de

Desarrollo de las Ciencias Básicas (PEDECIBA)" Uruguay, and "Programa para Grupo de I+D Comisión Sectorial de Investigación Científica, Universidad de la República", Uruguay.

9 Acknowledgments

Authors thank Ricardo Larraya for technical assistance, Andrés Di Paolo for assistance in confocal microscopy analysis and Federico Santiñaque for flow cytometry analysis of DNA content.

10 References

Afgan, E., Baker, D., Batut, B., van den Beek, M., Bouvier, D., Čech, M., *et al.* (2018). The Galaxy platform for accessible, reproducible and collaborative biomedical analyses: 2018 update. Nucleic Acids Res. 46, W537–W544. doi:10.1093/nar/gky379.

Allen, M. D., Yamasaki, K., Ohme-Takagi, M., Tateno, M., and Suzuki, M. (1998). A novel mode of DNA recognition by a beta-sheet revealed by the solution structure of the GCC-box binding domain in complex with DNA. EMBO J. 17, 5484-96. doi:10.1093/emboj/17.18.5484.

Alvarez, A., Montesano, M., Schmelz, E., and Ponce de León, I. (2016). Activation of shikimate, phenylpropanoid, oxylipins, and auxin pathways in *Pectobacterium carotovorum* elicitors-treated moss. Front. Plant Sci. 7, 328. doi:10.3389/fpls.2016.00328.

Ashton, N.W., and Cove, D. (1977). The isolation and preliminary characterization of auxotrophic and analogue resistant mutants of the moss, *Physcomitrella patens*. Mol. Genet. Genomics 154, 87-95. doi:10.1007/BF00265581.

Aukerman, M. J., and Sakai, H. (2003). Regulation of flowering time and floral organ identity by a microRNA and lts APETALA2-like target genes. Plant Cell 15, 2730–2741. doi:10.1105/tpc.016238.

Benjamini, Y., and Hochberg, Y. (1995). Controlling the false discovery rate - a practical and powerful approach to multiple testing. J. R. Stat. Soc. Ser. B Methodol. 57, 289-300. doi:10.2307/2346101.

Berrocal-Lobo, M., Molina, A., and Solano, R. (2002). Constitutive expression of ETHYLENE-RESPONSE-FACTOR1 in Arabidopsis confers resistance to several necrotrophic fungi. Plant J. 29, 23–32. doi:10.1046/j.1365-313x.2002.01191.x.

Bowman, J.L., Kohchi, T., Yamato, K.T., Jenkins, J., Shu, S., Ishizaki, K. *et al.* (2017). Insights into land plant evolution garnered from the *Marchantia polymorpha* genome. Cell 171, 287-304.e15. doi:10.1016/j.cell.2017.09.030.

Brown, R.L., Kazan, K., McGrath, K.C., Maclean, D.J., and Manners, J.M. (2003). A role for the GCC-box in jasmonate-mediated activation of the PDF1.2 gene of Arabidopsis. Plant Physiol. 132, 1020–1032. doi:10.1104/pp.102.017814.

Castro, A., Vidal, S., and Ponce de León, I. (2016). Moss Pathogenesis-Related-10 protein enhances resistance to *Pythium irregulare* in *Physcomitrella patens* and *Arabidopsis thaliana*. Front. Plant Sci. 7, 580. doi:10.3389/fpls.2016.00580.

Charfeddine, M., Samet, M., Charfeddine, S., Bouaziz, D., and Bouzid, R.G. (2019). Ectopic expression of StERF94 transcription factor in potato plants improved resistance to *Fusarium solani* infection. Plant Mol. Biol. Reporter 37, 450–463. doi:10.1007/s11105-019-01171-4.

Chen, L., Zhang, Z., Liang, H., Liu, H., Du, L., Xu, H. *et al.* (2008). Overexpression of TiERF1 enhances resistance to sharp eyespot in transgenic wheat. J. Exp. Bot. 59, 4195-204. doi:10.1093/jxb/ern259.

Chen, Q., Dong, C., Sun, X., Zhang, Y., Dai, H., and Bai, S. (2020). Overexpression of an apple LysM-containing protein gene, MdCERK1–2, confers improved resistance to the pathogenic fungus, *Alternaria alternata*, in *Nicotiana benthamiana*. BMC Plant Biol. 20, 146. doi:10.1186/s12870-020-02361-z.

Chowdhury, J., Lück, S., Rajaraman, J., Douchkov, D., Shirley, N.J., Schwerdt, J.G., *et al.* (2017). Altered expression of genes implicated in xylan biosynthesis affects penetration resistance against powdery mildew. Front. Plant Sci. 8, 445. doi:10.3389/fpls.2017.00445.

Curtis, M.D., and Grossniklaus, U. (2003). A Gateway cloning vector set for high-throughput functional analysis of genes in planta. Plant Physiol. 133, 462–469. doi:10.1104/pp.103.027979.

Duan, C., Argout, X., Gebelin, V., Summo, M., Dufayard, J.F., Leclercq, J., *et al.* (2013). Identification of the *Hevea brasiliensis* AP2/ERF superfamily by RNA sequencing. BMC Genom. 14:30. doi:10.1186/1471-2164-14-30.

539 Drozdetskiy, A., Cole, C., Procter, J., and Barton, G.J. (2015). JPred4: a protein secondary structure
540 prediction server. Nucleic Acids Res. 43, W389–W394. doi:10.1093/nar/gkv332.

541 Dubouzet, J.G., Sakuma, Y., Ito, Y., Kasuga, M., Dubouzet, E.G., Miura, S., *et al.* (2003). Os-DREB
542 genes in rice, *Oryza sativa* L., encode transcription activators that function in drought-, high-
543 salt- and cold-responsive gene expression. Plant J. 33, 751–763. doi:10.1046/j.1365-313X.

544 Erxleben, A., Gessler, A., Vervliet-Scheebaum, M., and Reski, R. (2012). Metabolite profling of the
545 moss *Physcomitrella patens* reveals evolutionary conservation of osmoprotective substances.
546 Plant Cell Rep. 31, 427–436. doi.org/10.1007/s00299-011-1177-9.

547 Frank, W., Ratnadewi, D., and Reski, R. (2005). *Physcomitrella patens* is highly tolerant against
548 drought, salt and osmotic stress. Planta 220, 384–394. doi:10.1007/s00425-004-1351-1.

549 Götz, S., Garcia-Gomez, J.M., Terol, J., Williams, T.D., Nagaraj, S.H., Nueda, M.J., *et al.* (2008).
550 High-throughput functional annotation and data mining with the Blast2GO suite. Nucleic
551 Acids Res. 36, 3420-3435. doi:10.1093/nar/gkn176.

552 Huckelhoven, R. (2005). Powdery mildew susceptibility and biotrophic infection strategies. FEMS
553 Microbiol. Lett. 245, 9–17. doi:10.1016/j.femsle.2005.03.001.

554 Katoh, K., Rozewicki, J., and Yamada, K. (2019). MAFFT online service: multiple sequence
555 alignment, interactive sequence choice and visualization. Brief. Bioinformatics 20 (4): 1160-
556 1166. doi.org/10.1093/bib/bbx108.

557 Kim, D., Langmead, B., and Salzberg, S. (2015). HISAT: a fast spliced aligner with low memory
558 requirements. Nat. Methods 12, 357-360. doi.org/10.1038/nmeth.3317.

559 Kim, N.Y., Jang, Y.J. and Park, O.K. (2018), AP2/ERF Family transcription factors ORA59 and
560 RAP2.3 interact in the nucleus and function together in ethylene responses. Front. Plant Sci.
561 9, 1675. doi:10.3389/fpls.2018.01675.

562 Jin, J.P., Tian, F., Yang, D.C., Meng, Y.Q., Kong, L., Luo, J.C., et al. (2017). PlantTFDB 4.0:
563 toward a central hub for transcription factors and regulatory interactions in plants. Nucleic
564 Acids Res. 45, D1040-D1045. doi: 10.1093/nar/gkw982.

Jofuku, K.D., den Boer, B.G., Van Montagu, M., and Okamuro, J.K. (1994). Control of Arabidopsis flower and seed development by the homeotic gene APETALA2. Plant Cell 6, 1211–1225. doi: 10.1105/tpc.6.9.1211.

Kirbis, A., Waller, M., Ricca, M., Bont, Z., Neubauer, A., Goffinet, B. et al. (2020). Transcriptional landscapes of divergent sporophyte development in two mosses, *Physcomitrium* (*Physcomitrella*) *patens* and *Funaria hygrometrica*. Front. Plant Sci. 11, 747. doi: 10.3389/fpls.2020.00747.

Lang, D., Ullrich, K.K., Murat, F., Fuchs, J., Jenkins, J., Haas, F.B., et al. (2018). The *Physcomitrella patens* chromosome-scale assembly reveals moss genome structure and evolution. Plant J. 93, 515-533. doi: 10.1111/tpj.13801.

Lata, C., and Prasad, M. (2011). Role of DREBs in regulation of abiotic stress responses in plants. J. Exp. Bot. 62, 4731–4748. doi.org/10.1093/jxb/err210.

Lehtonen, M.T., Akita, M., Kalkkinen, N., Ahola-Iivarinen, E., Rönnholm, G., Somervuo, P. et al (2009). Quickly-released peroxidase of moss in defense against fungal invaders. New Phytol. 183, 432–443. doi.org/10.1111/j.1469-8137.2009.02864.x.

Lehtonen, M.T., Akita, M., Frank, W., Reski, R., and Valkonen, J.P. (2012). Involvement of a class III peroxidase and the mitochondrial protein TSPO in oxidative burst upon treatment of moss plants with a fungal elicitor. Mol. Plant Microbe Interact. 25, 363–371. doi.org/10.1094/MPMI-10-11-0265.

Letunic, I., Khedkar, S., and Bork, P. (2021). SMART: recent updates, new developments and status in 2020, Nucleic Acids Res. 49, D458-460. doi.org/10.1093/nar/gkaa937.

Letunic, I., and Bork, P. (2021). Interactive Tree Of Life (iTOL) v5: an online tool for phylogenetic tree display and annotation, Nucleic Acids Res. 49, W293–W296. https://doi.org/10.1093/nar/gkab301

Levine, A., Tenhaken, R., Dixon, R., and Lamb, C. (1994). H2O2 from the oxidative burst orchestrates the plant hypersensitive disease resistance response. Cell 79, 583–593. doi: 10.1016/0092-8674(94)90544-4.

592 Licausi, F., Ohme-Takagi, M., and Perata, P. (2013). APETALA2/Ethylene Responsive Factor
593 (AP2/ERF) transcription factors: mediators of stress responses and developmental programs.
594 New Phytol. 199, 639–649. doi: 10.1111/nph.12291.

595 Li, H., Handsaker, B., Wysoker, A., Fennell, T., Ruan, J., Homer, N., et al. (2009). The Sequence
596 Alignment/Map format and SAMtools. Bioinformatics 25, 2078-2079.
597 doi.org/10.1093/bioinformatics/btp352.

598 Li, X., Gao, B., Zhang, D., Liang, Y., Liu, X., Zhao, J., et al. (2018). Identification, classification,
599 and functional analysis of AP2/ERF family genes in the desert moss *Bryum argenteum*. Int. J.
600 Mol. Sci. 19, 3637. doi: 10.3390/ijms19113637.

601 Li, L., Peng, H., Tan, S., Zhou, J., Fang, Z., Hu, Z., *et al.* (2020). Effects of early cold stress on gene
602 expression in *Chlamydomonas reinhardtii*, Genomics 112, 1128-1138.
603 https://doi.org/10.1016/j.ygeno.2019.06.027.

604 Liao, Y., Smyth, G.K., and Shi, W. (2014). FeatureCounts: an efficient general purpose program for
605 assigning sequence reads to genomic features. Bioinformatics 30, 923-930.
606 doi.org/10.1093/bioinformatics/btt656.

607 Liu, R., Holik, A.Z., Su, S., Jansz, N., Chen, K., Leong, H.S., et al. (2015). Why weight? Modelling
608 sample and observational level variability improves power in RNA-seq analyses. Nucleic
609 Acids Res. 43, e97. doi: 10.1093/nar/gkv412.

610 McGrath, K.C., Dombrecht, B., Manners, J.M., Schenk, P.M., Edgar, C.I., Maclean, D.J., et al.
611 (2005) Repressor- and activator-type ethylene response factors functioning in jasmonate
612 signaling and disease resistance identified via a genome-wide screen of Arabidopsis
613 transcription factor gene expression. Plant Physiol. 139, 949–959.
614 doi:10.1104/pp.105.068544.

615 Minh, B. Q., Nguyen, M. A. T., von Haeseler, A. (2013). Ultrafast approximation for phylogenetic
616 bootstrap. Mol. Biol. Evol. 30:1188-1195. doi: 10.1093/molbev/mst024.

617 Müller, M., and Munné-Bosch, S. (2015). Ethylene Response Factors: A key regulatory hub in
618 hormone and stress signaling. Plant Physiol. 169, 32-41. doi:10.1104/pp.15.00677.

619 Nakano, T., Suzuki, K., Fujimura, T., Shinshi, H. (2006). Genome-wide analysis of the ERF gene
620 family in Arabidopsis and rice. Plant Physiol. 140:411–432. doi: 10.1104/pp.105.073783.

621 Nguyen, L. T., Schmidt, H. A., von Haeseler, A., and Minh B. Q. (2015). IQ-TREE: A Fast and
622 Effective Stochastic Algorithm for Estimating Maximum-Likelihood Phylogenies. Mol. Biol.
623 Evol. 32(1): 268-274. doi.org/10.1093/molbev/msu300.

624 Okamuro, J.K., Caster, B., Villarroel, R., Van Montagu, M., and Jofuku, K.D. (1997). The AP2
625 domain of APETALA2 defines a large new family of DNA binding proteins in Arabidopsis.
626 Proc. Natl. Acad. Sci. USA 94, 7076–7081. doi: 10.1073/pnas.94.13.7076.

627 Oliver, J. P., Castro, A., Gaggero, C., Cascón, T., Schmelz, E. A., Castresana, C., et al. (2009).
628 *Pythium* infection activates conserved plant defense responses in mosses. Planta 230, 569–
629 579. doi:10.1007/s00425-009-0969-4.

630 Oñate-Sánchez, L., Anderson, J.P., Young, J., and Singh, K.B. (2007). AtERF14, a member of the
631 ERF family of transcription factors, plays a nonredundant role in plant defense. Plant Physiol.
632 143, 400–409. doi:10.1104/pp.106.086637.

633 Otero-Blanca, A., Pérez-Llano, Y., Reboledo-Blanco, G., Lira-Ruan, V., Padilla-Chacon, D., Folch-
634 Mallol, J.L., et al. (2021). *Physcomitrium patens* infection by *Colletotrichum gloeosporioides*:
635 understanding the fungal–bryophyte interaction by microscopy, phenomics and RNA
636 sequencing. J. Fungi 7, 677. https://doi.org/10.3390/jof7080677.

637 Perroud, P. F., Cove, D. J., Quatrano, R. S., and McDaniel, S. F. (2011). An experimental method to
638 facilitate the identification of hybrid sporophytes in the moss *Physcomitrella patens* using
639 fluorescent tagged lines. New Phytol. 191, 301–306. doi:10.1111/j.1469-8137.2011.03668.x.

640 Ponce de León, I., Oliver, J.P., Castro, A., Gaggero, C., Bentancor, M., and Vidal, S. (2007). *Erwinia*
641 *carotovora* elicitors and *Botrytis cinerea* activate defense responses in *Physcomitrella patens*.
642 BMC Plant Biol. 7, 52. doi:10.1186/1471-2229-7-52.

643 Ponce De León, I., Schmelz, E.A., Gaggero, C., Castro, A., Álvarez, A., and Montesano, M. (2012).
644 *Physcomitrella patens* activates reinforcement of the cell wall, programmed cell death and
645 accumulation of evolutionary conserved defence signals, such as salicylic acid and 12-oxo-

phytodienoic acid, but not jasmonic acid, upon *Botrytis cinerea* infection. Mol. Plant Pathol. 13, 960–974. doi:10.1111/j.1364-3703.2012.00806.x.

Ponce de León, I., and Montesano, M. (2017). Adaptation mechanisms in the evolution of moss defenses to microbes. Front. Plant Sci. 8, 1–14. doi:10.3389/fpls.2017.00366.

Pré, M., Atallah, M., Champion, A., De Vos, M., Pieterse, C.M.J., and Memelink, J. (2008). The AP2/ERF domain transcription factor ORA59 integrates jasmonic acid and ethylene signals in plant defense. Plant Physiol. 147, 1347–1357. doi:10.1104/pp.108.117523.

Nakano, T., Suzuki, K., Fujimura, T., and Shinshi, H. (2006). Genome-wide analysis of the ERF gene family in Arabidopsis and rice. Plant Physiol. 140, 411–432. doi: 10.1104/pp.105.073783.

Rantakari, A., Virtaharju, O., Vähämiko, S., Taira, S., Palva, E. T., Saarilahti, H. T., et al. (2001). Type III secretion contributes to the pathogenesis of the soft-rot pathogen *Erwinia carotovora* partial characterization of the hrp gene cluster. Mol. Plant Microbe Interact. 14, 962–968. doi:10.1094/MPMI.2001.14.8.962.

Reboledo, G., del Campo, R., Alvarez, A., Montesano, M., Mara, H., and Ponce de León, I. (2015). *Physcomitrella patens* activates defense responses against the pathogen *Colletotrichum gloeosporioides*. Int. J. Mol. Sci. 16, 22280–22298. doi:10.3390/ijms160922280.

Reboledo, G., Agorio, A., Vignale, L., Batista-García, R.A., and Ponce De León, I. (2021). Transcriptional profiling reveals conserved and species-specific plant defense responses during the interaction of *Physcomitrium patens* with *Botrytis cinerea*. Plant Mol. Biol. 107, 365-385. doi:10.1007/s11103-021-01116-0.

Reboledo, G., Agorio, A., and Ponde De león, I. (2022). Moss transcription factors regulating development and defense responses to stress. J. Exp. Bot., erac055. https://doi.org/10.1093/jxb/erac055. *In press.*

Richter, H., Lieberei, R., Strnad, M., Novák, O., Gruz, J., Rensing, S.A., et al. (2012). Polyphenol oxidases in Physcomitrella: functional PPO1 knockout modulates cytokinin dependent development in the moss Physcomitrella patens. J. Exp. Bot. 63, 5121–5135. doi:10.1093/jxb/ers169.

674 Robinson, M.D., McCarthy, D.J., and Gordon, K. (2010). Smyth, edgeR: a Bioconductor package for
675 differential expression analysis of digital gene expression data. Bioinformatics 26, 139-140.
676 doi:10.1093/bioinformatics/btp616.

677 Sahu, S.S., Loaiza, C.D., and Kaundal, R. (2020). Plant-mSubP: a computational framework for the
678 prediction of single- and multi-target protein subcellular localization using integrated
679 machine-learning approaches, AoB PLANTS 12, plz068. doi:10.1093/aobpla/plz068.

680 Sakuma, Y., Liu, Q., Dubouzet, J.G., Abe, H., and Shinozaki, K. (2002). DNA-binding specificity of
681 the ERF/AP2 domain of Arabidopsis DREBs, transcription factors involved in dehydration-
682 and cold-inducible gene expression. Biochem. Biophys. Res. Commun. 290, 998-1009.
683 doi:10.1006/bbrc.2001.6299.

684 Schindelin, J., Arganda-Carreras, I., Frise, E., Kaynig, V., Longair, M., Pietzsch, T., et al. (2012).
685 Fiji: an open-source platform for biological-image analysis. Nat. Methods, 9, 676–682.
686 doi:10.1038/nmeth.2019.

687 Schaefer, D., Zryd, J. P., Knight, C. D., and Cove, D. J. (1991). Stable transformation of the moss
688 *Physcomitrella patens*. Mol. Gen. Genet. 226, 418–424. doi:10.1007/BF00260654

689 Solano, R., Stepanova, A., Chao, Q., and Ecker, J.R. (1998). Nuclear events in ethylene signaling: a
690 transcriptional cascade mediated by ETHYLENEINSENSITIVE3 and ETHYLENE-
691 RESPONSE-FACTOR1. Genes Dev. 12, 3703–3714. doi:10.1101/gad.12.23.3703.

692 Tsutsui, T., Kato, W., Asada, Y., Sako, K., Sato, T., Sonoda, Y. et al. (2009). DEAR1, a
693 transcriptional repressor of DREB protein that mediates plant defense and freezing stress
694 responses in Arabidopsis. J. Plant Res. 122, 633–643. doi:10.1007/s10265-009-0252-6.

695 Wang X, Chen X, Liu Y, Gao H, Wang Z, Sun G. (2011). CkDREB gene in Caragana korshinskii is
696 involved in the regulation of stress response to multiple abiotic stresses as an AP2/EREBP
697 transcription factor. Mol Biol Rep. 38(4):2801-11. doi: 10.1007/s11033-010-0425-3.

698 Wang, J.H., Gu, K.D., Han, P.L., Yu, J.Q., Wang, C.K., Zhang, Q.Y., et al. (2020). Apple ethylene
699 response factor MdERF11 confers resistance to fungal pathogen *Botryosphaeria dothidea*.
700 Plant Sci. 291, 110351. doi:10.1016/j.plantsci.2019.110351.

Windram, O., Madhou, P., McHattie, S., Hill, C., Hickman, R., Cooke, E. et al (2012). Arabidopsis defense against *Botrytis cinerea*: chronology and regulation deciphered by high-resolution temporal transcriptomic analysis. Plant Cell 24, 3530–3557. doi:10.1105/tpc.112.102046.

Yang, H., Shen, F., Wang, H., Zhao, T., Zhang, H., Jiang, J., and Xu, X. (2020a). Functional analysis of the SlERF01 gene in disease resistance to *S. lycopersici*. BMC Plant Biol. 20: 376. doi: 10.1186/s12870-020-02588-w.

Yang, Y., Li, R., and Qi, M. (2000b). *In vivo* analysis of plant promoters and transcription factors by agroinfiltration of tobacco leaves. Plant J. 22, 543–551. doi:10.1046/j.1365-313x.2000.00760.x

Xu, Z.S., Chen, M., Li, L.C., and Ma, Y.Z. (2011). Functions and application of the AP2/ERF transcription factor family in crop improvement. J. Integr. Plant. Biol. 53, 570-85. doi:10.1111/j.1744-7909.2011.01062.x.

Zhuang, J., Cai, B., Peng, R.H., Zhu, B., Jin, X.F., Xue, Y., et al. (2008). Genome-wide analysis of the AP2/ERF gene family in *Populus trichocarpa*. Biochem. Biophys. Res. Commun. 371, 468–474. doi:10.1016/j.bbrc.2008.04.087.

Table legend

Table 1. Pp3c11_14690 (PpERF24) protein best blast hits in mosses, liverwort and vascular plants genomes.

Figure legends

Figure 1. **Unrooted phylogenetic tree of AP2 domain of *P. patens*, moss and *A. thaliana*.** Unrooted maximum-likehood phylogenetic tree was visualized with iTOL. Subfamilies are indicated with different colors; ERFs (blue), DREBs (red) and moss-specific proteins (green). *A. thaliana* groups are indicated based on the classification published by Nakano *et al.* (2006). For proper visualization only bootstraps values for moss-specific, DREB and ERF clades, and PpERF24 and Pp3c22_20520 subclades are indicated. Pp3c11_14690 (PpERF24) is highlighted in green.

Figure 2. **Conserved motifs in the AP2 domain of mosses ERF family clades** (**A**) Sequence logos of AP2 domain from *P. patens* DREB clade, *P. patens* ERF clade and moss-specific clades. (**B**)

729 Alignment of PpERF24 and Pp3c22_20520 subclades AP2 domains and corresponding sequence
730 logos. Conserved YRG and RAYD elements are indicated with a black line and conserved amino
731 acids 14 and 19 for members of the DREB and ERF clades and 15 and 20 for PpERF24 and
732 Pp3c22_20520 subclades were marked with red arrows. The β-sheets and α-helix predicted for
733 PpERF24 are shown.

734 **Figure 3**. **Subcellular localization of PpERF24 in agroinfiltrated *N. tabacum* leaves**. Confocal
735 microscopy images of *N. tabacum* leaves taken 2 days after agroinfiltration. *N. tabacum* leaves were
736 transformed with the pMDC83 vector (GFP alone, upper panels) or with pMDC83-PpERF24-
737 mGFP6his construct (PpERF24 fused to GFP, lower panels). Visible cell nuclei are marked with a
738 white asterisk in bright field and merged panels. From left to right: GFP, chloroplasts, bright field
739 and merged images. The scale bars represent 50 μm.

740 **Figure 4. Cell death measurement in wild type and PpERF24 overexpressing plants**.

741 Measurement of cell death by Evans blue staining 24 h after inoculation of wild type, PpERF24-OX-
742 2 (OX2) and PpERF24-OX-4 (OX4) moss colonies with *B. cinerea*, *P. irregulare* and treatment with
743 elicitors of *P.c. carotovorum*. Cell death measurement for plant tissues inoculated with *C.*
744 *gloeosporioides* was performed at 72 hpi, Data were expressed as the absorbance (Abs) at 600 nm per
745 milligram of dry weight (DW). Values are means with standard deviations of eight independent
746 replicate moss samples. Experiments were repeated thrice with similar results. Asterisks indicate a
747 statistically significant difference between the wild type and overexpressing PpERF24 plants [two-
748 way ANOVA test, with Tukey's Honest Significant Difference test as post-hoc test using $P \leq 0.001$
749 (***)].

750 **Figure 5. Differentially expressed genes of wild type and PpERF24-OX-4 overexpressing line**
751 **during control treatment and *B. cinerea* infection**. (**A**) Number of differentially expressed genes
752 (DEGs), up and downregulated, in wild type versus PpERF24-OX-4 (OX4) tissues treated with water
753 (Ctrl), and wild type (Wt) and PpERF24-OX-4 tissues inoculated with *B. cinerea* (Bcin) versus
754 water-treated tissues at 24 hpi. (**B**) Venn diagram of *B. cinerea*-responsive *P. patens* genes in wild
755 type and PpERF24-OX-4 plants, and PpERF24-OX-4 versus wild type control tissues. Genes were
756 considered as DEGs when $|\log2\ FC| \geq 1$ and $FDR \leq 0.05$.

757 **Figure 6: Heatmap of hierarchical clustering of wild type and PpERF24-OX-4 overexpressing**
758 **line during control treatment and *B. cinerea* infection**. DEGs correspond to the 391 DEGs of

PpERF24-OX-4 control versus wild type control plants. Selected DEGs had |log2 FC| ≥ 1 and FDR ≤ 0.05. See Supplementary Table 4 for complete information.

Supplementary Material

Supplementary Figure 1. Alignment of the AP2 domain of the *P. patens* and *A. thaliana* DREB clades. Alignments include AP2 domain sequences from DREB clade in the unrooted phylogenetic tree shown in Fig. 1. *P. patens* DREB realignment was used to obtain DREB sequence logo showed in Fig. 2 A, without Pp3c8_24200, Pp3c10_680 and Pp3c6_9830 from *P. patens* and AT3G54320 and AT4G13040 from *A. thaliana* considering that they did not show conserved positions 14 and 19 and were not included in Nakano *et al.* (2006) ERF classification.

Supplementary Figure 2. Alignment of the AP2 domain of the *P. patens* and *A. thaliana* ERF clades. Alignments include AP2 domain sequences from ERF clade in the unrooted phylogenetic tree shown in Fig. 1. *P. patens* ERF alignment was used to obtain ERF sequence logo showed in Fig. 2 A.

Supplementary Figure 3. Alignment of the AP2 domain of the moss-specific clade. Alignment include AP2 domain sequences from moss-specific clade in the unrooted phylogenetic tree shown in Fig. 1. Alignment was used to obtain moss-specific sequence logo showed in Fig. 2 A.

Supplementary Figure 4. Generation of PpERF24 overexpression *P. patens* plants. (**A**) Transcript levels of PpERF24 in untreated (Control) and *B. cinerea* inoculated wild type (Wt) plants, and untreated PpERF24-OX-1 (OX-1), PpERF24-OX-2 (OX-2), PpERF24-OX-3 (OX-3), and PpERF24-OX-4 (OX-4) plants. (**B**) Phenotype of wild type, PpERF24-OX-2 and PpERF24-OX-4 moss colonies.

Supplementary Table 1. Members of the AP2/ERF superfamily of *P. patens*.

Supplementary Table 2. Summary of mapped reads of the RNA-Seq libraries.

Supplementary Table 3. List of *P. patens* differentially expressed genes (DEGs) in wild type and PpERF-OX-4 during control treatment and *B. cinerea* infection.

Supplementary Table 4. Enriched gene ontology (GO) terms (over-representation) for biological processes and molecular function in wild type and PpERF24-OX-4 during control treatment and *B. cinerea* infection.

Supplementary Table 5. List of 391 *P. patens* DEGs that were differentially expressed when wild type and PpERF24-OX-4 control samples were compared. DEGs were considered when $|\log2\ FC| \geq 1$ and FDR ≤ 0.05. Data corresponds to Heatmap shown in Figure 6.

4.3.1. Tabla y figuras Capítulo III

Table 1. Pp3c11_14690 (PpERF24) protein best blast hits in mosses, liverwort and vascular plants genomes.

Plant species		Protein	Protein size	Pp3c11_14690V3.1 protein aligned region (aa position)	aa identity in aligned region	E-value
Physcomitrium patens	moss	Pp3c7_10780V3.1.p	177	20-177	67%	3e-48
		Pp3c2_25760V3.4.p	224	19-177	63%	4e-45
		Pp3c1_14230V3.1.p	191	20-177	58%	1e-39
		Pp3c21_21070V3.1.p	204	39-99	69%	3e-24
		Pp3c22_20520V3.1.p	204	39-99	69%	4e-24
		Pp3c18_1800V3.1.p	202	39-99	69%	4e-24
		Pp3c19_10050V3.1.p	203	39-99	69%	6e-24
Funaria hygrometrica	moss	Fh_17935 *	184	18-177	81%	4e-66
		Fh_23703 *	191	29-177	63%	2e-51
Ceratodon purpureus	moss	CepurR40.9G091300.1.p	193	38-177	68%	5e-45
		CepurR40.11G133100.1.p	201	39-99	69%	2e-24
Bryum argenteum	moss	TR55251mRNA **	193	31-177	66%	1e-39
		TR125756 mRNA **	216	39-109	63%	4e-25
Syntrichia caninervis	moss	DREB5-9 mRNA **	201	39-109	63%	7e-25
Sphagnum fallax	moss	Sphfalx11G110500.1.p	205	38-95	84%	2e-28
Sphagnum magellanicum	moss	Sphmag11G113800.1.p	212	21-95	71%	6e-29
Marchantia polymorpha	liverwort	Mapoly0166s0010.2.p	443	38-98	46%	5e-09
Selaginella moellendorffii	vascular plant	S.moellendorffii v1.0|68470	131	20-85	38%	1e-09
Arabidopsis thaliana	vascular plant	AT4G06746.1	150	38-90	54%	3e-11
Glycina max	vascular plant	Glyma.15G180000.1.p	213	36-101	49%	3e-11
Solanum lycopersicum	vascular plant	Solyc06g054630.3.1	237	37-99	52%	3e-13
Vitis vinifera	vascular plant	VIT_204s0008g02230.1	192	38-99	51%	3e-11
Oriza sativa	vascular plant	LOC_Os09g39810.1	131	35-81	49%	1e-09

* Protein sequence obtained from Kirbis *et al*. 2020, used as query sequence in blast analysis against *P. patens* genome at phtozome.

** Protein sequence retrieved from tblastn analysis at NCBI, using Pp3c11_14690V3.1 as a query sequence (excluding *P. patens* in the search); TR55251mRNA, TR125756 mRNA and DREB5-9 mRNA corresponds to accession MK170311.1, MK170349.1, and KU613417.1, respectively.

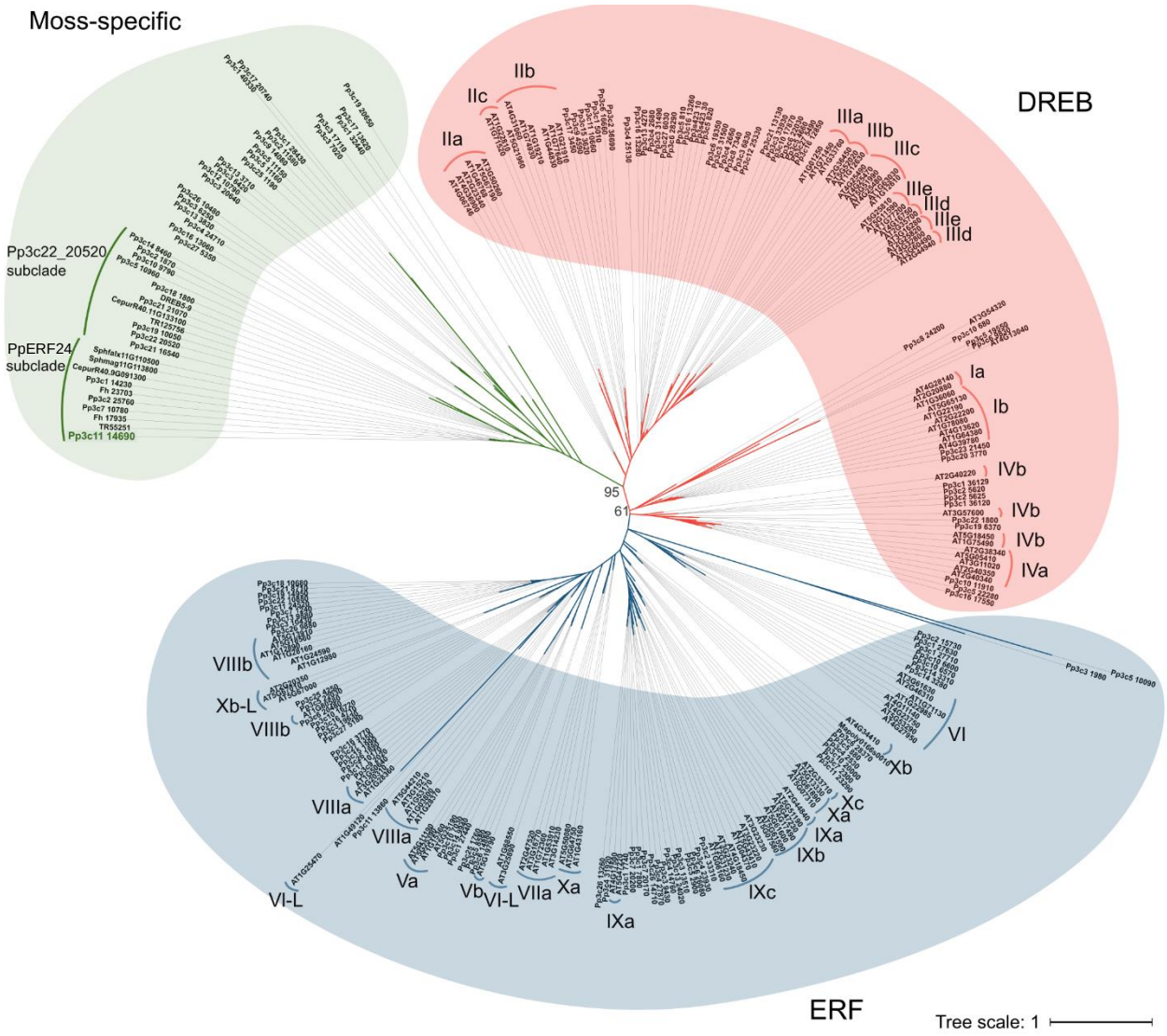

Figure 1. Unrooted phylogenetic tree of AP2 domain of *P. patens*, moss and *A. thaliana*. Unrooted maximum-likehood phylogenetic tree was visualized with iTOL. Subfamilies are indicated with different colors; ERFs (blue), DREBs (red) and moss-specific proteins (green). *A. thaliana* groups are indicated based on the classification published by Nakano et al. (2006). For proper visualization only bootstraps values for moss-specific, DREB and ERF clades, and PpERF24 and Pp3c22_20520 subclades are indicated. Pp3c11_14690 (PpERF24) is highlighted in green.

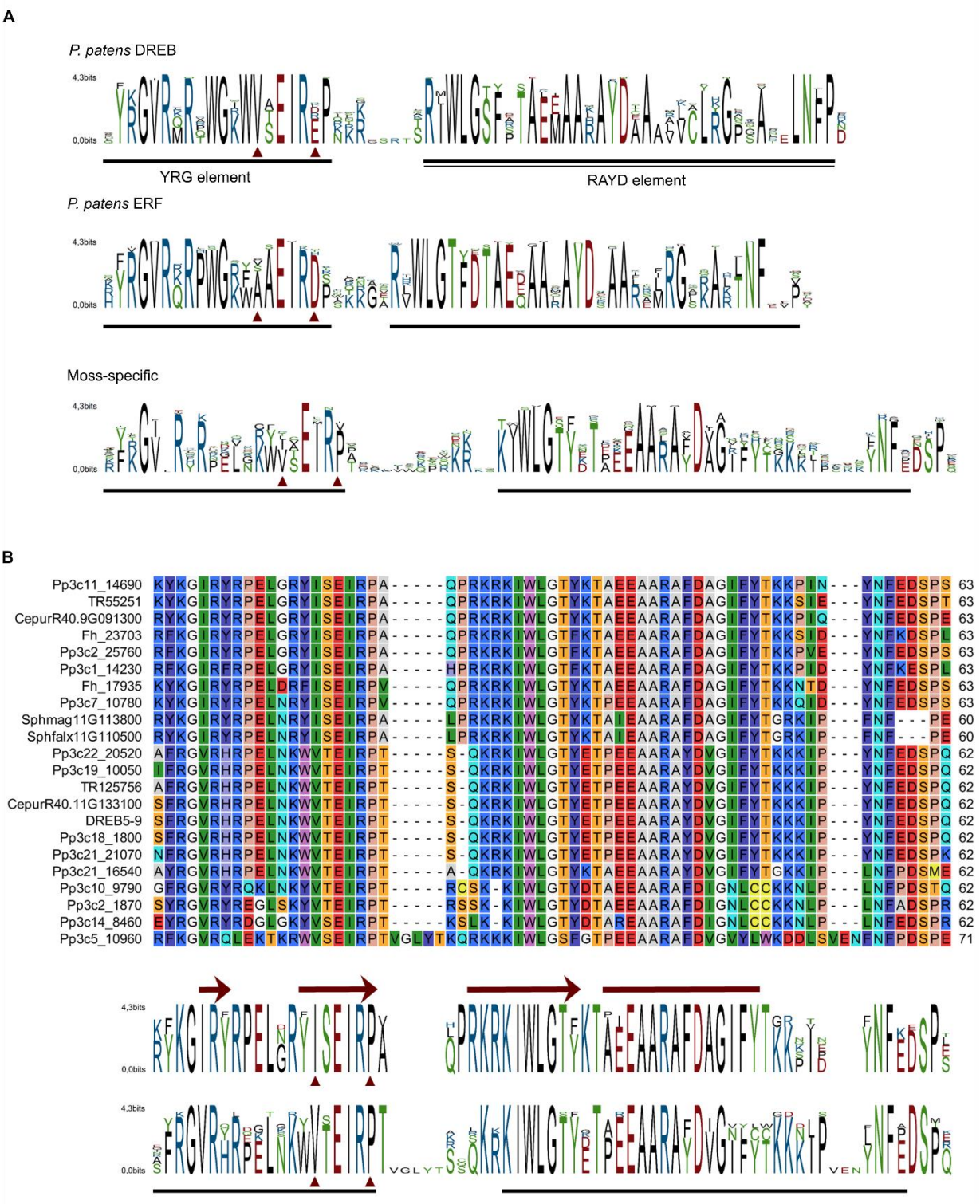

Figure 2. Conserved motifs in the AP2 domain of mosses ERF family clades (A) Sequence logos of AP2 domain from *P. patens* DREB clade, *P. patens* ERF clade and moss-specific clades. **(B)** Alignment of PpERF24 and Pp3c22_20520 subclades AP2 domains and corresponding sequence logos. Conserved YRG and RAYD elements are indicated with a black line and conserved amino acids 14 and 19 for members of the DREB and ERF clades and 15 and 20 for PpERF24 and Pp3c22_20520 subclades were marked with red arrows. The β-sheets and α-helix predicted for PpERF24 are shown.

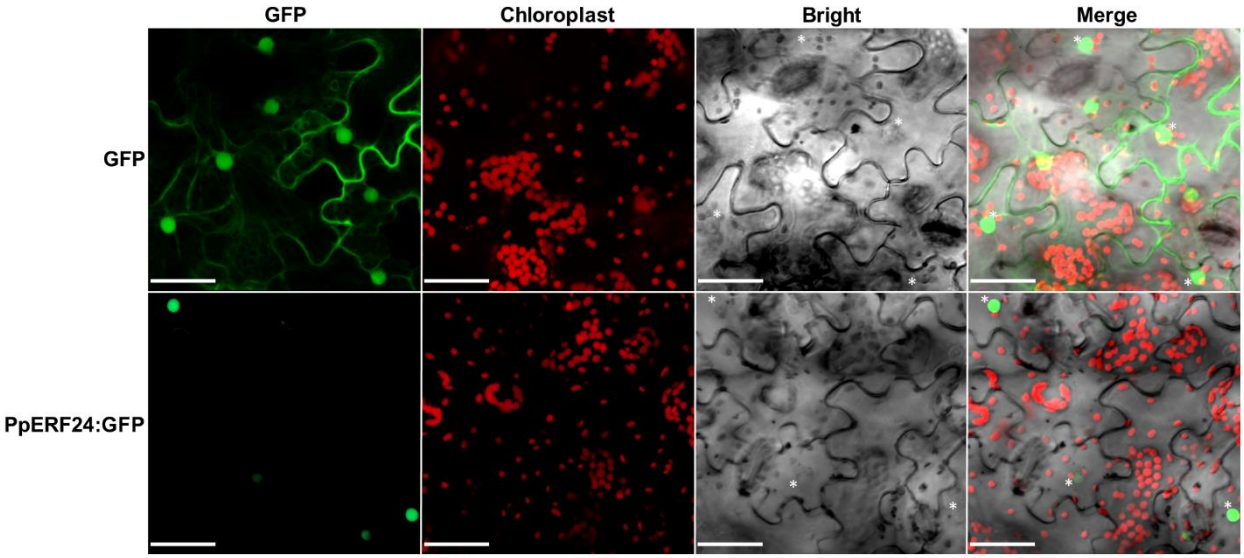

Figure 3. **Subcellular localization of PpERF24 in agroinfiltrated *N. tabacum* leaves**. Confocal microscopy images of *N. tabacum* leaves taken 2 days after agroinfiltration. *N. tabacum* leaves were transformed with the pMDC83 vector (GFP alone, upper panels) or with pMDC83-PpERF24-mGFP6his construct (PpERF24 fused to GFP, lower panels). Visible cell nuclei are marked with a white asterisk in bright field and merged panels. From left to right: GFP, chloroplasts, bright field and merged images. The scale bars represent 50 μm.

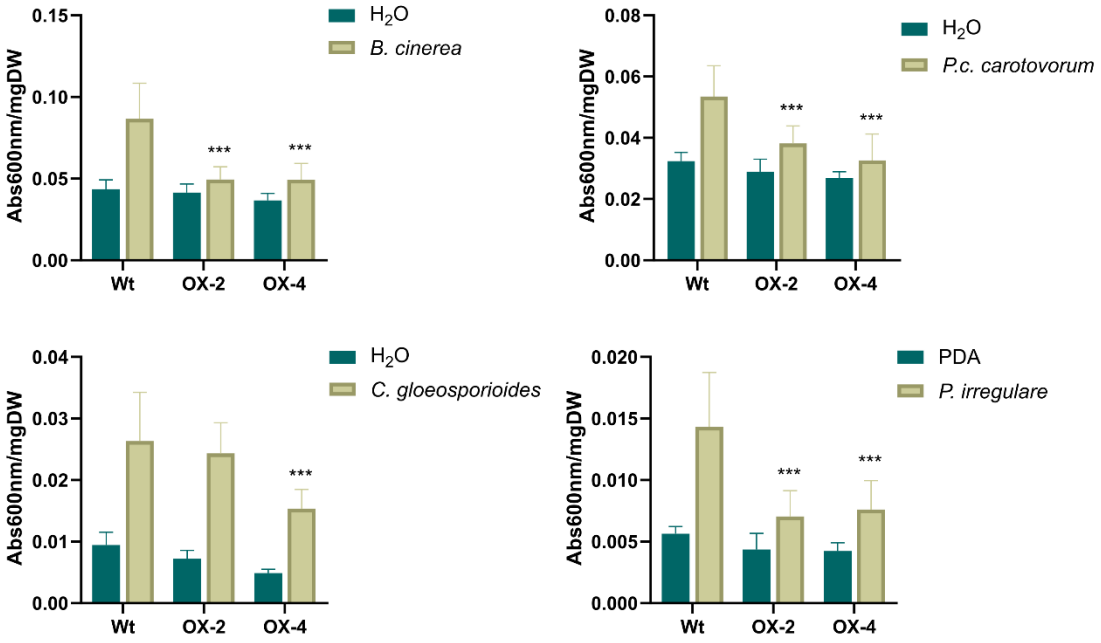

Figure 4. Cell death measurement in wild type and PpERF24 overexpressing plants. Measurement of cell death by Evans blue staining 24 h after inoculation of wild type, PpERF24-OX-2 (OX2) and PpERF24-OX-4 (OX4) moss colonies with *B. cinerea*, *P. irregulare* and treatment with elicitors of *P.c. carotovorum*. Cell death measurement for plant tissues inoculated with *C. gloeosporioides* was performed at 72 hpi, Data were expressed as the absorbance (Abs) at 600 nm per milligram of dry weight (DW). Values are means with standard deviations of eight independent replicate moss samples. Experiments were repeated thrice with similar results. Asterisks indicate a statistically significant difference between the wild type and overexpressing PpERF24 plants [two-way ANOVA test, with Tukey's Honest Significant Difference test as post-hoc test using $P \leq 0.001$ (***)].

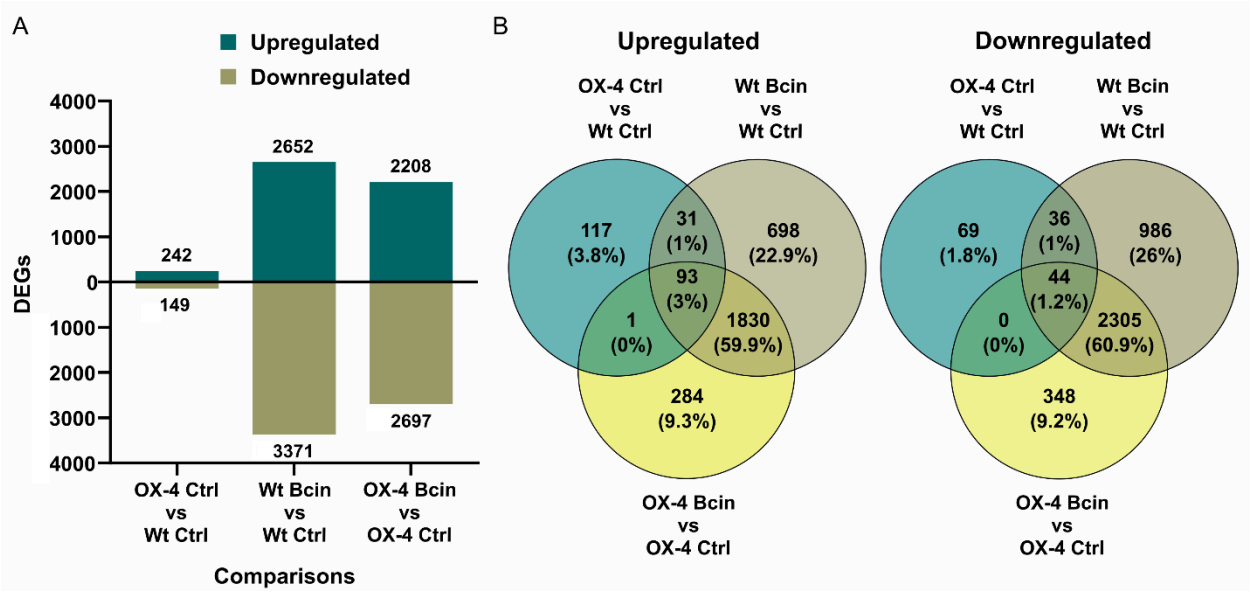

Figure 5. Differentially expressed genes of wild type and PpERF24-OX-4 overexpressing line during control treatment and *B. cinerea* infection. (A) Number of differentially expressed genes (DEGs), up and downregulated, in wild type versus PpERF24-OX-4 (OX4) tissues treated with wáter (Ctrl), and wild type (Wt) and PpERF24-OX-4 tissues inoculated with *B. cinerea* (Bcin) versus water-treated tissues at 24 hpi. (B) Venn diagram of *B. cinerea*-responsive *P. patens* genes in wild type and PpERF24-OX-4 plants, and PpERF24-OX-4 versus wild type control tissues. Genes were considered as DEGs when $|\log2\ FC| \geq 1$ and $FDR \leq 0.05$.

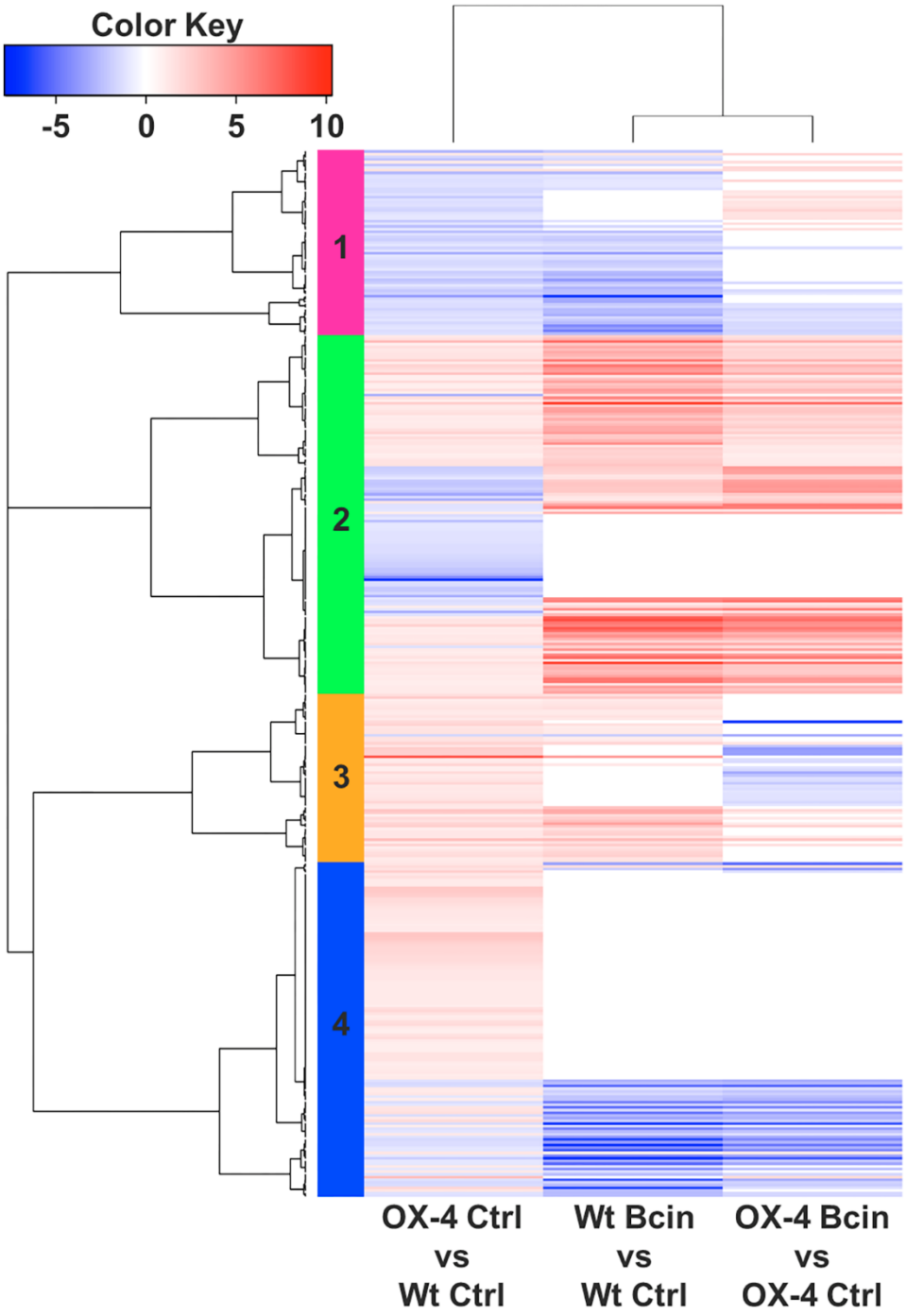

Figure 6: Heatmap of hierarchical clustering of wild type and PpERF24-OX-4 overexpressing line during control treatment and *B. cinerea* infection. DEGs correspond to the 391 DEGs of PpERF24-OX-4 control versus wild type control plants. Selected DEGs had |log2 FC| ≥ 1 and FDR ≤ 0.05. See Supplementary Table 4 for complete information.

4.3.2. Figuras suplementarias Capítulo III

AP2 domain sequences from *P. patens* proteins in DREB clade.

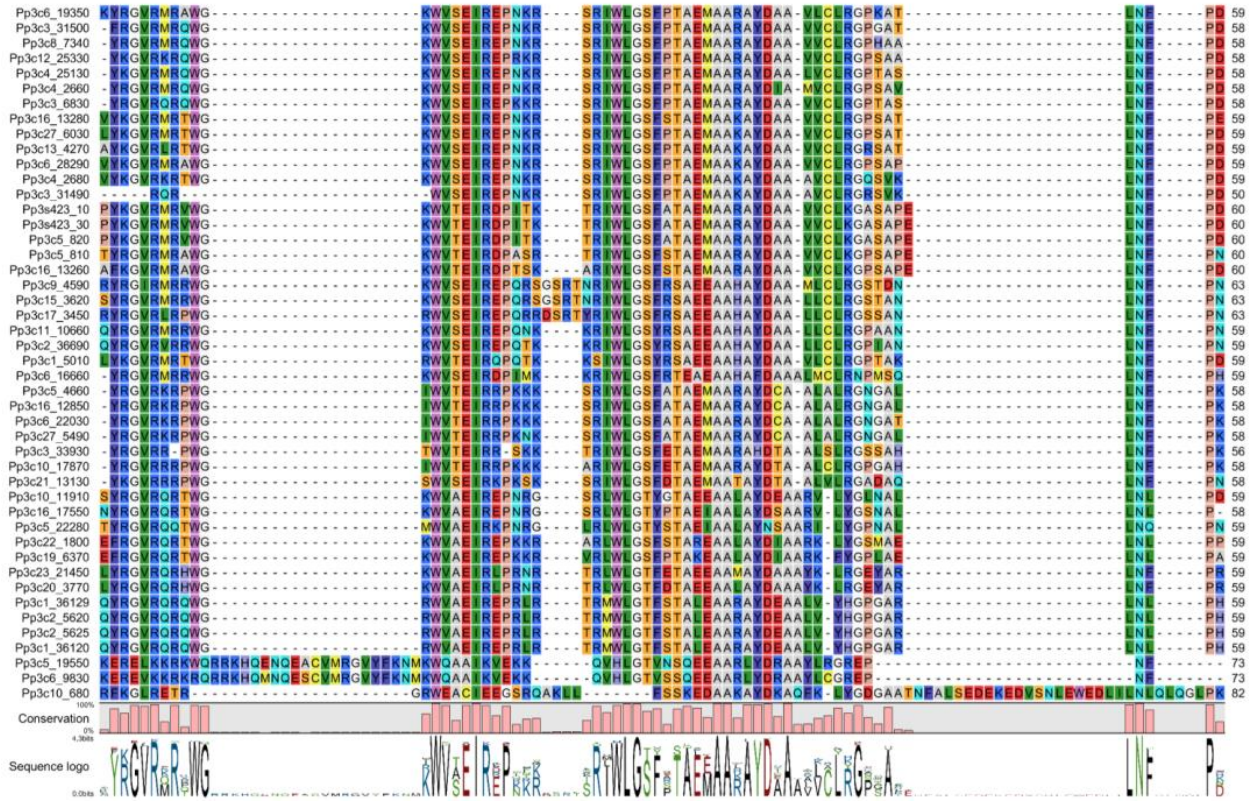

AP2 domain sequences from *A. thaliana* proteins in DREB clade.

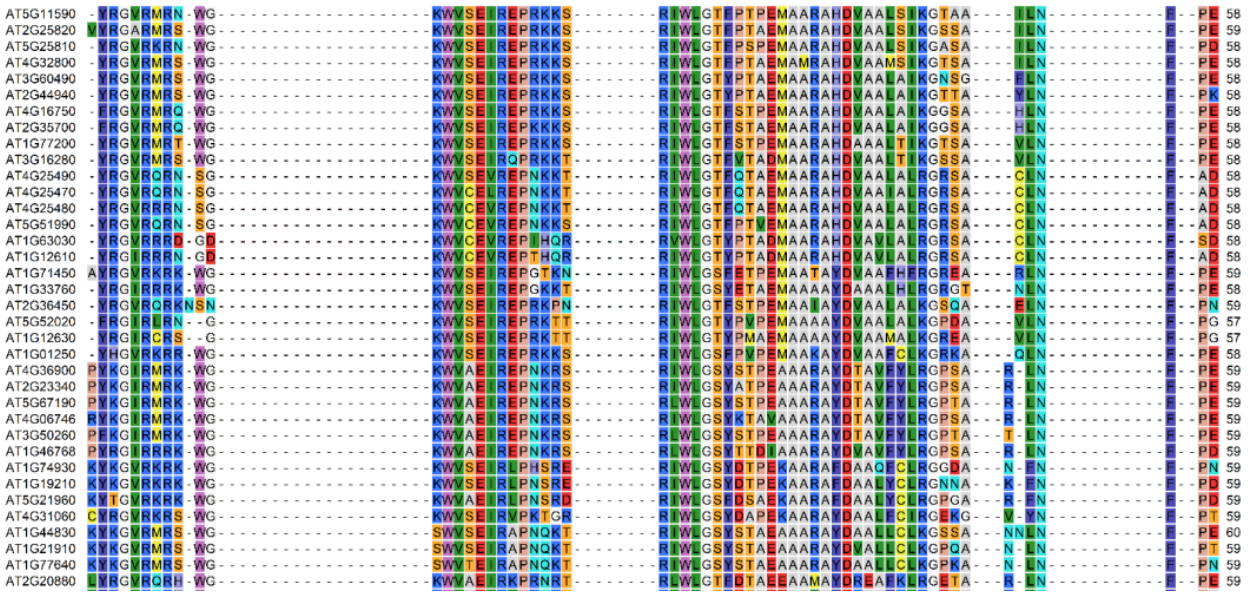

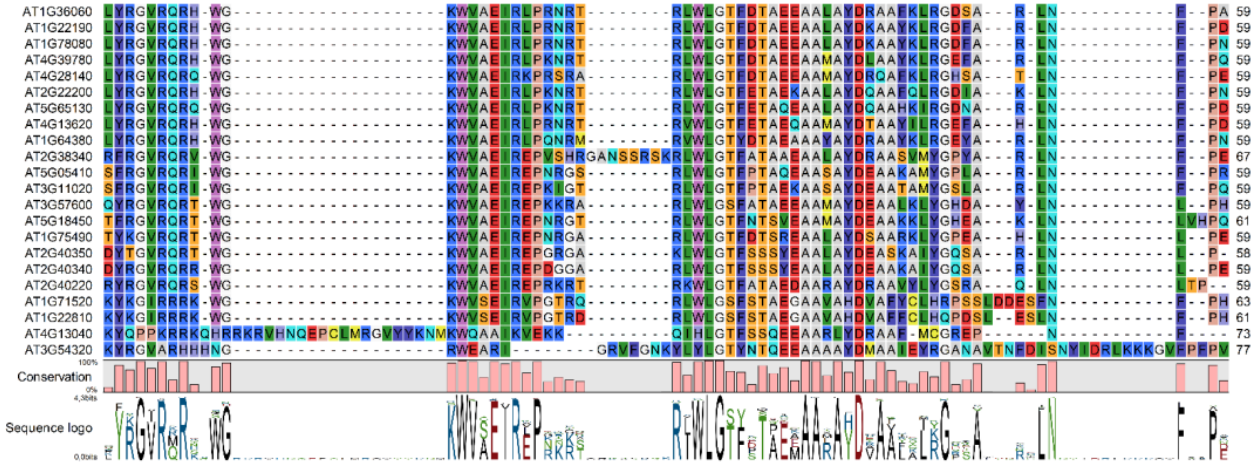

Supplementary Figure 1. Alignment of the AP2 domain of the *P. patens* and *A. thaliana* DREB clades. Alignments include AP2 domain sequences from DREB clade in the unrooted phylogenetic tree shown in Fig. 1. *P. patens* DREB realignment was used to obtain DREB sequence logo showed in Fig. 2 A, without Pp3c8_24200, Pp3c10_680 and Pp3c6_9830 from *P. patens* and AT3G54320 and AT4G13040 from *A. thaliana* considering that they did not show conserved positions 14 and 19 and were not included in Nakano *et al.* (2006) ERF classification.

AP2 domain sequences from *P. patens* proteins in ERF clade.

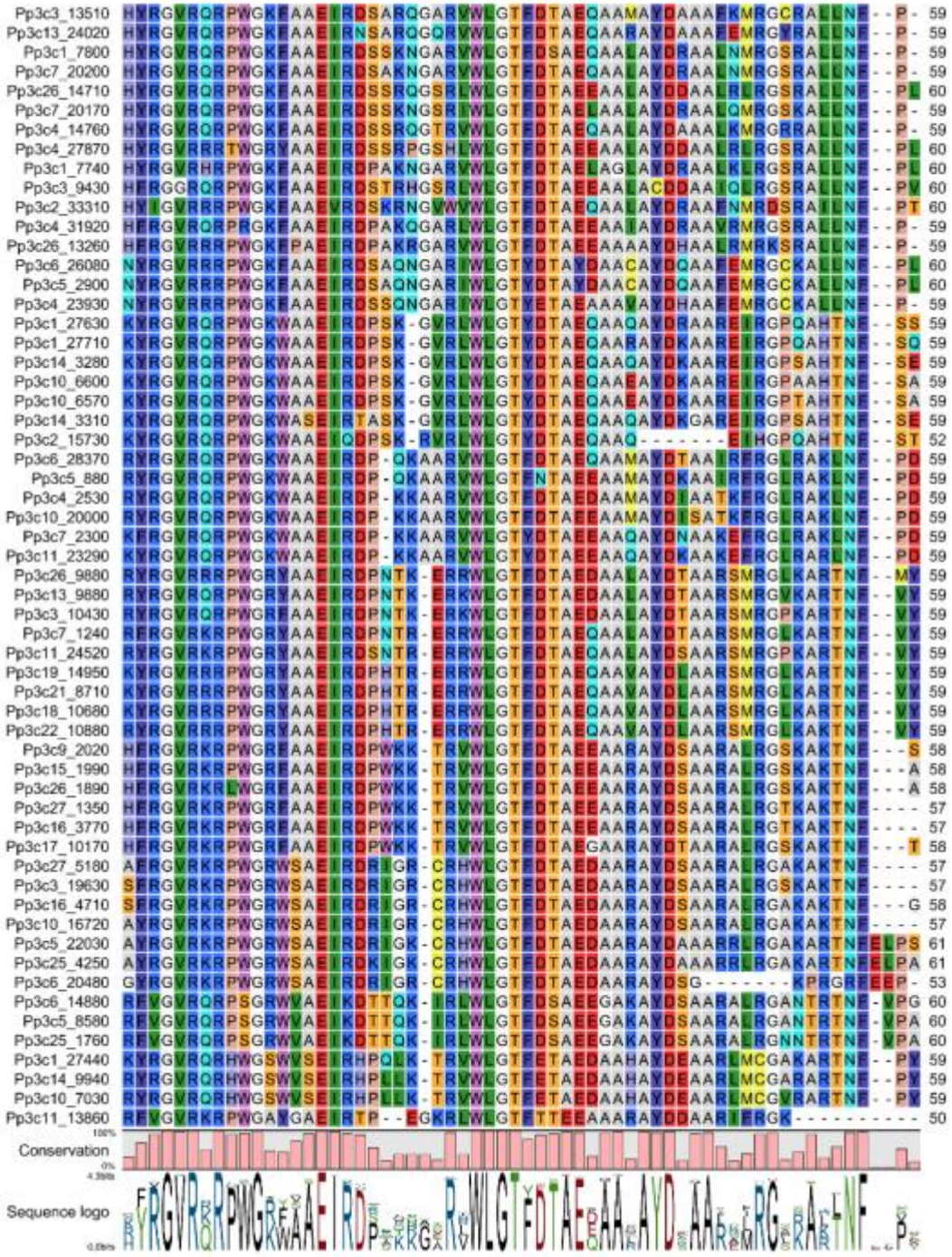

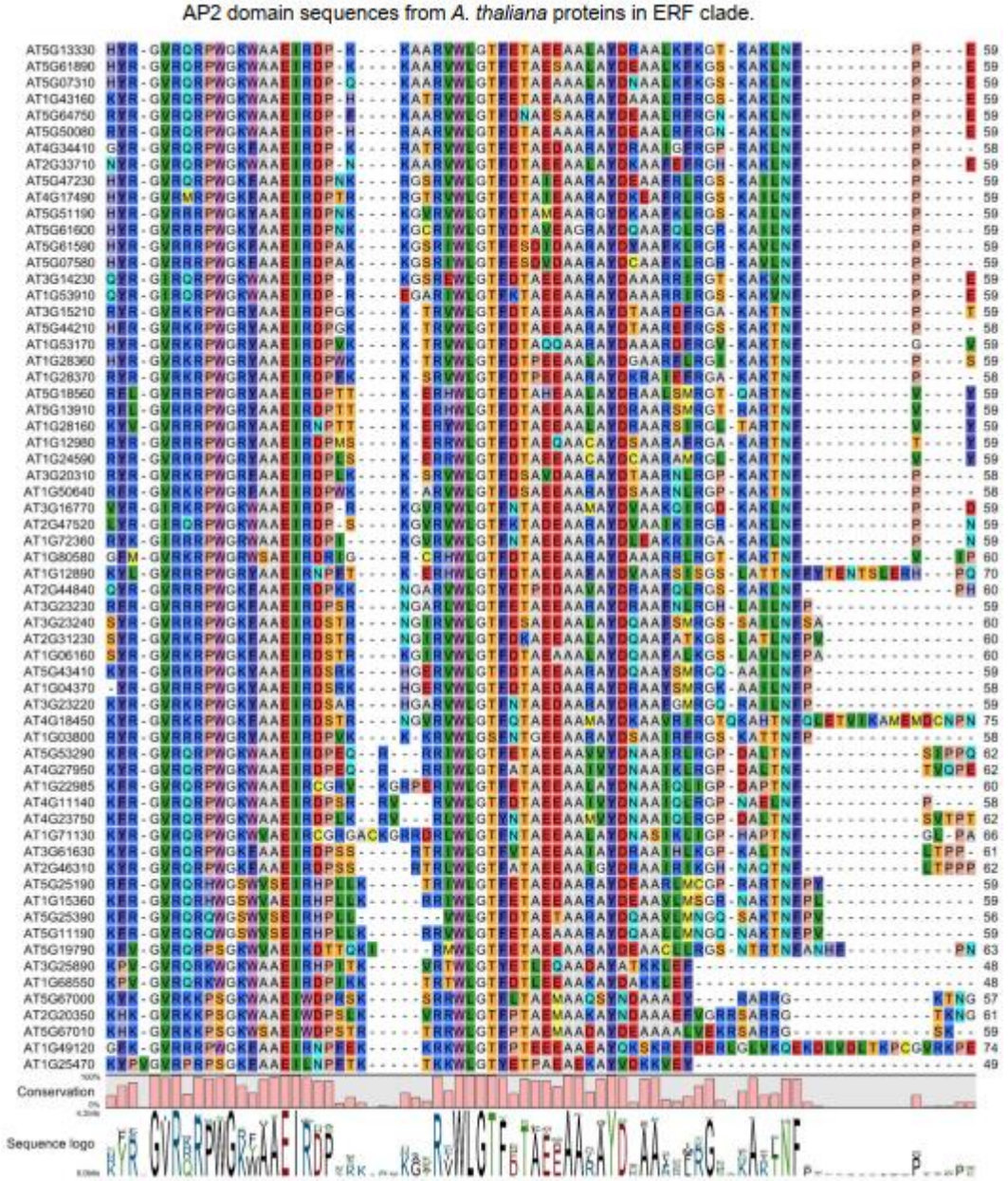

Supplementary Figure 2. Alignment of the AP2 domain of the *P. patens* and *A. thaliana* ERF clades. Alignments include AP2 domain sequences from ERF clade in the unrooted phylogenetic tree shown in Fig. 1. *P. patens* ERF alignment was used to obtain ERF sequence logo showed in Fig. 2 A.

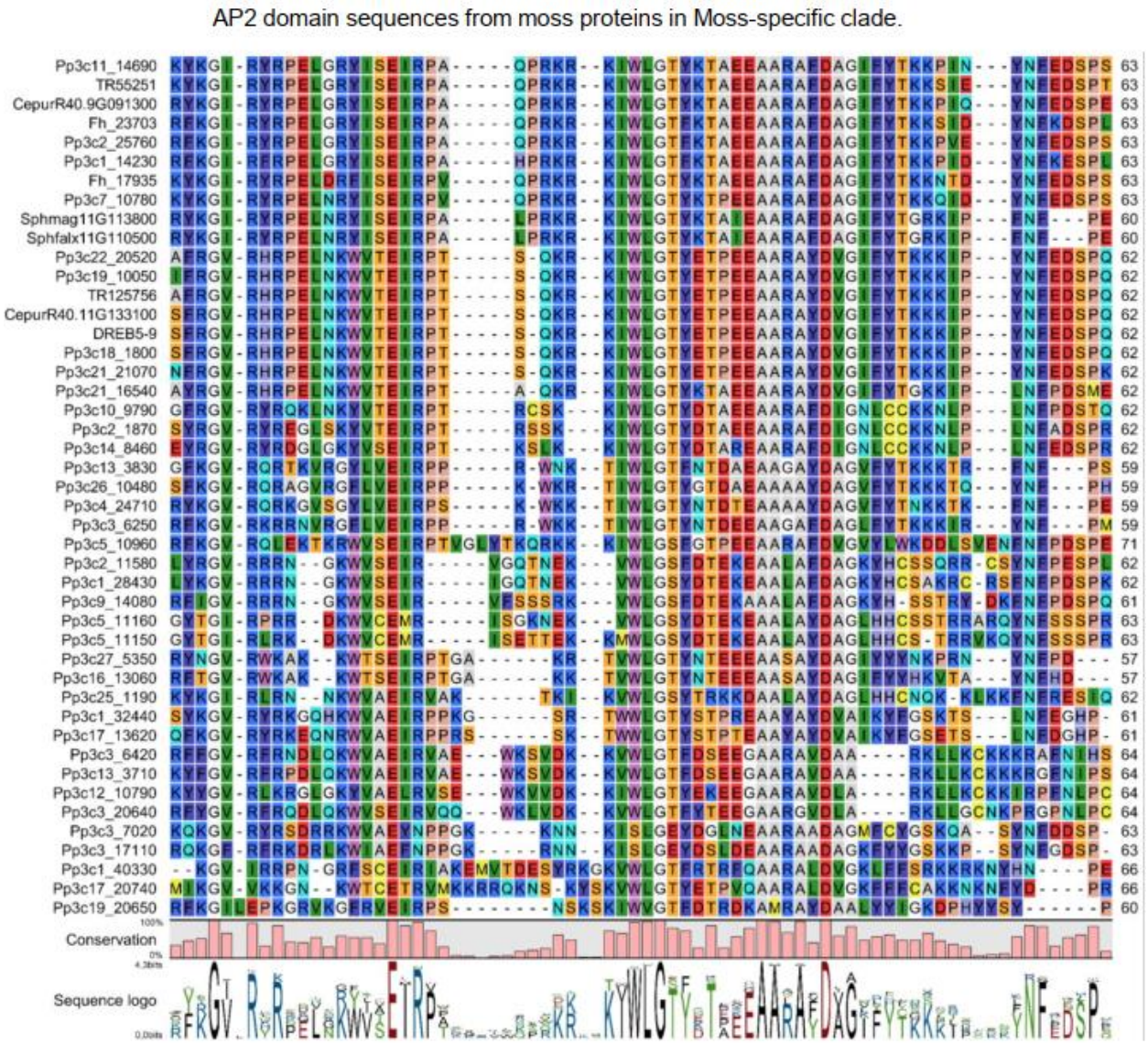

Supplementary Figure 3. Alignment of the AP2 domain of the moss-specific clade. Alignment include AP2 domain sequences from moss-specific clade in the unrooted phylogenetic tree shown in Fig. 1. Alignment was used to obtain moss-specific sequence logo showed in Fig. 2 A.

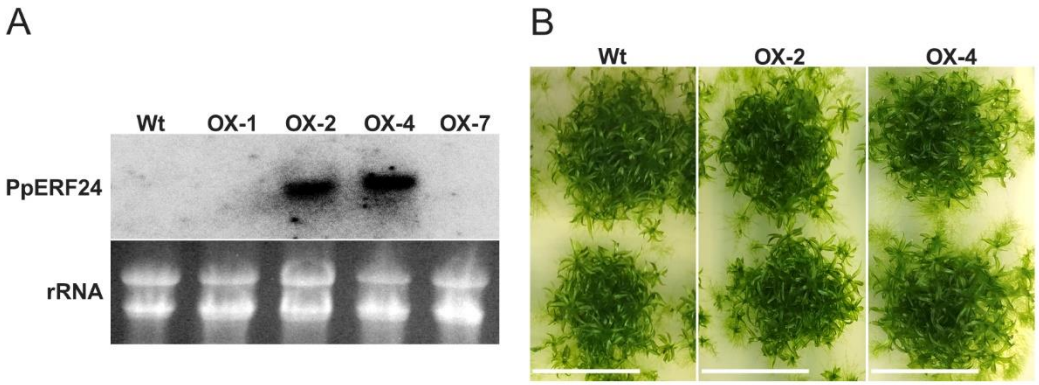

Supplementary Figure 4. Generation of PpERF24 overexpression *P. patens* plants. (A) Transcript levels of PpERF24 in untreated (Control) and *B. cinerea* inoculated wild type (Wt) plants, and untreated PpERF24-OX-1 (OX-1), PpERF24-OX-2 (OX-2), PpERF24-OX-3 (OX-3), and PpERF24-OX-4 (OX-4) plants. (B) Phenotype of wild type, PpERF24-OX-2 and PpERF24-OX-4 moss colonies.

5. Perspectivas

Los análisis transcriptómicos por RNA-Seq arrojaron una gran cantidad de datos los cuales permitirán seguir profundizando en los mecanismos de defensa de *P. patens* en respuesta a patógenos. Estos resultados podrán ser utilizados para comparar los mecanismos de defensa que activan las briofitas en respuesta a patógenos y las diferencias y similitudes que existen con las angiospermas. La comparación entre las bases moleculares de la respuesta de defensa de briofitas y angiospermas frente a patógenos permite identificar aquellos mecanismos de defensa que son compartidos y por lo tanto están presentes en el ancestro en común, así como identificar respuestas de defensa hasta ahora desconocidas y musgo especifica.

Varios resultados interesantes obtenidos a partir del análisis de los datos transcriptómicos requieren de más estudio. Por ejemplo, se observó la inducción de una gran cantidad de genes PRR, principalmente RLKs del tipo LRR, demostrando la importancia de expresar varios receptores que podrían detectar componentes moleculares del patógeno y así activar la respuesta de defensa de la planta. Dentro de los PRR inducidos en la planta durante la infección por *B. cinerea*, se encontró uno de los tres miembros de la familia LYK5 como diferencialmente expresado de forma significativa. El silenciamiento de los tres miembros de esta familia en *P. patens*, lleva a la insensibilización de la quitina (Orr et al., 2020). Sin embargo, sería interesante mutar el gen *PpLYK5* que se encontró inducido en la infección por *B. cinerea* y evaluar específicamente su papel en la defensa de la planta. Por otra parte, la infección de *P. patens* por el hongo *B. cinerea* alteró la expresión de solamente tres genes NLR. Esto es llamativo dada la gran cantidad de genes NLR que presenta este musgo, y siendo que en otras interacciones planta-*B. cinerea* la cantidad de genes NLR diferencialmente expresados es mayor. También resulta interesante poder profundizar en el rol de los NLR en la defensa de la planta, así como también estudiar la acción de los efectores del patógeno que interfieren con la defensa vegetal. Mediante la generación de líneas mutantes en genes individuales y varios genes NLR por CRISPR-CAS (Rensing et al., 2020; Trogu et al., 2021), así como también mutantes en genes efectores de *B. cinerea*, se podrían estudiar las diferencias en la susceptibilidad y el posible rol de cada uno de estos genes en la defensa vegetal y virulencia del patógeno.

Según nuestros resultados, varias de las hormonas relacionadas con la defensa participan en la respuesta de *P. patens* frente a patógenos. En el laboratorio hemos generado plantas transgénicas que degradan el SA mediante la enzima salicilato hidroxilasa (NahG) de *Pseudomonas putida*, las cuales podrán ser utilizadas para evaluar el rol del SA en la defensa de *P. patens*. También, se observó que varios genes que codifican para AP2/ERFs aumentan su expresión durante la infección por *B. cinérea*. Este aumento, junto con el aumento en la expresión del receptor del ET (ETR) (Yasumura et al., 2012), el cual se encuentra vinculado a la respuesta adaptativa de *P. patens* a sequía y sumersión, indica que el ET se encuentra probablemente involucrado en la respuesta de defensa contra estrés biótico. El uso de mutantes en los receptores para el SA, el OPDA y el ET permitirán evaluar la participación de las hormonas en respuesta a *B. cinerea* y otros patógenos así como a distintos estreses abióticos.

Resultó muy interesante el gran número de genes huérfanos que se vieron diferencialmente expresados durante el proceso de infección de *P. patens* por *B. cinerea*. Por esto, descifrar el rol que tienen los genes huérfanos, de los cuales la gran mayoría carece de anotación, durante el estrés biótico y abiótico en *P. patens* ayudará a entender su participación en los mecanismos de adaptación al estrés de este musgo. Sería interesante seleccionar de estos genes aquellos con mayor inducción para generar líneas mutantes y sobreexpresantes de *P. patens* en estos genes y evaluar la respuesta de dichas plantas a distintos patógenos. También se podría evaluar cuáles de estos genes huérfanos son específicos de distintos tipos de estrés bióticos y abióticos.

Para poder estudiar aquellos mecanismos moleculares involucrados en la virulencia del hongo y el proceso de infección que son diferentes entre *P. patens* y angiospermas, como es el caso de los diferentes patrones de expresión de los genes CAZymes del hongo y posibles transportadores MFS, se necesitan más estudios de interacción planta-hongo. Por ejemplo, conocer la diana en la pared celular de la planta donde las CAZymes actúan, así como también la identidad de metabolitos con actividad antifúngica de las proteínas codificadas por *P. patens*. Esto aumentará nuestro conocimiento sobre las interacciones briofitas-hongo. Además, el uso de mutantes de *B. cinerea* contribuirá a descubrir los mecanismos moleculares de patogenicidad y la red regulatoria usada por este patógeno durante la infección del musgo y su rol durante la co-evolución entre patógenos y plantas.

Demostramos que PpERF24, el cual es específico de musgos, aumenta la resistencia ante hongos, oomicetes y filtrado acelular de cultivo de bacteria. Otros estudios sobre los ERFs específicos de los musgos, incluyendo PpERF24, contribuirán a revelar los mecanismos moleculares que subyacen a su acción, incluyendo los elementos de unión al ADN, otras proteínas que interactúan y los genes diana y su contribución a la defensa de los musgos. Sería interesante estudiar con mayor profundidad los motivos de unión al ADN de los ERFs específicos de musgos. Además, dado que el clado musgo-especifico es inducido en su totalidad por los patógenos *B. cinerea* y *C. gloeosporioides*, resultaría interesante generar líneas mutantes en dichos genes y evaluar su rol en la defensa de la planta ante estos hongos y otros patógenos.

Además de las perspectivas anteriores y aprovechando los datos de RNA-Seq generados durante este trabajo y los existentes en base de datos públicas, y dado que los análisis transcriptómicos aquí presentados se realizaron a partir de la expresión genes nucleares, sería interesante estudiar la expresión de GDEs en los distintos organelos de la planta al comparar entre diferentes tipos de estrés bióticos y/o abióticos, así como también entre líneas de *P. patens* resistentes y susceptibles.

En resumen, más estudios sobre las interacciones entre *P. patens* y distintos patógenos, contribuirán a descubrir aquellos mecanismos moleculares que subyacen a las defensas específicas de los musgos y su implicación en la co-evolución de las plantas terrestres y los patógenos.

6. Referencias

AbuQamar, S., Moustafa, K., and Tran, L. S. P. (2017). Mechanisms and strategies of plant defense against Botrytis cinerea. *Crit. Rev. Biotechnol.* 37, 262–274. doi:10.1080/07388551.2016.1271767.

Adachi, H., Derevnina, L., and Kamoun, S. (2019). NLR singletons, pairs, and networks: evolution, assembly, and regulation of the intracellular immunoreceptor circuitry of plants. *Curr. Opin. Plant Biol.* 50, 121–131. doi:10.1016/j.pbi.2019.04.007.

Albert, I., Hua, C., Nürnberger, T., Pruitt, R. N., and Zhang, L. (2020). Surface sensor systems in plant immunity. *Plant Physiol.* 182, 1582–1596. doi:10.1104/PP.19.01299.

Alonso, J. M., Stepanova, A. N., Solano, R., Wisman, E., Ferrari, S., Ausubel, F. M., et al. (2003). Five components of the ethylene-response pathway identified in a screen for weak ethylene-insensitive mutants in Arabidopsis. *Proc. Natl. Acad. Sci. U. S. A.* 100, 2992–2997. doi:10.1073/pnas.0438070100.

Alvarez, A., Montesano, M., Schmelz, E., and Ponce de León, I. (2016). Activation of Shikimate, Phenylpropanoid, Oxylipins, and Auxin Pathways in Pectobacterium carotovorum Elicitors-Treated Moss. *Front. Plant Sci.* 7, 1–14. doi:10.3389/fpls.2016.00328.

Andolfo, G., Di Donato, A., Chiaiese, P., De Natale, A., Pollio, A., Jones, J. D. G., et al. (2019). Alien Domains Shaped the Modular Structure of Plant NLR Proteins. *Genome Biol. Evol.* 11, 3466–3477. doi:10.1093/gbe/evz248.

Arenas, Y. C., Kalkman, E. R. I. C., Schouten, A., Dieho, M., Vredenbregt, P., Uwumukiza, B., et al. (2010). Functional analysis and mode of action of phytotoxic Nep1-like proteins of Botrytis cinerea. *Physiol. Mol. Plant Pathol.* 74, 376–386. doi:10.1016/j.pmpp.2010.06.003.

Arif, M. A., Hiss, M., Tomek, M., Busch, H., Meyberg, R., Tintelnot, S., et al. (2019). ABA-Induced Vegetative Diaspore Formation in Physcomitrella patens. *Front. Plant Sci.* 10, 1–18. doi:10.3389/fpls.2019.00315.

Asai, T., Tena, G., Plotnikova, J., Willmann, M. R., Chiu, W.-L., Gomez-Gomez, L., et al. (2002). MAP kinase signalling cascade in Arabidopsis innate immunity. *Nature* 415, 977–983. doi:10.1038/415977a.

Baillo, E. J., Kimotho, R. N., Zhang, Z., and Xu, P. (2019). Transcription Factors Associated with Abiotic and Biotic Stress Tolerance and Their Potential for Crops Improvement. *Genes (Basel).* 10, 771. doi:10.3390/genes10100771.

Beike, A. K., Lang, D., Zimmer, A. D., Wüst, F., Trautmann, D., Wiedemann, G., et al. (2015). Insights from the cold transcriptome of Physcomitrella patens: Global specialization pattern of conserved transcriptional regulators and identification of orphan genes involved in cold acclimation. *New Phytol.* 205, 869–881. doi:10.1111/nph.13004.

Bernoux, M., Burdett, H., Williams, S. J., Zhang, X., Chen, C., Newell, K., et al. (2016). Comparative analysis of the flax immune receptors L6 and L7 suggests an equilibrium-based switch activation model. *Plant Cell* 28, 146–159. doi:10.1105/tpc.15.00303.

Berrocal-Lobo, M., Molina, A., and Solano, R. (2002). Constitutive expression of ETHYLENE-RESPONSE-FACTOR1 in Arabidopsis confers resistance to several necrotrophic fungi. *Plant J.* 29, 23–32. doi:10.1046/j.1365-313x.2002.01191.x.

Bi, G., Su, M., Li, N., Liang, Y., Dang, S., Xu, J., et al. (2021). The ZAR1 resistosome is a calcium-permeable channel triggering plant immune signaling. *Cell* 184, 3528-3541.e12. doi:10.1016/j.cell.2021.05.003.

Bi, G., Zhou, Z., Wang, W., Li, L., Rao, S., Wu, Y., et al. (2018). Receptor-like cytoplasmic kinases directly link diverse pattern recognition receptors to the activation of mitogen-activated protein kinase cascades in arabidopsis. *Plant Cell* 30, 1543–1561. doi:10.1105/tpc.17.00981.

Bilgin, D. D., Zavala, J. A., Zhu, J., Clough, S. J., Ort, D. R., and Delucia, E. H. (2010). Biotic stress globally downregulates photosynthesis genes. *Plant, Cell Environ.* 33, 1597–1613. doi:10.1111/j.1365-3040.2010.02167.x.

Boller, T., and Felix, G. (2009). A renaissance of elicitors: perception of microbe-associated molecular patterns and danger signals by pattern-recognition receptors. *Annu. Rev. Plant Biol.* 60, 379–406. doi:10.1146/annurev.arplant.57.032905.105346.

Bonardi, V., Tang, S., Stallmann, A., Roberts, M., Cherkis, K., and Dangl, J. L. (2011). Expanded functions for a family of plant intracellular immune receptors beyond specific recognition of pathogen effectors. *Proc. Natl. Acad. Sci. U. S. A.* 108, 16463–16468. doi:10.1073/pnas.1113726108.

Boutrot, F., and Zipfel, C. (2017). Freddy Boutrot and Cyril Zipfel. *Annu. Rev. Phytopathol.* 55, 1–30.

Bowman, J. L., Kohchi, T., Yamato, K. T., Jenkins, J., Shu, S., Ishizaki, K., et al. (2017). Insights into Land Plant Evolution Garnered from the Marchantia polymorpha Genome. *Cell* 171, 287-304.e15. doi:10.1016/j.cell.2017.09.030.

Bressendorff, S., Azevedo, R., Kenchappa, C. S., de León, I. P., Olsen, J. V., Rasmussen, M. W., et al. (2016). An Innate Immunity Pathway in the Moss Physcomitrella patens. *Plant Cell* 28, 1328–1342. doi:10.1105/tpc.15.00774.

Buscaill, P., and Rivas, S. (2014). Transcriptional control of plant defence responses. *Curr. Opin. Plant Biol.* 20, 35–46. doi:10.1016/j.pbi.2014.04.004.

Cao, Y., Liang, Y., Tanaka, K., Nguyen, C. T., Jedrzejczak, R. P., Joachimiak, A., et al. (2014). The kinase LYK5 is a major chitin receptor in Arabidopsis and forms a chitin-induced complex with related kinase CERK1. *Elife* 3, 1–19. doi:10.7554/eLife.03766.

Cesari, S. (2018). Multiple strategies for pathogen perception by plant immune receptors. *New Phytol.* 219, 17–24. doi:10.1111/nph.14877.

Cesari, S., Bernoux, M., Moncuquet, P., Kroj, T., and Dodds, P. N. (2014). A novel conserved mechanism for plant NLR protein pairs: The “integrated decoy” hypothesis. *Front. Plant Sci.* 5, 1–10. doi:10.3389/fpls.2014.00606.

Césari, S., Kanzaki, H., Fujiwara, T., Bernoux, M., Chalvon, V., Kawano, Y., et al. (2014). The NB - LRR proteins RGA 4 and RGA 5 interact functionally and physically to confer disease resistance . *EMBO J.* 33, 1941–1959. doi:10.15252/embj.201487923.

Chakravarthy, S., Tuori, R. P., D'Ascenzo, M. D., Fobert, P. R., Després, C., and Martin, G. B. (2003). The Tomato Transcription Factor Pti4 Regulates Defense-Related Gene Expression via GCC Box and Non-GCC Box cis Elements. *Plant Cell* 15, 3033–3050. doi:10.1105/tpc.017574.

Chakravarthy, S., Velásquez, A. C., Ekengren, S. K., Collmer, A., and Martin, G. B. (2010). Identification of Nicotiana benthamiana Genes Involved in Pathogen-Associated Molecular Pattern-Triggered Immunity. *Mol. Plant. Microbe. Interact.* 23, 715–726. doi:10.1094/MPMI-23-6-0715.

Charfeddine, M., Samet, M., Charfeddine, S., Bouaziz, D., and Gargouri Bouzid, R. (2019). Ectopic Expression of StERF94 Transcription Factor in Potato Plants Improved Resistance to Fusarium solani Infection. *Plant Mol. Biol. Report.* 37, 450–463. doi:10.1007/s11105-019-01171-4.

Chen, L., Zhang, Z., Liang, H., Liu, H., Du, L., Xu, H., et al. (2008). Overexpression of TiERF1 enhances resistance to sharp eyespot in transgenic wheat. *J. Exp. Bot.* 59, 4195–4204. doi:10.1093/jxb/ern259.

Chen, Q., Dong, C., Sun, X., Zhang, Y., Dai, H., and Bai, S. (2020). Overexpression of an apple LysM-containing protein gene, MdCERK1–2, confers improved resistance to the pathogenic fungus, Alternaria alternata, in Nicotiana benthamiana. *BMC Plant Biol.* 20, 146. doi:10.1186/s12870-020-02361-z.

Chiang, Y.-H., and Coaker, G. (2015). Effector Triggered Immunity: NLR Immune Perception and Downstream Defense Responses. *Arab. B.* 13, e0183. doi:10.1199/tab.0183.

Choi, J., Tanaka, K., Cao, Y., Qi, Y., Qiu, J., Liang, Y., et al. (2014). Identification of a plant receptor for extracellular ATP. *Science (80-.).* 343, 290–294. doi:10.1126/science.343.6168.290.

Choquer, M., Fournier, E., Kunz, C., Levis, C., Pradier, J. M., Simon, A., et al. (2007). Botrytis cinerea virulence factors: New insights into a necrotrophic and polyphageous pathogen. *FEMS Microbiol. Lett.* 277, 1–10. doi:10.1111/j.1574-6968.2007.00930.x.

Chung, H. S., Koo, A. J. K., Gao, X., Jayanty, S., Thines, B., Jones, A. D., et al. (2008). Regulation and function of arabidopsis JASMONATE ZIM-domain genes in response to wounding and herbivory. *Plant Physiol.* 146, 952–964. doi:10.1104/pp.107.115691.

Clark, C. A., and Lorbeer, J. W. (1976). Comparative Histopathology of Botrytis squamosa and B. cinerea on Onion Leaves. *Phytopathology*1289–1279, 66 . Available at: https://www.apsnet.org/publications/phytopathology/backissues/Documents/1976Articles/Phyto66n11_1279.PDF.

Collado, I. G., and Viaud, M. (2016). "Secondary Metabolism in Botrytis cinerea : Combining Genomic and Metabolomic Approaches," in *Botrytis – the Fungus, the Pathogen and its Management in Agricultural Systems* (Springer Cham), 291–313. doi:10.1007/978-3-319-23371-0.

Colmenares, A. J., Aleu, J., Durán-Patrón, R., Collado, I. G., and Hernández-Galán, R. (2002). The putative role of botrydial and related metabolites in the infection mechanism of Botrytis cinerea. *J. Chem. Ecol.* 28, 997–1005. doi:10.1023/A:1015209817830.

Comménil, P., Belingheri, L., Sancholle, M., and Dehorter, B. (1995). Purification and properties

of an extracellular lipase from the fungus Botrytis cinerea. *Lipids* 30, 351–356. doi:10.1007/BF02536044.

Coram, T. E., Wang, M., and Chen, X. (2008). Transcriptome analysis of the wheat-Puccinia striiformis f. sp. tritici interaction. *Mol. Plant Pathol.* 9, 157–169. doi:10.1111/j.1364-3703.2007.00453.x.

Corina Vlot, A., Dempsey, D. A., and Klessig, D. F. (2009). Salicylic acid, a multifaceted hormone to combat disease. *Annu. Rev. Phytopathol.* 47, 177–206. doi:10.1146/annurev.phyto.050908.135202.

Coudert, Y., Palubicki, W., Ljung, K., Novak, O., Leyser, O., and Harrison, C. J. (2015). Three ancient hormonal cues co-ordinate shoot branching in a moss. *Elife* 4, e06808. doi:10.7554/eLife.06808.

Couto, D., and Zipfel, C. (2016). Regulation of pattern recognition receptor signalling in plants. *Nat. Rev. Immunol.* 16, 537–552. doi:10.1038/nri.2016.77.

Cove, D. J., Knight, C. D., and Lamparter, T. (1997). Mosses as model systems. *Trends Plant Sci.* 2, 99–105.

Cui, M., Haider, M. S., Chai, P., Guo, J., Du, P., Li, H., et al. (2021). Genome-Wide Identification and Expression Analysis of AP2/ERF Transcription Factor Related to Drought Stress in Cultivated Peanut (Arachis hypogaea L.). *Front. Genet.* 12, 750761. doi:10.3389/fgene.2021.750761.

Dangl, J. L., and Jones, J. D. (2001). Plant pathogens and integrated defence responses to infection. *Nature* 411, 826–833. doi:10.1038/35081161.

Davin, L. B., and Lewis, N. G. (2000). Dirigent Proteins and Dirigent Sites Explain the Mystery of Specificity of Radical Precursor Coupling in Lignan and Lignin Biosynthesis. *Plant Physiol.* 123, 453–461. doi:10.1104/pp.123.2.453.

de Vries, J., and Archibald, J. M. (2018). Plant evolution: landmarks on the path to terrestrial life. *New Phytol.* 217, 1428–1434. doi:10.1111/nph.14975.

Dean, R., Van Kan, J. A. L., Pretorius, Z. A., Hammond-Kosack, K. E., Di Pietro, A., Spanu, P. D., et al. (2012). The Top 10 fungal pathogens in molecular plant pathology. *Mol. Plant Pathol.* 13, 414–430. doi:10.1111/j.1364-3703.2011.00783.x.

DeFalco, T. A., and Zipfel, C. (2021). Molecular mechanisms of early plant pattern-triggered immune signaling. *Mol. Cell* 81, 3449–3467. doi:10.1016/j.molcel.2021.07.029.

Delaux, P. M., Hetherington, A. J., Coudert, Y., Delwiche, C., Dunand, C., Gould, S., et al. (2019). Reconstructing trait evolution in plant evo–devo studies. *Curr. Biol.* 29, R1110–R1118. doi:10.1016/j.cub.2019.09.044.

Denancé, N., Sánchez-Vallet, A., Goffner, D., and Molina, A. (2013). Disease resistance or growth: The role of plant hormones in balancing immune responses and fitness costs. *Front. Plant Sci.* 4, 1–12. doi:10.3389/fpls.2013.00155.

Dievart, A., Gottin, C., Peacuterin, C., Ranwez, V., and Chantret, N. (2020). Origin and Diversity of Plant Receptor-Like Kinases. *Annu. Rev. Plant Biol.* 71, 131–156. doi:10.1146/annurev-arplant-073019-025927.

Ding, Y., Sun, T., Ao, K., Peng, Y., Zhang, Y., Li, X., et al. (2018). Opposite Roles of Salicylic Acid Receptors NPR1 and NPR3/NPR4 in Transcriptional Regulation of Plant Immunity. *Cell* 173, 1454-1467.e10. doi:10.1016/j.cell.2018.03.044.

Dixon, R. A., and Paiva, N. L. (1995). Stress-Induced Phenylpropanoid Metabolism. *Plant Cell* 7, 1085–1097. doi:10.1105/tpc.7.7.1085.

Dubiella, U., Seybold, H., Durian, G., Komander, E., Lassig, R., Witte, C. P., et al. (2013). Calcium-dependent protein kinase/NADPH oxidase activation circuit is required for rapid defense signal propagation. *Proc. Natl. Acad. Sci. U. S. A.* 110, 8744–8749. doi:10.1073/pnas.1221294110.

Dubos, C., Stracke, R., Grotewold, E., Weisshaar, B., Martin, C., and Lepiniec, L. (2010). MYB transcription factors in Arabidopsis. *Trends Plant Sci.* 15, 573–581. doi:10.1016/j.tplants.2010.06.005.

El Ouakfaoui, S., Schnell, J., Abdeen, A., Colville, A., Labbé, H., Han, S., et al. (2010). Control of somatic embryogenesis and embryo development by AP2 transcription factors. *Plant Mol. Biol.* 74, 313–326. doi:10.1007/s11103-010-9674-8.

Emiliani, G., Fondi, M., Fani, R., and Gribaldo, S. (2009). A horizontal gene transfer at the origin of phenylpropanoid metabolism: A key adaptation of plants to land. *Biol. Direct* 4, 1–12. doi:10.1186/1745-6150-4-7.

Erpen, L., Devi, H. S., Grosser, J. W., and Dutt, M. (2018). Potential use of the DREB/ERF, MYB, NAC and WRKY transcription factors to improve abiotic and biotic stress in transgenic plants. *Plant Cell, Tissue Organ Cult.* 132, 1–25. doi:10.1007/s11240-017-1320-6.

Erxleben, A., Gessler, A., Vervliet-Scheebaum, M., and Reski, R. (2012). Metabolite profiling of the moss Physcomitrella patens reveals evolutionary conservation of osmoprotective substances. *Plant Cell Rep.* 31, 427–436. doi:10.1007/s00299-011-1177-9.

Feng, K., Hou, X.-L., Xing, G.-M., Liu, J.-X., Duan, A.-Q., Xu, Z.-S., et al. (2020). Advances in AP2/ERF super-family transcription factors in plant. *Crit. Rev. Biotechnol.* 40, 750–776. doi:10.1080/07388551.2020.1768509.

Fernandez-Pozo, N., Haas, F. B., Meyberg, R., Ullrich, K. K., Hiss, M., Perroud, P. F., et al. (2020). *PEATmoss (Physcomitrella Expression Atlas Tool): a unified gene expression atlas for the model plant Physcomitrella patens*. doi:10.1111/tpj.14607.

Field, K. J., Pressel, S., Duckett, J. G., Rimington, W. R., and Bidartondo, M. I. (2015). Symbiotic options for the conquest of land. *Trends Ecol. Evol.* 30, 477–486. doi:10.1016/j.tree.2015.05.007.

Flor, H. H. (1971). Current Status of the Gene-For-Gene Concept. *Annu. Rev. Phytopathol.* 9, 275–296. doi:10.1146/annurev.py.09.090171.001423.

Fritz-Laylin, L. K., Krishnamurthy, N., Tör, M., Sjölander, K. V., and Jones, J. D. G. (2005). Phylogenomic analysis of the receptor-like proteins of rice and Arabidopsis. *Plant Physiol.* 138, 611–623. doi:10.1104/pp.104.054452.

Fu, M., Kang, H. K., Son, S. H., Kim, S. K., and Nam, K. H. (2014). A subset of arabidopsis RAV transcription factors modulates drought and salt stress responses independent of ABA.

Plant Cell Physiol. 55, 1892–1904. doi:10.1093/pcp/pcu118.

Fu, Z. Q., and Dong, X. (2013). Systemic acquired resistance: Turning local infection into global defense. *Annu. Rev. Plant Biol.* 64, 839–863. doi:10.1146/annurev-arplant-042811-105606.

Fu, Z. Q., Yan, S., Saleh, A., Wang, W., Ruble, J., Oka, N., et al. (2012). NPR3 and NPR4 are receptors for the immune signal salicylic acid in plants. *Nature* 486, 228–232. doi:10.1038/nature11162.

Fürst-Jansen, J. M. R., De Vries, S., De Vries, J., and De Vries, J. (2020). Evo-physio: On stress responses and the earliest land plants. *J. Exp. Bot.* 71, 3254–3269. doi:10.1093/jxb/eraa007.

Galotto, G., Abreu, I., Sherman, C., Liu, B., Gonzalez-Guerrero, M., and Vidali, L. (2020). Chitin Triggers Calcium-Mediated Immune Response in the Plant Model Physcomitrella patens. *Mol. Plant-Microbe Interact.* 33, 911–920. doi:10.1094/MPMI-03-20-0064-R.

Gimenez-Ibanez, S., Zamarreño, A. M., García-Mina, J. M., and Solano, R. (2019). An Evolutionarily Ancient Immune System Governs the Interactions between Pseudomonas syringae and an Early-Diverging Land Plant Lineage. *Curr. Biol.* 29, 2270-2281.e4. doi:10.1016/j.cub.2019.05.079.

Glazebrook, J. (2005). Contrasting Mechanisms of Defense Against Biotrophic and Necrotrophic Pathogens. *Annu. Rev. Phytopathol.* 43, 205–227. doi:10.1146/annurev.phyto.43.040204.135923.

Gourgues, M., Brunet-Simon, A., Lebrun, M. H., and Levis, C. (2004). The tetraspanin BcPIs1 is required for appressorium-mediated penetration of Botrytis cinerea into host plant leaves. *Mol. Microbiol.* 51, 619–629. doi:10.1046/j.1365-2958.2003.03866.x.

Govrin, E. M., and Levine, A. (2000). The hypersensitive response facilitates plant infection by the necrotrophic pathogen Botrytis cinerea. *Curr. Biol.* 10, 751–757. doi:10.1016/S0960-9822(00)00560-1.

Grant, M., Brown, I., Adams, S., Knight, M., Ainslie, A., and Mansfield, J. (2000). The RPM1 plant disease resistance gene facilitates a rapid and sustained increase in cytosolic calcium that is necessary for the oxidative burst and hypersensitive cell death. *Plant J.* 23, 441–450. doi:10.1046/j.1365-313X.2000.00804.x.

Greenberg, J. T., and Yao, N. (2004). The role of regulation of programmed cell death in plant-pathogen interactions. *Cell. Microbiol.* 6, 201–211. doi:10.1111/j.1462-5822.2004.00361.x.

Gu, C., Guo, Z. H., Hao, P. P., Wang, G. M., Jin, Z. M., and Zhang, S. L. (2017). Multiple regulatory roles of AP2/ERF transcription factor in angiosperm. *Bot. Stud.* 58, 6. doi:10.1186/s40529-016-0159-1.

Guan, L., Denkert, N., Eisa, A., Lehmann, M., Sjuts, I., Weiberg, A., et al. (2019). JASSY, a chloroplast outer membrane protein required for jasmonate biosynthesis. *Proc. Natl. Acad. Sci. U. S. A.* 116, 10568–10575. doi:10.1073/pnas.1900482116.

Gust, A. A., Pruitt, R., and Nürnberger, T. (2017). Sensing Danger: Key to Activating Plant Immunity. *Trends Plant Sci.* 22, 779–791. doi:10.1016/j.tplants.2017.07.005.

Hahn, M. (2014). The rising threat of fungicide resistance in plant pathogenic fungi: Botrytis as a case study. *J. Chem. Biol.* 7, 133–141. doi:10.1007/s12154-014-0113-1.

Haile, Z. M., Nagpala-De Guzman, E. G., Moretto, M., Sonego, P., Engelen, K., Zoli, L., et al. (2019). Transcriptome Profiles of Strawberry (Fragaria vesca) Fruit Interacting With Botrytis cinerea at Different Ripening Stages. *Front. Plant Sci.* 10, 1–17. doi:10.3389/fpls.2019.01131.

Halim, V. A., Eschen-Lippold, L., Altmann, S., Birschwilks, M., Scheel, D., and Rosahl, S. (2007). Salicylic Acid Is Important for Basal Defense of Solanum tuberosum Against Phytophthora infestans. *Mol. Plant. Microbe. Interact.* 20, 1346–1352. doi:10.1094/MPMI-20-11-1346.

Harrison, C. J., Roeder, A. H. K., Meyerowitz, E. M., and Langdale, J. A. (2009). Local Cues and Asymmetric Cell Divisions Underpin Body Plan Transitions in the Moss Physcomitrella patens. *Curr. Biol.* 19, 461–471. doi:10.1016/j.cub.2009.02.050.

Hiss, M., Laule, O., Meskauskiene, R. M., Arif, M. A., Decker, E. L., Erxleben, A., et al. (2014). Large-scale gene expression profiling data for the model moss Physcomitrella patens aid understanding of developmental progression, culture and stress conditions. *Plant J.* 79, 530–539. doi:10.1111/tpj.12572.

Hong, J. C. (2015). "General Aspects of Plant Transcription Factor Families," in *Plant Transcription Factors: Evolutionary, Structural and Functional Aspects*, ed. D. H. Gonzalez (Elsevier), 35–56. doi:10.1016/B978-0-12-800854-6.00003-8.

Hou, J., Feng, H. Q., Chang, H. W., Liu, Y., Li, G. H., Yang, S., et al. (2020). The H3K4 demethylase Jar1 orchestrates ROS production and expression of pathogenesis-related genes to facilitate Botrytis cinerea virulence. *New Phytol.* 225, 930–947. doi:10.1111/nph.16200.

Hu, Y. X., Wang, Y. H., Liu, X. F., and Li, J. Y. (2004). Arabidopsis RAV1 is down-regulated by brassinosteroid and may act as a negative regulator during plant development. *Cell Res.* 14, 8–15. doi:10.1038/sj.cr.7290197.

Hutcheson, S. W. (1998). Current concepts of active defense in plants. *Annu. Rev. Phytopathol.* 36, 59–90. doi:10.1146/annurev.phyto.36.1.59.

Inagaki, H., Miyamoto, K., Ando, N., Murakami, K., Sugisawa, K., Morita, S., et al. (2021). Deciphering OPDA Signaling Components in the Momilactone-Producing Moss Calohypnum plumiforme. *Front. Plant Sci.* 12, 1–14. doi:10.3389/fpls.2021.688565.

Iqbal, Z., Iqbal, M. S., Hashem, A., Abd_Allah, E. F., and Ansari, M. I. (2021). Plant Defense Responses to Biotic Stress and Its Interplay With Fluctuating Dark/Light Conditions. *Front. Plant Sci.* 12, 1–22. doi:10.3389/fpls.2021.631810.

Ish-Shalom, S., Gafni, A., Lichter, A., and Levy, M. (2011). Transformation of Botrytis cinerea by direct hyphal blasting or by wound-mediated transformation of sclerotia. *BMC Microbiol.* 11. doi:10.1186/1471-2180-11-266.

Ishikawa, M., Murata, T., Sato, Y., Nishiyama, T., Hiwatashi, Y., Imai, A., et al. (2011). Physcomitrella Cyclin-Dependent Kinase A Links Cell Cycle Reactivation to Other Cellular Changes during Reprogramming of Leaf Cells. *Plant Cell* 23, 2924–2938. doi:10.1105/tpc.111.088005.

Jensen, M. K., Hagedorn, P. H., de Torres-Zabala, M., Grant, M. R., Rung, J. H., Collinge, D. B., et al. (2008). Transcriptional regulation by an NAC (NAM-ATAF1,2-CUC2) transcription

factor attenuates ABA signalling for efficient basal defence towards Blumeria graminis f. sp. hordei in Arabidopsis. *Plant J.* 56, 867–880. doi:10.1111/j.1365-313X.2008.03646.x.

Jin, J., Tian, F., Yang, D. C., Meng, Y. Q., Kong, L., Luo, J., et al. (2017). PlantTFDB 4.0: Toward a central hub for transcription factors and regulatory interactions in plants. *Nucleic Acids Res.* Jan4, D1040–D1045. doi:10.1093/nar/gkw982.

Jones, J. D. G., and Dangl, J. L. (2006). The plant immune system. *Nature* 444, 323–329. doi:10.1038/nature05286.

Jurkowski, G. I., Smith, R. K., Yu, I. C., Ham, J. H., Sharma, S. B., Klessig, D. F., et al. (2004). Arabidopsis DND2, a second cyclic nucleotide-gated ion channel gene for which mutation causes the "defense, no death" phenotype. *Mol. Plant-Microbe Interact.* 17, 511–520. doi:10.1094/MPMI.2004.17.5.511.

Kadota, Y., Sklenar, J., Derbyshire, P., Stransfeld, L., Asai, S., Ntoukakis, V., et al. (2014). Direct Regulation of the NADPH Oxidase RBOHD by the PRR-Associated Kinase BIK1 during Plant Immunity. *Mol. Cell* 54, 43–55. doi:10.1016/j.molcel.2014.02.021.

Kanehisa, M., Sato, Y., and Kawashima, M. (2022). KEGG mapping tools for uncovering hidden features in biological data. *Protein Sci.* 31, 47–53. doi:10.1002/pro.4172.

Kazan, K., and Manners, J. M. (2013). MYC2: The Master in Action. *Mol. Plant* 6, 686–703. doi:10.1093/mp/sss128.

Kendrick, M. D., and Chang, C. (2008). Ethylene signaling: new levels of complexity and regulation. *Curr. Opin. Plant Biol.* 11, 479–485. doi:10.1016/j.pbi.2008.06.011.

Kimura, S., Hunter, K., Vaahtera, L., Tran, H. C., Citterico, M., Vaattovaara, A., et al. (2020). CRK2 and C-terminal phosphorylation of NADPH oxidase RBOHD regulate reactive oxygen species production in arabidopsis. *Plant Cell* 32, 1063–1080. doi:10.1105/tpc.19.00525.

Krings, M., Taylor, T. N., Hass, H., Kerp, H., Dotzler, N., and Hermsen, E. J. (2007). Fungal endophytes in a 400-million-yr-old land plant: Infection pathways, spatial distribution, and host responses. *New Phytol.* 174, 648–657. doi:10.1111/j.1469-8137.2007.02008.x.

Kroj, T., Chanclud, E., Michel-Romiti, C., Grand, X., and Morel, J. B. (2016). Integration of decoy domains derived from protein targets of pathogen effectors into plant immune receptors is widespread. *New Phytol.* 210, 618–626. doi:10.1111/nph.13869.

Kutschera, A., Dawid, C., Gisch, N., Schmid, C., Raasch, L., Gerster, T., et al. (2019). Bacterial medium-chain 3-hydroxy fatty acid metabolites trigger immunity in Arabidopsis plants. *Science (80-.).* 364, 178–181. doi:10.1126/science.aau1279.

Lang, D., Ullrich, K. K., Murat, F., Fuchs, J., Jenkins, J., Haas, F. B., et al. (2018). The Physcomitrella patens chromosome-scale assembly reveals moss genome structure and evolution. *Plant J.* 93, 515–533. doi:10.1111/tpj.13801.

Lawton, M., and Saidasan, H. (2009). Pathogenesis in mosses. *Annu. Plant Rev.* 36, 298–339.

Le Roux, C., Huet, G., Jauneau, A., Camborde, L., Trémousaygue, D., Kraut, A., et al. (2015). A receptor pair with an integrated decoy converts pathogen disabling of transcription factors to immunity. *Cell* 161, 1074–1088. doi:10.1016/j.cell.2015.04.025.

Lecourieux, D., Lamotte, O., Bourque, S., Wendehenne, D., Mazars, C., Ranjeva, R., et al. (2005). Proteinaceous and oligosaccharidic elicitors induce different calcium signatures in the nucleus of tobacco cells. *Cell Calcium* 38, 527–538. doi:10.1016/j.ceca.2005.06.036.

Lee, D. H., Lal, N. K., Lin, Z. J. D., Ma, S., Liu, J., Castro, B., et al. (2020). Regulation of reactive oxygen species during plant immunity through phosphorylation and ubiquitination of RBOHD. *Nat. Commun.* 11. doi:10.1038/s41467-020-15601-5.

Lee, D. H., Lee, H. S., and Belkhadir, Y. (2021). Coding of plant immune signals by surface receptors. *Curr. Opin. Plant Biol.* 62, 102044. doi:10.1016/j.pbi.2021.102044.

Lehti-Shiu, M. D., Zou, C., Hanada, K., and Shiu, S. H. (2009). Evolutionary history and stress regulation of plant receptor-like kinase/pelle genes. *Plant Physiol.* 150, 12–26. doi:10.1104/pp.108.134353.

Lehtonen, M. T., Akita, M., Frank, W., Reski, R., and Valkonen, J. P. T. (2012). Involvement of a Class III Peroxidase and the Mitochondrial Protein TSPO in Oxidative Burst Upon Treatment of Moss Plants with a Fungal Elicitor. *Mol. Plant-Microbe Interact.* 25, 363–371. doi:10.1094/MPMI-10-11-0265.

Lehtonen, M. T., Akita, M., Kalkkinen, N., Ahola-Iivarinen, E., Rönnholm, G., Somervuo, P., et al. (2009). Quickly-released peroxidase of moss in defense against fungal invaders. *New Phytol.* 183, 432–443. doi:10.1111/j.1469-8137.2009.02864.x.

Leroch, M., Plesken, C., Weber, R. W. S., Kauff, F., Scalliet, G., and Hahn, M. (2013). Gray mold populations in German strawberry fields are resistant to multiple fungicides and dominated by a novel clade closely related to Botrytis cinerea. *Appl. Environ. Microbiol.* 79, 159–167. doi:10.1128/AEM.02655-12.

Li, C. W., Su, R. C., Cheng, C. P., Sanjaya, You, S. J., Hsieh, T. H., et al. (2011). Tomato RAV transcription factor is a pivotal modulator involved in the AP2/EREBP-mediated defense pathway. *Plant Physiol.* 156, 213–227. doi:10.1104/pp.111.174268.

Li, L., Aslam, M., Rabbi, F., Vanderwel, M. C., Ashton, N. W., and Suh, D.-Y. (2018). PpORS, an ancient type III polyketide synthase, is required for integrity of leaf cuticle and resistance to dehydration in the moss, Physcomitrella patens. *Planta* 247, 527–541. doi:10.1007/s00425-017-2806-5.

Li, L., Li, M., Yu, L., Zhou, Z., Liang, X., Liu, Z., et al. (2014). The FLS2-associated kinase BIK1 directly phosphorylates the NADPH oxidase RbohD to control plant immunity. *Cell Host Microbe* 15, 329–338. doi:10.1016/j.chom.2014.02.009.

Li, Q., Zheng, J., Li, S., Huang, G., Skilling, S. J., Wang, L., et al. (2017). Transporter-Mediated Nuclear Entry of Jasmonoyl-Isoleucine Is Essential for Jasmonate Signaling. *Mol. Plant* 10, 695–708. doi:10.1016/j.molp.2017.01.010.

Licausi, F., Giorgi, F. M., Zenoni, S., Osti, F., Pezzotti, M., and Perata, P. (2010). Genomic and transcriptomic analysis of the AP2/ERF superfamily in Vitis vinifera. *BMC Genomics* 11, 719. doi:10.1186/1471-2164-11-719.

Lorenzo, O., and Solano, R. (2005). Molecular players regulating the jasmonate signalling network. *Curr. Opin. Plant Biol.* 8, 532–540. doi:10.1016/j.pbi.2005.07.003.

Luo, X., Wu, W., Liang, Y., Xu, N., Wang, Z., Zou, H., et al. (2020). Tyrosine phosphorylation

of the lectin receptor-like kinase LORE regulates plant immunity. *EMBO J.* 39, 1–16. doi:10.15252/embj.2019102856.

Manteau, S., Abouna, S., Lambert, B., and Legendre, L. (2003). Differential regulation by ambient pH of putative virulence factor secretion by the phytopathogenic fungus Botrytis cinerea. *FEMS Microbiol. Ecol.* 43, 359–366. doi:10.1016/S0168-6496(02)00439-7.

Medina, R., Johnson, M. G., Go, B., Liu, Y., Wickett, N. J., and Shaw, A. J. (2019). Phylogenomic delineation of Physcomitrium (Bryophyta : Funariaceae) based on targeted sequencing of nuclear exons and their fl anking regions rejects the retention of Physcomitrella , Physcomitridium and Aphanorrhegma. doi:10.1111/jse.12516.

Monte, I., Ishida, S., Zamarreño, A. M., Hamberg, M., Franco-Zorrilla, J. M., García-Casado, G., et al. (2018). Ligand-receptor co-evolution shaped the jasmonate pathway in land plants. *Nat. Chem. Biol.* 14, 480–488. doi:10.1038/s41589-018-0033-4.

Nakajima, M., and Akutsu, K. (2014). Virulence factors of Botrytis cinerea. *J. Gen. Plant Pathol.* 80, 15–23. doi:10.1007/s10327-013-0492-0.

Nakano, T., Suzuki, K., Fujimura, T., and Shinshi, H. (2006). Genome-Wide Analysis of the ERF Gene Family in Arabidopsis and Rice. *Plant Physiol.* 140, 411–432. doi:10.1104/pp.105.073783.currently.

Nakashima, K., Takasaki, H., Mizoi, J., Shinozaki, K., and Yamaguchi-Shinozaki, K. (2012). NAC transcription factors in plant abiotic stress responses. *Biochim. Biophys. Acta - Gene Regul. Mech.* 1819, 97–103. doi:10.1016/j.bbagrm.2011.10.005.

Ngou, B. P. M., Ahn, H.-K., Ding, P., and Jones, J. D. G. (2021). Mutual potentiation of plant immunity by cell-surface and intracellular receptors. *Nature* 592. doi:10.1038/s41586-021-03315-7.

Ngou, B. P. M., Ahn, H. K., Ding, P., Redkar, A., Brown, H., Ma, Y., et al. (2020). Estradiol-inducible AvrRps4 expression reveals distinct properties of TIR-NLR-mediated effector-triggered immunity. *J. Exp. Bot.* 71, 2186–2197. doi:10.1093/jxb/erz571.

Nuruzzaman, M., Sharoni, A. M., and Kikuchi, S. (2013). Roles of NAC transcription factors in the regulation of biotic and abiotic stress responses in plants. *Front. Microbiol.* 4, 1–16. doi:10.3389/fmicb.2013.00248.

Okamuro, J. K., Caster, B., Villarroel, R., Van Montagu, M., and Jofuku, K. D. (1997). The AP2 domain of APETALA2 defines a large new family of DNA binding proteins in Arabidopsis. *Proc. Natl. Acad. Sci. U. S. A.* 94, 7076–7081. doi:10.1073/pnas.94.13.7076.

Oliver, J. P., Castro, A., Gaggero, C., Cascón, T., Schmelz, E. A., Castresana, C., et al. (2009). Pythium infection activates conserved plant defense responses in mosses. *Planta* 230, 569–579. doi:10.1007/s00425-009-0969-4.

Orr, R. G., Foley, S. J., Sherman, C., Abreu, I., Galotto, G., Liu, B., et al. (2020). Robust Survival-Based RNA Interference of Gene Families Using in Tandem Silencing of Adenine Phosphoribosyltransferase. *Plant Physiol.* 184, 607–619. doi:10.1104/pp.20.00865.

Ortiz-Ramírez, C., Hernandez-Coronado, M., Thamm, A., Catarino, B., Wang, M., Dolan, L., et al. (2016). A Transcriptome Atlas of Physcomitrella patens Provides Insights into the Evolution and Development of Land Plants. *Mol. Plant* 9, 205–220.

doi:10.1016/j.molp.2015.12.002.

Otero-Blanca, A., Pérez-Llano, Y., Reboledo-Blanco, G., Lira-Ruan, V., Padilla-Chacon, D., Folch-Mallol, J. L., et al. (2021). Physcomitrium patens Infection by Colletotrichum gloeosporioides: Understanding the Fungal–Bryophyte Interaction by Microscopy, Phenomics and RNA Sequencing. *J. Fungi* 7, 677. doi:10.3390/jof7080677.

Pandey, S. P., and Somssich, I. E. (2009). The Role of WRKY Transcription Factors in Plant Immunity. *Plant Physiol.* 150, 1648–1655. doi:10.1104/pp.109.138990.

Perroud, P. F., Haas, F. B., Hiss, M., Ullrich, K. K., Alboresi, A., Amirebrahimi, M., et al. (2018). The Physcomitrella patens gene atlas project: large-scale RNA-seq based expression data. *Plant J.* 95, 168–182. doi:10.1111/tpj.13940.

Pieterse, C. M. J., Leon-Reyes, A., Van der Ent, S., and Van Wees, S. C. M. (2009). Networking by small-molecule hormones in plant immunity. *Nat. Chem. Biol.* 5, 308–316. doi:10.1038/nchembio.164.

Pirrello, J., Prasad, B. C. N., Zhang, W., Chen, K., Mila, I., Zouine, M., et al. (2012). Functional analysis and binding affinity of tomato ethylene response factors provide insight on the molecular bases of plant differential responses to ethylene. *BMC Plant Biol.* 12. doi:10.1186/1471-2229-12-190.

Ponce de León, I., and Montesano, M. (2013). Activation of Defense Mechanisms against Pathogens in Mosses and Flowering Plants. *Int. J. Mol. Sci.* 14, 3178–3200. doi:10.3390/ijms14023178.

Ponce de León, I., and Montesano, M. (2017). Adaptation Mechanisms in the Evolution of Moss Defenses to Microbes. *Front. Plant Sci.* 8, 1–14. doi:10.3389/fpls.2017.00366.

Ponce de León, I., Oliver, J. P., Castro, A., Gaggero, C., Bentancor, M., and Vidal, S. (2007). Erwinia carotovora elicitors and Botrytis cinerea activate defense responses in Physcomitrella patens. *BMC Plant Biol.* 7. doi:10.1186/1471-2229-7-52.

Ponce de León, I., Schmelz, E., GAGGERO, C., CASTRO, A., ÁLVAREZ, A., and MONTESANO, M. (2012). Physcomitrella patens activates reinforcement of the cell wall, programmed cell death and accumulation of evolutionary conserved defence signals, such as salicylic acid and 12-oxo-phytodienoic acid, but not jasmonic acid, upon Botrytis cinerea infection. *Mol. Plant Pathol.* 13, 960–974. doi:10.1111/j.1364-3703.2012.00806.x.

Pré, M., Atallah, M., Champion, A., De Vos, M., Pieterse, C. M. J., and Memelink, J. (2008). The AP2/ERF Domain Transcription Factor ORA59 Integrates Jasmonic Acid and Ethylene Signals in Plant Defense. *Plant Physiol.* 147, 1347–1357. doi:10.1104/pp.108.117523.

Pu, X., Yang, L., Liu, L., Dong, X., Chen, S., Chen, Z., et al. (2020). Genome-wide analysis of the MYB transcription factor superfamily in physcomitrella patens. *Int. J. Mol. Sci.* 21, 1–18. doi:10.3390/ijms21030975.

Ranf, S., Eschen-Lippold, L., Pecher, P., Lee, J., and Scheel, D. (2011). Interplay between calcium signalling and early signalling elements during defence responses to microbe- or damage-associated molecular patterns. *Plant J.* 68, 100–113. doi:10.1111/j.1365-313X.2011.04671.x.

Reboledo, G., Agorio, A., and De León, I. P. (2022). Transcription factors in moss development

and defenses against biotic and abiotic stress. *J. Exp. Bot.*, erac055. doi:10.1093/jxb/erac055.

Reboledo, G., del Campo, R., Alvarez, A., Montesano, M., Mara, H., and Ponce de León, I. (2015). Physcomitrella patens Activates Defense Responses against the Pathogen Colletotrichum gloeosporioides. *Int. J. Mol. Sci.* 16, 22280–22298. doi:10.3390/ijms160922280.

Reddy, A. S. N., Ali, G. S., Celesnik, H., and Day, I. S. (2011). Coping with stresses: Roles of calcium- and calcium/calmodulin-regulated gene expression. *Plant Cell* 23, 2010–2032. doi:10.1105/tpc.111.084988.

Reis, H., Pfiff, S., and Hahn, M. (2005). Molecular and functional characterization of a secreted lipase from Botrytis cinerea. *Mol. Plant Pathol.* 6, 257–267. doi:10.1111/j.1364-3703.2005.00280.x.

Rensing, S. A. (2016). (Why) Does Evolution Favour Embryogenesis ? *Trends Plant Sci.* 21, 562–573. doi:10.1016/j.tplants.2016.02.004.

Rensing, S. A., Goffinet, B., Meyberg, R., Wu, S. Z., and Bezanilla, M. (2020). The moss physcomitrium (Physcomitrella) patens: A model organism for non-seed plants. *Plant Cell* 32, 1361–1376. doi:10.1105/tpc.19.00828.

Rensing, S. A., Lang, D., Zimmer, A. D., Terry, A., Salamov, A., Shapiro, H., et al. (2008). The Physcomitrella Genome Reveals Evolutionary Insights into the Conquest of Land by Plants. *Science (80-.).* 319, 64–69. doi:10.1126/science.1150646.

Reski, R., and Abel, W. O. (1985). Planta Induction of budding on chloronemata and cau of the moss , Physcomitrella patens ,. *Planta* 165, 354–358.

Richter, H., Lieberei, R., Strnad, M., Novák, O., Gruz, J., Rensing, S. A., et al. (2012). Polyphenol oxidases in Physcomitrella: functional PPO1 knockout modulates cytokinin-dependent developmentin the moss Physcomitrella patens. *J. Exp. Bot.* 63, 5121–5135. doi:10.1093/jxb/ers169.

Riechmann, J. L., Heard, J., Martin, G., Reuber, L., Jiang, C.-Z., Keddie, J., et al. (2000). Arabidopsis Transcription Factors: Genome-Wide Comparative Analysis Among Eukaryotes. *Science (80-.).* 290, 2105–2110. doi:10.1126/science.290.5499.2105.

Riechmann, J. L., and Meyerowitz, E. M. (1998). The AP2/EREBP family of plant transcription factors. *Biol. Chem.* 379, 633–646. doi:10.1515/bchm.1998.379.6.633.

Rinerson, C. I., Rabara, R. C., Tripathi, P., Shen, Q. J., and Rushton, P. J. (2015). The evolution of WRKY transcription factors. *BMC Plant Biol.* 15, 1–18. doi:10.1186/s12870-015-0456-y.

Roux, M., Schwessinger, B., Albrecht, C., Chinchilla, D., Jones, A., Holton, N., et al. (2011). The Arabidopsis leucine-rich repeat receptor-like kinases BAK1/SERK3 and BKK1/SERK4 are required for innate immunity to hemibiotrophic and biotrophic pathogens. *Plant Cell* 23, 2440–2455. doi:10.1105/tpc.111.084301.

Sakuma, Y., Liu, Q., Dubouzet, J. G., Abe, H., Shinozaki, K., and Yamaguchi-Shinozaki, K. (2002). DNA-Binding Specificity of the ERF/AP2 Domain of Arabidopsis DREBs, Transcription Factors Involved in Dehydration- and Cold-Inducible Gene Expression.

Biochem. Biophys. Res. Commun. 290, 998–1009. doi:10.1006/bbrc.2001.6299.

Sarris, P. F., Duxbury, Z., Huh, S. U., Ma, Y., Segonzac, C., Sklenar, J., et al. (2015). A plant immune receptor detects pathogen effectors that target WRKY transcription factors. *Cell* 161, 1089–1100. doi:10.1016/j.cell.2015.04.024.

Sasaki, K., Mitsuhara, I., Seo, S., Ito, H., Matsui, H., and Ohashi, Y. (2007). Two novel AP2/ERF domain proteins interact with cis-element VWRE for wound-induced expression of the Tobacco tpoxN1 gene. *Plant J.* 50, 1079–1092. doi:10.1111/j.1365-313X.2007.03111.x.

Schaefer, D. G. (2002). A New Moss Genetics: Targeted Mutagenesis in Physcomitrella patens. *Annu. Rev. Plant Biol.* 53, 477–501. doi:10.1146/annurev.arplant.53.100301.135202.

Schaller, A., and Stintzi, A. (2009). Enzymes in jasmonate biosynthesis - Structure, function, regulation. *Phytochemistry* 70, 1532–1538. doi:10.1016/j.phytochem.2009.07.032.

Shigyo, M., and Ito, M. (2004). Analysis of gymnosperm two-AP2-domain-containing genes. *Dev. Genes Evol.* 214, 105–114. doi:10.1007/s00427-004-0385-5.

Siegmund, U., and Viefhues, A. (2015). "Reactive Oxygen Species in the Botrytis – Host Interaction," in *Botrytis - The Fungus, the Pathogen and its Management in Agricultural Systems* (Springer Cham), 269–289. doi:10.1007/978-3-319-23371-0.

Siewers, V., Viaud, M., Jimenez-teja, D., Collado, I. G., Gronover, C. S., Pradier, J., et al. (2005). Functional Analysis of the Cytochrome P450 Monooxygenase Gene bcbot1 of Botrytis cinerea Indicates That Botrydial Is a Strain-Specific Virulence Factor. *Mol. Plant-Microbe Interact.* 18, 602–612. doi:https://doi.org/10.1094/MPMI-18-0602.

Sigel, E. M., Schuettpelz, E., Pryer, K. M., Der, J. P., Christian, C., and Chater, C. (2018). Overlapping Patterns of Gene Expression Between Gametophyte and Sporophyte Phases in the Fern Polypodium amorphum (Polypodiales). *Front. Plant Sci.* 9. doi:https://doi.org/10.3389/fpls.2018.01450.

Sohn, K. H., Lee, S. C., Jung, H. W., Hong, J. K., and Hwang, B. K. (2006). Expression and functional roles of the pepper pathogen-induced transcription factor RAV1 in bacterial disease resistance, and drought and salt stress tolerance. *Plant Mol. Biol.* 61, 897–915. doi:10.1007/s11103-006-0057-0.

Spoel, S. H., Johnson, J. S., and Dong, X. (2007). Regulation of tradeoffs between plant defenses against pathogens with different lifestyles. *Proc. Natl. Acad. Sci. U. S. A.* 104, 18842–18847. doi:10.1073/pnas.0708139104.

Stracke, R., Werber, M., and Weisshaar, B. (2001). The R2R3-MYB gene family in Arabidopsis thaliana. *Curr. Opin. Plant Biol.* 4, 447–456. doi:10.1016/S1369-5266(00)00199-0.

Strotbek, C., Krinninger, S., and Frank, W. (2013). The moss Physcomitrella patens: Methods and tools from cultivation to targeted analysis of gene function. *Int. J. Dev. Biol.* 57, 553–564. doi:10.1387/ijdb.130189wf.

Strullu-Derrien, C. (2018). Fossil filamentous microorganisms associated with plants in early terrestrial environments. *Curr. Opin. Plant Biol.* 44, 122–128. doi:10.1016/j.pbi.2018.04.001.

Su, J., Yang, L., Zhu, Q., Wu, H., He, Y., Liu, Y., et al. (2018). Active photosynthetic inhibition mediated by MPK3/MPK6 is critical to effector-triggered immunity. *PLoS Biol.* 16, 1–29. doi:10.1371/journal.pbio.2004122.

Sugimoto, K., Gordon, S. P., and Meyerowitz, E. M. (2011). Regeneration in plants and animals: Dedifferentiation, transdifferentiation, or just differentiation? *Trends Cell Biol.* 21, 212–218. doi:10.1016/j.tcb.2010.12.004.

Sugiura, C., Kobayashi, Y., Aoki, S., Sugita, C., and Sugita, M. (2003). Complete chloroplast DNA sequence of the moss Physcomitrella patens: Evidence for the loss and relocation of rpoA from the chloroplast to the nucleus. *Nucleic Acids Res.* 31, 5324–5331. doi:10.1093/nar/gkg726.

Tamborski, J., and Krasileva, K. V. (2020). Evolution of Plant NLRs: From Natural History to Precise Modifications. *Annu. Rev. Plant Biol.* 71, 355–378. doi:10.1146/annurev-arplant-081519-035901.

Tang, D., Wang, G., and Zhou, J. M. (2017). Receptor kinases in plant-pathogen interactions: More than pattern recognition. *Plant Cell* 29, 618–637. doi:10.1105/tpc.16.00891.

Teixeira, P. J. P., Colaianni, N. R., Fitzpatrick, C. R., and Dangl, J. L. (2019). Beyond pathogens: microbiota interactions with the plant immune system. *Curr. Opin. Microbiol.* 49, 7–17. doi:10.1016/j.mib.2019.08.003.

Terasawa, K., Odahara, M., Kabeya, Y., Kikugawa, T., Sekine, Y., Fujiwara, M., et al. (2007). The mitochondrial genome of the moss physcomitrella patens sheds new light on mitochondrial evolution in land plants. *Mol. Biol. Evol.* 24, 699–709. doi:10.1093/molbev/msl198.

Thaler, J. S., Humphrey, P. T., and Whiteman, N. K. (2012). Evolution of jasmonate and salicylate signal crosstalk. *Trends Plant Sci.* 17, 260–270. doi:10.1016/j.tplants.2012.02.010.

Trogu, S., Ermert, A. L., Stahl, F., Nogué, F., Gans, T., and Hughes, J. (2021). Multiplex CRISPR-Cas9 mutagenesis of the phytochrome gene family in Physcomitrium (Physcomitrella) patens. *Plant Mol. Biol.* 107, 327–336. doi:10.1007/s11103-020-01103-x.

Tsuda, K., Mine, A., Bethke, G., Igarashi, D., Botanga, C. J., Tsuda, Y., et al. (2013). Dual Regulation of Gene Expression Mediated by Extended MAPK Activation and Salicylic Acid Contributes to Robust Innate Immunity in Arabidopsis thaliana. *PLoS Genet.* 9. doi:10.1371/journal.pgen.1004015.

Tsuda, K., and Somssich, I. E. (2015). Transcriptional networks in plant immunity. *New Phytol.* 206, 932–947. doi:10.1111/nph.13286.

Valero-Jiménez, C. A., Veloso, J., Staats, M., and van Kan, J. A. L. (2019). Comparative genomics of plant pathogenic Botrytis species with distinct host specificity. *BMC Genomics* 20, 203. doi:10.1186/s12864-019-5580-x.

Van Der Biezen, E. A., and Jones, J. D. G. (1998). Plant disease-resistance proteins and the gene-for-gene concept. *Trends Biochem. Sci.* 23, 454–456. doi:10.1016/S0968-0004(98)01311-5.

Van Kan, J. A. L. (2006). Licensed to kill: the lifestyle of a necrotrophic plant pathogen. *Trends*

Plant Sci. 11, 247–253. doi:10.1016/j.tplants.2006.03.005.

Van Kan, J. A. L., Stassen, J. H. M., Mosbach, A., Van Der Lee, T. A. J., Faino, L., Farmer, A. D., et al. (2017). A gapless genome sequence of the fungus Botrytis cinerea. *Mol. Plant Pathol.* 18, 75–89. doi:10.1111/mpp.12384.

Van Kan, J. A. L., Van't Klooster, J. W., Wagemakers, C. A. M., Dees, D. C. T., and Van Der Vlugt-Bergmans, C. J. B. (1997). Cutinase A of Botrytis cinerea is expressed, but not essential, during penetration of gerbera and tomato. *Mol. Plant-Microbe Interact.* 10, 30–38. doi:10.1094/MPMI.1997.10.1.30.

van Wersch, S., Tian, L., Hoy, R., and Li, X. (2020). Plant NLRs: The Whistleblowers of Plant Immunity. *Plant Commun.* 1, 100016. doi:10.1016/j.xplc.2019.100016.

VanEtten, H., Temporini, E., and Wasmann, C. (2001). Phytoalexin (and phytoanticipin) tolerance as a virulence trait: Why is it not required by all pathogens? *Physiol. Mol. Plant Pathol.* 59, 83–93. doi:10.1006/pmpp.2001.0350.

Wang, C., Zhou, M., Zhang, X., Yao, J., Zhang, Y., and Mou, Z. (2017). A lectin receptor kinase as a potential sensor for extracellular nicotinamide adenine dinucleotide in arabidopsis thaliana. *Elife* 6, 1–23. doi:10.7554/eLife.25474.

Wang, J.-H., Gu, K.-D., Han, P.-L., Yu, J.-Q., Wang, C.-K., Zhang, Q.-Y., et al. (2020). Apple ethylene response factor MdERF11 confers resistance to fungal pathogen Botryosphaeria dothidea. *Plant Sci.* 291, 110351. doi:10.1016/j.plantsci.2019.110351.

Wang, J., Hu, M., Wang, J., Qi, J., Han, Z., Wang, G., et al. (2019a). Reconstitution and structure of a plant NLR resistosome conferring immunity. *Science (80-.).* 364, eaav5870. doi:10.1126/science.aav5870.

Wang, J., Wang, J., Hu, M., Wu, S., Qi, J., Wang, G., et al. (2019b). Ligand-triggered allosteric ADP release primes a plant NLR complex. *Science (80-.).* 364, eaav5868. doi:10.1126/science.aav5868.

Wang, K. L. C., Li, H., and Ecker, J. R. (2002). Ethylene biosynthesis and signaling networks. *Plant Cell* 14, 131–151. doi:10.1105/tpc.001768.

Wessler, S. R. (2005). Homing into the origin of the AP2 DNA binding domain. *Trends Plant Sci.* 10, 54–56. doi:http://dx.doi.org/10.1016/j.tplants.2004.12.007.

Wildermuth, M. C., Dewdney, J., Wu, G., and Ausubel, F. M. (2001). Isochorismate synthase is required to synthesize salicylic acid for plant defence. *Nature* 414, 562–565. doi:10.1038/35107108.

Williamson, B., Tudzynski, B., Tudzynski, P., and Van Kan, J. A. L. (2007). Botrytis cinerea: The cause of grey mould disease. *Mol. Plant Pathol.* 8, 561–580. doi:10.1111/j.1364-3703.2007.00417.x.

Willmann, R., Lajunen, H. M., Erbs, G., Newman, M. A., Kolb, D., Tsuda, K., et al. (2011). Arabidopsis lysin-motif proteins LYM1 LYM3 CERK1 mediate bacterial peptidoglycan sensing and immunity to bacterial infection. *Proc. Natl. Acad. Sci. U. S. A.* 108, 19824–19829. doi:10.1073/pnas.1112862108.

Windram, O., Madhou, P., Mchattie, S., Hill, C., Hickman, R., Cooke, E., et al. (2012).

Arabidopsis defense against Botrytis cinerea: Chronology and regulation deciphered by high-resolution temporal transcriptomic analysis. *Plant Cell* 24, 3530–3557. doi:10.1105/tpc.112.102046.

Wu, C.-H., Derevnina, L., and Kamoun, S. (2018). Receptor networks underpin plant immunity. *Science (80-.).* Jun 22, 1300–1301.

Wu, L., Zhang, Z., Zhang, H., Wang, X. C., and Huang, R. (2008). Transcriptional modulation of ethylene response factor protein JERF3 in the oxidative stress response enhances tolerance of tobacco seedlings to salt, drought, and freezing. *Plant Physiol.* 148, 1953–1963. doi:10.1104/pp.108.126813.

Xu, G., Greene, G. H., Yoo, H., Liu, L., Marqués, J., Motley, J., et al. (2017). Global translational reprogramming is a fundamental layer of immune regulation in plants. *Nature* 545, 487–490. doi:10.1038/nature22371.

Xu, Z. S., Chen, M., Li, L. C., and Ma, Y. Z. (2011). Functions and Application of the AP2/ERF Transcription Factor Family in Crop Improvement. *J. Integr. Plant Biol.* 53, 570–585. doi:10.1111/j.1744-7909.2011.01062.x.

Yamada, K., Yamaguchi, K., Shirakawa, T., Nakagami, H., Mine, A., Ishikawa, K., et al. (2016). The Arabidopsis CERK 1-associated kinase PBL 27 connects chitin perception to MAPK activation . *EMBO J.* 35, 2468–2483. doi:10.15252/embj.201694248.

Yan, H., Zhao, Y., Shi, H., Li, J., Wang, Y., and Tang, D. (2018). BRASSINOSTEROID-SIGNALING kinase1 phosphorylates MAPKKK5 to regulate immunity in arabidopsis. *Plant Physiol.* 176, 2991–3002. doi:10.1104/pp.17.01757.

Yang, H., Shen, F., Wang, H., Zhao, T., Zhang, H., Jiang, J., et al. (2020). Functional analysis of the SlERF01 gene in disease resistance to S. lycopersici. *BMC Plant Biol.* 20, 376. doi:10.1186/s12870-020-02588-w.

Yang, Y.-X., Jalal Ahammed, G., Wu, C., Fan, S., and Zhou, Y.-H. (2015). Crosstalk among Jasmonate, Salicylate and Ethylene Signaling Pathways in Plant Disease and Immune Responses. *Curr. Protein Pept. Sci.* 16, 450–461.

Yasumura, Y., Pierik, R., Fricker, M. D., Voesenek, L. A. C. J., and Harberd, N. P. (2012). Studies of Physcomitrella patens reveal that ethylenemediated submergence responses arose relatively early in land-plant evolution. *Plant J.* 72, 947–959. doi:10.1111/tpj.12005.

Yoo, H., Greene, G. H., Yuan, M., Xu, G., Burton, D., Liu, L., et al. (2019). Translational Regulation of Metabolic Dynamics during Effector-Triggered Immunity. *Mol. Plant*, 88–98. doi:10.1016/j.molp.2019.09.009.

Yu, X., Feng, B., He, P., and Shan, L. (2017). From Chaos to Harmony : Responses and Signaling Upon Microbial Pattern Recognition. *Annu. Rev. Phytopathol.* 55, 1–29.

Yuan, M., Jiang, Z., Bi, G., Nomura, K., Liu, M., Wang, Y., et al. (2021a). Pattern-recognition receptors are required for NLR-mediated plant immunity. *Nature* 592. doi:10.1038/s41586-021-03316-6.

Yuan, M., Ngou, B. P. M., Ding, P., and Xin, X.-F. (2021b). PTI-ETI crosstalk: an integrative view of plant immunity. *Curr. Opin. Plant Biol.* 62, 102030. doi:10.1016/j.pbi.2021.102030.

Zhang, M., Chiang, Y. H., Toruño, T. Y., Lee, D. H., Ma, M., Liang, X., et al. (2018). The MAP4 Kinase SIK1 Ensures Robust Extracellular ROS Burst and Antibacterial Immunity in Plants. *Cell Host Microbe* 24, 379-391.e5. doi:10.1016/j.chom.2018.08.007.

Zhang, M. Z., Sun, C. H., Liu, Y., Feng, H. Q., Chang, H. W., Cao, S. N., et al. (2020). Transcriptome analysis and functional validation reveal a novel gene, BcCGF1, that enhances fungal virulence by promoting infection-related development and host penetration. *Mol. Plant Pathol.* 21, 834–853. doi:10.1111/mpp.12934.

Zhang, Z., Liu, Y., Huang, H., Gao, M., Wu, D., Kong, Q., et al. (2017). The NLR protein SUMM 2 senses the disruption of an immune signaling MAP kinase cascade via CRCK 3 . *EMBO Rep.* 18, 292–302. doi:10.15252/embr.201642704.

Zhao, S., and Li, Y. (2021). Current understanding of the interplays between host hormones and plant viral infections. *PLoS Pathog.* 17, 1–18. doi:10.1371/JOURNAL.PPAT.1009242.

Zhou, J. M., and Zhang, Y. (2020). Plant Immunity: Danger Perception and Signaling. *Cell* 181, 978–989. doi:10.1016/j.cell.2020.04.028.

Zhuang, J., Cai, B., Peng, R.-H., Zhu, B., Jin, X.-F., Xue, Y., et al. (2008). Genome-wide analysis of the AP2/ERF gene family in Populus trichocarpa. *Biochem. Biophys. Res. Commun.* 371, 468–474. doi:10.1016/j.bbrc.2008.04.087.